Asymptotic limit of the Landau-de Gennes model for liquid crystals around an inclusion

Dominik Stantejsky

INSTITUT POLYTECHNIQUE DE PARIS

NNT : 2022IPPAX066

Thèse de doctorat

Asymptotic Limit of the Landau-de Gennes Model for Liquid Crystals Around an Inclusion

Thèse de doctorat de l'Institut Polytechnique de Paris
préparée à l'École polytechnique

École doctorale n°574 École doctorale de mathématiques Hadamard (EDMH)
Spécialité de doctorat : Mathématiques appliquées

Thèse présentée et soutenue à Palaiseau, le 22 Septembre 2022, par

DOMINIK STANTEJSKY

Composition du Jury :

Grégoire ALLAIRE Professeur, École Polytechnique (CMAP)	Président
Lia BRONSARD Professeure, McMaster University (Dept of Math and Stats)	Rapporteure
Vincent MILLOT Professeur, Université Paris-Est (LAMA)	Rapporteur
Fabrice BETHUEL Professeur, Sorbonne Université (LJLL)	Examinateur
Felix OTTO Professeur, Max-Planck-Institut (MPI MIS)	Examinateur
François ALOUGES Professeur, École Polytechnique (CMAP)	Directeur de thèse
Antonin CHAMBOLLE Directeur de Recherche, Université Paris-Dauphine (CEREMADE)	Directeur de thèse

Das Instrument, welches die Vermittlung bewirkt zwischen Theorie und Praxis, zwischen Denken und Beobachten, ist die Mathematik; sie baut die verbindende Brücke und gestaltet sie immer tragfähiger. Daher kommt es, dass unsere ganze gegenwärtige Kultur, soweit sie auf der geistigen Durchdringung und Dienstbarmachung der Natur beruht, ihre Grundlage in der Mathematik findet.

– David Hilbert, 1930

Remerciements

La rédaction d'une thèse et des remerciements marque l'étape finale d'un travail de plusieurs années. Je souhaite ainsi adresser mes remerciements à toutes ces personnes qui y ont contribué et qui m'ont soutenu dans son aboutissement.

D'abord, j'adresse tout mes remerciements, chaleureusement et pleinement, à mes directeurs de thèse, François et Antonin, pour leur encadrement impeccable, toutes les heures de travail productives et amicales passées ensemble, le soutien constant, les conseils précieux, mais aussi pour la liberté qu'ils m'ont donnée de poursuivre mes idées et les discussions hors sujet.

J'aimerais également remercier Lia Bronsard et Vincent Millot d'avoir accepté d'être rapporteurs, et Grégoire Allaire, Fabrice Béthuel et Felix Otto pour leur participation au jury. Je suis reconnaissant pour toutes les discussions que j'ai eues avec différentes personnes lors de conférences et de séminaires, qui m'ont permis de me plonger dans le sujet et d'élargir mes horizons. En particulier, je remercie Xavier Lamy pour les discussions que nous avons eues et le soutien qu'il m'a apporté. Je tiens également à remercier Christophe Geuzaine, dont l'aide a été précieuse pour surmonter mes difficultés rencontrées dans le cadre de mon travail avec GMSH. Un grand merci aussi à tout ceux et celles qui ont relu mon manuscrit et qui m'ont aidé à l'améliorer.

Le travail scientifique nécessite un cadre administratif. Dans cet esprit, merci à l'équipe administrative du laboratoire, en particulier Nasséra et Alex, et du DEPMAP, notamment Nicoletta et Leyla, pour les aimables réponses à toutes mes questions naïves et pour la résolution de tous les petits et grands problèmes. En même temps, je remercie l'équipe informatique autour de Sylvain, Pierre et Laurent pour leur soutien, surtout au cours de mon 3ème année. Pour toute question et problème administratif hors travail, je remercie Science Accueil et notamment Jean, son président.

Je tiens également à remercier les permanents et post-doctorants qui m'ont accompagné pendant mon temps au CMAP, avant tout Aline, Hanieh et Marcella. Mes remerciements vont aussi aux doctorants du CMAP (je parle de vous Apolline, Arthur, Clément, Constantin, Jessie, Louis, Thomas et Yohannn), d'autres labos (Elise, Mehdi et Yvonne), et particulièrement le bureau 00.20.15, Claire, Corentin, Eugénie, Ignatio, Michaël, Morfal et Solange. En commençant par des collègues, vous êtes devenus des amis.

Ein besonderer Dank gilt meiner Familie, insbesondere meinen Eltern und meinem Bruder, welche seit mehr als 27 Jahren immer für mich da sind, mich unterstützen und ermutigen, und meinen Großeltern, die mich stets auf meinem Weg begleitet und bestärkt haben.

During the past years, you have become my second family: Akadshi (including the zoo members), Elissa, Giulia and Moira. Do I need to say more? Potatoes will potate. I'm also sending a thank you all around the world to Akhila, Alina, Celesta, Denis, Harsh, Josh, Kaitlin, Marcos, Martina, Mona and Sebi. I feel deep gratitude for the time we spend together (and will in the future).

Coming towards the end, as not to disappoint certain people, a statement shall be added, in order to address, in unsurpassable clarity and without wasting any further words, a matter which is not without a certain importance, and to mention certain, may it be hidden or superficially apparent, influences that led, at the end of the day, after cycles of extending, altering and abbreviating, to the ultimate arrangement and expressive, some say peculiar, phrasing from which this passage derives its overall significance: as the attentive reader has surely noticed by now, the subjects of concern are John Cleese and Sir Humphrey Appleby for providing the emotion of thriving cheerfulness, especially related to the acquisition of linguistic expressions of doubtful utility, and for the elevating and stimulating influence brought upon the intellect and creativity of the individuum currently pouring his thoughts onto this 210×297 mm piece of processed cellulose fibres, as it is about to define itself by the means of the perpendicular pronoun.

Merci.	Thank you.	Danke.	Takk.	Спасибо.	شكرا.	Děkuji.	متشكرم.
𓈖𓉔𓅓𓀁.	धन्यवाद	Gracias.	谢谢。	Kiitos.	Kösz.	ευχαριστω	Grazie.

Abstract

Liquid crystals are a type of matter which share properties with both liquids and crystalline solids, i.e. the molecules of such materials can move but exhibit a positional and orientational order. One of the most remarkable characteristics is the formation of defect structures, in particular point and line singularities. In this work we use a version of the Landau-de Gennes model for nematic liquid crystals with an external magnetic field to describe the Saturn ring effect around an immersed particle. In an asymptotic regime where both point and line singularities occur, we derive an effective energy describing the formation and transition between different singularities.

The first chapter deals with the physically relevant case of a spherical particle. After a rescaling of the physical energy, a limit energy in the sense of $\Gamma-$convergence, stated on the particle surface, is derived. Studying the limit problem, we explain the transition between the dipole and Saturn ring configurations and the occurrence of a hysteresis phenomenon.

In the second chapter we consider the general case of an arbitrary closed and sufficiently smooth particle. In contrast to spherical (or more general convex) particle, we obtain an additional term in the limit energy, showing quantitatively that the close-to-minimal energy is asymptotically concentrated on lines and surfaces nearby or on the particle. We also discuss regularity of minimizers and optimality conditions for the limit energy.

The third chapter is dedicated to the numerical investigation of the limit energy and the development and implementation of adapted numerical methods. We verify the results of the first chapter for the sphere and then study the defect structures in the case of a peanut and croissant-like particle.

Résumé

Les cristaux liquides sont des matériaux avec des propriétés intermédiaires entre celles des liquides et des solides cristallins, c'est-à-dire les molécules peuvent se déplacer mais montrent un ordre de position et d'orientation. L'une de leurs caractéristiques les plus remarquables est la formation naturelle de structures de défauts, en particulier des singularités ponctuelles ou en lignes. Dans ce travail on considère une version du modèle de Landau-de Gennes pour les cristaux liquides nématiques avec un champ magnétique externe modélisant l'effet de l'anneau de Saturne autour d'une particule immergée. Dans un régime asymptotique où les singularités ponctuelles et de lignes se produisent, nous dérivons une énergie effective décrivant la formation et la transition entre les différentes singularités.

Le premier chapitre porte sur le cas physique le plus étudié d'une particule sphérique. Après une remise à l'échelle de l'énergie physique, une énergie limite au sens de la $\Gamma-$convergence, énoncée à la surface de la particule, est dérivée. En étudiant le problème limite, nous expliquons la transition entre la configuration du dipôle et de l'anneau de Saturne ainsi que l'apparition d'un phénomène d'hystérésis.

Dans le deuxième chapitre, nous considérons le cas général d'une particule quelconque fermée et suffisamment lisse. Contrairement à une particule sphérique (ou plus généralement convexe), nous obtenons un terme supplémentaire dans l'énergie limite, montrant quantitativement que l'énergie proche du minimum est asymptotiquement concentrée sur des lignes et des surfaces proches de la particule voire collées à sa surface. Nous discutons également la régularité des minimiseurs et les conditions d'optimalité de l'énergie limite.

Le troisième chapitre est consacré à l'étude numérique de l'énergie limite et au développement et à la mise en œuvre de méthodes numériques adaptées. Nous vérifions les résultats du premier chapitre pour la sphère, puis nous étudions les structures de défauts dans le cas d'une particule en forme de cacahuète ou de croissant.

Zusammenfassung

Flüssigkristalle sind Materialien, die Eigenschaften von sowohl Flüssigkeiten als auch von kristallinen Feststoffen aufweisen, d.h. die Moleküle dieser Materialien können sich bewegen, weisen aber eine Ordnung bezüglich ihrer Positions- oder Orientierung auf. Eine der bemerkenswertesten Eigenschaften ist die Bildung von Defektstrukturen, insbesondere von Punkt- und Liniensingularitäten. In dieser Arbeit verwenden wir eine Version des Landau-de Gennes-Modells für nematische Flüssigkristalle mit einem externen Magnetfeld um den Saturnring-Effekt um ein eingetauchtes Teilchen zu beschreiben. In einem asymptotischen Parameterbereich, in dem sowohl Punkt- als auch Liniensingularitäten auftreten, leiten wir eine effektive Energie ab, welche die Bildung und den Übergang zwischen den verschiedenen Singularitäten beschreibt.

Das erste Kapitel befasst sich mit dem physikalisch relevanten Fall eines kugelförmigen Teilchens. Nach einer Reskalierung der physikalischen Energie wird eine auf der Teilchenoberfläche gegebene Grenzenergie im Sinne der $\Gamma-$Konvergenz hergeleitet. Bei der Untersuchung des Limitproblems erklären wir den Übergang zwischen der Dipol- und der Saturnring-Konfiguration und das Auftreten eines Hysteresephänomens.

Im zweiten Kapitel betrachten wir den allgemeinen Fall eines beliebigen geschlossenen und hinreichend glatten Teilchens. Im Gegensatz zu kugelförmigen (oder allgemeiner konvexen) Partikeln, erhalten wir einen zusätzlichen Term in der Grenzwert-Energie und zeigen quantitativ, dass die nahezu-minimale Energie asymptotisch auf Linien und Oberflächen in der Nähe oder auf dem Teilchen konzentriert ist. Wir befassen uns auch mit der Regularität der Minimierer und den Optimalitätsbedingungen der Grenzwert-Energie.

Das dritte Kapitel widmet sich der numerischen Untersuchung der Grenzenergie und der Entwicklung und Implementierung geeigneter numerischer Methoden. Wir verifizieren die Ergebnisse des ersten Kapitels für die Sphäre und studieren die Defektstrukturen im Falle eines Erdnuss- und Croissantförmigen Teilchens.

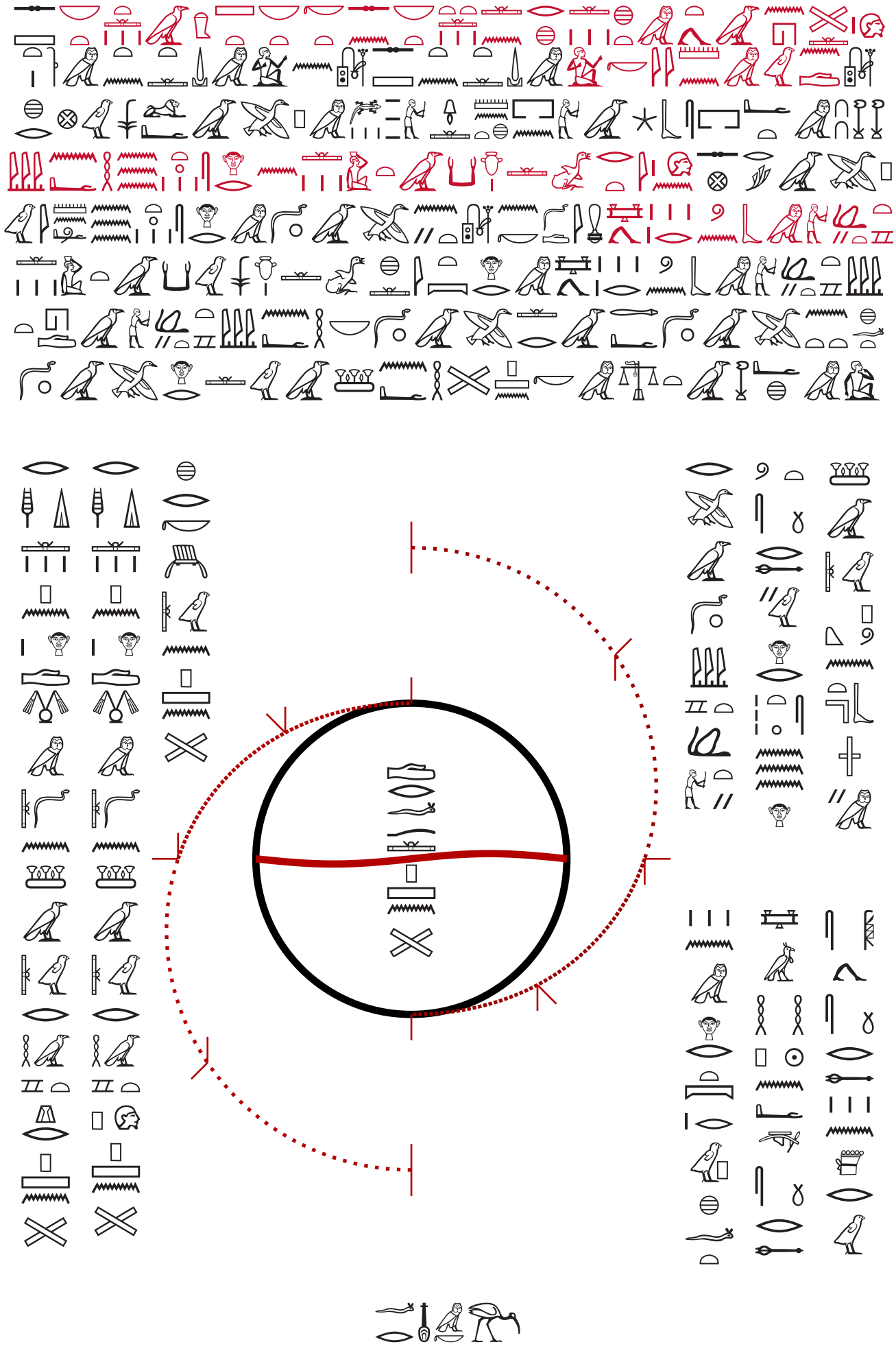

Contents

Chapter 1

Introduction générale

1.1 Les cristaux liquides nématiques

1.1.1 Physique et description

En 1888, le chimiste autrichien Friedrich Reinitzer observe un "phénomène étrange de la présence de deux points de fusion" dans le benzoate de cholestéryle [54, 141]. Par la suite c'est le physicien et cristallographe allemand Otto Lehmann qui lui donne son nom *cristal fluide* [106]. D'un point de vue contemporain, les cristaux liquides représentent un état de la matière molle aux propriétés intermédiaires entre les liquides et les solides cristallins. Ils peuvent former des gouttes comme un fluide, bien qu'ils présentent des anisotropies, par exemple de leurs propriétés électromagnétiques. C'est pourquoi ils sont parfois appelés des *fluides anisotropes*. En raison de ces propriétés uniques, les cristaux liquides présentent des structures et des applications dans beaucoup de domaines. Omniprésents au quotidien dans les écrans à cristaux liquides ("LCD"), l'emploi dans d'autres domaines électro-optiques, chimiques [58, Ch. IX] ainsi que dans les nano-, micro- et biotechnologies [102] est également pertinent.

Pour former un cristal liquide, les molécules doivent être *nématogènes* et avoir des interactions qui leurs permettent de s'ordonner. Habituellement ces matériaux sont constitués de molécules en forme de bâtonnet (bien qu'il existe d'autres molécules en forme de disque, par exemple) dont l'ordre de position et d'orientation peut varier dans l'espace, le temps et en fonction des paramètres tels que la température. Contrairement aux cristaux qui présentent un ordre de position et d'orientation à l'échelle moléculaire et aux liquides qui ne sont pas structurés, les cristaux liquides peuvent être classés en plusieurs types selon l'ordre qu'ils présentent. Les plus proches d'un liquide sont les cristaux *nématiques* dont la position des molécules est distribuée de façon aléatoire, mais leurs orientations sont en moyenne alignées. Un autre type de cristaux liquides est appelé *cholestérique* dans lequel les molecules sont positionnées de façon hélicoïdale. Ensuite, les *smectiques* s'organisent dans des couches, avec leur orientation perpendiculaire à la normale du plan (*smectique A*) ou pas (*smectique C*). Pour une introduction générale, nous référons le lecteur à [13, 58].

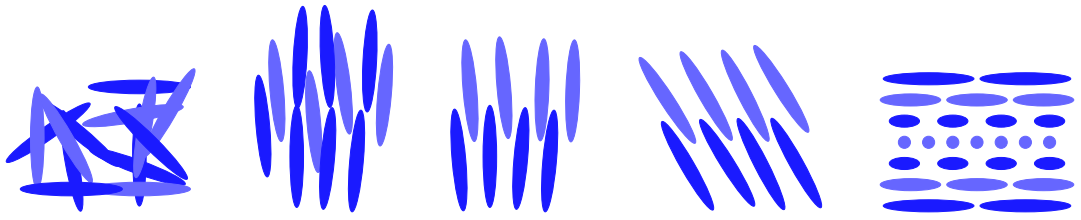

Figure 1.1: Représentation schématique d'une phase de cristal liquide isotrope, nématique, smectique A, smectique C et cholestérique (de gauche à droite).

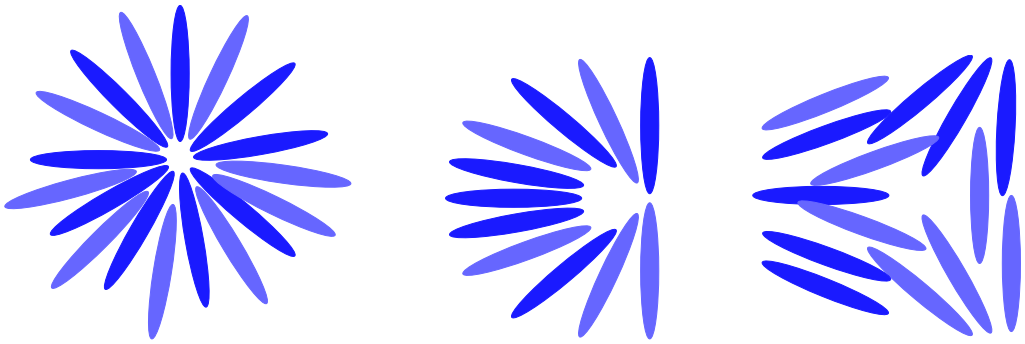

Figure 1.2: Représentation schématique des défauts de degré $+1$, $+\frac{1}{2}$ et $-\frac{1}{2}$ (de gauche à droite).

Afin de modéliser la direction des molécules à un endroit donné, on utilise le fait qu'en moyenne, les molécules d'un cristal liquide sont alignées le long d'un directeur $\mathbf{n} \in \mathbb{S}^2$. Il est commode d'introduire un champ de vecteurs $\mathbf{n} : \Omega \to \mathbb{S}^2$ qui pointe dans la direction des molécules en chaque point du matériau Ω. En pratique, il est possible de détecter le directeur car les cristaux liquides sont *biréfringents* et l'axe optique coïncide avec $\mathbf{n}$. Puisque les molécules sont souvent symétriques le long de l'axe (au sens qu'elles ne sont pas polaires), on ne distingue pas entre $\mathbf{n}$ et $-\mathbf{n}$ et donc on peut penser que le champ $\mathbf{n}$ prend plutôt des valeurs dans $\mathbb{R}P^2$. Un tel champ $\mathbf{n}$ est appelé *champ de directeurs* et il est à la base des modèles des cristaux liquides nématiques que nous regarderons par la suite [21].

L'état naturel d'un cristal liquide est $\nabla \mathbf{n} \equiv 0$, c'est-à-dire que les molécules sont toutes alignées dans la même direction. À cause d'inhomogénéités et impuretés du matériau (mélange avec d'autres substances ou particules immergées), d'autres influences extérieures (champs magnétiques, électriques, flux) ou la présence de bords [91], on observe $\nabla \mathbf{n} \not\equiv 0$ mais aussi l'apparition de structures de défauts. Schématiquement, un défaut est une singularité du champ $\mathbf{n}$, voir Figure 1.2, mais nous allons préciser dans les chapitres suivants ce que nous entendons par défaut, après avoir introduit le modèle que nous allons utiliser.

Cette thèse est consacrée à l'étude du cas où l'on considère une seule particule rigide immergée avec ancrage homéotropique en présence d'un champ magnétique externe homogène et constant. Dans ces conditions, il est possible d'observer l'effet dit "anneau de Saturne" : dans certaines circonstances, la structure de défauts qui se forme afin d'équilibrer les conditions imposées par l'objet immergé prend la forme d'un anneau autour de la particule, voir Figure 1.3. Des structures plus exotiques telles que des nœuds sont également possibles, nous renvoyons à [133] pour un aperçu. En plus des singularités de ligne (d'où le nom *nématique* du mot grèque $\nu\eta\mu\alpha$ ("fil")), on peut aussi observer différents types de singularités de point. Le cas le plus simple est appelé "dipôle", car il y a un seul point singulier qui compense la charge topologique de la particule. En outre, un champ électromagnétique peut être utilisé pour manipuler l'apparition d'un anneau de Saturne ou du dipôle et de passer d'une configuration à l'autre [12, 71–73, 112, 113, 165] .

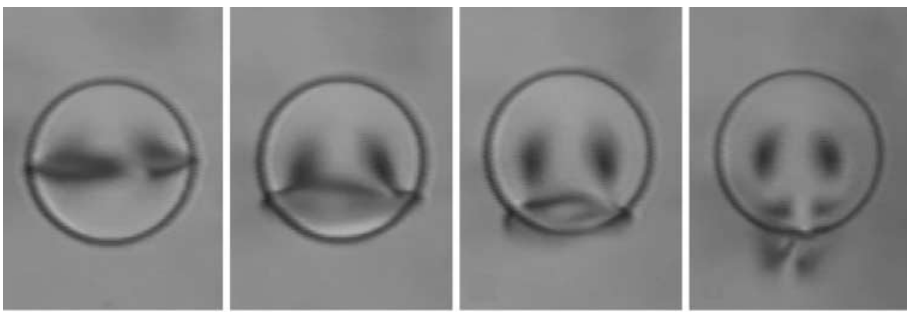

Figure 1.3: Changement d'une singularité de ligne ("anneau de Saturne") autour d'une particule sphérique à un défaut ponctuel sous l'influence d'un champ électrique, de [112, Fig. 1].

1.1.2 Le modèle de Landau-de Gennes

En raison des phénomènes intéressants qu'ils font apparaître et de leur importance considérable dans les applications, les cristaux liquides sont devenus une riche source de problèmes mathématiques à l'interface entre élasticité, géométrie, topologie et analyse. Certaines parties de ces études sont également intéressantes dans un cadre plus abstrait, par exemple les espaces fonctionnels [18] et les revêtements [88, 121], les $Q-$tenseurs [34, 132], la formation de singularités topologiques [157] ou des énergies similaires [49, 144], notamment le modèle de Ginzburg-Landau en micromagnétisme [30, 79, 92]. La source de ces liens provient de la diversité de modèles qui ont été proposés pour la modélisation de cristaux liquides [21]. Nous allons brièvement présenter les plus importants d'entre eux. Une introduction plus détaillée aux différents modèles peut être trouvée dans [20, 163].

D'un point de vue phénoménologique, une idée logique serait d'utiliser le champ de directeur $\mathbf{n} : \Omega \to \mathbb{S}^2$ comme objet central de l'étude. Ceci a été fait par le physicien suédois Carl Wilhelm Oseen [136] et le physicien anglais Frederick Charles Frank [70] qui ont développé une théorie variationnelle basée sur le champ de directeur $\mathbf{n}$ qu'on appelle aujourd'hui le modèle de *Oseen-Frank*. Bien que fructueux, ce modèle présente des problèmes d'orientabilité, car si $\mathbf{n} \in \mathbb{S}^2$, la symétrie $\mathbf{n} \leftrightarrow -\mathbf{n}$ n'est pas prise en compte. Cela conduit au problème suivant : seuls les défauts ponctuels entiers peuvent être représentés. Aucune ligne de défaut de demi-degré ne peut apparaître.

Une autre approche est de décrire la structure d'un cristal liquide par une distribution de probabilité ρ sur la sphère des directions. En tenant compte du fait que les points opposés ont la même probabilité, le premier moment d'une telle distribution ρ disparaît par symétrie. En décalant le second moment par une distribution uniforme, nous obtenons un tenseur Q symétrique sans trace ($Q-$tenseur)

$$Q \;=\; \int_{\mathbb{S}^2} \mathbf{n}(x) \otimes \mathbf{n}(\otimes)\, \mathrm{d}\rho(x) - \frac{1}{3}\mathrm{Id} \in \mathrm{Sym}_0 \;:=\; \{Q \in \mathbb{R}^{3\times 3} \;:\; Q^\top = Q\,,\; \mathrm{tr}(Q) = 0\}\,, \tag{1.1}$$

qui est utilisé pour modéliser ρ, même si de nombreuses informations sur ρ sont perdues dans ce processus. C'est la base même de ce que l'on appelle le modèle de *Landau-de Gennes*. Plus précisément, Pierre-Gilles de Gennes, physicien français, a utilisé la théorie du physicien soviétique Lev Landau pour décrire la transition de phase isotrope à nématique avec un paramètre d'ordre tensoriel pour obtenir le développement suivant de l'énergie libre au-dessus de la température de transition nématique-isotrope T_c [57, p.77]

$$f(Q) \;=\; C - \frac{a}{2}\mathrm{tr}(Q^2) - \frac{b}{3}\mathrm{tr}(Q^3) + \frac{c}{4}(\mathrm{tr}(Q^2))^2\,. \tag{1.2}$$

Nous remarquons que si $\rho = \frac{1}{2}(\delta_{\mathbf{n}} + \delta_{-\mathbf{n}})$ pour un $\mathbf{n} \in \mathbb{S}^2$, alors Q défini dans (1.1) est donné par $Q = (\mathbf{n} \otimes \mathbf{n} - \frac{1}{3}\mathrm{Id})$ ce qui donne un lien avec la théorie d'Oseen-Frank. Il est possible de montrer que si la constante C est bien choisie et $b, c > 0$, alors f est positive ou nulle et s'annule précisement sur des tenseurs Q de la forme $Q = s_*(\mathbf{n} \otimes \mathbf{n} - \frac{1}{3}\mathrm{Id})$, pour un $\mathbf{n} \in \mathbb{S}^2$ et un paramètre $s_* > 0$ qui dépend de a, b et c. De tels tenseurs Q sont appelés *uniaxiaux* et $\mathbf{n}$ est alors un vecteur propre de Q qui correspond à la plus grande valeur propre $\lambda_1(Q)$, les autres valeurs propres $\lambda_2(Q) = \lambda_3(Q) < 0$ étant égales et négatives. Afin de définir l'ensemble singulier dans la suite, nous introduisons également l'ensemble des $Q-$tenseurs $\mathcal{C}$ pour lesquels les deux valeurs propres principales sont égales, c'est-à-dire $\mathcal{C} = \{Q \in \mathrm{Sym}_0 \;:\; \lambda_1(Q) = \lambda_2(Q)\}$. Par ailleurs, pour intégrer des forces élastiques, on ajoute à la densité d'énergie

$$f_{\mathrm{el}}(Q) = \frac{L_1}{2}\sum_{i,j,k=1}^{3} \partial_k Q_{ij}\partial_k Q_{ij} \;+\; \frac{L_2}{2}\sum_{i,j,k=1}^{3} \partial_i Q_{ik}\partial_j Q_{jk} \;+\; \frac{L_3}{2}\sum_{i,j,k=1}^{3} \partial_i Q_{jk}\partial_i Q_{jk}\,. \tag{1.3}$$

Dans cette thèse nous nous restreindrons au cas le plus simple ("one constant approximation"), pour lequel $L_1 = L > 0$ et $L_2 = L_3 = 0$. Enfin, on peut inclure les effets d'un champ magnétique externe $\mathbf{H}$ via [139, Ch. 6, Secs. 3-4 et Ch. 10, Sec. 2.3]

$$f_{\mathrm{mag}}(Q) = -\frac{1}{2}\chi_a \mathbf{H} \otimes \mathbf{H} : Q\,, \tag{1.4}$$

où χ_a est l'anisotropie magnétique. Cela favorise que le vecteur propre principal soit dans la direction $\pm\mathbf{e}_3$. Intégrées sur un domaine Ω, (1.2),(1.3) et (1.4) donnent l'énergie

$$\mathcal{E}(Q) \;=\; \int_\Omega \frac{L}{2}|\nabla Q|^2 + C_0 - \frac{a}{2}\mathrm{tr}(Q^2) - \frac{b}{3}\mathrm{tr}(Q^3) + \frac{c}{4}(\mathrm{tr}(Q^2))^2 - \frac{1}{2}\chi_a \mathbf{H}\otimes\mathbf{H} : Q \,\mathrm{d}x\,. \tag{1.5}$$

Des théories dynamiques qui prennent en compte les écoulements de cristaux liquides ont également été développées : le mathématicien américain Jerald Ericksen [61, 62] et le physicien mathématicien écossais Frank Matthews Leslie [107] ont créé une approche basée sur la représentation avec un champ de directeurs, tandis que les chimistes américains Antony Beris et Brian Edwards ont fondé leur modèle sur les $Q-$tenseurs [26].

Enfin, des efforts considérables ont été déployés pour élaborer des théories statistiques sur les cristaux liquides. Les plus connues sont celles de Lars Onsager, physico-chimiste américain d'origine norvégienne [135] dont le modèle repose sur des forces d'ordre purement entropiques basées sur la répulsion à courte portée des molécules, et celui des physiciens allemands Wilhelm Maier et Alfred Saupe qui ont developpé une théorie du champ moyen fondée sur les forces de dispersion de London attractives [118].

En général, il est difficile de donner une description précise des minimiseurs des fonctionnelles d'énergie associées à l'un des modèles de manière explicite, sauf dans certains cas très particuliers comme dans [169] ou pour la solution appelée "hérisson" [120].

1.2 Le cas d'une inclusion sphérique

Le premier résultat de cette thèse concerne la forme des configurations minimisantes autour d'une particule sphérique. Avant de présenter le résultat, nous allons adimensionner l'énergie dans (1.5). Pour cela, notons r_0 le rayon de la particule sphérique et $\Omega_{r_0} = \mathbb{R}^3 \setminus \overline{B_{r_0}(0)}$ la région de l'espace occupée par le cristal liquide. En changeant l'échelle $x \rightsquigarrow r_0 x$, il est possible de travailler sur le domaine fixe $\Omega := \mathbb{R}^3 \setminus \overline{B_1(0)}$. Après division par Lr_0, on retrouve une version adimensionnée de l'énergie (1.5) qui s'écrit

$$\mathcal{E}_{\eta,\xi}(Q) \;=\; \int_\Omega \frac{1}{2}|\nabla Q|^2 + \frac{1}{\xi^2} f(Q) + \frac{1}{\eta^2} g(Q) + C_0 \,\mathrm{d}x\,. \tag{1.6}$$

Le paramètre sans dimension $\eta = \sqrt{\frac{L}{2\chi_a r_0^2 h^2}}$ décrit le rapport entre la densité d'énergie magnétique et celles des énergies élastique et volumique. De la même manière, $\xi = \sqrt{\frac{L}{cr_0^2}}$ est également sans dimension et déterminé par le ratio entre les densités des énergies élastique et volumique.

La fonction f est encore de la forme (1.2), mais avec différents paramètres a, b, c et C qui n'ont en particulier plus de dimension. Venant de (1.5), la fonction g est donnée par $g(Q) = Q_{33}$, mais d'un point de vue mathématique, d'autres fonctions g pourraient être utilisées sans modifier l'analyse. Nous avons également ajouté la constante C_0 qui dépend de ξ et η pour rendre la densité d'énergie positive ou nulle.

Nous nous focalisons sur des régimes asymptotiques pour lesquels ξ, η et C_0 tendent vers 0 d'une façon qui sera précisée par la suite.

Pour compléter notre modèle, nous imposons une condition au bord d'ancrage fort sur $\partial\Omega$ qui s'écrit

$$Q(x) \;=\; s_*\left(\nu(x)\otimes\nu(x) - \frac{1}{3}\mathrm{Id}\right) \quad \text{pour tout } x \in \partial\Omega\,, \tag{1.7}$$

où ν est la normale sortante de $\partial\Omega$ et correspond à un champ directeur radial $\mathbf{n} = \mathbf{e}_r$.

Selon le modèle de Landau-de Gennes, une configuration d'équilibre est trouvée par la minimisation de l'énergie libre (1.6) avec la condition au bord (1.7).

Il est possible d'envisager différents régimes concernant la vitesse de convergence relative des deux paramètres ξ et η tendant vers 0. Un premier régime a été traité dans [4] où les auteurs observent un anneau de Saturne. Cela correspond au cas des champs forts où $\eta|\ln(\xi)| \ll 1$. Le cas $\eta|\ln(\xi)| \sim 1$, où la transition entre le dipôle et l'anneau de Saturne a lieu, est le cadre de cette thèse et il nous permet également de raisonner sur ce qui se passe si $\eta|\ln(\xi)| \gg 1$ où nous nous attendons uniquement à des configurations de dipôle.

Le resultat principal de cette partie de la thèse est le Théorème 2.3.1 qui montre dans l'esprit de la $\Gamma-$convergence que dans la limite $\eta, \xi \to 0$ dans le régime où $\eta|\ln(\xi)| \to \beta \in (0, \infty)$, l'énergie se réduit à une énergie $\mathcal{E}_0$ énoncée à la surface de la sphère $\mathbb{S}^2 = \partial\Omega$ donnée par

$$\mathcal{E}_0(F) = 2s_*c_* \int_F (1 - \cos(\theta))\, \mathrm{d}\omega + 2s_*c_* \int_{F^c} (1 + \cos(\theta))\, \mathrm{d}\omega + \frac{\pi}{2} s_*^2 \beta |D\chi_F|(\mathbb{S}^2)\,, \tag{1.8}$$

où $s_*, c_* > 0$ sont des paramètres en fonction de f et g, $F \subset \mathbb{S}^2$ est un ensemble de périmètre fini, F^c est le complément de F dans $\mathbb{S}^2$ et $|D\chi_F|(\mathbb{S}^2)$ désigne le périmètre de F. Dans l'expression ci-dessus, θ représente l'angle entre la normale sortante à un point ω sur la sphère (voir la condition au bord) et $\mathbf{e}_3$ (la direction du champ externe). Le rapport entre $\mathcal{E}_{\eta,\xi}(Q_{\eta,\xi})$ et $\mathcal{E}_0(F)$ se présente comme suit : si $Q_{\eta,\xi} : \Omega \to \mathrm{Sym}_0$ est une suite bornée en énergie qui vérifie les conditions au bord (1.7), alors on trouve un champ de directeur $\mathbf{n}_{\eta,\xi} : \Omega \to \mathbb{S}^2$ qui est proche d'un revêtement de $Q_{\eta,\xi}$ (qui n'existe pas partout dans Ω pour des raisons topologiques). En choisissant une orientation de $\mathbf{n}_{\eta,\xi}$ à l'infini, il est possible d'identifier des régions sur $\partial\Omega$ où $\mathbf{n}_{\eta,\xi}$ s'aligne avec la normale sortante de ∂B_1 (ce qui donne une approximation de F) où avec la normale entrante (approximation de F^c).

Nous interprétons le terme de périmètre dans (1.8) comme la représentation d'une singularité de ligne. Il nous indique que le passage d'une orientation à l'autre a un coût, qui dépend de la longueur de la ligne de défaut et de l'équilibre entre les forces modélisées par β, s_* qui est lié aux propriétés du cristal liquide et c_* qui dépend de l'interaction entre le champ magnétique et le cristal liquide.

Cette étude est réalisée sous l'hypothèse d'une équivariance rotationnelle, c'est-à-dire qu'on peut se restreindre à un problème posé sur un domaine bidimensionnel $\Omega' = \{(\rho, z) \ : \ \rho^2 = x^2 + y^2,\ (x, y, z) \in \Omega\}$ qui représente une tranche de Ω. Ceci est une simplification majeure pour l'analyse puisqu'au lieu de singularités de ligne, nous devons seulement considérer leur intersection avec la tranche, c'est-à-dire des points. Mais d'un autre côté, cela restreint les configurations admissibles pour Q et F à une classe beaucoup plus petite. Le cas général traité dans la section suivante abandonnera donc cette hypothèse.

La preuve du théorème est divisée en deux parties principales : $\Gamma-$liminf et $\Gamma-$limsup. Une estimation du type $\Gamma-$liminf signifie que pour toute suite $Q_{\eta,\xi}$, il existe un ensemble $F \subset \mathbb{S}^2$ tel que l'on trouve un champ $\mathbf{n}_{\eta,\xi}$ comme décrit ci-dessus qui fait le lien entre $Q_{\eta,\xi}$ et F et que la liminf de $\mathcal{E}_{\eta,\xi}(Q_{\eta,\xi})$ majore $\mathcal{E}_0(F)$. Pour montrer cela, l'idée principale sera de remplacer les fonctions $Q_{\eta,\xi}$ par les minimiseurs d'un problème d'approximation et ensuite d'utiliser la régularité améliorée de ces minimiseurs pour dériver une borne inférieure sur le coût énergétique d'une singularité. Après, nous montrons d'abord que si l'énergie est uniformément bornée, alors il existe seulement un nombre fini de singularités, pour ensuite calculer la limite inférieure asymptotiquement exacte pour l'énergie près d'une singularité. Ceci est l'étape principale pour justifier le terme du périmètre dans (1.8). Pour les deux termes surfaciques, nous introduisons un problème auxiliaire radial comme dans [4]. Étant donné un rayon partant de la surface $\partial\Omega$ vers l'infini tel que $Q_{\eta,\xi}$ est proche d'être uniaxial, nous pouvons remplacer $Q_{\eta,\xi}$ par $\mathbf{n}_{\eta,\xi}$ qui est proche de $Q_{\eta,\xi}$. On peut calculer explicitement l'énergie nécessaire pour le champ de vecteurs $\mathbf{n}_{\eta,\xi}$ pour tourner le long du rayon partant de $\mathbf{n}_{\eta,\xi}(x) = x$ sur le bord de Ω à la configuration parallèle au champ externe dans la direction $\pm\mathbf{e}_3$ à l'infini qui est favorisée par l'énergie. En combinant les résultats, nous sommes capables de prouver la partie de la borne inférieure du théorème principal.

La partie $\Gamma-$limsup se résume à construire une suite de fonctions $Q_{\eta,\xi}$ pour un $F \subset \mathbb{S}^2$ donné tel que la limsup de $\mathcal{E}_{\eta,\xi}(Q_{\eta,\xi})$ minore $\mathcal{E}_0(F)$ et qui vérifie le lien entre $Q_{\eta,\xi}$ et F décrit auparavant (il s'agit de l'étape appelée "recovery sequence" dans la littérature). Nous utilisons nos connaissances sur l'interaction des trois parties de l'énergie pour définir des régions approximatives proches de la particule dans lesquelles l'énergie des deux premiers termes de $\mathcal{E}_0$ est concentrée et Q est uniaxial.

Nous profitons ici de l'expression exacte du profil optimal issu du problème auxiliaire radial. En dehors de ces régions, nous construisons les singularités qui donnent lieu au terme de périmètre de $\mathcal{E}_0$. Entre les deux, nous utilisons un argument d'interpolation pour relier les deux régions.

Avec l'énergie limite que nous obtenons, il est possible de calculer explicitement les minimiseurs (en fonction de β) et de comparer leur énergie avec celle d'un dipôle et d'un anneau de Saturne à la même valeur de β. Intuitivement, on pourrait s'attendre à ce que les configurations minimisantes changent graduellement d'un anneau de Saturne à l'équateur en passant par des configurations d'anneau à des angles intermédiaires pour finalement se rapprocher d'une singularité de point à l'un des deux pôles de la particule sphérique. Contrairement à cette intuition, les seuls minimieurs locaux sont l'anneau de Saturne à l'équateur et le dipôle. Puisque les anneaux intermédiaires ont une plus grande énergie, il n'est pas favorable de passer d'une configuration localement minimisante à une configuration globalement minimisante tant que β ne prend pas des valeurs extrêmes où le minimum local perd sa stabilité. En conséquence, nous constatons qu'en faisant varier β, un phénomène d'hystérésis se produit. Même si, à notre connaissance, ce phénomène d'hystérésis n'a pas encore été observé dans une expérience physique, nos résultats expliquent rigoureusement les simulations numériques et les raisonnements physiques connus dans [105, 154].

1.3 Le cas d'une inclusion générale

Même si la majorité des expériences physiques sont réalisées avec des particules colloïdales sphériques, on s'intéresse de plus en plus à l'utilisation d'autres formes, par exemple des particules en forme de tore [147], de cube [156], de cacahuète [143], de fer à cheval [15] ou même de fractale [133]. D'un point de vue purement mathématique, il est également intéressant d'étudier le cas des particules non sphériques et particulièrement non convexes, comme nous le verrons dans la suite, car nous généraliserons le résultat évoqué dans la section précédente et la structure des défauts deviendra beaucoup plus riche mais aussi plus compliquée. En même temps, nous supprimons également l'hypothèse d'équivariance rotationnelle, ce qui donne une preuve tridimensionnelle sans l'hypothèse de symétrie du résultat précédent pour la sphère. Pour les raisons susmentionnées, nous aurons besoin d'outils techniques plus avancés, notamment du vocabulaire et des résultats de la théorie géométrique de la mesure.

L'interaction entre les problèmes variationnels et la géométrie existe depuis longtemps. Parmi les problèmes à motivation géométrique les plus connus, on trouve celui de la courbe brachistochrone [27, 137], le principe de Fermat en optique [31], la science des matériaux [19] et la relativité générale [85, 122]. Un problème particulièrement important se pose lorsque la taille des objets géométriques eux-mêmes doit être minimisée, ce qui conduit à ce que l'on appelle des *surfaces minimales* [103]. Un exemple classique est le film de savon bidimensionnel s'étendant entre des courbes limites prédéfinies et fixés, appelé problème de Plateau [59, 140, 155].

Un cadre général pour résoudre cette question et d'autres questions connexes est appelé théorie de la mesure géométrique et l'un de ses objets fondamentaux sont les chaînes bémol ("flat chains") [65, 131]. L'énoncé de notre théorème principal faisant intervenir des chaînes bémol, nous allons donc donner un rapide aperçu des notions les plus importantes. Nous introduisons d'abord l'ensemble $\mathcal{P}^k$ des chaînes bémol polyhédrales avec des coefficients dans $\mathbb{Z}_2$ de dimension k dans $\mathbb{R}^3$. C'est l'ensemble des sommes formelles de polyèdres compacts, convexes et orientés de dimension k dans $\mathbb{R}^3$ avec des coefficients dans le groupe $\mathbb{Z}_2$. Avec l'addition naturelle et l'identification d'un polyèdre qui résultent du collage d'une face commune avec la somme des polyèdres individuels, l'ensemble forme un groupe. Notez que pour un groupe de coefficients général G, il faut également prendre en compte les orientations des polyèdres, ce qui n'est pas nécessaire pour notre cas simple de coefficients qui appartiennent à $\mathbb{Z}_2$. Un élément $P \in \mathcal{P}^k$ peut donc être écrit comme la somme

$$P \;=\; \sum_{i=1}^{p} 1_{\mathbb{Z}_2}\, \sigma_i\,, \tag{1.9}$$

où les σ_i sont des polyèdres compacts, convexes et orientés qui peuvent être choisis pour ne pas se superposer. Le *bord* $\partial\sigma$ d'un polyèdre σ est la somme formelle des faces polyédriques

$(k-1)-$dimensionnelles de σ avec l'orientation induite et le coefficient 1 sous les identifications mentionnées ci-dessus. Notons que $\partial(\partial\sigma) = 0$. Nous pouvons étendre linéairement cet opérateur à un opérateur de bord $\partial : \mathcal{P}^k \to \mathcal{P}^{k-1}$. Pour une chaîne polyédrale $P \in \mathcal{P}^k$ écrite comme dans (1.9), nous définissons la *masse* $\mathbb{M}(P) = \sum_{i=1}^{p} \mathcal{H}^k(\sigma_i)$ et la *norme bémol* $\mathbb{F}(P)$ par l'infimum de $\mathbb{M}(Q) + \mathbb{M}(R)$ parmi les $Q \in \mathcal{P}^{k+1}$ et $R \in \mathcal{P}^k$ vérifient $P = \partial Q + R$. L'espace des *chaînes bémol* $\mathcal{F}^k$ est alors défini comme étant la complétion de $\mathcal{P}^k$ par rapport à la norme $\mathbb{F}$. L'opérateur limite ∂ s'étend à un opérateur continu $\partial : \mathcal{F}^k \to \mathcal{F}^{k-1}$ et nous désignons toujours par $\mathbb{M}$ la plus grande extension semi-continue inférieure de la masse qui a été définie sur $\mathcal{P}^k$. De plus, pour tout $A \in \mathcal{F}^k$,

$$\mathbb{F}(A) \;=\; \inf\{\mathbb{M}(Q) + \mathbb{M}(R) \;:\; A = \partial Q + R\,, Q \in \mathcal{F}^{k+1}\,, R \in \mathcal{F}^k\}\,.$$

Comme nous l'avons noté lors de la présentation du modèle de Landau-de Gennes, f est minimisé par des $Q-$tenseurs uniaxiaux $Q \in \mathcal{N}$ dont le vecteur propre correspondant à la valeur propre dominante $\mathbf{n}$ est $\pm\mathbf{e}_3$ et donc la région dans laquelle Q est proche de ce $Q-$tenseur ne portera presque pas d'énergie. En cherchant un ensemble où l'énergie se concentrera, on peut considérer l'ensemble $\{\mathbf{n}_3 = 0\}$. Plus précisément, nous définissons $\mathcal{T}$ comme le sous-ensemble de Sym_0 tel que, pour $Q \in \mathcal{T}$, la plus grande valeur propre $\lambda_1(Q)$ de Q est strictement plus grande que la deuxième plus grande et telle que le vecteur propre $\mathbf{n}$ correspondant à $\lambda_1(Q)$ a une troisième composante nulle $\mathbf{n}_3 = 0$.

Avec ces notations, notre théorème principal peut être résumé comme suit : soit $E \subset \mathbb{R}^3$ un ensemble (la particule solide) avec un bord $\mathcal{M} := \partial E$ de classe $C^{1,1}$ et posons la condition au bord (1.7) où ν est la normale sortante de ∂E. Soit $\Gamma := \{\omega \in \mathcal{M} \;:\; \nu_3(\omega) = 0\}$ une (union de) courbe de classe C^2. Si de plus $\eta|\ln(\xi)| \to \beta \in (0,\infty)$ lorsque $\eta, \xi \to 0$, alors $\eta\,\mathcal{E}_{\eta,\xi} \to \mathcal{E}_0$ dans un sens variationnel pour l'énergie limite $\mathcal{E}_0$ donnée par

$$\mathcal{E}_0(T,S) \;=\; 2s_*c_*E_0(\mathcal{M},\mathbf{e}_3) + 4s_*c_*\int_{\mathcal{M}} |\cos(\theta)|\,\mathrm{d}\mu_{T\llcorner\Omega} + 4s_*c_*\mathbb{M}(T\llcorner\Omega) + \frac{\pi}{2}s_*^2\beta\mathbb{M}(S)\,, \quad (1.10)$$

où $T \in \mathcal{F}^2, S \in \mathcal{F}^1$ sont des chaînes bémol dans $\overline{\Omega}$ avec $\partial T = S + \Gamma$ et

$$E_0(\mathcal{M},\mathbf{e}_3) := \int_{\{\nu_3>0\}} (1-\cos(\theta))\,\mathrm{d}\omega + \int_{\{\nu_3\le 0\}} (1+\cos(\theta))\,\mathrm{d}\omega\,.$$

La convergence variationnelle doit être comprise de la manière suivante : quitte à régulariser $Q_{\eta,\xi}$ et ajouter une petite perturbation (qui disparaît dans la limite), on trouve des chaînes bémol $T_{\eta,\xi}$ et $S_{\eta,\xi}$ comme préimages de $\mathcal{T}$ et $\mathcal{C}$ qui convergent localement vers des chaînes bémol T et S pour la norme $\mathbb{F}$ et $\partial T = S + \Gamma$. Pour des T et S construits de cette manière, on a l'estimation de type $\Gamma-$liminf

$$\liminf_{\eta\to 0} \eta\,\mathcal{E}_{\eta,\xi}(Q_{\eta,\xi}) \ge \mathcal{E}_0(T,S)\,.$$

Réciproquement, pour toutes chaînes bémol T, S tel que $\partial T = S + \Gamma$, on peut construire une suite $Q_{\eta,\xi}$ qui vérifie la convergence variationnelle décrite en haut vers T, S et telle que

$$\limsup_{\eta\to 0} \eta\,\mathcal{E}_{\eta,\xi}(Q_{\eta,\xi}) \le \mathcal{E}_0(T,S)\,.$$

Avant de donner quelques éléments de preuve, nous allons d'abord expliquer le lien entre l'énergie (1.10) pour des particules convexes et celle du cas de l'inclusion sphérique (1.8). Notons d'abord que si la particule E est convexe, alors on peut projeter T et S sur $\mathcal{M}$, ceci diminuant l'énergie et on obtient $\mathbb{M}(T\llcorner\Omega) = 0$. De plus, il est possible d'écrire $\mu_{T\llcorner\mathcal{M}} = \chi_G\mathcal{H}^2\llcorner\mathcal{M}$ pour un ensemble mesurable $G \subset \mathcal{M}$ et donc on peut definir

$$F = \{\omega \in \mathcal{M}\setminus G \;:\; \nu(\omega)\cdot\mathbf{e}_3 > 0\} \cup \{\omega \in \mathcal{M}\cap G \;:\; \nu(\omega)\cdot\mathbf{e}_3 \le 0\}\,.$$

L'énergie (1.10) devient donc

$$\mathcal{E}_0(T,S) \;=\; 2s_*c_*\int_F (1-\cos(\theta))\,\mathrm{d}\omega + 2s_*c_*\int_{\mathcal{M}\setminus F} (1+\cos(\theta))\,\mathrm{d}\omega \;+\; \frac{\pi}{2}s_*^2\beta\mathbb{M}(S) \;=\; \mathcal{E}_0(F)\,,$$

car on peut exprimer $\partial F = \partial T + \Gamma = S$. Dans ce sens, l'énergie (1.10) est une généralisation de $\mathcal{E}_0$ définie en (1.8).

La première étape pour démontrer la partie $\Gamma-$liminf est de régulariser la suite $Q_{\eta,\xi}$ et de prouver que les deux suites sont proches en énergie. Si on admet que $Q_{\eta,\xi}$ est suffisamment régulier, par exemple comme minimiseur de $\mathcal{E}_{\eta,\xi}$, cette étape n'est pas nécessaire. Ensuite on utilise le théorème de transversalité de Thom pour définir les chaînes bémol $T_{\eta,\xi} := (Q_{\eta,\xi} - Y_{\eta,\xi})^{-1}(\mathcal{T})$ et $S_{\eta,\xi} := (Q_{\eta,\xi} - Y_{\eta,\xi})^{-1}(\mathcal{C})$ pour une petite perturbation $Y_{\eta,\xi} \in \mathrm{Sym}_0$. Les propriétés de $S_{\eta,\xi}$ ont été étudiées dans [43, 44] et nous nous en servons. Notamment, $S_{\eta,\xi}$ est une ligne de longueur contrôlée par l'énergie. Avec un argument classique du type Modica et Mortola [127], nous démontrons ensuite que $T_{\eta,\xi}$ est une surface de masse finie si $Q_{\eta,\xi}$ est proche d'un tenseur uniaxial. La partie la plus délicate est d'estimer la taille de $T_{\eta,\xi}$ proche de son bord. Autour de S dans Ω, nous utilisons une construction inspirée par le théorème de déformation pour remplacer un morceau de $T_{\eta,\xi}$ par des parties de facettes de cubes dont nous contrôlons l'aire surfacique tout en gardant la propriété que le bord de $T_{\eta,\xi}$ coincide avec $S_{\eta,\xi}$ dans cette zone. Une procédure de blow-up donne ensuite l'estimation précise de l'énergie venant de $T_{\eta,\xi}$. Après avoir obtenu une borne uniforme sur la masse de $T_{\eta,\xi}$ et $S_{\eta,\xi}$, la convergence par rapport à la norme $\mathbb{F}$ est une conséquence du théorème de compacité pour les chaînes bémol.

La construction de $Q_{\eta,\xi}$ pour l'inégalité du $\Gamma-$limsup procède en deux étapes. Premièrment, nous montrons que n'importe quelle chaîne bémol T d'énergie $\mathcal{E}_0(T) < \infty$ peut être approchée dans la norme $\mathbb{F}$ par une chaîne bémol qui est plus régulière. Pour cela, nous prenons un minimiseur T_n de la fonctionnelle $\tilde{T} \mapsto \mathcal{E}_0(\tilde{T}) + n\mathbb{F}(T - \tilde{T})$. En utilisant des idées de la théorie de régularité pour les surfaces minimales, il est possible de montrer que T_n a des propriétés bien meilleures que T qui nous serviront dans la suite. Deuxièmement, nous définissons la suite $Q_{\eta,\xi,n}$ en fonction de la distance et les vecteurs normaux et tangents de T_n et ∂T_n en utilisant les profils déjà utilisés dans le cas sphérique. Avec un argument diagonal, on obtient une suite $Q_{\eta,\xi}$ qui vérifie l'inégalité de $\Gamma-$limsup.

La dernière partie du chapitre est consacrée à la question de la régularité et des conditions d'optimalité. Un premier résultat de régularité a déjà été montré pour la borne supérieure et, en appliquant [130], il devient clair que les minimiseurs sont même lisses dans Ω. Les conditions d'optimalité peuvent être déduites simplement comme dans le cas des surfaces minimales ou des forces capillaires.

1.4 Résolution numérique du problème limite

Dans le cas d'une inclusion sphérique, nous avons pu déterminer analytiquement les minimiseurs du problème limite. Comme le problème de trouver des minimiseurs de $\mathcal{E}_0$ pour une inclusion générale semble inabordable, la question d'une approximation numérique de ces minimiseurs se pose naturellement.

La simplification principale consiste à remplacer les chaînes bémol à valeurs dans $\mathbb{Z}_2$ par des courants à valeurs dans $\mathbb{R}$. On utilisera une représentation de T via un champ de vecteurs qui peut être vu comme le champ de normale de T et son bord par le rotationnel de u pointant dans la direction tangentielle à ∂T. La masse de T (resp. ∂T) et ainsi représentée par la norme L^1 de u (resp. $\mathrm{curl}(u)$). D'un point de vue numérique, nous discrétisons la particule par une triangulation en utilisant un maillage adapté. L'intérieur de la particule est enlevé et une couche limite $\mathcal{M}_h$ remplace la surface $\mathcal{M}$. Nous choisissons d'approcher la fonction u par u_h appartenant à l'espace des éléments finis de Nédélec en notant que $\mathrm{curl}(u_h) \in \mathbb{P}^0$. La courbe Γ est également approchée par un champ de vecteurs tangentiels, construit comme rotationnel d'une fonction u_0. La surface de T s'écrit ainsi $\mathbb{M}(T) = \|u_h\|_{L^1}$ et la longueur de S est donnée par $\mathbb{M}(S) = \|\mathrm{curl}(u_h)\|_{L^1}$. Pour la minimisation nous utilisons *l'algorithme des directions alternées* (ADA, ou ADMM en anglais) pour lequel notre problème est le suivant :

$$\min_{\substack{p,q\in\mathbb{P}^0,\\ u\in\mathrm{Ned}}} \|p_{\max} p\|_{L^1} + \|q_{\max} q\|_{L^1}, \tag{1.11}$$

sous la contrainte que

$$\begin{pmatrix} 1 \\ \mathrm{curl} \end{pmatrix} u \; + \; \begin{pmatrix} -1 & 0 \\ 0 & -1 \end{pmatrix} \begin{pmatrix} p \\ q \end{pmatrix} \; = \; \begin{pmatrix} 0 \\ \mathrm{curl}(u_0) \end{pmatrix}.$$

Les fonctions $p_{\max}, q_{\max}$ sont choisies pour prendre en compte la particule et la couche limite, c'est-à-dire $p_{\max}$ et $q_{\max}$ sont grandes à l'intérieur de la particule pour ne pas créer de T ni de S dans cette zone, en dehors $q_{\max} = \beta_h$ et $p_{\max} = 1$, à l'exception de $\mathcal{M}_h$ où on pose $p_{\max} = |\nu_3|$, ν étant une extension de la normale de $\mathcal{M}$.

Nous avons fait le choix d'étudier les trois formes représentées dans la Figure 1.4 :

1. une *sphère* qui est la particule la plus utilisée dans la littérature des colloïdes et pour laquelle on possède des résultats analytiques concernant les configurations minimisantes et le comportement de l'énergie. Ce cas peut donc nous servir comme cas de validation pour notre algorithme;
2. une particule sous forme de *cacahuète* avec une symétrie radiale autour d'un axe qui donc permet d'étudier l'influence sur les singularités venant de l'orientation de la particule par rapport au champ externe;
3. une particule de type *croissant* qui sert comme exemple que la ligne S et la surface T peuvent se détacher de $\mathcal{M}$ sous des conditions appropriées. De plus, cette forme peut être vue comme une simple version d'un fer à cheval considerée dans la littérature [15] grâce à ces applications potentielles.

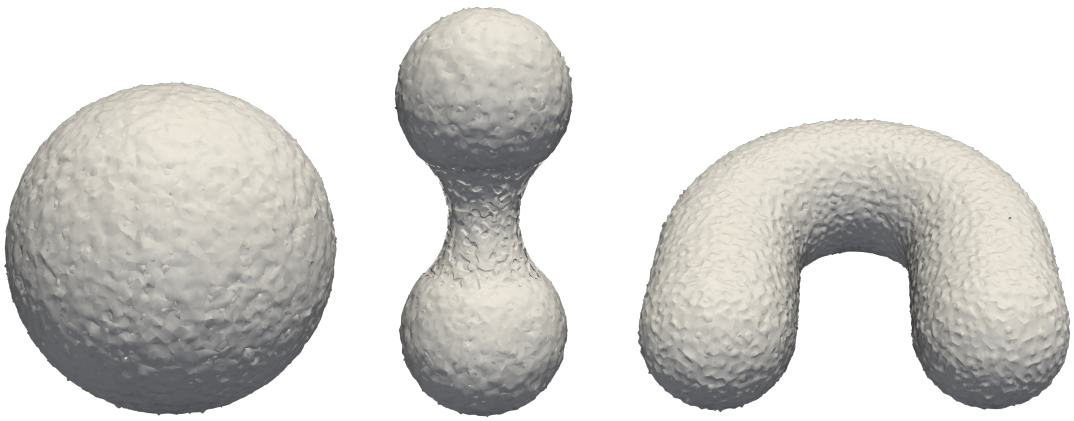

Figure 1.4: Les inclusions considérées dans les simulations numériques : sphère, cacahuète et croissant (de gauche à droite).

Avec les simulations autour de la sphère, on confirme les résultats obtenus théoriquement. On trouve que les seules configurations minimisantes sont l'anneau de Saturne à l'équateur et le dipôle, voir Figure (1.5a),(1.5d). On retrouve aussi la croissance linéaire de l'énergie E_h en fonction de β_h dans le cas de l'anneau de Saturne, et l'énergie constante pour le dipole.

Pour la cacahuète nous observons une plus grande variété de structures de défauts, en fonction de β_h et l'angle ϕ entre l'axe de symétrie de la particule et le champ extérieur $\mathbf{H}$. Lorsque ϕ est petit, la ligne Γ est composée de trois composantes et donc pour β_h petit on y trouve trois anneaux de Saturne (Figure 1.5 (b)). Pour β_h plus grand, on observe encore un anneau tandis que les deux autres anneaux ont été remplacés par la surface T joignant les deux composantes de Γ sur $\mathcal{M}$ (Figure 1.5 (e)). Si β_h devient encore plus grand, on retrouve un dipôle créé par deux morceaux de T collés à la surface $\mathcal{M}$ (Figure 1.5 (g)). Si ϕ est proche de $\frac{\pi}{2}$, la situation est comparable à celle de la sphère. Il n'y a que deux états que l'on observe : l'anneau de Saturne représenté par la

ligne S à l'équateur (pour β_h petit), et le dipole représenté par T couvrant la moitié de la surface de la cacahuète (pour β_h grand). Pour β_h donné, on trouve que l'angle pour lequel l'énergie est minimale est proche de $\phi = \frac{\pi}{2}$ (pour β_h petit) ou proche de $\phi = 0$ (pour β_h grand).

Enfin, nous donnons un aperçu des structures qu'il est possible d'observer pour le croissant. En plus des structures déjà observées dans les cas précédents, le croissant nous permet de voir numériquement qu'il existe des situations où il est énergétiquement favorable que la surface T se détache de $\mathcal{M}$. Notamment, la Figure 1.5 (h) montre un T qui s'est formé dans Ω, avec un bord qui est formé d'une partie de Γ et une autre partie de $S \llcorner \Omega$.

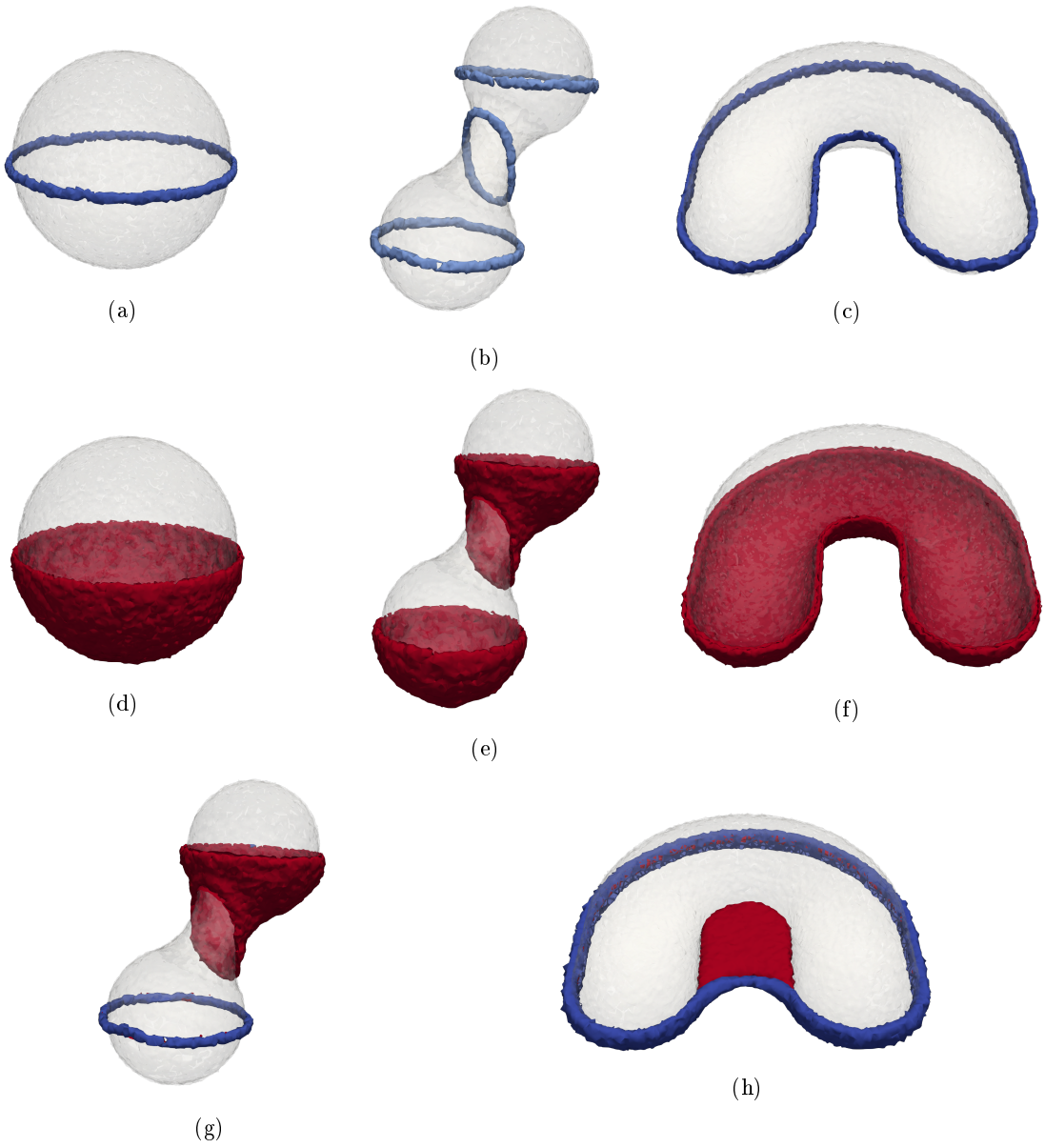

Figure 1.5: Minimiseurs de l'énergie $\mathcal{E}_0$ pour différentes valeurs de β_h et differentes inclusions. On trouve des configurations du type anneau de Saturne (a)-(c), du type dipôle (d)-(f) ainsi que des configurations intermédiaires (g)-(h).

1.5 Conclusion et perspectives

Pour résumer, l'objectif de cette thèse est d'étudier mathématiquement l'interaction complexe entre un cristal liquide nématique, une particule immergée et un champ magnétique externe appliqué. Dans le cas d'une seule particule sphérique, nous avons dérivé une énergie effective posée à la surface de la particule qui peut décrire et expliquer les différentes structures de défauts ainsi que les transitions entre elles. Nous avons vu comment ce modèle peut être généralisé pour décrire également les singularités autour d'une particule quelconque (régulière). Nous avons implémenté un algorithme numérique qui nous permet de calculer la forme et l'énergie des configurations globalement minimisantes, nous aidant à comprendre quelles formes nous observons dans la réalité pour des géométries compliquées.

Bien entendu, il ne s'agit que d'une première étape dans la compréhension des colloïdes dans les cristaux liquides ce qui ouvrirait la voie à la manipulation des propriétés des cristaux liquides eux-mêmes et à l'assemblage de microstructures dans un milieu de cristaux liquides. Plusieurs orientations futures pourraient être envisagées à partir de là :

1. Comme nous nous intéressons aux colloïdes, une question naturelle serait de savoir s'il est possible de décrire des assemblages de plusieurs particules dans le même cadre que celui que nous avons utilisé dans cette thèse. Il est connu que si les particules sont suffisamment proches, des lignes de singularité peuvent se former de manière à enchevêtrer plusieurs d'entre elles et à former des chaînes ou des couches. De plus, la topologie de ces lignes devient intéressante car dans les expériences, on observe des nœuds et des liens, contrairement aux anneaux de Saturne de topologie triviale que nous avons décrits dans ce travail.

2. D'un point de vue théorique, il serait aussi souhaitable de dériver un modèle d'ordre supérieur. En effet, alors que dans la réalité l'anneau de Saturne reste à une certaine distance de la particule, dans notre modèle il est, la plupart du temps, confiné à la surface de la particule. Une énergie incluant des termes d'ordre linéaire dans η pourrait être en mesure de fournir des estimations sur la distance du défaut par rapport à la surface.

3. L'algorithme numérique que nous proposons ici doit être étudié et amélioré. Pour être justifié, la preuve d'un résultat de consistance générale est nécessaire en plus des arguments que nous donnons ici. Il serait également intéressant de prouver la convergence de notre méthode et d'obtenir des estimations sur le taux de convergence.

4. Dans le cadre de la modélisation des cristaux liquides, on pourrait également analyser comment nos résultats dépendent du modèle de Landau-de Gennes que nous avons choisi d'étudier. On pourrait essayer de prouver des résultats analogues pour différents potentiels f, en allant au-delà de l'approximation à une constante, en faisant varier la température ou en considérant un champ externe non homogène. Comme nous nous intéressons à la transition entre les singularités, on peut aussi se demander si l'on peut dériver une version dynamique de notre modèle à partir du modèle de Beris-Edwards, en décrivant l'évolution des singularités par celles de S et T.

Chapter 2

The case of a spherical particle

This chapter has been published under the title "The Saturn Ring Effect in Nematic Liquid Crystals with External Field: Effective Energy and Hysteresis" in the journal "Archive for Rational Mechanics and Analysis" in 2021, see [8].

Abstract

In this work we consider the Landau-de Gennes model for liquid crystals with an external magnetic field to model the occurrence of the Saturn ring effect under the assumption of rotational equivariance. After a rescaling of the energy, a variational limit is derived. Our analysis relies on precise estimates around the singularities and the study of a radial auxiliary problem in regions, where a continuous director field exists. Studying the limit problem, we explain the transition between the dipole and Saturn ring configuration and the occurence of a hysteresis phenomenon, giving a rigorous explanation of what was derived and simulated previously by [H. Stark, Eur. Phys. J. B 10, 311–321 (1999)].

2.1 Introduction

Liquid crystals represent a state of matter with properties intermediate between liquids and crystalline solids. They are commonly referred to as rod like molecules (although there are other e.g. disk shaped molecules) whose positional and orientational order may vary within space, time and parameters such as temperature. For a general and complete introduction, we refer to [13, 58]. Depending on the alignment of the molecules and its symmetries, liquid crystals are generally divided into nematic, smectic and cholesteric. Due to their unique properties, liquid crystals exhibit remarkable structures and applications, see for example [100, 115, 133].

From a mathematical point of view, several models have been introduced to study the phenomena arising from liquid crystals [21]. Roughly speaking, the Oseen-Frank model describes liquid crystals by a unit vector field $\mathbf{n}$, that represents the preferred direction of the molecules at a point, averaging the fluctuations of the molecules. A peculiarity is, that in practice we do not distinguish between $\mathbf{n}$ and $-\mathbf{n}$, so that $\mathbf{n}$ should rather take values in a projective space $\mathbb{R}P^2$ to avoid problems with orientability.

In order to represent local averages of the directions of the molecules, one gets an additional degree of freedom. Models describing the liquid crystal with such a variable include e.g. the Ericksen model [63], [161, Ch.6]. The Landau-de Gennes model goes one step further by using the idea to describe the arrangement of a liquid crystal by a probability distribution ρ on the sphere of directions, taking into account that opposite points have the same probability. Then the first moment vanishes and the (shifted) second moment Q is a symmetric traceless tensor, which is used to model ρ. This allows to incorporate both the Oseen-Frank and Ericksen model into the Landau-

de Gennes model. A more detailed introduction to the various models and even for more refined generalizations of the Landau-de Gennes model, e.g. the Onsager model or Maier-Saupe model, can be found in [20, 163]. For the challenges and a comparison of the mentioned descriptions, see [22, 23, 25, 37, 142]. In general, it is difficult to give precise descriptions of minimizers of the energy functionals associated with one of the models explicitly, except in some very special cases such as in [169] or for the radial hedgehog solution in [120].

Mathematically speaking, liquid crystal theory shares several techniques and results with other subjects, for example the Ginzburg-Landau model in micromagnetics, [30, 79, 92]. Also parts of the description, such as function spaces [18] and liftings [88, 121], $Q-$tensors [34, 132], the formation of topological singularities [157] or similar energy functionals [49, 144] are of interest in a more abstract setting.

One interesting pattern one can observe in liquid crystals is the so called "Saturn ring" effect. Under certain circumstances the defect structure forming in order to balance a topological charge on the surface of an immersed object in liquid crystals, takes the form of a ring around the particle, see [2, 3, 83, 133]. Also more exotic structures such as knots are possible, we refer to [133] for an overview. In addition, an electromagnetic field can be used to manipulate the occurrence of a Saturn ring. While this is known in physics for several years [12, 71–73, 112, 113, 165], there are only few mathematical results [4]. Starting from the Landau-de Gennes model, an equilibrium configuration is found by minimization of the dimensionless free energy

$$\mathcal{E}_{\eta,\xi}(Q) = \int_\Omega \frac{1}{2}|\nabla Q|^2 + \frac{1}{\xi^2} f(Q) + \frac{1}{\eta^2} g(Q) + C_0(\xi,\eta)\, \mathrm{d}x$$

under suitable anchoring boundary conditions. Here Ω is the region filled with the liquid crystal, in our case the complement of the unit ball, i.e. $\Omega = \mathbb{R}^3 \setminus B_1(0)$ and $C_0(\xi,\eta)$ is a renormalization constant such that the energy is finite. The first term is the density for the elastic energy, while f is a potential inducing a force which tends to push the material into an ordered state. The parameter ξ describes the ratio between elastic and bulk energy. We are going to consider the limit of ξ converging to zero, which can be interpreted as the limit for large particle. The effect of an external magnetic field is described by the function g, with the parameter η coupling the field to the elastic and bulk energy densities. We will consider a regime where also $\eta \to 0$, not much slower than ξ. In our limit of $\xi, \eta \to 0$, C_0 converges to zero. To complete our model, we impose a strong anchoring boundary condition on $\partial\Omega$ that corresponds to a radial director field $\mathbf{n} = \mathbf{e}_r$. With ξ and η converging to zero, we can consider different regimes regarding the relative speed of convergence of both parameters.

1. The case of strong fields $\eta|\ln(\xi)| \ll 1$, where we expect to observe a Saturn ring was treated in [4].
2. The case $\eta|\ln(\xi)| \sim 1$, where the transition between dipole and Saturn ring takes place is precisely the purpose of this paper.
3. In the case $\eta|\ln(\xi)| \gg 1$ we expect only dipole configurations, see Remark 2.3.3.

Our work is organized as follows. In the first section we define the different parts of the free energy carefully, establish fundamental properties and discuss their effects in the minimizing process.

The second section contains the rescaling and states our main theorem, a sort of $\Gamma-$convergence result in a sense that will be precised later. We will prove, that in the limit $\eta, \xi \to 0$ in our regime and under the assumption of rotational equivariance, the model reduces to a simple energy stated on the surface of the sphere $\mathbb{S}^2 = \partial\Omega$, of the form

$$\mathcal{E}_0(F) = 2s_*c_* \int_F (1 - \cos(\theta))\, \mathrm{d}\omega + 2s_*c_* \int_{F^c} (1 + \cos(\theta))\, \mathrm{d}\omega + \frac{\pi}{2} s_*^2 \beta |D\chi_F|(\mathbb{S}^2)\,,$$

where $s_*, c_* > 0$ is a parameter depending on f and $F \subset \mathbb{S}^2$ is a set of finite perimeter that can be seen as the projection of the region, in which a lifting of Q from $\mathbb{R}P^2$ to $\mathbb{S}^2$ exists and the orientation at infinity agrees with the outward normal of ∂B_1. In the same spirit, F^c stands for the region, where the lifting has the opposite orientation and $|D\chi_F|(\mathbb{S}^2)$ denotes the perimeter of F

in $\mathbb{S}^2$. In the above expression, θ stands for the angle between a point ω on the sphere and $\mathbf{e}_3$. We see the latter perimeter term as representation of a defect line. It tells us that switching from one orientation to the other comes with a cost, depending on the balance between the forces (modelled by β), s_* which is related to the liquid crystal properties, c_* which depends on the interaction between magnetic field and liquid crystal and the length of the defect line. This is the result we are going to prove in the next two sections.

Section 3 is divided into three parts: We first show that the energy bound implies the existence of only a finite number of singularities if we are at some distance from the $\mathbf{e}_3-$axis. The main idea will be to replace our functions $Q_{\eta,\xi}$ by the minimizers of approximate problems and then use the higher regularity to derive a lower bound on the energy cost of a singularity. The energy bound then implies that in fact only finitely many singularities can occur. Next, we provide asymptotically exact lower bounds for the energy near those singularities. Then, the radial auxiliary problem is introduced. Given a ray from the surface $\partial\Omega$ to infinity such that $Q_{\eta,\xi}$ is close to being uniaxial with prescribed scalar order parameter, we can explicitly calculate the energy necessary to turn along the ray from our boundary conditions to the preferred configuration parallel to the external field in $\pm\mathbf{e}_3-$direction. Combining the results, we are able to prove the lower bound part of the main theorem.

The construction of a recovery sequence is made in section four. We use our knowledge about the interplay of the three parts of the energy to define approximate regions close to the particle in which the energy of the first two terms of $\mathcal{E}_0$ is concentrated and Q is uniaxial. Here we profit from the exact formula of the optimal profile from the radial auxiliary problem. Apart from these regions, we construct the singularities that give rise to the perimeter term of $\mathcal{E}_0$.

The remaining section deals with the limit energy. We calculate the minimizers (depending on β) and compare their energy with that of a dipole and a Saturn ring at the same $\beta-$value. We find that by varying β a hysteresis phenomenon occurs. Our findings rigorously explain known numerical simulations and physical reasoning in [105, 154].

2.2 Scaling, definitions and preliminaries

Starting from the one constant approximation of the Landau-de Gennes free energy [139, Ch. 6, Secs. 3-4 and Ch. 10, Sec. 2.3] (see also [57, Ch. 3, Secs. 1-2]) in $\Omega_{r_0} = \mathbb{R}^3 \setminus \overline{B_{r_0}(0)}$ we find

$$\mathcal{E}(Q) = \int_{\Omega_{r_0}} \frac{L}{2}|\nabla Q|^2 - \frac{a}{2}\mathrm{tr}(Q^2) - \frac{b}{3}\mathrm{tr}(Q^3) + \frac{c}{4}(\mathrm{tr}(Q^2))^2 - \frac{1}{2}\chi_a \mathbf{H}\otimes\mathbf{H} : Q \,\mathrm{d}x\,, \tag{2.1}$$

where the last term is added to the Landau-de Gennes model to incorporate the effect of the external magnetic field $\mathbf{H}$. The length r_0 is the particle radius, the parameter L is the elastic constant, a, b, c are the bulk constants depending on the liquid crystal material. They can be temperature dependent, although it is usually assumed that only a has a linear dependence, i.e. $a = a_0(T - T_*)$ for a reference temperature T_* [132]. However, this case will not be discussed here. As already noted, $\mathbf{H}$ is the magnetic field, which we choose to be parallel to $\mathbf{e}_3$, i.e. $\mathbf{H} = h\mathbf{e}_3$ and χ_a denotes the magnetic anisotropy. See [77] for more details on the modelling, in particular how magnetic fields differ from electric and gravitational fields.

In order to be able to work on a fixed domain, we apply the rescaling $\Omega := \frac{1}{r_0}\Omega_{r_0}$ and $\tilde{x} = x/r_0$. We introduce the new function $\widetilde{Q}(\tilde{x}) = Q(r_0\tilde{x}) = Q(x)$ and $\widetilde{\nabla} = \nabla_{\tilde{x}} = \frac{1}{r_0}\nabla_x$. Furthermore, we write $\tilde{a} = \frac{a}{c}$ and $\tilde{b} = \frac{b}{c}$. Then

$$\mathcal{E}(Q) = \int_\Omega \frac{Lr_0^3}{2r_0^2}|\nabla\widetilde{Q}|^2 + r_0^3 c\left(-\frac{\tilde{a}}{2}\mathrm{tr}(\widetilde{Q}^2) - \frac{\tilde{b}}{3}\mathrm{tr}(\widetilde{Q}^3) + \frac{1}{4}(\mathrm{tr}(\widetilde{Q}^2))^2\right) - \frac{1}{2}\chi_a h^2 r_0^3 \widetilde{Q}_{33}\,\mathrm{d}\tilde{x}\,.$$

Dividing by Lr_0, we can define

$$\widetilde{\mathcal{E}}(\widetilde{Q}) = \int_\Omega \frac{1}{2}|\widetilde{\nabla}\widetilde{Q}|^2 + \frac{1}{\xi^2}\left(-\frac{\tilde{a}}{2}\mathrm{tr}(\widetilde{Q}^2) - \frac{\tilde{b}}{3}\mathrm{tr}(\widetilde{Q}^3) + \frac{1}{4}(\mathrm{tr}(\widetilde{Q}^2))^2\right) - \frac{1}{\eta^2}\widetilde{Q}_{33}\,\mathrm{d}\tilde{x}\,, \tag{2.2}$$

where we introduced the new dimensionless parameters $\xi = \sqrt{\frac{L}{cr_0^2}}$ and $\eta = \sqrt{\frac{L}{2\chi_a r_0^2 h^2}}$. We choose the coefficients $\tilde{a}, \tilde{b}$ to be fixed from now on, which corresponds to choosing a material and keeping the physical system at a constant temperature. For a common liquid crystal material such as MBBA at a temperature of $25°C$ we roughly find $\tilde{a} \approx 2.4$, $\tilde{b} \approx 1.8$ [139, p.168]. The analysis and particularly the constants in the estimates that appear in the following will generally depend on f and thus on $\tilde{a}$ and $\tilde{b}$, even if we do not explicitly state this dependence.

We are interested in the limit $\eta, \xi \to 0$. In the standard Landau-de Gennes model, $\xi \to 0$ can be interpreted as increasing the particle radius (see [76] for a detailed discussion). We impose the asymptotic relation $\eta |\ln(\xi)| \to \beta \in (0, \infty)$ which can be seen as a coupling of the parameters r_0 and h, i.e. slowly decreasing the field strength h, while increasing the particle radius in a way that keeps the system in a state where both Saturn ring and dipole configurations are likely to appear.

It is convenient to introduce a constant C_0 in the integral of (2.1) to obtain a non-negative energy density. In our case, this constant depends on ξ and η, but tends towards a constant independent of those parameters as $\xi, \eta \to 0$. We will discuss the issue later in this section.

From now on, we will only consider the rescaled model and thus drop all tildes in our notation. We continue this section by giving precise definitions for the function f modelling the bulk term and quantities mentioned in the introduction. We will furthermore introduce a more general function g for the magnetic term in (2.1).

Definition 2.2.1. *We denote by* Sym_0 *the space of symmetric matrices with vanishing trace*

$$\mathrm{Sym}_0 := \{Q \in \mathbb{R}^{3\times 3} \,:\, Q^\top = Q\,,\ \mathrm{tr}(Q) = 0\}\,,$$

equipped with the norm $|Q| = \sqrt{\mathrm{tr}(Q^2)}$*. Furthermore, for* $a, b, c \in \mathbb{R}$*,* $b, c > 0$ *we define*

$$f(Q) = C - \frac{a}{2}\mathrm{tr}(Q^2) - \frac{b}{3}\mathrm{tr}(Q^3) + \frac{c}{4}\left(\mathrm{tr}(Q^2)\right)^2. \tag{2.3}$$

As we stated in the introduction, the definition of Sym_0 is motivated by the second order moment of a probability distribution ρ on a sphere. The symmetry between $\pm\mathbf{n}$ reads $\rho(\mathbf{n}) = \rho(-\mathbf{n})$ for all $\mathbf{n} \in \mathbb{S}^2$, i.e. the expectation value of $\mathbf{n}$ vanishes, $\int_{\mathbb{S}^2} \mathbf{n}\, \mathrm{d}\rho = 0$. The second moment $\int_{\mathbb{S}^2} \mathbf{n}\otimes\mathbf{n}\, \mathrm{d}\rho$ is symmetric and has trace 1. From this we subtract the second moment of a uniform distribution on $\mathbb{S}^2$, i.e. $\overline{\rho} = \frac{1}{4\pi}$ to get the symmetric and traceless tensor Q.

The specific form of the function f comes from the requirement of being invariant under rotations. Indeed, assuming a polynomial function f and demanding frame indifference for the bulk energy (and of course for the elastic energy) we find that f has to satisfy $f(Q) = f(R^\top Q R)$ for all $R \in O(3)$. This implies that f is the linear combination of $\mathrm{tr}(Q^2)$, $\mathrm{tr}(Q^3)$, $(\mathrm{tr}(Q)^2)^2$, $\mathrm{tr}(Q^2)\mathrm{tr}(Q^3)$, $\mathrm{tr}(Q^2)^2$, $\mathrm{tr}(Q^3)^2$, etc (see [20, Lemma 3]). It is convenient to consider only the first three terms although one could in principle add more. The constant C in (2.3) is chosen such that f is non-negative and vanishes on uniaxial $Q-$tensors of a prescribed scalar order parameter (the set $\mathcal{N}$ in Proposition 2.2.2 below). This is the main property of f one should keep in mind during our analysis.

Proposition 2.2.2 (Properties of f)**.** *There exists a constant* C *such that* f *given by (2.3) satisfies*

1. $f(Q) \geq 0$ *for all* $Q \in \mathrm{Sym}_0$ *and* $\min_{Q\in\mathrm{Sym}_0} f(Q) = 0$*. Let*

$$\mathcal{N} := \left\{ s_* \left(\mathbf{n}\otimes\mathbf{n} - \frac{1}{3}\mathrm{Id} \right) \,:\, \mathbf{n} \in \mathbb{S}^2 \right\},$$

where $\mathbb{S}^2 \subset \mathbb{R}^3$ *is the unit sphere and* $s_* = \frac{1}{4}\left(\tilde{b} + \sqrt{\tilde{b}^2 + 24\tilde{a}}\right)$*. Then* $\mathcal{N} = f^{-1}(0)$ *is a smooth, compact, connected manifold without boundary diffeomorphic to* $\mathbb{R}P^2$*. The constant* C *can be explicitly be calculated as* $C = \frac{\tilde{a}}{3}s_*^2 + \frac{2\tilde{b}}{27}s_*^3 - \frac{1}{9}s_*^4$*.*

2. *Furthermore, there exist constants* $\delta_0, \gamma_1 > 0$ *such that if* $Q \in \mathrm{Sym}_0$ *satisfies* $\mathrm{dist}(Q, \mathcal{N}) \leq \delta_0$*, then*

$$f(Q) \geq \gamma_1 \,\mathrm{dist}^2(Q, \mathcal{N})\,.$$

3. *There exist constants $C_1, C_2 > 0$ such that for all $Q \in \mathrm{Sym}_0$*

$$f(Q) \geq C_1 \left(|Q|^2 - \frac{2}{3} s_*^2 \right)^2 , \qquad Df(Q) : Q \geq C_1 |Q|^4 - C_2 .$$

Note that all constants appearing in the above proposition are depending on $\tilde{a}$ and $\tilde{b}$.

Proof. A proof of the first statement can be found in [121, Proposition 15]. For the second result, we refer to [42, Lemma 2.4 (F_2)]. The last assertions follows by elementary calculations as in [42, Lemma 2.4 (F_0)]. □

The last two statements are of technical nature. The third property is used to establish $L^\infty-$bounds in Remark 2.3.2 and Proposition 2.4.4 and to establish Proposition 2.2.4 and Proposition 2.2.6. The estimate in 2. simply states that one can think of f as being quadratic close to its minimum which is attained on $\mathcal{N}$. The first statement gives an interesting connection between f and the space Sym_0. In fact, $\mathcal{N}$ plays an important role in our analysis as it will allow us to identify Q and $\pm\mathbf{n}$ and thus give a intuitive meaning to Q. This is formalized in the next proposition.

Proposition 2.2.3 (Structure of Sym_0)**.** *1. For all $Q \in \mathrm{Sym}_0$ there exist $s \in [0, \infty)$ and $r \in [0, 1]$ such that*

$$Q = s \left(\left(\mathbf{n} \otimes \mathbf{n} - \frac{1}{3}\mathrm{Id} \right) + r \left(\mathbf{m} \otimes \mathbf{m} - \frac{1}{3}\mathrm{Id} \right) \right) , \tag{2.4}$$

where $\mathbf{n}, \mathbf{m}$ are normalized, orthogonal eigenvectors of Q. The values s and r are continuous functions of Q.

2. *Let $\mathcal{C} = \{Q \in \mathrm{Sym}_0 : \lambda_1(Q) = \lambda_2(Q)\}$, where we denoted by λ_1, λ_2 the two leading eigenvalues of Q. Then*

$$\mathcal{C} = \{Q \in \mathrm{Sym}_0 \setminus \{0\} \ : \ r(Q) = 1\} \cup \{0\} \quad \text{and} \quad \mathcal{C} \setminus \{0\} \cong \mathbb{R}P^2 \times \mathbb{R} .$$

3. *There exists a continuous function $\mathcal{R} : \mathrm{Sym}_0 \setminus \mathcal{C} \to \mathcal{N}$ such that $\mathcal{R}(Q) = Q$ for all $Q \in \mathcal{N}$. In particular, $\mathrm{Sym}_0 \setminus \mathcal{C}$ and $\mathcal{N}$ are homotopic. The map $\mathcal{R}$ can be chosen to be the nearest point projection onto $\mathcal{N}$. In this case, for all $Q \in \mathrm{Sym}_0 \setminus \mathcal{C}$ decomposed as in (2.4), $\mathcal{R}$ is given by $\mathcal{R}(Q) = s_*(\mathbf{n} \otimes \mathbf{n} - \frac{1}{3}\mathrm{Id})$.*

Proof. The first part follows from [41, Lemma 1.3.1] for $s = 2\lambda_1 + \lambda_2$ and $r = (\lambda_1 + 2\lambda_2)/s$, where $\lambda_1 \geq \lambda_2$ are the two leading eigenvalues of Q. The second part is a consequence of the definition of s, r in terms of the eigenvalues and [41, Lemma 1.3.5]. The last part is a reformulation of Lemma 1.3.6 and Lemma 1.3.7 in [41], together with Lemma 2.2.2. □

The decomposition (2.4) provides us with a very useful tool to perform calculations, for example in Proposition 2.4.16, Proposition A.1.1 or Proposition A.1.2. In the second statement we introduce $\mathcal{C}$, a subset of the uniaxial $Q-$tensor, sometimes referred to as "oblate uniaxial" [69,119]. One can think of $\mathcal{C}$ as a cone over $\mathbb{R}P^2$. If a $Q-$tensor is not oblate uniaxial, there exists a retraction onto $\mathcal{N}$ which coincides with the nearest point projection and is given by the element of $\mathcal{N}$ corresponding to the dominating eigenvector of Q.

In the remaining part of this chapter we are concerned with the magnetic energy term, which will be modelled by a function g. We require $g : \mathrm{Sym}_0 \to \mathbb{R}$ to be of class C^2 away from 0 and to satisfy the following properties:

1. The function g does not grow faster than f, i.e. there exists a constant $C > 0$ such that for all $Q \in \mathrm{Sym}_0$

$$|g(Q)| \ \leq \ C \left(1 + |Q|^4\right), \tag{2.5}$$

$$|Dg(Q)| \ \leq \ C \left(1 + |Q|^3\right). \tag{2.6}$$

2. The preferred eigenvector of Q for g is $\mathbf{e}_3$ in the following sense: g is invariant by rotations around the $\mathbf{e}_3-$axis and the function $O(3) \ni R \mapsto g(R^\top QR)$ is minimal if $\mathbf{e}_3$ is eigenvector to the maximal eigenvalue of $R^\top QR$. Decomposing Q as in (2.4) with $\mathbf{n} = \mathbf{e}_3$ and keeping s and $\mathbf{m}$ fixed, then $g(Q)$ is minimal for $r = 0$. For a uniaxial $Q \in \mathcal{N}$, i.e. $Q = s_*(\mathbf{n} \otimes \mathbf{n} - \frac{1}{3}\mathrm{Id})$ for $s_* \geq 0$ and $\mathbf{n} \in \mathbb{S}^2$ we have

$$g(Q) = c_*^2(1 - \mathbf{n}_3^2)\,. \tag{2.7}$$

3. There exist constants $\delta_1, C > 0$ such that if $Q \in \mathrm{Sym}_0$ with $\mathrm{dist}(Q, \mathcal{N}) < \delta$ for $0 < \delta < \delta_1$, then

$$|g(Q) - g(\mathcal{R}(Q))| \leq C\,\mathrm{dist}(Q, \mathcal{N})\,. \tag{2.8}$$

The first and last conditions are technical assumptions. The former allows us to dominate g by f. This is necessary, since g may be negative. The latter states the Lipschitz continuity of g in a neighbourhood of $\mathcal{N}$ in normal direction. The second requirement contains the mathematical translation of the physical model. The homogeneous magnetic field parallel to $\mathbf{e}_3$ should favour the alignment of the dominating eigenvector of Q parallel to $\mathbf{e}_3$. Equation (2.7) expresses the compatibility of our $Q-$tensor analysis with the classical formulations for director fields. From a mathematical point of view, it is possible to replace (2.7) by (2.7')

$$g(Q) \geq c_*^2(1 - \mathbf{n}_3^2)\,, \tag{2.7'}$$

and to obtain a similar limit energy, see Remark 2.4.18.

We note that the functions g_1 and g_2, defined as

$$g_1(Q) = \frac{2}{3}s_* - Q_{33} \quad \text{and} \quad g_2(Q) = \begin{cases} \sqrt{\frac{2}{3}} - \frac{Q_{33}}{|Q|} & Q \in \mathrm{Sym}_0 \setminus \{0\} \\ 0 & Q = 0 \end{cases}, \tag{2.9}$$

satisfy the above assumptions on g (see Appendix). The function g_1 (with $c_*^2 = s_*$) is the natural (physical) term to model a magnetic field [139, Ch.10], we have used it to derive our scaling in (2.1), the constant $\frac{2}{3}s_*$ being part of C_0. Another possible choice is g_2, which is a useful approximation to g_1 introduced in [71] and used e.g. in [4]. In this case $c_*^2 = \sqrt{\frac{3}{2}}$.

We finish this section by two propositions. Note that if $g \geq 0$ (e.g. in the case $g = g_2$), then both propositions are trivial. The first proposition shows that under the above assumptions on f and g there exists a unique minimizer $Q_{\infty,\xi,\eta}$ of $\frac{1}{\xi^2}f(Q) + \frac{1}{\eta^2}g(Q)$. This allows us to characterize a constant $C_0(\xi, \eta)$ such that the bulk energy density becomes non-negative and vanishes only at $Q_{\infty,\xi,\eta}$. The second proposition expresses that if Q is close to $\mathcal{N}$ but the dominating eigenvector $\mathbf{n}$ far from $\mathbf{e}_3$, then g has to be strictly positive.

Proposition 2.2.4. *For $\xi, \eta > 0$ with $\xi \ll \eta$, there exists a unique $Q_{\infty,\xi,\eta} \in \mathrm{Sym}_0$ such that*

$$Q_{\infty,\xi,\eta} = \operatorname*{argmin}_{Q \in \mathrm{Sym}_0} \frac{1}{\xi^2}f(Q) + \frac{1}{\eta^2}g(Q)\,,$$

given by $s_{*,\xi^2/\eta^2}(\mathbf{e}_3 \otimes \mathbf{e}_3 - \frac{1}{3}\mathrm{Id})$, where $|s_{*,t} - s_*| \leq Ct$ with s_* as in Proposition 2.2.2. Hence, for $C_0(\xi, \eta) = -\frac{1}{\xi^2}f(Q_{\infty,\xi,\eta}) - \frac{1}{\eta^2}g(Q_{\infty,\xi,\eta}) \geq 0$ it also holds true that $C_0(\xi, \eta) \leq C\xi^2/\eta^4$.

Since $s_{*,\xi^2/\eta^2} \to s_{*,0} = s_*$ for $\xi, \eta \to 0$ in our regime, we denote $Q_\infty := s_*(\mathbf{e}_3 \otimes \mathbf{e}_3 - \frac{1}{3}\mathrm{Id})$.

In the physically relevant case of $g = g_1$, we have the expansion $s_{*,\xi^2/\eta^2} = s_* + (-\frac{2}{3}a - \frac{4}{9}bs_* + \frac{4}{3}cs_*^2)^{-1}\frac{\xi^2}{\eta^2} + O(\frac{\xi^4}{\eta^4})$.

Proof. Let $Q \in \mathrm{Sym}_0$ be of norm $\sqrt{\frac{2}{3}}s_*$ and let $t \geq 0$. Then we can estimate

$$\frac{1}{2\,\xi^2}f(tQ) + \frac{1}{\eta^2}g(tQ) \geq \frac{1}{2\xi^2}C_f(t^2 - 1)^2 - \frac{C_g}{\eta^2}(1 + t^4)\,.$$

So if we choose a $|t-1| \geq t_0 > 0$ and $\frac{\xi^2}{\eta^2} \leq \frac{C_f}{2C_g} \max_{|t-1|\geq t_0} \frac{(t^2-1)^2}{t^4+1}$, the above expression is positive. Let $||Q| - \sqrt{\frac{2}{3}} s_*| \leq \delta$ and $\operatorname{dist}(Q,\mathcal{N}) > \delta$. Then $f(Q) \geq f_{\min} := \min\{f(Q) \,:\, Q \in \operatorname{Sym}_0, \operatorname{dist}(Q,\mathcal{N}) > \delta\} > 0$ and

$$\frac{1}{2\,\xi^2} f(Q) + \frac{1}{\eta^2} g(Q) \geq \frac{f_{\min}}{2\xi^2} - \frac{C}{\eta^2}(1+\delta^3) > 0\,,$$

for $\xi^2/\eta^2 \leq \frac{f_{\min}}{2C(1+\delta^3)}$. By invariance of f under rotations and property 2. of g we know that a minimizer Q has the dominating eigenvector $\mathbf{e}_3$ or $-\mathbf{e}_3$ and has to verify $r = 0$. This allows us to write $Q_s = s(\mathbf{e}_3 \otimes \mathbf{e}_3 - \frac{1}{3}\mathrm{Id})$ for $s \in (-C\delta, C\delta)$ for a constant $C > 0$. Taking the derivative with respect to s in the energy of Q_s we get

$$\frac{\mathrm{d}}{\mathrm{d}s}\left(\frac{1}{\xi^2} f(Q_s) + \frac{1}{\eta^2} g(Q_s)\right) = \frac{1}{\xi^2}\left(-\frac{2}{3}as - \frac{2}{9}bs^2 + \frac{4}{9}cs^3\right) - \frac{1}{\eta^2} Dg(Q_s) : \left(\mathbf{e}_3 \otimes \mathbf{e}_3 - \frac{1}{3}\mathrm{Id}\right) = 0\,.$$

We multiply by ξ^2 and since $|Dg(Q_s)|$ is bounded and $\xi \ll \eta$ this equation admits a unique positive solution corresponding to a minimum in the energy density, which we call $s_{*,\xi^2/\eta^2}$. This gives the existence of a unique minimizer $Q_{\infty,\xi,\eta}$ and the claimed representation. By a standard perturbation theory argument we get the estimate $|s_{*,t} - s_*| \leq Ct$.

Since $|s_{*,\xi^2/\eta^2} - s_*| \leq C\xi^2/\eta^2$, we have the estimates $f(Q_{\infty,\xi,\eta}) \leq C(\xi^2/\eta^2)^2$ and $|g(Q_{\infty,\xi,\eta})| \leq C\xi^2/\eta^2$ from which we get

$$C_0(\xi,\eta) \;\leq\; C\frac{1}{\xi^2}\frac{\xi^4}{\eta^4} + C\frac{2}{\eta^2}\frac{\xi^2}{\eta^2} \;\leq\; C\frac{\xi^2}{\eta^4}\,.$$

□

Proposition 2.2.5. *There exist $\mathfrak{a}, \delta_0 > 0$ such that if $0 < \delta < \delta_0$, then*

$$\min\{g(Q) \,:\, Q \in \operatorname{Sym}_0 \text{ with } \operatorname{dist}(Q,\mathcal{N}) \leq \delta\,,\ |Q - Q_\infty| \geq \mathfrak{a}\sqrt{\delta}\} > 0\,.$$

Proof. Let $0 < \delta < \min \delta_1, 1$, where δ_1 is from (2.8). Let $Q \in \operatorname{Sym}_0$ such that $\operatorname{dist}(Q,\mathcal{N}) \leq \delta$. We can apply (2.8) to $g(Q)$ to get

$$g(Q) \;\geq\; g(\mathcal{R}(Q)) - C\operatorname{dist}(Q,\mathcal{N}) \;\geq\; c_*^2(1-\mathbf{n}_3^2) - C\delta\,,$$

where $\mathbf{n}_3$ is the third component of the dominating unit eigenvector of Q, see Proposition 2.2.3.

Since $|Q - \mathcal{R}(Q)| = \operatorname{dist}(Q,\mathcal{N}) \leq \delta$ and $|\mathbf{n}| = |\mathbf{e}_3| = 1$ we can estimate

$$|Q - Q_\infty|^2 \leq 2|Q - \mathcal{R}(Q)|^2 + 2|\mathcal{R}(Q) - Q_\infty|^2 \leq 2\delta^2 + 2s_*^2|\mathbf{n}\otimes\mathbf{n} - \mathbf{e}_3\otimes\mathbf{e}_3|^2 \leq 2\delta^2 + 4s_*^2(1-\mathbf{n}_3^2)\,,$$

and thus

$$g(Q) \geq \frac{c_*^2}{4s_*^2}|Q - Q_\infty|^2 - 4C\delta \geq \left(\frac{c_*^2}{4s_*^2}\mathfrak{a} - 4C\right)\delta > 0\,,$$

if $|Q - Q_\infty| \geq \mathfrak{a}\sqrt{\delta}$ for $\mathfrak{a} > 0$ large enough. In order to conclude, it remains to choose $0 < \delta_0 \leq \min\{\delta_1, 1\}$ in such a way that the set $\{Q \in \operatorname{Sym}_0 \text{ with } \operatorname{dist}(Q,\mathcal{N}) \leq \delta\,,\ |Q - Q_\infty| \geq \mathfrak{a}\sqrt{\delta}\}$ is non empty for all $\delta \in (0,\delta_0)$. Setting $\delta_0 = \min\{1, \delta_1, \frac{2}{3}s_*^2\mathfrak{a}^{-2}\}$, we have $\mathfrak{a}\sqrt{\delta} \leq \sqrt{\frac{2}{3}}s_* + \delta$ for all $\delta \in (0,\delta_0)$, i.e. the set is non-empty. □

As we have seen in Proposition 2.2.4, the minimizer $Q_{\infty,\xi,\eta}$ of the bulk term is not part of $\mathcal{N}$ (which has order parameter s_*). We will introduce a slightly modified manifold $\mathcal{N}_{\eta,\xi}$ such that $Q_{\infty,\xi,\eta} \in \mathcal{N}_{\eta,\xi}$ and such that $f(Q) + \frac{\xi^2}{\eta^2}g(Q) + \xi^2 C_0(\xi,\eta)$ controls the squared distance of Q to this new manifold, in analogy to $f(Q) \geq \gamma_1 \operatorname{dist}^2(Q,\mathcal{N})$ from Proposition 2.2.2.

Proposition 2.2.6. *If $\xi^2/\eta^2 \ll 1$, then there exists a smooth manifold $\mathcal{N}_{\eta,\xi} \subset \mathrm{Sym}_0$, diffeomorphic to $\mathcal{N}$ such that*

$$f(Q) + \frac{\xi^2}{\eta^2} g(Q) + \xi^2 C_0(\xi,\eta) \geq \gamma_2 \operatorname{dist}^2(Q, \mathcal{N}_{\eta,\xi}) \tag{2.10}$$

for a constant $\gamma_2 > 0$. In particular $Q_{\infty,\xi,\eta} \in \mathcal{N}_{\eta,\xi}$. Furthermore, there exists a constant $C > 0$ such that

$$\sup_{Q \in \mathcal{N}_{\eta,\xi}} \operatorname{dist}(Q, \mathcal{N}) \leq C \frac{\xi^2}{\eta^2}\,. \tag{2.11}$$

Proof. We introduce the notation $f_{\eta,\xi}(Q)$ for the LHS of (2.10).

Step 1: Definition of $\mathcal{N}_{\eta,\xi}$. Let $Q_0 \in \mathcal{N}$ and $\{P_1, P_2, P_3\}$ a orthonormal basis of $(T_{Q_0}\mathcal{N})^\perp$. For $t \in \mathbb{R}^3$ we define $F(Q_0, t) := D_\nu f_{\eta,\xi}(Q_0 + t_1P_1 + t_2P_2 + t_3P_3)$, where D_ν denotes the derivative normal to $\mathcal{N}$. From perturbation theory it follows that there exists a $t_0 \in \mathbb{R}^3$ with $|t_0| \leq C\frac{\xi^2}{\eta^2}$ such that $F(Q_0, t_0) = 0$. From Lemma 2.4 (F_1) in [42] we get that if $P \in \mathrm{Sym}_0$ orthogonal to $T_{Q_0}\mathcal{N}$, then $P \cdot (D^2 f(Q_0))P \geq \gamma \|P\|^2$. Hence, for $Q_t = Q_0 + t_1P_1 + t_2P_2 + t_3P_3$ it holds that

$$D_t F(Q_0, t_0) \;=\; D^2_\nu f(Q_t) + \frac{\xi^2}{\eta^2} D^2_\nu g(Q_t) \;\geq\; D^2_\nu f(Q_0) - C|t_0|\mathrm{Id} + \frac{\xi^2}{\eta^2} D^2_\nu g(Q_t) \;\geq\; \frac{\gamma}{2}\mathrm{Id}\,,$$

since $D^2 g$ is bounded in a compact neighbourhood of $\mathcal{N}$, $|t_0| \leq C\frac{\xi^2}{\eta^2}$ and $\frac{\xi^2}{\eta^2} \ll 1$. By the Implicit Function Theorem we conclude that there exists a smooth function $\psi : \mathcal{N} \to \mathbb{R}^3$ such that $F(Q_0, \psi(Q_0)) = 0$. Thus, $\mathcal{N}_{\eta,\xi} := \{Q_{t_0} \,:\, Q_0 \in \mathcal{N} \text{ and } t_0 = \psi(Q_0)\}$ is a smooth manifold, diffeomorphic to $\mathcal{N}$. Furthermore, since ψ is continuous and $\mathcal{N}$ is compact, we deduce that (2.11) holds.

Step 2: Control of the distance. Since ξ^2/η^2 is small and $f_{\eta,\xi}$ grows faster than the RHS of (2.10), we can use (2.11) and argue similar to Proposition 2.2.4 to deduce that (2.10) holds if $\operatorname{dist}(Q, \mathcal{N}_{\eta,\xi}) \geq \delta$ for some small but fixed $\delta > 0$. Because of this, it is enough to show that (2.10) holds for all $Q \in \mathrm{Sym}_0$ with $\operatorname{dist}(Q, \mathcal{N}_{\eta,\xi}) < \delta$. For such Q, we first define $Q_0 = \mathcal{R}(Q)$. Let $Q_1 \in \mathcal{N}_{\eta,\xi}$ be the element corresponding to Q_0 according to step 1. Then $Q - Q_1 \in (T_{Q_0}\mathcal{N})^\perp$ and by Taylor expansion it holds that

$$f_{\eta,\xi}(Q) \;\geq\; f_{\eta,\xi}(Q_1) + D_\nu f_{\eta,\xi}(Q_1) : (Q - Q_1) + \frac{1}{2}(Q - Q_1) \cdot D^2 f_{\eta,\xi}(Q_1)(Q - Q_1) - C\delta|Q - Q_1|^2\,.$$

Note that $f_{\eta,\xi}(Q) \geq 0$ and by construction $D_\nu f_{\eta,\xi}(Q_1) : (Q - Q_1) = 0$. Evoking again Lemma 2.4 in [42], we get

$$f_{\eta,\xi}(Q) \;\geq\; \Big(\frac{\gamma}{4} - C\delta\Big)|Q - Q_1|^2\,.$$

Choosing $\delta > 0$ small enough there exists a $\gamma_2 > 0$ such that $\frac{\gamma}{4} - C\delta \geq \gamma_2 > 0$ and since $\operatorname{dist}(Q, \mathcal{N}_{\eta,\xi}) \leq |Q - Q_1|$, (2.10) follows.

From Proposition 2.2.4 we know that $f_{\eta,\xi}(Q_{\infty,\xi,\eta}) = 0$ and hence by (2.10) it follows that $\operatorname{dist}(Q_{\infty,\xi,\eta}, \mathcal{N}_{\eta,\xi}) = 0$, i.e. $Q_{\infty,\xi,\eta} \in \mathcal{N}_{\eta,\xi}$. □

2.3 Statement of result

From equation (2.2) and using the notation introduced in the last section, we write our energy

$$\mathcal{E}_{\eta,\xi}(Q) = \int_\Omega \frac{1}{2}|\nabla Q|^2 + \frac{1}{\xi^2} f(Q) + \frac{1}{\eta^2} g(Q) + C_0(\xi,\eta)\,\mathrm{d}x\,, \tag{2.12}$$

which is the dimensionless free energy that was announced in the introduction. The natural space for this energy to be well defined is $H^1(\Omega, \mathrm{Sym}_0) + Q_{\infty,\xi,\eta}$ with $Q_{\infty,\xi,\eta}$ as in Proposition

2.2.4. Minimizing the first term would lead to a harmonic map, the second term prefers Q to be uniaxial with a certain scalar order parameter and hence norm, while the third term takes its minimum when the director is aligned parallel to $\mathbf{e}_3$. So the (spatially) constant uniaxial map $Q_{\infty,\xi,\eta} = s_{*,\xi^2/\eta^2}(\mathbf{e}_3 \otimes \mathbf{e}_3 - \frac{1}{3}\mathrm{Id})$ would be a minimizer of our free energy. However, this will violate the strong anchoring conditions we are going to impose on the boundary, namely we want $Q_{\eta,\xi} \in H^1(\Omega, \mathrm{Sym}_0) + Q_{\infty,\xi,\eta}$ to satisfy

$$Q_{\eta,\xi} = Q_b \quad \text{on} \quad \mathbb{S}^2\,, \tag{2.13}$$

where $Q_b(x) = s_*\left(\mathbf{x}\otimes\mathbf{x} - \frac{1}{3}\mathrm{Id}\right)$. The system is therefore frustrated and we expect the minimizer to be close to $s_*(\mathbf{e}_3\otimes\mathbf{e}_3 - \frac{1}{3}\mathrm{Id})$ everywhere, except for a transition zone near the boundary. In this boundary layer, which will turn out to be of thickness η, we will find tubes of cross sectional area ξ^2 containing the regions where $Q_{\eta,\xi}$ is biaxial.

Since the problem is equivariant with respect to rotations around the $\mathbf{e}_3-$axis, it is natural to consider only rotationally equivariant maps. We say that a map Q is *rotationally equivariant* if Q is equivariant with respect to rotations around the $\mathbf{e}_3$-axis. In other words, using cylindrical coordinates, one has

$$Q(\rho,\varphi,z) = R_\varphi^\top Q(\rho,0,z)R_\varphi\,, \qquad \text{where} \qquad R_\varphi = \begin{pmatrix}\cos\varphi & -\sin\varphi & 0\\ \sin\varphi & \cos\varphi & 0\\ 0 & 0 & 1\end{pmatrix}.$$

For uniaxial maps $Q = s_*(\mathbf{n}\otimes\mathbf{n} - \frac{1}{3}\mathrm{Id})$ this is equivalent to the usual notion of equivariance for vectors $\mathbf{n}(R_\varphi\mathbf{x}) = R_\varphi^\top\mathbf{n}(\mathbf{x})$. We define the set of admissible functions $\mathcal{A}$ to be the set of rotationally equivariant functions $Q_{\eta,\xi} \in H^1(\Omega,\mathrm{Sym}_0) + Q_{\infty,\xi,\eta}$ satisfying the boundary condition (2.13). This motivates the definition for $Q \in H^1(\Omega,\mathbb{R}^{3\times3}) + Q_{\infty,\xi,\eta}$

$$\mathcal{E}^{\mathcal{A}}_{\eta,\xi}(Q) = \begin{cases}\mathcal{E}_{\eta,\xi}(Q) & \text{if } Q\in\mathcal{A}\,,\\ \infty & \text{otherwise.}\end{cases}$$

We believe that minimizers of $\mathcal{E}_{\eta,\xi}$ are also rotationally equivariant, although this does not follow from our work and remains an open issue. We will remove the hypothesis of rotational equivariance in a work in preparation.

The following theorem is the main result of the paper.

Theorem 2.3.1. *Suppose that*

$$\eta|\ln(\xi)| \to \beta \in (0,\infty) \qquad \text{as } \eta\to 0\,. \tag{2.14}$$

Then $\eta\,\mathcal{E}^{\mathcal{A}}_{\eta,\xi} \to \mathcal{E}_0$ in a variational sense, where the limiting energy $\mathcal{E}_0$ for a set $F\subset\mathbb{S}^2$ is given by

$$\mathcal{E}_0(F) = 2s_*c_*\int_F(1-\cos(\theta))\,\mathrm{d}\omega + 2s_*c_*\int_{F^c}(1+\cos(\theta))\,\mathrm{d}\omega + \frac{\pi}{2}s_*^2\beta|D\chi_F|(\mathbb{S}^2)\,. \tag{2.15}$$

More precisely, we have the following statements:

1. *Compactness: For any sequence $Q_{\eta,\xi}\in\mathcal{A}$ such that $\eta\,\mathcal{E}_{\eta,\xi}(Q_{\eta,\xi}) \le C$, there exists a measurable set of finite perimeter $F\subset\mathbb{S}^2$ that is invariant under rotations w.r.t. the $\mathbf{e}_3-$axis, measurable functions $\mathbf{n}^\eta : \Omega\to\mathbb{S}^2$ and a set $\omega_\eta\subset\Omega$ with $\lim_{\eta\to0}|\omega_\eta| = 0$, $\Omega\setminus\omega_\eta$ simply connected, such that for all $\sigma>0$ it holds $\mathbf{n}^\eta\in C^0(\Omega\setminus(Z_\sigma\cup\omega_\eta),\mathbb{S}^2)$ and for all $R>0$*

$$\lim_{\eta\to0}\left\|s_*\left(\mathbf{n}^\eta\otimes\mathbf{n}^\eta - \frac{1}{3}\mathrm{Id}\right) - Q_{\eta,\xi}\right\|_{L^2(B_R(0)\setminus Z_\sigma)} = 0\,, \quad \chi_{F_\eta}\to\chi_F \text{ pointwise,} \tag{2.16}$$

   where $Z_\sigma = \{x\in\mathbb{R}^3 : x_1^2+x_2^2\le\sigma^2\}$ and $F_\eta = \{x\in\partial\Omega : \mathbf{n}^\eta(x)\cdot\nu(x) = -1\}$.

2. *$\Gamma-$liminf: For any sequence $Q_{\eta,\xi}\in\mathcal{A}$ and any measurable set of finite perimeter $F\subset\mathbb{S}^2$, measurable functions $\mathbf{n}^\eta:\Omega\to\mathbb{S}^2$ and a measurable set $\omega_\eta\subset\Omega$ that satisfy $\lim_{\eta\to0}|\omega_\eta| = 0$, $\Omega\setminus\omega_\eta$ simply connected with $\mathbf{n}^\eta\in C^0(\Omega\setminus(Z_\sigma\cup\omega_\eta),\mathbb{S}^2)$ and (2.16) hold for all $R,\sigma>0$, we have*

$$\liminf_{\eta\to0}\eta\,\mathcal{E}_{\eta,\xi}(Q_{\eta,\xi}) \ge \mathcal{E}_0(F)\,. \tag{2.17}$$

3. $\Gamma-$*limsup: For any measurable set of finite perimeter* $F \subset \mathbb{S}^2$ *that is invariant under rotations w.r.t. the* $\mathbf{e}_3-$*axis there exists a sequence* $Q_{\eta,\xi} \in \mathcal{A}$ *with* $\|Q_{\eta,\xi}\|_{L^\infty} \leq \sqrt{\frac{2}{3}} s_*$ *and measurable functions* $\mathbf{n}^\eta : \Omega \to \mathbb{S}^2$ *with* $\mathbf{n}^\eta \in C^0(\Omega \setminus \omega_\eta, \mathbb{S}^2)$, $\lim_{\eta\to 0} |\omega_\eta| = 0$, $\Omega \setminus \omega_\eta$ *simply connected, such that* (2.16) *holds for all* $R, \sigma > 0$ *and*

$$\limsup_{\eta\to 0} \eta\, \mathcal{E}_{\eta,\xi}(Q_{\eta,\xi}) \leq \mathcal{E}_0(F)\,. \tag{2.18}$$

Remark 2.3.2. *1. In view of (2.14) we can replace the bound* $\eta\, \mathcal{E}_{\eta,\xi}(Q_{\eta,\xi}) \leq C$, *by*

$$\mathcal{E}_{\eta,\xi}(Q_{\eta,\xi}) \leq C\ (1 + |\ln(\xi)|)\ . \tag{2.19}$$

2. *The convergence we show is not a* $\Gamma-$*convergence in the classical sense since the limit functional is defined on a different functions space.*

3. *The compactness can also be formulated globally: It holds*

$$\lim_{\eta\to 0} \int_{\Omega\setminus Z_\sigma} \mathrm{dist}^2(Q_{\eta,\xi}, \mathcal{N}_{\eta,\xi})\, \mathrm{d}x \ = \ 0$$

for the manifold $\mathcal{N}_{\eta,\xi}$ *as in Proposition 2.2.6 which is a small perturbation (at distance at most* $C\frac{\xi^2}{\eta^2}$*) from the manifold* $\mathcal{N}$. *In addition if* g *is non-negative (e.g. in the case* $g = g_2$*),* $\mathcal{N}_{\eta,\xi} = \mathcal{N}$ *and we have the convergence*

$$\lim_{\eta\to 0} \left\| s_* \left(\mathbf{n}^\eta \otimes \mathbf{n}^\eta - \frac{1}{3}\mathrm{Id} \right) - Q_{\eta,\xi} \right\|_{L^2(\Omega\setminus Z_\sigma)} \ = \ 0\,.$$

Remark 2.3.3. *If* $\beta = \infty$ *in* (2.14), *then Theorem 2.3.1 holds for* $F = \mathbb{S}^2$ *or* $F = \emptyset$, *i.e. no Saturn ring structure can occur in the limit. In the case of* g *being non-negative, this follows easily: For* $Q_{\eta,\xi} \in H^1(\Omega, \mathrm{Sym}_0) + Q_\infty$ *with* $\eta\mathcal{E}_{\eta,\xi}(Q_{\eta,\xi}) \leq C$ *we can introduce* $\tilde{\xi}$ *such that* $\eta|\ln(\tilde{\xi})| \to \beta \in (0,\infty)$, *i.e. this new sequence* $\tilde{\xi}$ *decreases more slowly than* ξ. *Hence* $\mathcal{E}_{\eta,\tilde{\xi}} \leq \mathcal{E}_{\eta,\xi}$. *Applying Theorem 2.3.1 to this new energy we get the existence of a set* $F_\beta \subset \mathbb{S}^2$ *such that*

$$\mathcal{E}_0(F_\beta) \leq \liminf_{\eta\to 0} \eta\, \mathcal{E}_{\eta,\xi}(Q_{\eta,\xi}) \leq C\,.$$

Since the RHS is independent of $\beta \in (0,\infty)$, *we find* $|D\chi_{F_\beta}|(\mathbb{S}^2) \to 0$ *as* $\beta \to \infty$. *From this we conclude* $F = \mathbb{S}^2$ *or* $F = \emptyset$ *which have the same energy* $\mathcal{E}_0$. *For the case of general* g *one cannot apply this trick, but using* (2.42) *it is possible to show that the perimeter of* F_η *converges to zero and that* $\mathcal{E}_0(\mathbb{S}^2)$ *is indeed a lower bound.*

2.4 Lower bound

In this section we prove the lower bound of Theorem 2.3.1. Our strategy to obtain the lower bound is the following: First, we approximate the sequence $Q_{\eta,\xi}$ by a more regular one named Q_ϵ. We use $\epsilon := \xi$ to meet the notation in [4, 40, 41] and let out η in our notation since η and ξ are related via (2.14), i.e. $\eta \sim \frac{\beta}{|\ln(\epsilon)|}$. We also write $\mathcal{E}_\epsilon$ instead of $\mathcal{E}_{\eta,\xi}$. We find that away from the $\mathbf{e}_3$-axis the sequence Q_ϵ has only finitely many singularities in the neighbourhood of which Q_ϵ is far from $\mathcal{N}$. Then we can estimate the energy of Q_ϵ nearby these points from below by balancing $|\nabla Q_\epsilon|^2$ and $f(Q_\epsilon)$. In the region where Q_ϵ is close to $\mathcal{N}$, we will use the optimal radial profile found in [4] by balancing $|\nabla Q_\epsilon|^2$ and $g(Q_\epsilon)$.

2.4.1 Preliminaries

The construction of the approximation Q_ϵ of $Q_{\eta,\xi}$ follows several steps. First, we are going to show that $Q_{\eta,\xi}$ can be approximated by another function $\widetilde{Q_{\eta,\xi}}$ which verifies an additional $L^\infty-$bound.

Proposition 2.4.1. *Let $Q_{\eta,\xi} \in H^1(\Omega, \mathrm{Sym}_0) + Q_{\infty,\xi,\eta}$ such that (2.19) holds. Then there exists a constant $C_1 > 0$ and $\widetilde{Q_{\eta,\xi}} \in H^1(\Omega, \mathrm{Sym}_0) + Q_{\infty,\xi,\eta}$ which decreases the energy $\mathcal{E}_{\eta,\xi}$, verifies*

$$\|\widetilde{Q_{\eta,\xi}}\|_{L^\infty(\Omega)} \leq C_1 \tag{2.20}$$

and $\widetilde{Q_{\eta,\xi}} - Q_{\eta,\xi} \to 0$ in L^2 as $\eta, \xi \to 0$.

Proof. Let $N > \sqrt{\frac{2}{3}} s_*$ to be chosen later. We can define $\widetilde{Q_{\eta,\xi}}$ as

$$\widetilde{Q_{\eta,\xi}} := \begin{cases} N \frac{Q_{\eta,\xi}}{|Q_{\eta,\xi}|} & \text{if } |Q_{\eta,\xi}| > N\,, \\ Q_{\eta,\xi} & \text{otherwise.} \end{cases}$$

This function is clearly admissible and has lower Dirichlet energy. Since we cannot conclude that $g(\widetilde{Q_{\eta,\xi}}) \leq g(Q_{\eta,\xi})$, we need to show that the (possible) increase of the energy in g is compensated by the decrease in f. So if $Q \in \mathrm{Sym}_0$ of norm 1 and $t > N$, we get by (2.6) and Proposition 2.2.2

$$\frac{\mathrm{d}}{\mathrm{d}t}\left(\frac{1}{\xi^2} f(tQ) + \frac{1}{\eta^2} g(tQ)\right) \;\geq\; C\frac{t^3}{\xi^2} - C\frac{1+t^3}{\eta^2} \;\geq\; 0$$

if $N \geq N_1$ with a certain N_1 large enough, depending on f and g. Hence, the sum of bulk and magnetic energy of $\widetilde{Q_{\eta,\xi}}$ is smaller than the one of $Q_{\eta,\xi}$ and we conclude $\mathcal{E}_{\eta,\xi}(\widetilde{Q_{\eta,\xi}}) \leq \mathcal{E}_{\eta,\xi}(Q_{\eta,\xi})$. The $L^\infty-$ bound is obvious. So it remains to show that $\|\widetilde{Q_{\eta,\xi}} - Q_{\eta,\xi}\|_{L^2(\Omega)}$ converges to zero as $\eta, \xi \to 0$. We decompose Ω into two sets

$$\Omega = \{x \,:\, |Q_{\eta,\xi}(x)| \leq N\} \cup \{x \,:\, |Q_{\eta,\xi}(x)| > N\}$$

and note that $\int |\widetilde{Q_{\eta,\xi}} - Q_{\eta,\xi}|^2 = 0$ if $|Q_{\eta,\xi}| \leq N$. Hence, we only need to estimate the difference $|\widetilde{Q_{\eta,\xi}} - Q_{\eta,\xi}|$ on the second set. By Proposition 2.2.2 and (2.5) we get that there exists $C, N_2 > 0$ (depending on f and g) such that if $N \geq N_2$, then for $Q \in \mathrm{Sym}_0$ with $|Q| \geq N$ it holds

$$\begin{aligned} \left|\frac{2}{3}s_*^2 - |Q|^2\right|^2 &\leq 2\left(\left|\frac{2}{3}s_*^2 - |Q|^2\right|^2 - \frac{\xi^2}{\eta^2}|Q|^4 + \xi^2 C_0(\xi,\eta)\right) \\ &\leq C\left(f(Q) + \frac{\xi^2}{\eta^2} g(Q) + \xi^2 C_0(\xi,\eta)\right). \end{aligned}$$

For $|Q| \geq \max\{N_1, N_2\}$ we additionally have $|Q_{\eta,\xi} - \widetilde{Q_{\eta,\xi}}| = |N - |Q_{\eta,\xi}||$. Taking N even bigger if necessary it holds that

$$\begin{aligned} \int_{|Q_{\eta,\xi}|>N} |Q_{\eta,\xi} - \widetilde{Q_{\eta,\xi}}|^2 \,\mathrm{d}x = \int_{|Q_{\eta,\xi}|>N} |N - |Q_{\eta,\xi}||^2 \,\mathrm{d}x &\leq C \int_{|Q_{\eta,\xi}|>N} \left|\frac{2}{3}s_*^2 - |Q_{\eta,\xi}|^2\right|^2 \mathrm{d}x \\ &\leq C \int_\Omega f(Q) + \frac{\xi^2}{\eta^2} g(Q) + \xi^2 C_0(\xi,\eta) \,\mathrm{d}x \leq C(1 + |\ln \xi|)\xi^2\,, \end{aligned}$$

which converges to zero as $\xi \to 0$. This proves our claim for $C_1 \geq N$. □

Since g may not be regular in $Q = 0$ (for example if $g = g_2$), we will replace g by $g\phi$, with a cut-off function ϕ such that $g\phi$ is smooth, but keeps the relevant information from g. In order to replace g in the energy, we just need to show that $\int (1-\phi) g(Q_{\eta,\xi}) \,\mathrm{d}x$ tends to zero in the limit $\xi, \eta \to 0$. This is made precise in the next proposition.

Proposition 2.4.2. *Let $\phi \in C^\infty([0,\infty),[0,1])$ be a cut-off function with $\phi = 1$ on $[q_0, \infty)$ and $\phi = 0$ on $[0, \frac{1}{2}q_0]$, where $q_0 \in (0, \sqrt{\frac{2}{3}} s_*)$. Then the function $Q \mapsto g(Q)\phi(|Q|)$ is smooth and there exists a constant $C > 0$ such that*

$$\int_\Omega (1 - \phi(|Q_{\eta,\xi}|)) g(Q_{\eta,\xi}) \,\mathrm{d}x \leq C\frac{\xi^2}{\eta}\,.$$

Proof. The smoothness of $g\phi$ is obvious, since ϕ is smooth and we supposed g smooth away from 0. So it remains the energy estimate. First note that if $Q \in \mathrm{Sym}_0$ with $|Q| \leq q_0$, then for ξ, η small enough $f(Q) + \frac{\xi^2}{\eta^2} g(Q) + \xi^2 C_0(\xi, \eta) \geq \frac{1}{2} f_{\min} > 0$, where $f_{\min} = \min\{f(Q) \,:\, Q \in \mathrm{Sym}_0,\, |Q| \leq q_0\}$. Indeed, by Proposition 2.2.2 $f_{\min} > 0$ and by (2.5) we can choose $\frac{\xi^2}{\eta^2}$ small enough such that $\frac{\xi^2}{\eta^2} g(Q) \leq \frac{1}{4} f_{\min}$. Since $\xi^2 C_0(\xi, \eta)$ converges to zero as $\xi, \eta \to 0$, this can equally be bounded by $\frac{1}{4} f_{\min}$. Hence

$$\begin{aligned} C &\geq \frac{\eta}{\xi^2} \int_{\{x \in \Omega \,:\, |Q_{\eta,\xi}(x)| \leq q_0\}} f(Q_{\eta,\xi}) + \frac{\xi^2}{\eta^2} g(Q_{\eta,\xi}) + \xi^2 C_0(\xi, \eta) \, \mathrm{d}x \\ &\geq \frac{1}{2} \frac{\eta}{\xi^2} f_{\min} |\{x \in \Omega \,:\, |Q_{\eta,\xi}(x)| \leq q_0\}| \,. \end{aligned}$$

Now we use this estimate to bound

$$\int_\Omega (1 - \phi(|Q_{\eta,\xi}|)) g(Q_{\eta,\xi}) \, \mathrm{d}x \leq C |\{x \in \Omega \,:\, |Q_{\eta,\xi}(x)| \leq q_0\}| \leq C \frac{\xi^2}{\eta} \,.$$

□

From now on, we simply write $g(Q)$ instead of $g(Q)\phi(|Q|)$. We will also replace η, ξ in our notation by ϵ, i.e. $\widetilde{Q_\epsilon} := \widetilde{Q_{\eta,\xi}}$. For the sake of readability, we introduce the notation $f_\epsilon(Q) := f(Q) + \frac{\epsilon^2}{\eta^2} g(Q) + \epsilon^2 C_0(\epsilon, \eta)$. The next step will be defining the more regular sequence Q_ϵ replacing $\widetilde{Q_\epsilon}$. In view of the lower bound for the claimed $\Gamma-$limit we still want Q_ϵ to be rotationally equivariant and that it converges to the same limit as $\widetilde{Q_\epsilon}$, while decreasing the energy.

We thus define the three dimensional approximate energy for $0 < \gamma < 2$ and $\omega \subset \Omega$

$$E_\epsilon^{3D}(Q, \omega) = \int_\omega \frac{1}{2} |\nabla Q|^2 + \frac{1}{\epsilon^2} f_\epsilon(Q) + \frac{1}{2\epsilon^\gamma} |Q - \widetilde{Q_\epsilon}|^2 \, \mathrm{d}x \,.$$

We seek Q_ϵ by minimizing $E_\epsilon^{3D}(Q, \Omega)$ among rotationally equivariant fields Q. Because of the equivariance, the problem can be stated as a two dimensional problem. Indeed, calculating $|\partial_\varphi Q|^2$ for a rotationally equivariant map $Q \in H^1(\Omega, \mathrm{Sym}_0) + Q_{\infty,\xi,\eta}$, and using the equivariance, we can write $Q(\rho, \varphi, z) = R_\varphi^\top Q(\rho, 0, z) R_\varphi$ and thus

$$|\partial_\varphi Q|^2 = \left|(\partial_\varphi R_\varphi)^\top Q R_\varphi + R_\varphi^\top Q (\partial_\varphi R_\varphi)\right|^2 = |Q|^2 + 6(Q_{12}^2 - Q_{11} Q_{22}) \,.$$

This expression does no longer depend on φ. In order to shorten notation, we introduce the matrix

$$Q_{2\times 2} := \frac{1}{2} \left(\frac{\partial}{\partial Q_{ij}} |\partial_\varphi Q|^2 \right)_{ij} = \begin{pmatrix} 2(Q_{11} - Q_{22}) & 4Q_{12} & Q_{13} \\ 4Q_{21} & 2(Q_{22} - Q_{11}) & Q_{23} \\ Q_{31} & Q_{32} & 0 \end{pmatrix} .$$

Note that, $Q_{2\times 2} : Q = \frac{1}{2} |\partial_\varphi Q|^2$. So the whole energy does not depend on φ any more and using cylindrical coordinates, it can be rewritten as

$$E_\epsilon^{3D}(Q_\epsilon, \Omega) = \int_0^{2\pi} E_\epsilon^{2D}(Q_\epsilon, \Omega') \, \mathrm{d}\varphi = 2\pi \, E_\epsilon^{2D}(Q_\epsilon, \Omega') \,,$$

where E_ϵ^{2D} is the two dimensional energy given by

$$E_\epsilon^{2D}(Q, \omega') = \int_{\omega'} \frac{\rho}{2} |\nabla' Q|^2 + \frac{1}{\rho} Q_{2\times 2} : Q + \frac{\rho}{\epsilon^2} f_\epsilon(Q) + \frac{\rho}{2\epsilon^\gamma} |Q - \widetilde{Q_\epsilon}|^2 \, \mathrm{d}\rho \, \mathrm{d}z \,,$$

where $\nabla' = (\partial_\rho, \partial_z)$ denotes the two dimensional gradient and $\omega' \subset \Omega' = \{(\rho, z) \in \mathbb{R}^2 \,:\, \rho > 0,\, \rho^2 + z^2 > 1\}$. In order to shorten notation, we are going to write $\frac{1}{2} |\nabla Q|^2$ instead of $\frac{1}{2} |\nabla' Q|^2 + \frac{1}{\rho^2} Q_{2\times 2} : Q$ whenever we make no use of this division of the gradient. Now we define Q_ϵ to be

$$Q_\epsilon := \operatorname*{argmin}_{Q \in \mathcal{A}'} E_\epsilon^{2D}(Q, \Omega') \,, \tag{2.21}$$

where $\mathcal{A}' = \{Q \in H^1(\Omega', \mathrm{Sym}_0) + Q_{\infty,\xi,\eta} : (2.13) \text{ holds for } \rho^2 + z^2 = 1\}$. We eventually extend Q_ϵ to a map in $H^1(\Omega, \mathrm{Sym}_0) + Q_{\infty,\xi,\eta}$ which we will also call Q_ϵ by defining $Q_\epsilon(\rho, \varphi, z) := R_\varphi^\top Q_\epsilon(\rho, z) R_\varphi$.

Remark 2.4.3. *1. Note that $\widetilde{Q_\epsilon}|_{\Omega'}$ is an admissible function in (2.21), so that Q_ϵ does exist.*

2. The function Q_ϵ has lower energy than $\widetilde{Q_\epsilon}$.

3. Thanks to the energy bound in (2.19) we know that

$$\|Q_\epsilon - \widetilde{Q_\epsilon}\|^2_{L^2(\Omega)} \leq C(|\ln\epsilon| + 1)\epsilon^\gamma \to 0 \quad \text{as } \epsilon \to 0\,,$$

i.e. the two sequences have the same limit for vanishing ϵ.

4. The minimizer Q_ϵ solves the two dimensional Euler-Lagrange equation

$$-\rho\Delta Q_\epsilon + \frac{1}{\rho}Q_{\epsilon,2\times 2} - \partial_\rho Q_\epsilon + \frac{\rho}{\epsilon^2}Df_\epsilon(Q) + \frac{\rho}{\epsilon^\gamma}(Q_\epsilon - \widetilde{Q_\epsilon}) = \Lambda\,\mathrm{Id}\,. \tag{2.22}$$

Note that the equation contains an additional term (RHS) due to the fact that Sym_0 is a subspace of the space of real matrices, i.e. a Lagrange multiplier Λ is needed to ensure the tracelessness constraint.

5. The function Q_ϵ also solves the three dimensional Euler-Lagrange equation

$$-\Delta Q_\epsilon + \frac{1}{\epsilon^2}Df_\epsilon(Q_\epsilon) + \frac{1}{\epsilon^\gamma}(Q_\epsilon - \widetilde{Q_\epsilon}) = \Lambda_{3D}\,\mathrm{Id}\,, \tag{2.23}$$

despite the fact that it does not need to be a minimizer of E^{3D}_ϵ. To see this, write

$$\begin{aligned}
\Lambda_{3D}\,\mathrm{Id} &= -\Delta Q_\epsilon + \frac{1}{\epsilon^2}Df_\epsilon(Q_\epsilon) + \frac{1}{\epsilon^\gamma}(Q_\epsilon - \widetilde{Q_\epsilon}) \\
&= -\partial^2_\rho Q_\epsilon - \frac{1}{\rho}\partial_\rho Q_\epsilon - \frac{1}{\rho^2}\partial^2_\varphi Q_\epsilon - \partial^2_z Q_\epsilon + \frac{1}{\epsilon^2}Df_\epsilon(Q) + \frac{1}{\epsilon^\gamma}(Q_\epsilon - \widetilde{Q_\epsilon}) \\
&= R_\varphi^\top\left(-\partial^2_\rho Q_\epsilon - \frac{1}{\rho}\partial_\rho Q_\epsilon - \partial^2_z Q_\epsilon + \frac{1}{\epsilon^\gamma}(Q_\epsilon - \widetilde{Q_\epsilon})\right)R_\varphi \\
&\quad - \frac{1}{\rho^2}\partial^2_\varphi(R_\varphi^\top Q_\epsilon R_\varphi) + \frac{1}{\epsilon^2}Df_\epsilon(R_\varphi^\top Q_\epsilon R_\varphi)\,.
\end{aligned}$$

One can explicitly calculate that $\partial^2_\varphi(R_\varphi^\top Q_\epsilon R_\varphi) = R_\varphi^\top Q_{2\times 2,\epsilon} R_\varphi$ and since f_ϵ is invariant under the change $Q \leftrightarrow R_\varphi^\top Q R_\varphi$, for symmetric matrices Q, we also have $Df_\epsilon(R_\varphi^\top Q_\epsilon R_\varphi) = R_\varphi^\top Df_\epsilon(Q_\epsilon)R_\varphi$. This implies that a rotationally equivariant extended solution of (2.22) is also solution of (2.23).

The last part of this subsection will be the following proposition which quantifies the regularity we have gained by replacing $\widetilde{Q_\epsilon}$ with Q_ϵ. This result relies on the three dimensional Euler-Lagrange equation. In fact, this is the only time we use (2.23) and cannot use (2.22) due to its singular behaviour near $\rho = 0$.

Proposition 2.4.4. *Let $\|\widetilde{Q_\epsilon}\|_{L^\infty} \leq C_1$ for a constant $C_1 \geq \sqrt{\frac{2}{3}}s_* > 0$ and let Q_ϵ be the rotationally equivariant extended minimizer of (2.21). Then $Q_\epsilon \in C^1(\Omega, \mathrm{Sym}_0)$,*

$$\|Q_\epsilon\|_{L^\infty} \leq C \quad \text{and} \quad \|\nabla Q_\epsilon\|_{L^\infty} \leq \frac{C}{\epsilon}\,.$$

Proof. From equation (2.23) and by elliptic regularity we deduce that for $\widetilde{Q_\epsilon} \in H^1$ we have $Q_\epsilon \in H^3$, i.e. $Q_\epsilon \in C^{1,\frac{1}{2}}$ since we are in dimension 3. Note that the boundary of Ω is smooth. To prove the L^∞-bounds we take a constant $C_2 > C_1$ such that $Df_\epsilon(Q) : Q \geq 0$ for all $Q \in \mathrm{Sym}_0$ with $|Q| \geq C_2$. This is possible due to Proposition 2.2.2 and (2.6). We define a comparison map

$$\overline{Q_\epsilon} := \begin{cases} C_2\frac{Q_\epsilon}{|Q_\epsilon|} & \text{if } |Q_\epsilon| > C_2\,, \\ Q_\epsilon & \text{otherwise.} \end{cases}$$

Then $|\nabla\overline{Q_\epsilon}| \leq |\nabla Q_\epsilon|$, $|\overline{Q_\epsilon} - \widetilde{Q_\epsilon}| \leq |Q_\epsilon - \widetilde{Q_\epsilon}|$ and $f_\epsilon(\overline{Q}) \leq f_\epsilon(Q_\epsilon)$ by Proposition 2.2.2 and our choice of C_2. Hence $E^{3D}_\epsilon(\overline{Q_\epsilon}, \Omega) \leq E^{3D}_\epsilon(Q_\epsilon, \Omega)$ with strict inequality unless $\overline{Q_\epsilon} = Q_\epsilon$. The estimate $\|\nabla Q_\epsilon\|_{L^\infty} \leq \frac{C}{\epsilon}$ follows from [29, Lemma A.2], using (2.23), (2.20) and $\gamma < 2$. □

2.4.2 Finite number of singularities away from $\rho = 0$

We introduce the notation $\Omega_\sigma := \{x \in \Omega : x_1^2 + x_2^2 \geq \sigma^2\} = \Omega \setminus Z_\sigma$ for $\sigma > 0$, with Z_σ defined as in Theorem 2.3.1. In the same spirit, we define the two dimensional analogue $\Omega'_\sigma = \{(\rho, z) \in \Omega' : \rho > \sigma\}$, i.e. Ω_σ can be obtained from Ω'_σ through rotation around the $\mathbf{e}_3-$axis.

The main theorem we want to prove in this subsection is the following:

Theorem 2.4.5. *For all $\sigma, \delta > 0$ there exists $\lambda_0, \epsilon_0 > 0$ such that for $\epsilon \leq \epsilon_0$ there is a set $X_\epsilon \subset \overline{\Omega'}$ which satisfies:*

1. *The set X_ϵ is finite and its cardinality is bounded independently of ϵ.*
2. *If $x \in \Omega'_\sigma$ and $\operatorname{dist}(x, X_\epsilon) > \lambda_0 \epsilon$, then $\operatorname{dist}(Q_\epsilon(x), \mathcal{N}) \leq \delta$.*

The general idea behind this subsection is the same as in [40, 41], where the analysis has been carried out for the case of minimizers of the energy $\int |\nabla Q_\epsilon|^2 + \frac{1}{\epsilon^2} f(Q_\epsilon)$ and uses ideas from [28]. We will show that in our situation with the modified bulk potential f_ϵ and the additional term $\frac{1}{\epsilon^\gamma}\|Q_\epsilon - \widetilde{Q_\epsilon}\|_{L^2}^2$ the same results hold. There are two main ingredients for the proof of Theorem 2.4.5: Proposition 2.4.11 that tells us that a singularity has an energy cost of order $|\ln \epsilon|$ and Proposition 2.4.7 that allows us to deduce that Q_ϵ is close to $\mathcal{N}$ (and hence being uniaxial) provided $\frac{1}{\epsilon^2}\int f_\epsilon(Q_\epsilon)$ is sufficiently small. While the second ingredient uses only the regularity of Q_ϵ, the first one makes use of equation (2.22) in the form of the following proposition.

Proposition 2.4.6 (Pohozaev identity)**.** *Let Q_ϵ be the minimizer of (2.21) and $\omega' \subset \Omega'$ open with Lipschitz boundary, $\overline{x} \in \omega'$. Then*

$$\begin{aligned}
&\int_{\partial\omega'} \rho((x-\overline{x})\cdot\nu)\left(\frac{1}{2}|\nabla' Q_\epsilon|^2 + \frac{1}{2\rho^2}|\partial_\varphi Q_\epsilon|^2 + \frac{1}{\epsilon^2} f_\epsilon(Q_\epsilon) + \frac{1}{2\epsilon^\gamma}|Q_\epsilon - \widetilde{Q_\epsilon}|^2\right) \\
&\quad = \frac{1}{2}\int_{\omega'} \rho|\nabla' Q_\epsilon|^2 + \frac{1}{2}\int_{\omega'} \frac{1}{\rho}|\partial_\varphi Q_\epsilon|^2 + \frac{3}{\epsilon^2}\int_{\omega'} \rho f_\epsilon(Q_\epsilon) + \frac{3}{2\epsilon^\gamma}\int_{\omega'} \rho|Q_\epsilon - \widetilde{Q_\epsilon}|^2 \\
&\qquad + \frac{1}{\epsilon^\gamma}\int_{\omega'} \rho(Q_\epsilon - \widetilde{Q_\epsilon}) : ((x-\overline{x})\cdot\nabla'\widetilde{Q}) + \int_{\partial\omega'} \rho\left((x-\overline{x})\cdot\nabla' Q_\epsilon\right) : \left(\nu\cdot\nabla' Q_\epsilon\right),
\end{aligned}$$

where ν denotes the outward unit normal vector on $\partial\omega'$.

Proof. To improve readability, we drop the subscripts ϵ in the proof. Our calculation only requires that Q is solution of equation (2.22).

Let $\omega' \subset \Omega'$ open with Lipschitz boundary and let $\overline{x} \in \omega'$ be an arbitrary point. By translation and without loss of generality we may assume that $\overline{x} = 0$. Testing the ij-component of equation (2.22) with $x_k\partial_k Q_{ij}$ and summing over i, j, k we find

$$\begin{aligned}
0 = &\sum_{i,j,k}\int_{\omega'} -\rho\Delta Q_{ij} x_k\partial_k Q_{ij} + \frac{1}{\epsilon^2}\int_{\omega'} \rho\frac{\partial f_\epsilon}{\partial Q_{ij}} x_k\partial_k Q_{ij} + \frac{1}{\epsilon^\gamma}\int_{\omega'} \rho(Q_{ij} - \widetilde{Q}_{ij}) x_k\partial_k Q_{ij} \\
&- \int_{\omega'} \partial_\rho Q_{ij} x_k\partial_k Q_{ij} + \int_{\omega'} \frac{1}{\rho} Q_{2\times 2,ij} x_k\partial_k Q_{ij} \\
=: &\, I + II + III + IV + V.
\end{aligned} \tag{2.24}$$

Note, that the RHS of (2.22) vanishes since Q_{ij} is traceless, i.e.

$$\sum_{i,j,k}\int_{\omega'} \Lambda\delta_{ij} x_k\partial_k Q_{ij} = \sum_k \int_{\omega'} \Lambda x_k\partial_k\left(\sum_{i,j}\delta_{ij}Q_{ij}\right) = \sum_k\int_{\omega'} \Lambda x_k\partial_k(\operatorname{tr}(Q)) = 0$$

For the first term (I) we calculate, using integration by parts

$$\begin{aligned}
\sum_{i,j,k,l}\int_{\omega'} -\rho\,\partial_l^2 Q_{ij} x_k\partial_k Q_{ij} = &\sum_{i,j,k,l}\int_{\omega'} \rho\,\partial_l Q_{ij}\delta_{lk}\partial_k Q_{ij} + \int_{\omega'} \rho\,\partial_l Q_{ij} x_k\partial_l\partial_k Q_{ij} \\
&- \int_{\partial\omega'} \rho\,\partial_l Q_{ij} x_k\partial_k Q_{ij}\nu_l + \int_{\omega'} \delta_{\rho l}\partial_l Q_{ij}\partial_k Q_{ij} x_k,
\end{aligned} \tag{2.25}$$

where ν is the outward-pointing normal vector on $\partial\omega'$. Note, that the last term reads $\int_{\omega'}(\partial_\rho Q) : ((x\cdot\nabla')Q)$ and thus is cancelled by (IV). We apply another integration by parts to the second term on the RHS of (2.25). This yields

$$\begin{aligned}\sum_{i,j,k,l}\int_{\omega'}\rho\,\partial_l Q_{ij}x_k\partial_l\partial_k Q_{ij} &= \sum_{i,j,k,l}\frac{1}{2}\int_{\omega'}\rho\,x_k\partial_k(\partial_l Q_{ij}\partial_l Q_{ij})\\ &= -\frac{2}{2}\sum_{i,j,l}\int_{\omega'}\rho\,\partial_l Q_{ij}\partial_l Q_{ij} + \sum_{i,j,k,l}\frac{1}{2}\int_{\partial\omega'}\rho\,\partial_l Q_{ij}\partial_l Q_{ij}x_k\nu_k\\ &\quad -\frac{1}{2}\int_{\omega'}\delta_{\rho k}x_k\partial_l Q_{ij}\partial_l Q_{ij}.\end{aligned}$$

Combined with (2.25) this gives

$$I+IV = \left(1-\frac{2}{2}-\frac{1}{2}\right)\int_{\omega'}\rho\,|\nabla' Q|^2 + \frac{1}{2}\int_{\partial\omega'}\rho\,|\nabla' Q|^2(x\cdot\nu) - \int_{\partial\omega'}\rho\,(x\cdot\nabla' Q):(\nu\cdot\nabla' Q). \tag{2.26}$$

The second integral (II) simply gives

$$II = \sum_k\frac{1}{\epsilon^2}\int_{\omega'}\rho\,\partial_k(f_\epsilon(Q))x_k = -\frac{1}{\epsilon^2}\int_{\omega'}3\rho\,f_\epsilon(Q) + \frac{1}{\epsilon^2}\int_{\partial\omega'}\rho\,f_\epsilon(Q)(x\cdot\nu). \tag{2.27}$$

For (III) we need to add (and subtract) the same integral with derivatives on $\widetilde{Q_{ij}}$. Then

$$\begin{aligned}III &= \frac{1}{\epsilon^\gamma}\int_{\omega'}\rho\,(Q_{ij}-\widetilde{Q}_{ij})\partial_k Q_{ij}x_k\\ &= \frac{1}{2\epsilon^\gamma}\int_{\omega'}\rho\,\partial_k(Q_{ij}-\widetilde{Q}_{ij})^2x_k + \frac{1}{\epsilon^\gamma}\int_{\omega'}\rho\,(Q_{ij}-\widetilde{Q}_{ij})\partial_k\widetilde{Q}_{ij}x_k\\ &= -\frac{3}{2\epsilon^\gamma}\int_{\omega'}\rho\,(Q_{ij}-\widetilde{Q}_{ij})^2 + \frac{1}{2\epsilon^\gamma}\int_{\partial\omega'}\rho\,(Q_{ij}-\widetilde{Q}_{ij})^2x_k\nu_k\\ &\quad + \frac{1}{\epsilon^\gamma}\int_{\omega'}\rho\,(Q_{ij}-\widetilde{Q}_{ij})\partial_k\widetilde{Q}_{ij}x_k.\end{aligned} \tag{2.28}$$

The fifth integral (V) simply gives

$$\begin{aligned}\int_{\omega'}\frac{1}{\rho}Q_{2\times2} : ((x\cdot\nabla')Q) &= \int_{\omega'}\frac{1}{2\rho}(x\cdot\nabla')(Q_{2\times2}:Q)\\ &= -\frac{1}{2}\int_{\omega'}\left(0+\frac{1}{\rho}\right)|\partial_\varphi Q|^2 + \frac{1}{2}\int_{\partial\omega'}(\nu\cdot x)\frac{1}{\rho}|\partial_\varphi Q|^2.\end{aligned} \tag{2.29}$$

Combining (2.26), (2.27), (2.28) and (2.29), the equality (2.24) reads

$$\begin{aligned}&\int_{\partial\omega'}\rho(x\cdot\nu)\left(\frac{1}{2}|\nabla' Q|^2 + \frac{1}{2\rho^2}|\partial_\varphi Q|^2 + \frac{1}{\epsilon^2}f_\epsilon(Q) + \frac{1}{2\epsilon^\gamma}|Q-\widetilde{Q}|^2\right)\\ &\qquad = \frac{1}{2}\int_{\omega'}\rho\,|\nabla' Q|^2 + \frac{1}{\rho}|\partial_\varphi Q|^2 + \frac{3}{\epsilon^2}\int_{\omega'}\rho\,f_\epsilon(Q) + \frac{3}{2\epsilon^\gamma}\int_{\omega'}\rho\,|Q-\widetilde{Q}|^2\\ &\qquad\quad + \frac{1}{\epsilon^\gamma}\int_{\omega'}\rho\,(Q-\widetilde{Q}):(x\cdot\nabla'\widetilde{Q}) + \int_{\partial\omega'}\rho\,(x\cdot\nabla' Q):(\nu\cdot\nabla' Q),\end{aligned}$$

which gives the result.

□

Since almost all term in consideration contain a ρ factor due to the passage from Ω to Ω'_σ, it is natural to introduce

$$\rho^\sigma_{\min}(x_0,l) := \inf\left\{\rho\ :\ (\rho,z)\in B_l(x_0)\cap\Omega'_\sigma\right\}, \tag{2.30}$$

for a point $x_0 \in \Omega'_\sigma$ and $l > 0$. Note that if we write $x_0 = (\rho_0, z_0)$, then $\rho^\sigma_{\min}(x_0, l) = \max\{\rho_0 - l, \sigma\}$. In particular, $\rho^\sigma_{\min}(x_0, l) \geq \sigma$.

The following proposition is a key ingredient in the proof of Theorem 2.4.5.

Proposition 2.4.7. *For all $\delta > 0$ there exist constants $\lambda_0, \mu_0 > 0$ such that for all $\sigma > 0$, $x_0 \in \Omega'_\sigma$, ϵ small enough and $l \in [\lambda_0\epsilon, 1]$ the following implication holds:*

$$\frac{1}{\epsilon^2}\int_{B_{2l}(x_0)\cap\Omega'_\sigma} \rho\, f_\epsilon(Q_\epsilon) \leq \mu_0\, \rho^\sigma_{\min}(x_0, 2l) \quad \Rightarrow \quad \operatorname{dist}(Q_\epsilon, \mathcal{N}) \leq \delta \text{ on } B_l(x_0)\cap\Omega'_\sigma\,.$$

Proof. We claim that λ_0, μ_0 can be defined as

$$\lambda_0 := \frac{\delta}{2C}\,, \quad \mu_0 := \frac{\pi}{8}\lambda_0^2 f_{\min}\,,$$

where C is a constant such that $\epsilon\|\nabla Q_\epsilon\|_{L^\infty} \leq C$ (see Proposition 2.4.4) and $f_{\min}$ is the minimum of f on the set $\{Q \in \mathrm{Sym}_0 \,:\, |Q| \leq \sqrt{\frac{2}{3}}s_*, \operatorname{dist}(Q, \mathcal{N}) \geq \delta/2\}$. Note that $f_{\min} > 0$ since on this compact set f is strictly positive. Furthermore, for ϵ small enough, we also have $f_\epsilon \geq \frac{1}{2}f_{\min}$ on this set.

In order to show that the definition indeed gives the desired implication, we argue by contradiction. Therefore we assume that there exists $x_0 \in \Omega$ and $l \in [\lambda_0\epsilon, 1]$ such that there is an $x \in B_l(x_0)\cap\Omega'_\sigma$ with $\frac{1}{\epsilon^2}\int_{B_{2l}(x_0)\cap\Omega'_\sigma} \rho\, f_\epsilon(Q_\epsilon) \leq \mu_0\rho^\sigma_{\min}(x_0, 2l)$ and $\operatorname{dist}(Q_\epsilon(x), \mathcal{N}) > \delta$.

This implies that $B_{\lambda_0\epsilon}(x) \subset B_{2l}(x_0)\cap(\mathbb{R}^2\setminus B_1(0))$. Indeed one can show that $\operatorname{dist}(x, \partial\Omega) > \lambda_0\epsilon$. Otherwise one would have $\operatorname{dist}(Q_\epsilon(x), \mathcal{N}) \leq \|\nabla Q_\epsilon\|_{L^\infty}\operatorname{dist}(x, \partial\Omega) \leq C\lambda_0 = \frac{\delta}{2}$ by definition of λ_0. This clearly contradicts the assumption that $\operatorname{dist}(Q_\epsilon(x), \mathcal{N}) > \delta$. Then, for all $y \in B_{\lambda_0\epsilon}(x)\cap\Omega'_\sigma$ by the triangle inequality

$$\operatorname{dist}(Q_\epsilon(y), \mathcal{N}) \geq \operatorname{dist}(Q_\epsilon(x), \mathcal{N}) - |Q_\epsilon(x) - Q_\epsilon(y)| > \delta - \lambda_0\epsilon\|\nabla Q_\epsilon\|_{L^\infty} \geq \frac{\delta}{2}\,.$$

By definition of $f_{\min}$ this implies $f_\epsilon(Q_\epsilon(y)) > \frac{1}{2}f_{\min}$. Since $B_{\lambda_0\epsilon}(x)\cap\Omega'_\sigma \subset B_{2l}(x_0)\cap\Omega'_\sigma$ and $|B_{\lambda_0\epsilon}(x)\cap\Omega'_\sigma| \geq \frac{1}{2}\pi(\lambda_0\epsilon)^2$ we know that

$$\begin{aligned}\frac{1}{\epsilon^2}\int_{B_{2l}(x_0)\cap\Omega'_\sigma} \rho\, f_\epsilon(Q_\epsilon) &\geq \frac{1}{\epsilon^2}\rho^\sigma_{\min}(x_0, 2l)\int_{B_{\lambda_0\epsilon}(x)\cap\Omega'_\sigma} f_\epsilon(Q_\epsilon)\\ &\geq \frac{1}{\epsilon^2}\rho^\sigma_{\min}(x_0, 2l)\frac{\pi}{2}(\lambda_0\epsilon)^2\frac{1}{2}f_{\min} = 2\mu_0\rho^\sigma_{\min}(x_0, 2l)\,,\end{aligned}$$

which contradicts our assumption. □

The next lemma basically tells us that for $\alpha \in (0, 1)$ there has to be some radius $r \leq \epsilon^{\alpha/2}$ so that we can control the energy on ∂B_r in terms of the energy on $B_{\epsilon^{\alpha/2}}$. It will become important later on when we will use it to bound the energy contributions of the boundary terms from Pohozaev identity (Proposition 2.4.6).

Lemma 2.4.8. *For all $x_0 \in \Omega'$ there exists $r \in (\epsilon^\alpha, \epsilon^{\frac{\alpha}{2}})$ (depending on x_0 and ϵ) such that*

$$\int_{\partial B_r(x_0)\cap\Omega'} \rho\left(\frac{1}{2}|\nabla Q_\epsilon|^2 + \frac{1}{\epsilon^2}f_\epsilon(Q_\epsilon) + \frac{1}{2\epsilon^\gamma}|Q_\epsilon - \widetilde{Q_\epsilon}|^2\right)\,\mathrm{d}x \leq \frac{4E^{2D}_\epsilon(Q_\epsilon, B_{\epsilon^{\alpha/2}}(x_0)\cap\Omega')}{\alpha r|\ln\epsilon|}\,.$$

Proof. The proof consists of an averaging argument. Assume that no such r exists. With the

notation $B' = B_{\epsilon^{\alpha/2}}(x_0) \cap \Omega'$, this would imply

$$\begin{aligned}
E_\epsilon^{2D}(Q_\epsilon, B') &= \int_0^{\epsilon^{\alpha/2}} \int_{\partial B_r(x_0)\cap\Omega'} \rho\left(\frac{1}{2}|\nabla Q_\epsilon|^2 + \frac{1}{\epsilon^2} f_\epsilon(Q_\epsilon) + \frac{1}{2\epsilon^\gamma}|Q_\epsilon - \widetilde{Q_\epsilon}|^2\right) \mathrm{d}x\, \mathrm{d}r \\
&\geq \int_{\epsilon^\alpha}^{\epsilon^{\alpha/2}} \int_{\partial B_r(x_0)\cap\Omega'} \rho\left(\frac{1}{2}|\nabla Q_\epsilon|^2 + \frac{1}{\epsilon^2} f_\epsilon(Q_\epsilon) + \frac{1}{2\epsilon^\gamma}|Q_\epsilon - \widetilde{Q_\epsilon}|^2\right) \mathrm{d}x\, \mathrm{d}r \\
&\geq \frac{4E_\epsilon^{2D}(Q_\epsilon, B')}{\alpha|\ln\epsilon|} \int_{\epsilon^\alpha}^{\epsilon^{\alpha/2}} \frac{1}{r}\, \mathrm{d}r \\
&= \frac{4E_\epsilon^{2D}(Q_\epsilon, B')}{\alpha|\ln\epsilon|} \frac{\alpha}{2}|\ln(\epsilon)| \\
&= 2E_\epsilon^{2D}(Q_\epsilon, B')\,.
\end{aligned}$$

This gives that $E_\epsilon^{2D}(Q_\epsilon, B') = 0$ and thus Q_ϵ is constant on B' and $Q_\epsilon = \widetilde{Q_\epsilon} \equiv Q_{\infty,\epsilon}$. But since the constant map $Q_{\infty,\epsilon}$ satisfies the lemma, we get a contradiction. □

The following two results (Lemma 2.4.10 and Proposition 2.4.11) are similar to [28], see also [41, Lemma 1.4.8, Proposition 1.4.9]. Lemma 2.4.10 states that we can derive a better bound (independent of ϵ) than (2.19) on balls B_{ϵ^α} for the energy contribution of f_ϵ. Then Proposition 2.4.11 tells us the cost in terms of energy for such a ball if Q_ϵ is not close to $\mathcal{N}$. Both results rely on the Pohozaev identity (Proposition 2.4.6) and Lemma 2.4.8. We start with a proposition that will help us in the proof of Lemma 2.4.10 to obtain estimates at the boundary of $\partial\Omega'$.

Proposition 2.4.9. *There exist constants $C_\Omega, \epsilon_1 > 0$ such that for all $0 < \epsilon \leq \epsilon_1$, $r \in (\epsilon^\alpha, \epsilon^{\frac{\alpha}{2}})$ and $y \in \Omega'$ there exists $z \in B_r(y) \cap \Omega'$ such that*

$$\nu(x) \cdot (x - z) \geq C_\Omega r \quad \forall x \in \partial\Omega' \cap B_r(y)\,,$$

where ν is the outward unit normal on $\partial\Omega'$.

Proof. Let us start by considering the domain $R = \{(x_1, x_2) \in \mathbb{R}^2 \,:\, x_1, x_2 > 0\}$. Let $y \in R$ and $r > 0$ such that $B_r(y) \cap \partial R \neq \emptyset$ (otherwise the result is trivial). Let $L_1 = |\{x_2 = 0\} \cap B_r(y)|$ and $L_2 = |\{x_1 = 0\} \cap B_r(y)|$. Then we define $z = y + \frac{r}{2}\left(R_1/L(0,1)^\top + L_1/L(1,0)^\top\right)$, where $L^2 = L_1^2 + L_2^2$. We will show that this definition of z indeed satisfies our claim. Without loss of generality we may assume that $y_1 \geq y_2$. We consider the following cases:

1. $(0,0) \in B_r(y)$. In this case, $L_1 = y_1 + \sqrt{r^2 - y_2^2}$ and $L_2 = y_2 + \sqrt{r^2 - y_1^2}$. Let $x = (x_1, 0)$. Then $\nu(x) = (0, -1)^\top$ and

   $$\nu(x) \cdot (x - z) = (y_2 - x_2) + \frac{r}{2}\frac{L_1}{L} \geq \frac{r}{2}\frac{L_1}{L}\,.$$

   Analogously, for $x = (0, x_2)$ we find $\nu \cdot (x - z) \geq \frac{r}{2}\frac{L_2}{L}$. Since $y_1 \geq y_2$ we have also the inequality $L_1 \geq L_2$. Minimizing L_2/L subject to the constraint $y_1 \geq y_2$ we get $y_1 = y_2$ and thus $L_1 = L_2$, i.e. $\nu(x) \cdot (x - z) \geq \frac{r}{2\sqrt{2}}$.

2. $L_2 \neq 0$ and $(0,0) \notin B_r(y)$. Then $L_1 = 2\sqrt{r^2 - y_2^2}$ and $L_2 = 2\sqrt{r^2 - y_1^2}$. A similar calculation as in the first case shows that $\nu(x) \cdot (x - z) \geq \frac{r}{2\sqrt{2}}$.

3. $L_2 = 0$. The lengths L_1, L_2 are given as in the second case, but since $L_2 = 0$ we get directly $\nu(x) \cdot (x - z) \geq \frac{r}{2}\frac{L_1}{L} = \frac{r}{2}$.

Now we consider the domain Ω'. For a radius $0 < r < \frac{1}{2}$ the angular difference between the normal vectors of Ω' and R is smaller than $\arccos(1 - r)$. Thus, for ϵ_1 small enough, $0 < \epsilon \leq \epsilon_1$, $r \in (\epsilon^\alpha, \epsilon^{\frac{\alpha}{2}})$, we can find $C_\Omega > 0$ such that

$$\nu(x) \cdot (x - z) \geq \frac{r}{2}\cos\left(\frac{\pi}{4} + \arccos(1 - r)\right) \geq \frac{r}{2}\cos\left(\frac{\pi}{4} + \arccos(1 - \epsilon_1^{\alpha/2})\right) \geq C_\Omega\, r > 0\,.$$

□

Lemma 2.4.10. *Let $x_0 \in \Omega'$. Then there exists a constant $C_\alpha > 0$ which depends only on α, γ, Ω, the energy bound in (2.19) and the boundary data in* (2.13) *such that if ϵ is small enough*

$$\frac{1}{\epsilon^2}\int_{B_{\epsilon^\alpha}(x_0)\cap\Omega'} \rho\, f_\epsilon(Q_\epsilon)\,\mathrm{d}x \le C_\alpha\,.$$

Proof. By Lemma 2.4.8 there exists $r \in (\epsilon^\alpha, \epsilon^{\frac{\alpha}{2}})$ and a constant $\overline{C} > 0$ such that for ϵ small enough

$$\int_{\partial B_r(x_0)\cap\Omega'} \rho\left(\frac{1}{2}|\nabla Q_\epsilon|^2 + \frac{1}{\epsilon^2} f_\epsilon(Q_\epsilon) + \frac{1}{2\epsilon^\gamma}|Q_\epsilon - \widetilde{Q_\epsilon}|^2\right) \le \frac{\overline{C}}{\alpha r}\,, \tag{2.31}$$

where we also used the energy bound (2.19).

Now assume in a first step that $B_r(x_0) \subset \Omega'$. Using the Pohozaev identity from Proposition 2.4.6 with $\omega' = B_r(x_0)$ and $\overline{x} = x_0$, we find

$$\begin{aligned}\frac{3}{\epsilon^2}\int_{B_r(x_0)} \rho\, f_\epsilon(Q_\epsilon) \le{}& \int_{\partial B_r(x_0)} \rho\,((x-x_0)\cdot\nu)\left(\frac{1}{2}|\nabla Q_\epsilon|^2 + \frac{1}{\epsilon^2} f_\epsilon(Q_\epsilon) + \frac{1}{2\epsilon^\gamma}|Q_\epsilon - \widetilde{Q_\epsilon}|^2\right)\\ &+ \frac{1}{\epsilon^\gamma}\int_{B_r(x_0)} \rho\,|Q_\epsilon - \widetilde{Q_\epsilon}||(x-x_0)\cdot\nabla'\widetilde{Q_\epsilon}|\\ &- \int_{\partial B_r(x_0)} \rho\,((x-x_0)\cdot\nabla' Q_\epsilon) : (\nu\cdot\nabla' Q_\epsilon)\,.\end{aligned} \tag{2.32}$$

Notice that since $x \in \partial B_r(x_0)$ we have $(x-x_0)\cdot\nabla' Q_\epsilon = r\nu\cdot\nabla' Q_\epsilon$, i.e.

$$((x-x_0)\cdot\nabla' Q_\epsilon) : (\nu\cdot\nabla' Q_\epsilon) = r\,|\nu\cdot\nabla' Q_\epsilon|^2 \ge 0\,,$$

and $(x-x_0)\cdot\nu = r|\nu|^2 = r$. Substituting this into (2.32), one gets

$$\begin{aligned}\frac{3}{\epsilon^2}\int_{B_r(x_0)} \rho\, f_\epsilon(Q_\epsilon) \le{}& r\int_{\partial B_r(x_0)} \rho\,\left(\frac{1}{2}|\nabla Q_\epsilon|^2 + \frac{1}{\epsilon^2} f_\epsilon(Q_\epsilon) + \frac{1}{2\epsilon^\gamma}|Q_\epsilon - \widetilde{Q_\epsilon}|^2\right)\\ &+ \frac{1}{\epsilon^\gamma}\int_{B_r(x_0)} \rho\,|Q_\epsilon - \widetilde{Q_\epsilon}||(x-x_0)\cdot\nabla'\widetilde{Q_\epsilon}|\,.\end{aligned}$$

By (2.31) and Cauchy-Schwarz inequality this entails

$$\begin{aligned}\frac{3}{\epsilon^2}\int_{B_r(x_0)} \rho\, f_\epsilon(Q_\epsilon)\,\mathrm{d}x &\le r\frac{\overline{C}}{\alpha r} + \frac{r}{\epsilon^\gamma}\left(\int_{B_r(x_0)} \rho\,|Q_\epsilon - \widetilde{Q_\epsilon}|^2\right)^{\frac{1}{2}}\left(\int_{B_r(x_0)} \rho\,|\nabla'\widetilde{Q_\epsilon}|^2\right)^{\frac{1}{2}}\\ &\le \frac{\overline{C}}{\alpha} + C\frac{\epsilon^{\frac{\alpha}{2}}}{\epsilon^\gamma}\left((1+|\ln\epsilon|)^2\epsilon^\gamma\right)^{\frac{1}{2}} \le \frac{\overline{C}}{\alpha} + C\epsilon^{(\alpha-\gamma)/4}\,,\end{aligned}$$

provided $\alpha > \gamma$ and ϵ small enough. This proves the claim in the case where $B_r(x_0) \subset \Omega'$.

In a second step we show that the result also holds if $B_r(x_0) \not\subseteq \Omega'$. We define $\Gamma = B_r(x_0)\cap\partial\Omega'$ which is now non-empty. This enables us to write $\partial(B_r(x_0)\cap\Omega') = \Gamma \cup (\partial B_r(x_0)\cap\Omega')$. Again we apply Proposition 2.4.6 with $\omega' = B_r(x_0)\cap\Omega'$ but this time we set $\overline{x} = z$, where $z \in \Omega'\cap B_r(x_0)$ is given by Proposition 2.4.9 for $y = x_0$. By Proposition 2.4.6 we get

$$\begin{aligned}\frac{3}{\epsilon^2}\int_{B_r(x_0)\cap\Omega'} \rho\, f_\epsilon(Q_\epsilon)\,\mathrm{d}x \le{}& \int_{\partial B_r(x_0)\cap\Omega'} \rho\,((x-\overline{x})\cdot\nu)\left(\frac{1}{2}|\nabla Q_\epsilon|^2 + \frac{1}{\epsilon^2} f_\epsilon(Q_\epsilon) + \frac{1}{2\epsilon^\gamma}|Q_\epsilon - \widetilde{Q_\epsilon}|^2\right)\\ &+ \int_\Gamma \rho\,((x-\overline{x})\cdot\nu)\left(\frac{1}{2}|\nabla Q_\epsilon|^2 + \frac{1}{\epsilon^2} f_\epsilon(Q_\epsilon) + \frac{1}{2\epsilon^\gamma}|Q_\epsilon - \widetilde{Q_\epsilon}|^2\right)\\ &- \frac{3}{2\epsilon^\gamma}\int_{B_r(x_0)\cap\Omega'} \rho\,|Q_\epsilon - \widetilde{Q_\epsilon}|^2 - \frac{1}{\epsilon^\gamma}\int_{B_r(x_0)\cap\Omega'} \rho\,(Q_\epsilon - \widetilde{Q_\epsilon}) : ((x-\overline{x})\cdot\nabla'\widetilde{Q})\\ &- \int_\Gamma \rho\,((x-\overline{x})\cdot\nabla' Q_\epsilon) : (\nu\cdot\nabla' Q_\epsilon) - \int_{\partial B_r(x_0)\cap\Omega'} \rho\,((x-\overline{x})\cdot\nabla' Q_\epsilon) : (\nu\cdot\nabla' Q_\epsilon)\,,\end{aligned}$$

where we denoted ν the unit outward normal. For the integrals on $\partial B_r(x_0)\cap\Omega'$ and $B_r(x_0)\cap\Omega'$ we proceed as before using $|(x-\overline{x})\cdot\nu|\le 2r$. Note, that this time $(x-\overline{x})\cdot\tau$ does not necessarily vanish. Nevertheless, the integral involving this term can be estimated from above by $\int_{\partial B_r\cap\Omega'} 2r\rho\,|\nabla' Q_\epsilon|^2$ and then be estimated using (2.31). Now we estimate the integrals involving Γ. First note that $Q_\epsilon = \widetilde{Q_\epsilon} = Q_b$ on $\Gamma\cap\partial\Omega$ with $f(Q_b)=0$, i.e. $\int_{\Gamma\cap\partial\Omega}\rho\, f(Q_\epsilon)=0$,$\int_{\Gamma\cap\partial\Omega}\rho\, f_\epsilon(Q_\epsilon)\le C_{Q_b}\epsilon^{\alpha/2}/\eta^2$ and $\int_{\Gamma\cap\partial\Omega}\rho\,|Q_\epsilon-\widetilde{Q_\epsilon}|^2=0$. On $\Gamma\setminus\partial\Omega\subset\{\rho=0\}$ we find that all integrals vanish because of the bounds in Q_ϵ established in Proposition 2.4.4. We are left with the two integrals on $\Gamma\cap\partial\Omega$ with gradients. The idea is now to split the gradient into a tangential and a normal part. The tangential part depends only on the boundary data Q_b, the normal part needs to be estimated. So let τ be the unit tangent vector on Γ. Decomposing $\nabla' Q_\epsilon = (\nu\cdot\nabla' Q_\epsilon)\nu + (\tau\cdot\nabla' Q_\epsilon)\tau$ and substituting this into $\int_{\Gamma\cap\partial\Omega}\rho(x-\overline{x})\cdot\nu\frac{1}{2}|\nabla' Q_\epsilon|^2$ yields

$$\begin{aligned}\frac{3}{\epsilon^2}\int_{B_r(x_0)\cap\Omega'}\rho\, f_\epsilon(Q_\epsilon)\,\mathrm{d}x &\le 4\frac{\overline{C}}{\alpha}+C\epsilon^{(\alpha-\gamma)/4}+C_{Q_b}\epsilon^{\alpha/4}-\int_{\Gamma\cap\partial\Omega}\rho\,((x-\overline{x})\cdot\nabla' Q_\epsilon):(\nu\cdot\nabla' Q_\epsilon)\\ &\quad+\frac{1}{2}\int_{\Gamma\cap\partial\Omega}\rho\,((x-\overline{x})\cdot\nu)|\nu\cdot\nabla' Q_\epsilon|^2+\frac{1}{2}\int_{\Gamma\cap\partial\Omega}\rho\,((x-\overline{x})\cdot\nu)|\tau\cdot\nabla' Q_\epsilon|^2\\ &\le 4\frac{\overline{C}}{\alpha}+C\epsilon^{(\alpha-\gamma)/4}+C_{Q_b}\epsilon^{\alpha/4}-\frac{1}{2}\int_{\Gamma\cap\partial\Omega}\rho\,((x-\overline{x})\cdot\nu)|\nu\cdot\nabla' Q_\epsilon|^2\\ &\quad-\int_{\Gamma\cap\partial\Omega}\rho\,((x-\overline{x})\cdot\tau)(\tau\cdot\nabla' Q_b):(\nu\cdot\nabla' Q_\epsilon)\,,\end{aligned}$$

where we used that $(x-\overline{x})=((x-\overline{x})\cdot\nu)\nu+((x-\overline{x})\cdot\tau)\cdot\tau$ and that $\tau\cdot\nabla' Q_\epsilon=\tau\cdot\nabla' Q_b$ only depends on the given boundary values. We apply the inequality $ab\le a^2/(2C^2)+C^2b^2/2$ with $C=\sqrt{C_\Omega/2}$ from Proposition 2.4.9 to get

$$\begin{aligned}\frac{3}{\epsilon^2}\int_{B_r(Q_\epsilon)\cap\Omega'}\rho\, f_\epsilon(Q_\epsilon)\,\mathrm{d}x &\le 4\frac{\overline{C}}{\alpha}+C\epsilon^{(\alpha-\gamma)/4}+C_{Q_b}\epsilon^{\alpha/4}-\frac{1}{2}\int_{\Gamma\cap\partial\Omega}\rho\,((x-\overline{x})\cdot\nu)|\nu\cdot\nabla' Q_\epsilon|^2\\ &\quad+\frac{1}{C_\Omega}\int_{\Gamma\cap\partial\Omega}\rho\,|(x-\overline{x})\cdot\tau||\tau\cdot\nabla' Q_b|^2+\frac{C_\Omega}{4}\int_{\Gamma\cap\partial\Omega}\rho\,|(x-\overline{x})\cdot\tau||\nu\cdot\nabla' Q_\epsilon|^2\,.\end{aligned}$$

Then we apply Proposition 2.4.9 to get

$$\begin{aligned}\frac{1}{\epsilon^2}\int_{B_r(Q_\epsilon)\cap\Omega'}\rho\, f_\epsilon(Q_\epsilon)\,\mathrm{d}x &\le 4\frac{\overline{C}}{\alpha}+C\epsilon^{(\alpha-\gamma)/4}+C_{Q_b}\epsilon^{\alpha/4}-\frac{1}{2}\int_{\Gamma\cap\partial\Omega}C_\Omega r\rho\,|\nu\cdot\nabla' Q_\epsilon|^2\\ &\quad+\frac{C_\Omega}{4}\int_{\Gamma\cap\partial\Omega}2r\rho\,|\nu\cdot\nabla' Q_\epsilon|^2\\ &=4\frac{\overline{C}}{\alpha}+C\epsilon^{(\alpha-\gamma)/4}+C_{Q_b}\epsilon^{\alpha/4}\,.\end{aligned}$$

□

We have now all the necessary tools to prove the second important ingredient for the proof of Theorem 2.4.5.

Proposition 2.4.11. *For all $\delta,\sigma>0$ there exist $\epsilon_2,\zeta_\alpha>0$ such that for $0<\epsilon\le\epsilon_2$ and $x_0\in\Omega'_\sigma$ the following implication holds:*

$$\mathrm{dist}(Q_\epsilon(x_0),\mathcal{N})>\delta \quad\Rightarrow\quad E_\epsilon^{2D}(Q_\epsilon,B_{\epsilon^\alpha}(x_0)\cap\Omega')\ge\zeta_\alpha(|\ln\epsilon|+1)\rho^\sigma_{\min}(x_0,\epsilon^\alpha)\,,$$

with $\rho^\sigma_{\min}\ge\sigma$ defined as in (2.30). The constant ζ_α can be chosen to be dependent only on α and δ, while ϵ_2 depends on $\delta,\sigma,\alpha,\gamma$.

Proof. Let's assume that the conclusion does not hold at $x_0\in\Omega'_\sigma$, i.e. $E_\epsilon^{2D}(Q_\epsilon,B_{\epsilon^\alpha}(x_0)\cap\Omega')\le\zeta_\alpha(|\ln\epsilon|+1)\rho^\sigma_{\min}(x_0,\epsilon^\alpha)$. Then there exists a radius $r\in(\epsilon^{2\alpha},\epsilon^\alpha)$ such that

$$\int_{\partial B_r(x_0)\cap\Omega'}\rho\left(\frac{1}{2}|\nabla Q_\epsilon|^2+\frac{1}{\epsilon^2}f_\epsilon(Q_\epsilon)+\frac{1}{2\epsilon^\gamma}|Q_\epsilon-\widetilde{Q_\epsilon}|^2\right)\mathrm{d}x\le\frac{2\zeta_\alpha\rho^\sigma_{\min}(x_0,\epsilon^\alpha)}{\alpha r}\,.\tag{2.33}$$

Indeed, otherwise

$$E_\epsilon^{2D}(Q_\epsilon, B_{\epsilon^\alpha}(x_0) \cap \Omega') \geq \int_{\epsilon^{2\alpha}}^{\epsilon^\alpha} \frac{2\zeta_\alpha \rho_{\min}^\sigma(x_0, \epsilon^\alpha)}{\alpha r} \, \mathrm{d}r = 2\zeta_\alpha \rho_{\min}^\sigma(x_0, \epsilon^\alpha) |\ln(\epsilon)| \,,$$

which clearly contradicts our assumption for $\epsilon < \frac{1}{e}$.

Replacing (2.31) by (2.33) in the proof of Lemma 2.4.10, i.e. $\overline{C} = 2\zeta_\alpha \rho_{\min}^\sigma(x_0, \epsilon^\alpha)$, we find

$$\frac{1}{\epsilon^2} \int_{B_r(x_0) \cap \Omega'} \rho \, f_\epsilon(Q_\epsilon) \leq \frac{8\zeta_\alpha \rho_{\min}^\sigma(x_0, \epsilon^\alpha)}{\alpha} + C\epsilon_2^{(\alpha-\gamma)/4} \,,$$

where the constant C can be chosen to be independent of α and ϵ. We choose ϵ_2 small enough such that it satisfies the estimate $\lambda_0 \epsilon_2 < \frac{1}{2}\epsilon_2^\alpha$. Now choose $\zeta_\alpha \leq \frac{\alpha \mu_0}{16}$ and $\epsilon_2 \leq (\frac{\mu_0 \sigma}{2C})^{\frac{4}{\alpha-\gamma}}$, where μ_0 is the constant from Proposition 2.4.7. These bounds imply that $\mu_0 \rho_{\min}^\sigma(x_0, \epsilon^\alpha) \geq \frac{8\zeta_\alpha \rho_{\min}^\sigma(x_0, \epsilon^\alpha)}{\alpha} + C\epsilon_2^{(\alpha-\gamma)/4}$, i.e. we can apply Proposition 2.4.7 with $l = \frac{1}{2}\epsilon^\alpha$. This implies $\operatorname{dist}(Q_\epsilon(x_0), \mathcal{N}) \leq \delta$, which proves the claim. □

Now we can finally prove Theorem 2.4.5 and define the set of singularities X_ϵ. To do this, one can proceed as follows: In a first step we cover Ω with balls of size ϵ^α and look for balls where the energy is large. The number of such balls has to be finite because of the energy bound. In view of Proposition 2.4.11, Q_ϵ will be almost uniaxial outside of these balls. In the second step we improve our estimates to the scale ϵ. We cover the balls with high energy from step one with balls of size ϵ and determine balls where f is large. By Lemma 2.4.10 this number will be finite too and Proposition 2.4.7 implies that Q_ϵ is indeed close to $\mathcal{N}$ on all other balls. We can then take X_ϵ to be the set of all centers of balls with large energy.

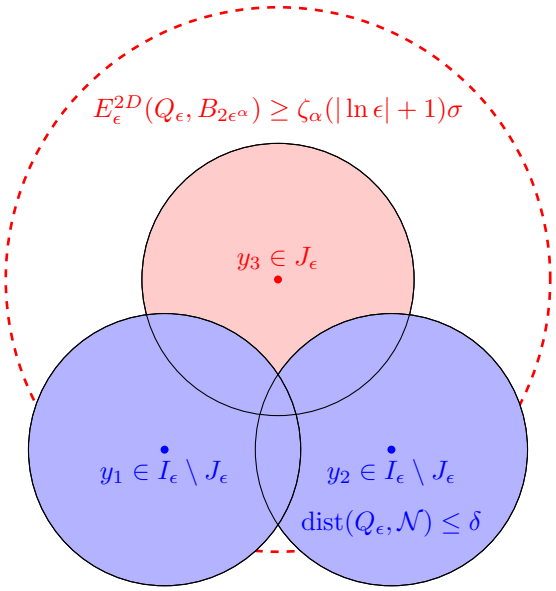

Figure 2.1: First covering argument: Find balls B_{ϵ^α}, where the energy is large

Proof of Theorem 2.4.5. Let $\delta, \sigma > 0$ be given and choose $\alpha \in (0,1)$. Let $\{B_{\epsilon^\alpha}(y) \,:\, y \in \Omega'\}$ be a covering of Ω'. By Vitali Covering Lemma there exists a countable family of points $\{y_i\}_{i \in I_\epsilon}$ such that

$$\Omega' \subset \bigcup_{i \in I_\epsilon} B_{\epsilon^\alpha}(y_i) \,, \quad B_{\frac{1}{5}\epsilon^\alpha}(y_i) \cap B_{\frac{1}{5}\epsilon^\alpha}(y_j) = \emptyset \text{ if } i \neq j \,.$$

Let $\zeta_\alpha > 0$ be given as in Proposition 2.4.11. We define

$$J_\epsilon := \left\{ i \in I_\epsilon \,:\, E_\epsilon^{2D}(Q_\epsilon, B_{2\epsilon^\alpha}(y_i) \cap \Omega') > \zeta_\alpha(1 + |\ln \epsilon|)\sigma \right\} .$$

Then by the energy bound (2.19),

$$\zeta_\alpha(1+|\ln\epsilon|)\sigma\#J_\epsilon \le \sum_{i\in J_\epsilon} E_\epsilon^{2D}(Q_\epsilon, B_{2\epsilon^\alpha}(y_i)\cap\Omega') \le CE_\epsilon^{2D}(Q_\epsilon,\Omega') \le C(1+|\ln\epsilon|)\,. \tag{2.34}$$

Indeed, note that there is a constant C depending only on the space dimension such that each point in Ω' is covered by at most C balls. This implies the second inequality in (2.34). From (2.34) we directly infer that the cardinality of J_ϵ is bounded by a constant dependent on δ,σ,α as well as the space dimension and the energy bound, but independent of ϵ. Let $i\in I_\epsilon\setminus J_\epsilon$ and $x_0\in B_{\epsilon^\alpha}(y_i)\cap\Omega'_\sigma$. If $\operatorname{dist}(Q_\epsilon(x_0),\mathcal{N})>\delta$ we deduce by Proposition 2.4.11 that $E_\epsilon^{2D}(Q_\epsilon, B_{2\epsilon^\alpha}(y_i)\cap\Omega') \ge E_\epsilon^{2D}(Q_\epsilon, B_{\epsilon^\alpha}(x_0)\cap\Omega') > \zeta_\alpha(|\ln(\epsilon)|+1)\sigma$, a contradiction to $i\in I_\epsilon\setminus J_\epsilon$. Hence

$$\operatorname{dist}(Q_\epsilon(x),\mathcal{N})\le\delta \quad \forall x\in B_{\epsilon^\alpha}(y_i)\cap\Omega'_\sigma, i\in I_\epsilon\setminus J_\epsilon\,.$$

See also Figure 2.1. Note, that this estimate is not good enough since we announced the radius around points in X_ϵ to be of order ϵ instead of ϵ^α.

Now fix $i\in J_\epsilon$. Again by Vitali Covering Lemma we can consider a covering of $B_{\epsilon^\alpha}(y_i)\cap\Omega'_\sigma$ of the form

$$B_{\epsilon^\alpha}(y_i)\cap\Omega'_\sigma \subset \bigcup_{j\in I_{\epsilon,i}} B_{\lambda_0\epsilon}(z_j)\,,\quad B_{\frac15\lambda_0\epsilon}(z_j)\cap B_{\frac15\lambda_0\epsilon}(z_k)=\emptyset \text{ if } j\neq k\,,$$

with all $z_j\in B_{\epsilon^\alpha}(y_i)$ and where λ_0 is given by Proposition 2.4.7. Furthermore, we define

$$J_{\epsilon,i} := \left\{ j\in I_{\epsilon,i} \,:\, \frac{1}{\epsilon^2}\int_{B_{2\lambda_0\epsilon}(z_j)\cap\Omega'_\sigma} \rho\, f_\epsilon(Q_\epsilon) \ge \mu_0\,\sigma \right\},$$

with μ_0 again from Proposition 2.4.7. By Lemma 2.4.10, recalling that $2\lambda_0\epsilon<\epsilon^\alpha$

$$\mu_0\,\sigma\,\#J_{\epsilon,i} \le \sum_{j\in J_{\epsilon,i}} \frac{1}{\epsilon^2}\int_{B_{2\lambda_0\epsilon}(z_j)\cap\Omega'_\sigma}\rho\, f_\epsilon(Q_\epsilon) \le \frac{C}{\epsilon^2}\int_{B_{\epsilon^\alpha}(y_i)\cap\Omega'}\rho\, f_\epsilon(Q_\epsilon)\le C_\alpha\,, \tag{2.35}$$

so that $\#J_{\epsilon,i}$ is also bounded independently of ϵ. Applying Proposition 2.4.7 to the sets $B_{2\lambda_0\epsilon}(z_j)$ for $j\in I_{\epsilon,i}\setminus J_{\epsilon,i}$ we get that $\operatorname{dist}(Q_\epsilon(x),\mathcal{N})\le\delta$ for all $x\in B_{\lambda_0\epsilon}(z_j)\cap\Omega'_\sigma$, see Figure 2.2. Thus, setting $X_\epsilon := \bigcup\{z_j \,:\, j\in\bigcup_{i\in J_\epsilon} J_{\epsilon,i}\}$ yields the result. □

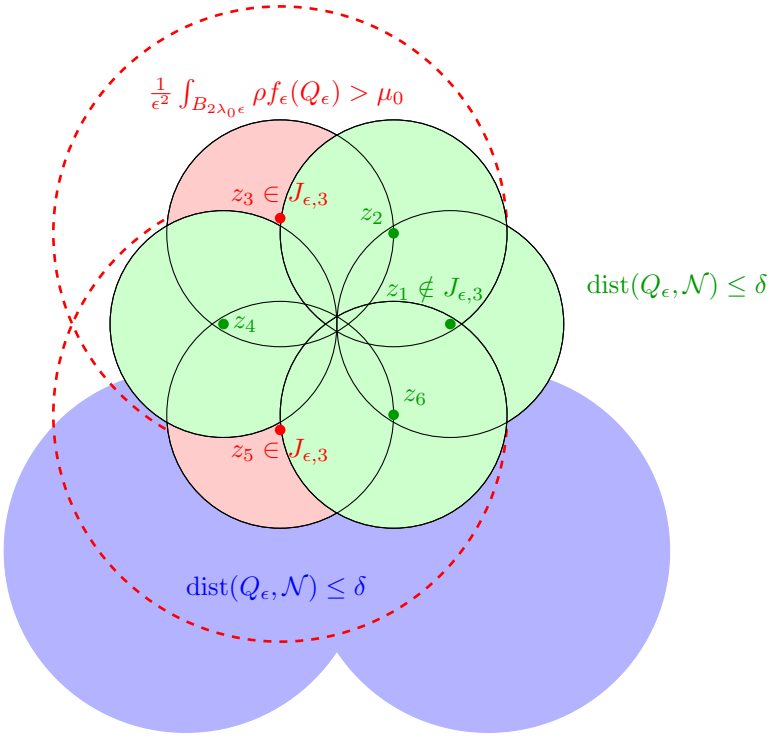

Figure 2.2: Second covering argument: Find balls, where $\frac{1}{\epsilon^2}\int\rho f_\epsilon(Q_\epsilon)$ is large

2.4.3 Lower bound near singularities

The goal of this subsection is to precisely determine the cost of a singularity. The plan is to use estimates as in [47, Chapter 6] which generalize the idea of [92, 144]. The general idea is to decompose the gradient of a function into a derivative of its norm and of its phase as for example

$$|\nabla u|^2 = |\nabla |u||^2 + |u|^2 \Big|\nabla \frac{u}{|u|}\Big|^2$$

for any vectorial function u that does not vanish. Following [41], we replace the phase $u/|u|$ by the projection of Q_ϵ onto $\mathcal{N}$. As a substitute for the norm, we introduce the auxiliary function ϕ.

Definition 2.4.12. *We define the function $\phi : \mathrm{Sym}_0 \to \mathbb{R}$ by*

$$\phi(Q) = \begin{cases} \frac{1}{s_*} s(Q)\,(1 - r(Q)) & Q \in \mathrm{Sym}_0 \setminus \{0\}\,, \\ 0 & Q = 0\,, \end{cases}$$

where s_* is given as in Proposition 2.2.2 and s, r are the parameters from the decomposition of Q in Proposition 2.2.3.

Proposition 2.4.13. *The function ϕ is Lipschitz continuous on Sym_0 and C^1 on $\mathrm{Sym}_0 \setminus \mathcal{C}$ with $\phi(Q) = 1$ for all $Q \in \mathcal{N}$. Furthermore, for a domain $\omega \subset \Omega$ and $Q \in C^1(\omega, \mathrm{Sym}_0)$, the function $\mathcal{R} \circ Q$ is C^1 on the open set $Q^{-1}(\mathrm{Sym}_0 \setminus \mathcal{C})$ and the following estimate holds:*

$$|\nabla Q|^2 \geq \frac{s_*^2}{3} |\nabla(\phi \circ Q)|^2 + (\phi \circ Q)^2 |\nabla(\mathcal{R} \circ Q)|^2 \quad \text{in } \omega\,,$$

where we use the convention that $(\phi \circ Q)^2 |\nabla(\mathcal{R} \circ Q)|^2 := 0$ if $Q(x) \in \mathcal{C}$.

Proof. The proposition follows directly from Lemma 2.2.3 and Lemma 2.2.7 in [41]. □

The next theorem gives the desired lower bound close to a singularity on a two dimensional unit disk. A proof of this can be found in [42, Proposition 2.5].Observe that we work here with the function f, not f_ϵ.

Theorem 2.4.14. *There exist constants $\kappa_*, C > 0$ such that for $Q \in H^1(B_1, \mathrm{Sym}_0)$ satisfying $Q(x) \notin \mathcal{C}$ for all $x \in B_1 \setminus B_{\frac{1}{2}}$ and $(\mathcal{R} \circ Q)|_{\partial B_1}$ is non-trivial, seen as element of $\pi_1(\mathcal{N})$ the following inequality holds*

$$\int_{B_1} \frac{1}{2} |\nabla' Q|^2 + \frac{1}{\epsilon^2} f(Q)\, \mathrm{d}x \geq \kappa_* \phi_0^2(Q, B_1 \setminus B_{\frac{1}{2}}) |\ln \epsilon| - C\,, \tag{2.36}$$

for a number $\phi_0(Q, B_1 \setminus B_{\frac{1}{2}}) := \operatorname{essinf}_{B_1 \setminus B_{\frac{1}{2}}} \phi(Q) > 0$. Furthermore, $\kappa_* = s_*^2 \frac{\pi}{2}$.

The constant κ_* can be calculated as in [42, Lemma 2.9] or [41, Lemma 1.3.4] and is specific for $\mathcal{N} \cong \mathbb{R}P^2$. For other manifolds, there are analogous results with different constants, see [47]. For our purposes, we will use the following version of Theorem 2.4.14.

Corollary 2.4.15. *Let $x_0 \in \Omega'$ such that $B_\eta(x_0) \subset \Omega'$. Let $Q \in H^1(B_\eta(x_0), \mathrm{Sym}_0)$ satisfying $Q(x) \notin \mathcal{C}$ for all $x \in B_\eta \setminus B_{\frac{1}{2}\eta}$ and $(\mathcal{R} \circ Q)|_{\partial B_\eta}$ is non-trivial, seen as element of $\pi_1(\mathcal{N})$. Then, with the same constant $C > 0$ as in Theorem 2.4.14*

$$\int_{B_\eta(x_0)} \frac{1}{2} |\nabla' Q|^2 + \frac{1}{\epsilon^2} f(Q)\, \mathrm{d}x \geq \kappa_* \phi_0^2(Q, B_\eta \setminus B_{\frac{1}{2}\eta}) \big(|\ln \epsilon| - |\ln \eta|\big) - C\,, \tag{2.37}$$

where $\kappa_* = s_*^2 \frac{\pi}{2}$.

Proof. By translating Ω' we can assume that $x_0 = 0$. In order to apply Theorem 2.4.14, we define $\overline{x} = \frac{1}{\eta}x$ and $\overline{Q}(\overline{x}) = Q(\eta\overline{x}) = Q(x)$. Therefore $\overline{Q} \in H^1(B_1(0), \mathrm{Sym}_0)$ and verifies the hypothesis of Theorem 2.4.14 with $\widetilde{\epsilon} = \epsilon\eta$, i.e.

$$\begin{aligned}\int_{B_\eta(x_0)} \frac{1}{2}|\nabla' Q|^2 + \frac{1}{\epsilon^2} f(Q)\,\mathrm{d}x &= \int_{B_1(x_0)} \frac{1}{2}|\nabla'\overline{Q}|^2 + \frac{1}{\eta^2\epsilon^2} f(\overline{Q})\,\mathrm{d}\overline{x} \\ &\geq \kappa_* \phi_0^2(\overline{Q}, B_1 \setminus B_{\frac{1}{2}})|\ln\widetilde{\epsilon}| - C \\ &\geq \kappa_* \phi_0^2(Q, B_\eta \setminus B_{\frac{1}{2}\eta})\big(|\ln\epsilon| - |\ln\eta|\big) - C\,.\end{aligned}$$

□

2.4.4 Lower bound away from singularities

The following proposition shows that we can uniformly bound the functions ϕ and ϕ_0 from the previous section if Q is close to $\mathcal{N}$.

Proposition 2.4.16. *Let* $\mathrm{dist}(Q, \mathcal{N}) \leq \delta$ *on* $\omega \subset \Omega$. *Then*

$$1 - \frac{\sqrt{3}}{s_*}\delta \leq (\phi \circ Q)(x) \leq 1 + \frac{\sqrt{3}}{s_*}\delta\,.$$

Proof. Let $Q \in \mathrm{Sym}_0$ with $\mathrm{dist}(Q, \mathcal{N}) \leq \delta$. In other words, $|Q - \mathcal{R}(Q)| \leq \delta$, since $\mathcal{R}$ is the nearest-point projection onto $\mathcal{N}$. We use Proposition 2.2.3 to write

$$Q = s\left(\left(\mathbf{n}\otimes\mathbf{n} - \frac{1}{3}\mathrm{Id}\right) + r\left(\mathbf{m}\otimes\mathbf{m} - \frac{1}{3}\mathrm{Id}\right)\right) \quad \text{and} \quad \mathcal{R}(Q) = s_*\left(\mathbf{n}\otimes\mathbf{n} - \frac{1}{3}\mathrm{Id}\right),$$

for $\mathbf{n}, \mathbf{m}$ orthonormal eigenvectors of Q, $s > 0$ and $r \in [0, 1)$. We can estimate

$$\begin{aligned}|Q - \mathcal{R}(Q)|^2 &= \left|(s - s_*)(\mathbf{n}\otimes\mathbf{n} - \frac{1}{3}\mathrm{Id}) + sr(\mathbf{m}\otimes\mathbf{m} - \frac{1}{3}\mathrm{Id})\right|^2 \\ &= \frac{2}{3}|s - s_*|^2 + \frac{2}{3}|sr|^2 - \frac{2}{3}sr(s - s_*) \\ &\geq \frac{1}{3}|s - s_*|^2 + \frac{1}{3}|sr|^2 + \frac{1}{3}|s - s_* - sr|^2\,,\end{aligned} \tag{2.38}$$

i.e. $\delta^2 \geq \frac{1}{3}|s(1-r) - s_*|^2 = \frac{s_*^2}{3}|\phi(Q) - 1|^2$. Hence $|\phi(Q) - 1| \leq \frac{\sqrt{3}}{s_*}\delta$. □

Away from singularities the main contribution to the energy comes from the Dirichlet term and the external field since Q_ϵ is close to $\mathcal{N}$. More precisely, we only need the energy in radial direction, i.e. $|\nabla Q_\epsilon|^2$ can be replaced by $|\partial_r Q_\epsilon|^2$ and the problem becomes essentially one dimensional. We formalize this thoughts by introducing the following auxiliary problem as in [4]

$$I(r_1, r_2, a, b) := \inf_{\substack{n_3 \in H^1([r_1, r_2], [0,1]) \\ n_3(r_1) = a,\ n_3(r_2) = b}} \int_{r_1}^{r_2} \frac{s_*^2 |n_3'|^2}{1 - n_3^2} + c_*^2(1 - n_3^2)\,\mathrm{d}r \tag{2.39}$$

for $0 \leq r_1 \leq r_2 \leq \infty$, $a, b \in [-1, 1]$. Note, that this is equivalent to minimizing $\int \left(\frac{1}{2}|\partial_r Q|^2 + g(Q)\right)\ \mathrm{d}r$ for a function Q taking values in $\mathcal{N}$ subject to suitable boundary conditions. For the infimum we have the following result.

Lemma 2.4.17. *Let* $0 \leq r_1 \leq r_2 \leq r_3 \leq \infty$ *and* $a, b, c \in [-1, 1]$. *Then*

1. $I(r_1, r_2, a, b) + I(r_2, r_3, b, c) \geq I(r_1, r_3, a, c)$.
2. $I(r_1, r_2, -1, 1) \geq 4 s_* c_*$.

3. *Let $\theta \in [0,\pi]$. Then*

$$I(0,\infty,\cos(\theta),\pm 1) = 2s_*c_*(1 \mp \cos(\theta))\,.$$

Furthermore, the minimizer $\mathbf{n}(r,\theta)$ of $I(0,\infty,\cos(\theta),1)$ is C^1 and $|\partial_\theta \mathbf{n}|^2, |\partial_r \mathbf{n}|^2, |\mathbf{n}-\mathbf{e}_3|$ decay exponentially as $r \to \infty$. The minimizer can be explicitly expressed as

$$\mathbf{n}(r,\theta) = \begin{pmatrix} \sqrt{1-\mathbf{n}_3^2} \\ 0 \\ \mathbf{n}_3 \end{pmatrix}, \quad \mathbf{n}_3(r,\theta) = \frac{A(\theta) - \exp(-2c_*/s_* r)}{A(\theta) + \exp(-2c_*/s_* r)}, \quad A(\theta) = \frac{1+\cos(\theta)}{1-\cos(\theta)}\,.$$

Proof. The first part follows directly from definition, since any function that is admissible for $I(r_1,r_2,a,b)$ combined with one for $I(r_2,r_3,b,c)$ is admissible for $I(r_1,r_3,a,c)$. For the second claim, we use the inequality $X^2+Y^2 \geq 2XY$ with $X = s_*|\mathbf{n}_3'|/\sqrt{1-\mathbf{n}_3^2}$ and $Y = c_*\sqrt{1-\mathbf{n}_3^2}$ to get

$$I(r_1,r_2,-1,1) \geq 2s_*c_* \int_{r_1}^{r_2} |\mathbf{n}_3'|\,\mathrm{d}r \geq 2s_*c_* \left| \int_{r_1}^{r_2} \mathbf{n}_3'\,\mathrm{d}r \right| = 2s_*c_*|\mathbf{n}_3(r_2) - \mathbf{n}_3(r_1)| = 4s_*c_*\,.$$

The third part follows from Lemma 3.4 and Remark 3.5 in [4]. □

Remark 2.4.18. *1. A close look at Lemma 2.4.17 reveals that it is enough to consider a rotationally symmetric function g which has a strict minimum on $\mathcal{N}$ at $Q = s_*(\mathbf{e}_3 \otimes \mathbf{e}_3 - \frac{1}{3}\mathrm{Id})$. Indeed, then for $Q = s_*(\mathbf{n}\otimes\mathbf{n} - \frac{1}{3}\mathrm{Id})$ we can write $\tilde{g}(n_3) = g(Q)$ and I becomes $I(r_1,r_2,a,b) = \inf \int_{r_1}^{r_2} \frac{s_*^2|n_3'|^2}{1-n_3^2} + \tilde{g}(n_3)\,\mathrm{d}r$. Taking a minimizer $n_3(r)$ for $n_3(0)=0$ and $\lim_{r\to\infty} n_3(r) = t$ we can define $G(t) = 2s_* \int \sqrt{\frac{\tilde{g}(n_3)}{1-n_3^2}}|n_3'|\,\mathrm{d}r$. One can then derive estimates analogous to Lemma 2.4.17, e.g. $I(r_1,r_2,-1,1) \geq 2G(1)$.*

2. Lemma 2.4.17 and (2.39) only uses the form of g on $\mathcal{N}$. As we have seen in Proposition 2.4.2, we can neglect the behaviour of g far from $\mathcal{N}$ for smaller norms of Q due to the dominating character of f in our asymptotic regime. With the same argument one could also introduce a cut-off for higher norms as long as the growth assumption (2.5) is satisfied. So the essential information about how g contributes to the energy is $g|_{\mathcal{N}}$, i.e. (2.7).

Now we can combine all our previous results to prove the lower bound of Theorem 2.3.1. The idea consists in replacing $\widetilde{Q_\epsilon}$ by its approximation Q_ϵ and use the equivariance to write the energy as a two dimensional integral. By Theorem 2.4.5 we can exclude regions in Ω_σ' where Q_ϵ is far from $\mathcal{N}$. Extending the sets if necessary, we can assure that the union has vanishing measure in the limit $\eta,\epsilon \to 0$ and that the complement Ω_0 is simply connected. The scaling of η and ϵ allows to apply Corollary 2.4.15 to each of these extended sets where the boundary datum is nontrivial. The expression we calculate here can later be identified as the perimeter term in $\mathcal{E}_0$. In the simply connected complement Ω_0 there exists a lifting $\mathbf{n}^\epsilon$ of Q_ϵ which fulfils the compactness (2.16). We then want to apply Lemma 2.4.17 to the rays in Ω_0 for the lower bound. We consider the rays with high energy (that we can estimate easily) and those with low energy where we need to be more precise about their behaviour far from the boundary $\partial\Omega$. Using a diagonal sequence, we can pass to the limit $\sigma \to 0$.

Proof of the lower bound (2.17) of Theorem 2.3.1. Let $\delta,\sigma > 0$ be arbitrary. We define Q_ϵ as in (2.21) and extend it rotationally equivariant. From Theorem 2.4.5 for $\epsilon \leq \epsilon_0$ we know that there exists a finite set X_ϵ of singular points $x_1^\epsilon, ..., x_{N_\epsilon}^\epsilon$ in Ω_σ'. In a first step, we suppose that all these points are included in the set $\Omega_R' = \Omega_\sigma' \cap B_R(0)$.

Since Ω_R' is bounded, there exists another finite set X, such that each sequence x_j^ϵ converges (up to a subsequence) to a point in X as $\epsilon,\eta \to 0$. Note that there may be more than one sequence converging to the same point in X and we a priori only know that $X \subset \overline{\Omega' \cap B_R}$.

We first assume that the set X is contained in $\Omega_\sigma' \setminus \partial\Omega$. Since $\eta|\ln\epsilon| \to \beta \in (0,\infty)$ we know that $\epsilon \leq C\exp(-\frac{1}{\eta})$. Assume that η is small enough such that $2\lambda_0\epsilon \leq \frac{1}{2}\eta$.

For $x_i \in X$ we define $\widetilde{\Omega_i^{\epsilon}}' = \mathrm{conv}\{B_\eta(x_i) \cup \{0\}\} \cap \Omega'$. If x_i is the only point of the set X that lies on the ray from 0 through x_i we define $\Omega_i^{\epsilon\prime} := \widetilde{\Omega_i^{\epsilon}}'$. If x_j for $j \in J \subset I$ define the same ray, i.e. lie on a common line through 0, then we set $\Omega_j^{\epsilon\prime} := \bigcup_{k\in J} \widetilde{\Omega_k^{\epsilon}}'$. After relabelling, we end up with a finite number N of sets $\Omega_k^{\epsilon\prime}$, $k = 1, ..., N$. We define $\Omega_0^{\epsilon\prime} := \Omega'_\sigma \setminus \bigcup_{k=1}^N \Omega_k^{\epsilon\prime}$ (see Figure 2.3). Since all points in X_ϵ converge to some point in X, we may assume that ϵ is small enough such that

$$\bigcup_{x\in X_\epsilon} B_{\lambda_0\epsilon}(x) \subset \bigcup_{x\in X} B_{2\lambda_0\epsilon}(x) \subset \bigcup_{k=1}^{N} \Omega_k^{\epsilon\prime} \subset \Omega'_\sigma \,. \tag{2.40}$$

We drop the ϵ in the notation of $\Omega_k^{\epsilon\prime}$ for simplicity and call Ω_k the three dimensional set defined by rotating Ω'_k around the $\mathbf{e}_3-$axis.

Using (2.21) and Remark 2.4.3 we can write

$$\begin{aligned}
\eta\, \mathcal{E}_\epsilon(\widetilde{Q_\epsilon}) &\geq \eta \int_\Omega \frac{1}{2}|\nabla Q_\epsilon|^2 + \frac{1}{\epsilon^2} f_\epsilon(Q_\epsilon) + \frac{1}{2\epsilon^\gamma}|Q_\epsilon - \widetilde{Q_\epsilon}|^2 \,\mathrm{d}x \\
&\geq \eta \int_{\Omega_0} \frac{1}{2}|\nabla Q_\epsilon|^2 + \frac{1}{\epsilon^2} f_\epsilon(Q_\epsilon) + \frac{1}{2\epsilon^\gamma}|Q_\epsilon - \widetilde{Q_\epsilon}|^2 \,\mathrm{d}x \\
&\quad + \eta \sum_{k=1}^{N} \int_0^{2\pi} \int_{\Omega'_k} \rho \left(\frac{1}{2}|\nabla Q_\epsilon|^2 + \frac{1}{\epsilon^2} f_\epsilon(Q_\epsilon) \right) \mathrm{d}\rho \,\mathrm{d}z \,\mathrm{d}\varphi \,.
\end{aligned} \tag{2.41}$$

For $x \in \Omega_0$ we know by Theorem 2.4.5 that $\mathrm{dist}(Q_\epsilon(x), \mathcal{N}) \leq \delta$. Since Ω'_0 and thus Ω_0 is simply connected there exist liftings $\pm\mathbf{n}^\epsilon : \Omega_0 \to \mathbb{S}^2$ such that

$$s_*\left(\mathbf{n}^\epsilon \otimes \mathbf{n}^\epsilon - \frac{1}{3}\mathrm{Id}\right) = \mathcal{R} \circ Q_\epsilon \quad \text{and} \quad \left\| s_*\left(\mathbf{n}^\epsilon \otimes \mathbf{n}^\epsilon - \frac{1}{3}\mathrm{Id}\right) - Q_\epsilon \right\|_\infty \leq \delta \quad \text{on } \Omega_0 \,.$$

In particular, $Q_\epsilon(x) \in \mathrm{Sym}_0 \setminus \mathcal{C}$ for all $x \in \partial\Omega'_k$ for all $k = 1, ..., N$. Let $\mathcal{M} \subset \{1, ..., N\}$ be the set of elements $k \in \{1, ..., N\}$ such that $(\mathcal{R} \circ Q_\epsilon)|_{\partial\Omega'_k}$ is non-trivial as an element of $\pi_1(\mathcal{N})$. On $B_\eta(x_k)$ we apply Corollary 2.4.15 to $\int_{B_\eta(x_k)} \frac{1}{2}|\nabla Q_\epsilon|^2 + \frac{1}{\epsilon^2} f(Q_\epsilon)$. The term $\eta \int_{B_\eta(x_k)} \frac{1}{\eta^2}|g(Q_\epsilon)| + C_0(\epsilon, \eta)$ is seen to be bounded by $C\eta$. On the remaining $\Omega'_k \setminus B_\eta(x_k)$ we use that the energy density $\frac{1}{2}|\nabla Q_\epsilon|^2 + \frac{1}{\epsilon^2} f_\epsilon(Q_\epsilon) \geq 0$ is non-negative. Hence we get

$$\begin{aligned}
\eta \sum_{k=1}^{N} \int_{\Omega'_k} \rho \left(\frac{1}{2}|\nabla Q_\epsilon|^2 + \frac{1}{\epsilon^2} f_\epsilon(Q_\epsilon) \right) \mathrm{d}\rho \,\mathrm{d}z &\geq \eta \sum_{k=1}^{N} \inf_{\Omega'_k} \rho \int_{\Omega'_k} \left(\frac{1}{2}|\nabla Q_\epsilon|^2 + \frac{1}{\epsilon^2} f(Q_\epsilon) \right) \mathrm{d}\rho \,\mathrm{d}z - C\eta \\
&\geq \eta \sum_{k\in\mathcal{M}} \kappa_* \phi_0^2(Q_\epsilon, B_\eta(x_k) \setminus B_{\frac{1}{2}\eta}(x_k)) \frac{\rho_k^\epsilon - \eta}{|x_k^\epsilon|} |\ln \epsilon| \eta \\
&\quad - C\phi_0^2(Q_\epsilon, B_\eta(x_k) \setminus B_{\frac{1}{2}\eta}(x_k))\, \eta |\ln \eta| - C\eta \\
&\geq \left(1 - \frac{\sqrt{3}}{s_*}\delta\right)^2 \sum_{k\in\mathcal{M}} \frac{\rho_k^\epsilon - \eta}{|x_k^\epsilon|} \frac{\pi}{2} s_*^2 \eta |\ln(\epsilon)| \\
&\quad - C\left(1 + \frac{\sqrt{3}}{s_*}\delta\right)^2 \eta |\ln \eta| - C\eta \,,
\end{aligned} \tag{2.42}$$

where we also applied Proposition 2.4.16 to estimate ϕ_0 from below.

Before estimating the energy coming from Ω_0, we need an additional information, namely we want to show that $\mathbf{n}^\epsilon(r\omega)$ approaches $+\mathbf{e}_3$ and $-\mathbf{n}^\epsilon(r\omega)$ approximates $-\mathbf{e}_3$ (or vice versa) as $r \to \infty$ for a.e. $\omega \in \mathbb{S}^2$. However, it will be enough for our analysis to just show that $\mathbf{n}^\epsilon$ is close to either $+\mathbf{e}_3$ or $-\mathbf{e}_3$ up to some factor times $\sqrt{\delta}$. To start with, we show that the vector $\mathbf{n}^\epsilon(r\omega)$ for $r \to \infty$ is close to $+\mathbf{e}_3$ or $-\mathbf{e}_3$ almost everywhere. By (2.21) and the energy bound we know, that for a.e. $\omega \in \mathbb{S}^2$ the integral

$$\int_R^\infty \frac{\eta}{\epsilon^2} f(Q_\epsilon) + \frac{1}{\eta} g(Q_\epsilon(r\omega)) + \eta C_0(\epsilon, \eta) \,\mathrm{d}r < \infty \,. \tag{2.43}$$

We argue by contradiction, i.e. assume that there exists some $\omega \in \mathbb{S}^2$ satisfying (2.43) such that $\limsup_{r\to\infty} ||\mathbf{n}_3^\epsilon(r\omega)| - 1| > 2\mathfrak{C}\mathfrak{a}\sqrt{\delta}$ for a $\mathfrak{C} > 0$ to be specified later and $\mathfrak{a}$ is the constant from Proposition 2.2.5. This implies that there exists a sequence r_ℓ such that $r_\ell \to \infty$ as $\ell \to \infty$ and $|\mathbf{n}_3^\epsilon(r_\ell\omega)| < 1 - 2\mathfrak{C}\mathfrak{a}\sqrt{\delta}$ for all $\ell \in \mathbb{N}$ or in other words $|Q_\epsilon - s_*(\mathbf{e}_3 \otimes \mathbf{e}_3 - \frac{1}{3}\mathrm{Id})| > 2\mathfrak{a}\sqrt{\delta}$ for a suitably chosen $\mathfrak{C}$ (A calculation shows that $\mathfrak{C} \geq \frac{5}{4\sqrt{2}s_*}$ is sufficient). By Lipschitz continuity of Q_ϵ this implies $|Q_\epsilon - s_*(\mathbf{e}_3 \otimes \mathbf{e}_3 - \frac{1}{3}\mathrm{Id})| > \mathfrak{a}\sqrt{\delta}$ for all $r \in I_\ell := (r_\ell - \frac{\epsilon\mathfrak{C}\mathfrak{a}\sqrt{\delta}}{C}, r_\ell + \frac{\epsilon\mathfrak{C}\mathfrak{a}\sqrt{\delta}}{C})$. This implies that $g(Q_\epsilon) \geq g_{\min} > 0$ for such points in I_ℓ, where we used $g_{\min} = \min\left\{g(Q) : Q \in \mathrm{Sym}_0\,, \mathrm{dist}(Q, \mathcal{N}) \leq \delta\,, |Q - s_*(\mathbf{e}_3 \otimes \mathbf{e}_3 - \frac{1}{3}\mathrm{Id})| \geq \mathfrak{a}\sqrt{\delta}\right\} > 0$ by Proposition 2.2.5. With this estimate in mind it becomes clear that we have the lower bound

$$\frac{1}{\eta}\int_{I_\ell} \frac{\eta}{\epsilon^2} f(Q_\epsilon) + \frac{1}{\eta} g(Q_\epsilon(r\omega)) + \eta C_0(\epsilon,\eta)\,\mathrm{d}r \geq \frac{1}{\eta} g_{\min}|I_\ell| = \frac{1}{\eta} g_{\min} \frac{2\epsilon\mathfrak{C}\mathfrak{a}\sqrt{\delta}}{C} > 0\,.$$

Summing over disjoint intervals yields a contradiction to (2.43).

This implies that either $\limsup_{r\to\infty} \mathbf{n}_3^\epsilon(r\omega) \geq 1 - 2\mathfrak{C}\mathfrak{a}\sqrt{\delta}$ or $\liminf_{r\to\infty} \mathbf{n}_3^\epsilon(r\omega) \leq -1 + 2\mathfrak{C}\mathfrak{a}\sqrt{\delta}$. Indeed, $\mathbf{n}_3^\epsilon(r\omega)$ cannot alternate between ± 1 since by continuity this yields a contradiction for δ small enough such that $2\mathfrak{C}\mathfrak{a}\sqrt{\delta} \ll \frac{1}{2}$. Next, consider the lifting $\mathbf{n}^\epsilon$ and suppose that there exist directions $\omega_+, \omega_- \in \mathbb{S}^2$ such that $\mathbf{n}^\epsilon(r\omega_+)$ is close to $+\mathbf{e}_3$ (resp. $\mathbf{n}^\epsilon(r\omega_-)$ close to $-\mathbf{e}_3$) as $r \to \infty$. Since our previous analysis holds a.e., we can assume that the angle between ω_+ and ω_- is smaller than π and that $\omega_\pm$ are not parallel to $\mathbf{e}_3$. Let $v = \omega_+ - \omega_-$ and $w = \omega_+ + \omega_-$. We estimate the energy in new coordinates (r, s) in the segment between the rays defined through ω_+ and ω_- to get

$$\begin{aligned} C &\geq \int_{R+1}^{\tilde{R}} \int_{-r|v|/2}^{r|v|/2} \rho\left(\frac{\eta}{2}\Big|\nabla' Q_\epsilon\Big(r\frac{v}{|v|} + s\frac{w}{|w|}\Big)\Big|^2 + \frac{1}{\eta} g\Big(Q_\epsilon\Big(r\frac{v}{|v|} + s\frac{w}{|w|}\Big)\Big)\right) \mathrm{d}s\,\mathrm{d}r \\ &\geq C(1-C\delta)^2 \int_{(R+1)}^{\tilde{R}} \int_{r|v|/2}^{r|v|/2} \rho\left(\eta s_*^2 \Big|\frac{v}{|v|}\cdot\nabla'\mathbf{n}^\epsilon\Big|^2 + \frac{1}{\eta}c_*^2(1-\mathbf{n}_3^\epsilon) - C\delta\right) \mathrm{d}s\,\mathrm{d}r\,. \end{aligned}$$

Lemma 2.4.17 gives the lower bound $\int_{-r|v|/2}^{r|v|/2} \left(\eta s_*^2 |\frac{v}{|v|}\cdot\nabla'\mathbf{n}^\epsilon|^2 + \frac{1}{\eta}c_*^2(1-\mathbf{n}_3^\epsilon)\right) \mathrm{d}s \geq 4c_*s_* - C\sqrt{\delta}$. Using $\rho \geq r\min\{\sin(\theta_+), \sin(\theta_-)\}$ for $\theta_\pm$ being the angular coordinate of $\omega_\pm$, we end up with

$$C \geq C(1-C\delta)^2 \int_{R+1}^{\tilde{R}} r(4c_*s_* - C\sqrt{\delta})\,\mathrm{d}r \geq C_R(1-\sqrt{\delta})\tilde{R}^{\frac{3}{2}} > 0\,,$$

provided $\delta > 0$ small enough. Sending $\tilde{R}$ to infinity, we get a contradiction. Hence, $\mathbf{n}^\epsilon$ has to approach either $+\mathbf{e}_3$ or $-\mathbf{e}_3$ a.e. and thus we can distinguish the two liftings by their asymptotics far from $\partial\Omega$.

We now introduce sets $F_{\sigma,\epsilon}$, $\widetilde{F_{\sigma,\epsilon}}$ which we use later to prove the compactness result. First choose one of the two possible liftings $\mathbf{n}^\epsilon \in C^0(\Omega_0, \mathbb{S}^2)$. Without loss of generality we choose the lifting such that $\mathbf{n}^\epsilon(r\omega)$ is close to $+\mathbf{e}_3$ as $r \to \infty$. The boundary conditions (2.13) imply that $\mathbf{n}^\epsilon(\omega) = \pm\nu(\omega)$, where ν is the outward normal on $\mathbb{S}^2$ for all $\omega \in \partial\Omega_0 \cap \mathbb{S}^2$. We define $F_{\sigma,\epsilon} := \{\omega \in \mathbb{S}^2 \cap \partial\Omega_0 : \mathbf{n}^\epsilon(\omega)\cdot\nu(\omega) = 1\}$. Conversely, $\widetilde{F_{\sigma,\epsilon}}$ is then given by $\widetilde{F_{\sigma,\epsilon}} = \{\omega \in \mathbb{S}^2 \cap \partial\Omega_0 : \mathbf{n}^\epsilon(\omega)\cdot\nu(\omega) = -1\}$. The remaining part of $\mathbb{S}^2 \cap \Omega_\sigma$ is denoted $S_{\sigma,\epsilon} = (\mathbb{S}^2 \cap \Omega_\sigma) \setminus (F_{\sigma,\epsilon} \cup \widetilde{F_{\sigma,\epsilon}}) = \bigcup_{k\geq 1}(\mathbb{S}^2 \cap \partial\Omega_k)$. Note that the sets $F_{\sigma,\epsilon}$, $\widetilde{F_{\sigma,\epsilon}}$ and $S_{\sigma,\epsilon}$ are rotationally symmetric with respect to the φ coordinate. Since the $\theta-$angular size of all Ω_k converges to zero (i.e. $|S_{\sigma,\epsilon}| \to 0$ as $\epsilon \to 0$) and $\mathbb{S}^2 \cap \Omega_\sigma$ is compact, we get that (up to extracting a subsequence) $\chi_{F_{\sigma,\epsilon}}$ (resp. $\chi_{\widetilde{F_{\sigma,\epsilon}}}$) converges pointwise to a characteristic function χ_{F_σ} (resp. $\chi_{\widetilde{F_\sigma}}$). By triangle inequality we get $\mathrm{dist}(\widetilde{Q_\epsilon}, \mathcal{N}_\epsilon) \leq \mathrm{dist}(Q_\epsilon, \mathcal{N}_\epsilon) + |Q_\epsilon - \widetilde{Q_\epsilon}|$, where $\mathcal{N}_\epsilon$ is the manifold $\mathcal{N}_{\eta,\xi}$ introduced in Proposition 2.2.6. By Remark 2.4.3, Proposition 2.2.6 and the energy bound (2.19) we get that $\int_{\Omega_0} \mathrm{dist}^2(\widetilde{Q_\epsilon}, \mathcal{N}_\epsilon)\,\mathrm{d}x \to 0$ as $\epsilon, \eta \to 0$. On bounded sets additionally use (2.11) to get the claimed L^2-convergence in (2.16).

As a last step, it remains the energy estimate on Ω_0. We split the integral over Ω_0 in (2.41) in several parts: For $\omega \in F_{\sigma,\epsilon}$ such that the energy on the ray in direction ω is large, i.e. $\int_1^\infty \frac{\eta}{2}|\nabla Q_\epsilon|^2 +$

$\frac{\eta}{\epsilon^2} f(Q_\epsilon) + \frac{1}{\eta} g(Q_\epsilon) + \eta C_0(\epsilon,\eta) + \frac{\eta}{2\epsilon^\gamma} |Q_\epsilon - \widetilde{Q_\epsilon}|^2 \, \mathrm{d}r \geq 4 s_* c_*$, we can use Lemma 2.4.17 that implies

$$\int_1^\infty \frac{\eta}{2}|\nabla Q_\epsilon|^2 + \frac{\eta}{\epsilon^2} f(Q_\epsilon) + \frac{1}{\eta} g(Q_\epsilon) + \eta C_0(\epsilon,\eta) + \frac{\eta}{2\epsilon^\gamma}|Q_\epsilon - \widetilde{Q_\epsilon}|^2 \, \mathrm{d}r \geq 4 s_* c_* \geq I(1,\infty,\nu_3(\omega),+1)\,. \tag{2.44}$$

Analogously, for points $\omega \in \widetilde{F_{\sigma,\epsilon}}$ with energy greater than $4 s_* c_*$ we use $I(1,\infty,\nu_3(\omega),-1)$ as a lower bound. Let's consider the set of points $\omega \in \mathbb{S}^2 \cap \partial\Omega_0$ such that the energy on the ray through ω is smaller than $4 s_* c_*$. We claim that there exists a constant $\overline{C} > 0$ independent of ω and a radius $R_{\eta,\omega} \in (R - \overline{C}\eta, R]$ such that $||\mathbf{n}_3^\epsilon(R_{\eta,\omega}\omega)| - 1| \leq 2\mathfrak{C}\mathfrak{a}\sqrt{\delta} \ll 1$. Indeed, if $||\mathbf{n}_3^\epsilon(R_{\eta,\omega}\omega)| - 1| > 2\mathfrak{C}\mathfrak{a}\sqrt{\delta}$ on $(R - \overline{C}\eta, R]$ then on this set $|Q_\epsilon - s_*(\mathbf{e}_3 \otimes \mathbf{e}_3 - \frac{1}{3}\mathrm{Id})| \geq 2\mathfrak{a}\sqrt{\delta}$. Hence for $\overline{C}$ large enough this contradicts $4 s_* c_* \geq \int \frac{\eta}{\epsilon^2} f(Q_\epsilon) + \frac{1}{\eta} g(Q_\epsilon) + \eta C_0(\epsilon,\eta) \, \mathrm{d}r \geq (R - (R - \overline{C}\eta)) \frac{C\mathfrak{a}\sqrt{\delta}}{\eta}$. In order to conclude that the energy from 1 to $R_{\eta,\omega}$ is (up to some small contributions of size $\sqrt{\delta}$) close to $I(1,\infty,\nu_3(\omega),\pm 1)$ we need to show that for $\omega \in F_{\sigma,\epsilon}$ the vector $\mathbf{n}^\epsilon(R_{\eta,\omega})$ is close to $+\mathbf{e}_3$ and not $-\mathbf{e}_3$ (and vice versa for $\omega \in \widetilde{F_{\sigma,\epsilon}}$). Again we argue by contradiction, i.e. we assume that $|\mathbf{n}^\epsilon(R_{\eta,\omega}) + \mathbf{e}_3| \leq 2\mathfrak{C}\mathfrak{a}\sqrt{\delta}$. We subdivide the ray in direction ω from R to infinity into segments of length 1, identified with the intervals $J_\ell = [\ell, \ell+1]$ for the radial variable, for integers $\ell \geq R$. On every segment, the energy bound on the ray implies the existence of two points $a_\ell, b_\ell \in J_\ell$ with $|a_\ell - \ell| \leq \overline{C}\eta$, $|b_\ell - (\ell+1)| \leq \overline{C}\eta$ such that $||\mathbf{n}_3^\epsilon(a_\ell)| - 1| \leq 2\mathfrak{C}\mathfrak{a}\sqrt{\delta}$, $||\mathbf{n}_3^\epsilon(b_\ell)| - 1| \leq 2\mathfrak{C}\mathfrak{a}\sqrt{\delta}$. Since we assumed $\mathbf{n}^\epsilon(R_{\omega,\eta})$ close to $-\mathbf{e}_3$ and $\mathbf{n}^\epsilon$ approaches $+\mathbf{e}_3$ for $\ell \to \infty$, there exists some integer $\ell \geq R$ such that $|\mathbf{n}_3^\epsilon(a_\ell) + 1| \leq 2\mathfrak{C}\mathfrak{a}\sqrt{\delta}$, $|\mathbf{n}_3^\epsilon(b_\ell) - 1| \leq 2\mathfrak{C}\mathfrak{a}\sqrt{\delta}$. Together with (2.8) this implies

$$\int_{J_\ell} \frac{\eta}{2}|\nabla Q_\epsilon|^2 + \frac{1}{\eta} g(Q_\epsilon) \, \mathrm{d}r \geq I(\ell, \ell+1, \mathbf{n}_3^\epsilon(a_\ell), \mathbf{n}_3^\epsilon(b_\ell)) - C(\mathfrak{C}\mathfrak{a}+1)\sqrt{\delta} \geq 4 s_* c_* - C\sqrt{\delta}\,.$$

In order to show that for δ and ϵ small enough this contradicts the assumption of the ray having energy smaller than $4 s_* c_*$, we prove that the energy coming from the segment $[0, R]$ has to be positive with a uniform lower bound. Since $\omega \in F_{\sigma,\epsilon} \subset \partial\Omega_\sigma$ one can show as in 2. in Lemma 2.4.17 that on such a ray $\int_1^R \frac{\eta}{2}|\nabla Q_\epsilon|^2 + \frac{1}{\eta} g(Q_\epsilon) \, \mathrm{d}r \geq 4 s_* c_* (\frac{1}{2}\sigma^2 - 8\mathfrak{C}\mathfrak{a}\sqrt{\delta})$. So combining this result and the estimate for J_k we get

$$4 s_* c_* \geq 4 s_* c_* - C\sqrt{\delta} + 2 s_* c_* \Big(\frac{1}{2}\sigma^2 - 8\mathfrak{C}\mathfrak{a}\sqrt{\delta}\Big)\,,$$

which yields a contradiction for δ, ϵ small enough. For $\omega \in F_{\sigma,\epsilon}$ we then use the change of variables $r = 1 + \eta\tilde{r}$, (2.8), Proposition 2.4.13 and Proposition 2.4.16 to get

$$\begin{aligned}
\int_1^R \frac{\eta}{2}|\nabla Q_\epsilon|^2 + \frac{1}{\eta} g(Q_\epsilon) \, \mathrm{d}r &\geq \int_0^{(R-1)/\eta} \frac{1}{2}|\nabla Q_\epsilon|^2 + g(\mathcal{R} \circ Q_\epsilon) - C \operatorname{dist}(Q_\epsilon, \mathcal{N}) \, \mathrm{d}\tilde{r} \\
&\geq (1 - C\delta)^2 \int_0^{(R-1)/\eta} \frac{1}{2}|\nabla(\mathcal{R} \circ Q_\epsilon)|^2 + g(R \circ Q_\epsilon) \, \mathrm{d}\tilde{r} - C\delta \qquad (2.45) \\
&\geq I(0, (R_{\eta,\omega} - 1)/\eta, \nu_3(\omega), \mathbf{n}_3^\epsilon((R_{\eta,\omega} - 1)/\eta)) - C\delta \\
&\geq I(0, (R_{\eta,\omega} - 1/\eta, \nu_3(\omega), +1) - C\delta\,,
\end{aligned}$$

where we also used Proposition 2.2.6 to get

$$\operatorname{dist}(Q_\epsilon, \mathcal{N}) \leq \operatorname{dist}\Big(Q_\epsilon, \mathcal{N}_\epsilon\Big) + C\frac{\epsilon^2}{\eta^2} \leq C\Big(f(Q_\epsilon) + \frac{\epsilon^2}{\eta^2} g(Q_\epsilon) + \epsilon^2 C_0(\epsilon,\eta)\Big)^{\frac{1}{2}} + C\frac{\epsilon^2}{\eta^2}$$

and thus by Cauchy-Schwarz inequality and the energy bound on the ray $\int_0^{(R-1)/\eta} \operatorname{dist}(Q_\epsilon, \mathcal{N}) \, \mathrm{d}\tilde{r} \leq C\sqrt{R}\frac{\epsilon}{\sqrt{\eta}} + CR\frac{\epsilon^2}{\eta^3}$. So by (2.44) and (2.45) we get that for $\omega \in F_{\sigma,\epsilon}$ we have

$$\int_1^\infty \frac{\eta}{2}|\nabla Q_\epsilon|^2 + \frac{1}{\eta} g(Q_\epsilon) \, \mathrm{d}r \geq \min\{I(0,\infty,\nu_3(\omega),+1),\, I(0,(R_{\eta,\omega} - 1/\eta, \nu_3(\omega), +1) - C\delta\}\,.$$

Furthermore, by compactness, $\chi_{F_{\sigma,\epsilon}}$ converges point wise a.e. to χ_{F_σ}. Since $(R_{\eta,\omega} - 1)/\eta \to \infty$ as

$\eta \to \infty$ we can apply Fatou's Lemma to get the energy contribution from Ω_0 related to $F_{\sigma,\epsilon}$ by

$$\begin{aligned}
&\liminf_{\epsilon,\eta\to 0} \int_{F_{\sigma,\epsilon}} \int_1^\infty \frac{\eta}{2}|\nabla Q_\epsilon|^2 + \frac{\eta}{\epsilon^2} f(Q_\epsilon) + \frac{1}{\eta} g(Q_\epsilon) + \eta C_0(\epsilon,\eta)\, \mathrm{d}r\, \mathrm{d}\omega \\
&\quad \geq \int_{\mathbb{S}^2\cap\partial\Omega_0} \liminf_{\epsilon,\eta\to 0} \min\{I(0,\infty,\nu_3(\omega),+1),\, I(0,(R_{\eta,\omega}-1/\eta,\nu_3(\omega),+1) - C\delta\}\chi_{F_{\sigma,\epsilon}}(\omega)\, \mathrm{d}\omega \\
&\quad \geq \int_{F_\sigma} I\left(0,\infty,\nu_3(\omega),+1\right)\, \mathrm{d}\omega - C\delta\,.
\end{aligned}$$

Now combine this estimate, the analogous result for $\widetilde{F_{\sigma,\epsilon}}$, the formulae for $I(0,\infty,\nu_3(\omega),\pm 1)$ from Lemma 2.4.17 and (2.42) to get

$$\begin{aligned}
\liminf_{\epsilon,\eta\to 0} \eta\mathcal{E}_{\eta,\xi}(Q_{\eta,\xi}) \geq \int_{F_\sigma} 2s_*c_*(1-\cos(\theta))\, \mathrm{d}\omega + \int_{\widetilde{F_\sigma}} 2s_*c_*(1+\cos(\theta))\, \mathrm{d}\omega \\
+ (1-C\delta)^2 \sum_{k\in\mathcal{M}} \frac{\rho_k - \eta}{|x_k|}\pi^2 s_*^2\beta - C\delta\,,
\end{aligned}$$

for the points $x_k = (\rho_k, \theta_k) \in X$.

It remains to show that for all $k \in \mathcal{M}$, the point $x_k/|x_k|$ corresponds to a jump between F_σ and $\widetilde{F_\sigma}$. For this it is enough to show that the orientation of $\mathbf{n}^\epsilon$ relative to the normal on $\partial\Omega$ changes when following $\partial\Omega_k' \cap \Omega'$ for all $k \in \mathcal{M}$. So let $k \in \mathcal{M}$ and consider the curve $\Gamma : \partial\Omega_k' \to \mathbb{S}^2$ defined by $\mathbf{n}^\epsilon|_{\partial\Omega_k'}$. By definition of $\mathcal{M}$, the curve is non-trivial in $\pi_1(\mathcal{N})$, i.e. Γ jumps an odd number of times from one vector to its antipodal vector on the sphere. Hence, the orientation has to change. In the limit $\epsilon, \eta \to 0$, this implies that

$$2\pi \sum_{k\in\mathcal{M}} \frac{\rho_k}{|x_k|} = |D\chi_{F_\sigma}|(\mathbb{S}^2 \cap \{\rho > \sigma\})\,.$$

This implies our result in the case $X_\epsilon, X \subset (\Omega' \cap B_R(0)) \setminus \partial\Omega$.

We now explain the changes in our construction if there are some $x_i \in X \cap \mathbb{S}^2$. Basically, we use the same construction as before, but we need to take care that the lower bound involving Corollary 2.4.15 stays applicable. To see this, we extend the map Q_ϵ outside of Ω using the boundary values. We define

$$\overline{Q_\epsilon}(x) = \begin{cases} Q_\epsilon(x) & x \in B_\eta(x_i) \cap \Omega\,, \\ s_*\left(\frac{x}{|x|} \otimes \frac{x}{|x|} - \frac{1}{3}\mathrm{Id}\right) & x \in B_\eta(x_i) \cap B_1(0)\,. \end{cases}$$

Then $f(\overline{Q_\epsilon}) = 0$ and $|\nabla\overline{Q_\epsilon}|^2, |g(\overline{Q_\epsilon})| \leq C$ on $B_\eta(x_i) \cap B_1(0)$, i.e.

$$\int_{B_\eta(x_i)\cap B_1(0)} \frac{1}{2}|\nabla\overline{Q_\epsilon}|^2 + \frac{1}{\epsilon^2} f(\overline{Q_\epsilon}) + \frac{1}{\eta^2} g(\overline{Q_\epsilon}) + C_0(\epsilon,\eta)\, \mathrm{d}x \leq C_1\,.$$

So if $(\mathcal{R}\circ Q_\epsilon)|_{\partial\Omega_i'}$ is non-trivial as element of $\pi_1(\mathcal{N})$, we can apply Corollary 2.4.15 to the extension $\overline{Q_\epsilon}$, i.e.

$$\begin{aligned}
\eta \int_{B_\eta(x_i)\cap\Omega'} \frac{1}{2}|\nabla Q_\epsilon|^2 + \frac{1}{\epsilon^2} f(Q_\epsilon)\, \mathrm{d}x &\geq \eta \int_{B_\eta(x_i)\cap\mathbb{R}^2} |\nabla'\overline{Q_\epsilon}|^2 + \frac{1}{\epsilon^2} f(\overline{Q_\epsilon})\, \mathrm{d}x - \eta\, C_1 \\
&\geq \left(1 - \frac{\sqrt{3}}{s_*}\delta\right)^2 \frac{\pi}{2} s_*^2 \eta |\ln\epsilon| - C\,\eta|\ln\eta| - C\,\eta\,.
\end{aligned}$$

If $(\mathcal{R}\circ Q_\epsilon)|_{\partial\Omega_i'}$ is trivial, then we just estimate as before, using that the energy is non-negative.

It remains one last case. Assume that there is a point $x_k^\epsilon \in X_\epsilon$ such that $|x_k^\epsilon| \to \infty$ as $\epsilon \to 0$. This causes two modifications to our previous results: This time, we define $\widetilde{\Omega_k^\epsilon}' = \mathrm{conv}\{B_\eta(x_k^\epsilon) \cup \{0\}\} \cap \Omega'$. Doing so, we risk to exclude a region from Ω_0 that is too large for proving the compactness, namely when we define the set ω_η afterwards. But in fact this is not

really a difficulty for two reasons: First, it is possible to extend $\mathbf{n}^\epsilon$ continuously in $\widetilde{\Omega_k^\epsilon}' \setminus \widehat{\Omega_k^\epsilon}'$, with $\widehat{\Omega_k^\epsilon}' = (B_\eta(x_k^\epsilon) \cup [0, x_k^\epsilon]) \cap \Omega'$, where $[0, x_k^\epsilon]$ is the line segment between the points 0 and x_k^ϵ. Second, in order to conclude that also the measure of $\widehat{\Omega_k^\epsilon}$ is bounded, we need to show that ρ_k^ϵ cannot grow to infinity. To see this, note that $x_k^\epsilon \in \Omega_\sigma$ and by applying Proposition 2.4.11 one gets from the energy bound that $\rho_{\min}^\sigma(x_k^\epsilon, \epsilon^\alpha)$ is indeed bounded. All estimates for the lower bound that we have done before stay valid in this setting.

So far, we have established the inequality

$$\begin{aligned}\liminf_{\eta,\xi\to 0} \eta\mathcal{E}_{\eta,\xi}(Q_{\eta,\xi}) \geq (1-C\delta)^2 \frac{\pi}{2} s_*^2 \beta |D\chi_{F_\sigma}|(\mathbb{S}^2 \cap \{\rho \geq \sigma\}) \\ + \int_{F_\sigma} 2s_*c_*(1-\cos(\theta))\,\mathrm{d}\omega + \int_{\widetilde{F_\sigma}} 2s_*c_*(1+\cos(\theta))\,\mathrm{d}\omega - C\sqrt{\delta}\,.\end{aligned} \tag{2.46}$$

We now define the set $\omega_{\sigma,\epsilon}$ as proxy for the set ω_η from Theorem 2.3.1. Let $\omega'_{\sigma,\epsilon} := \bigcup_{k\geq 1} \widehat{\Omega_k^\epsilon}'$, where the sets $\widehat{\Omega_k^\epsilon}' = \Omega_k^\epsilon{}'$ for bounded sequences $|x_k^\epsilon|$, and given as in the second construction if $|x_k^\epsilon|$ diverges. This is well defined for ϵ (and therefore η) small, depending on σ and δ. Recall that since $\eta|\ln\epsilon| \to \beta \in (0,\infty)$, we have the asymptotic $\eta \sim |\ln\epsilon|^{-1}$. Let $\omega_{\sigma,\epsilon}$ be the corresponding rotational symmetric extended set. Then $|\omega'_{\sigma,\epsilon}| \leq C|\bigcup_{x\in X_\epsilon} B_\eta(x)| \leq C\eta^2|X_\epsilon| \leq C\frac{\eta^2}{\delta^4\sigma^2}$, i.e. choosing η small we can force the measure of $\omega'_{\sigma,\epsilon}$ to vanish in the limit. Note that this also implies that the measure of $\omega_{\sigma,\epsilon}$ vanishes because we have an upper bound on the $\rho-$component of points in X_ϵ.

We now want to send $\sigma \to 0$ and choose a diagonal sequence with the properties announced in the theorem. From our previous construction, for a sequence $\sigma_k \searrow 0$ there exist corresponding sequences $\delta_k \searrow 0$, $\eta_k \searrow 0$ and $\epsilon_k \searrow 0$ such that from (2.46)

$$\begin{aligned}\eta\mathcal{E}_{\eta,\xi}(Q_{\eta,\xi}) \geq \frac{\pi}{2} s_*^2 \beta |D\chi_{F_{\sigma_k,\epsilon}}|(\mathbb{S}^2 \cap \{\rho \geq \sigma_k\}) \\ + \int_{F_{\sigma_k,\epsilon}} 2s_*c_*(1-\cos(\theta))\,\mathrm{d}\omega + \int_{\widetilde{F_{\sigma_k,\epsilon}}} 2s_*c_*(1+\cos(\theta))\,\mathrm{d}\omega - \frac{1}{k}\,,\end{aligned}$$

and furthermore $|\omega_{\sigma_k,\epsilon}| \leq \frac{1}{k}$, $|\mathbb{S}^2 \setminus (F_{\sigma_k,\epsilon} \cup \widetilde{F_{\sigma_k,\epsilon}})| \leq \frac{1}{k}$ and $\int_{\Omega_{\sigma_k}\setminus\omega_{\sigma,\epsilon}} \mathrm{dist}^2(\widetilde{Q_\epsilon}, \mathcal{N}_\epsilon)\,\mathrm{d}x \leq \frac{1}{k^2}$ for $\epsilon \leq \epsilon_k$ and $\eta \leq \eta_k$. The sequences ϵ_k and η_k depend on σ_k and δ_k and are related via $\eta_k|\ln\epsilon_k| \to \beta$ as $k \to \infty$.

So we can define the function $\mathbf{n}^\eta : \Omega \to \mathbb{S}^2$ announced in the theorem as $\mathbf{n}^\eta := \mathbf{n}^\epsilon$ on $\Omega_{\sigma_k} \setminus \omega_\eta$ for $\eta \in (\eta_{k+1}, \eta_k)$, $\omega_\eta := \omega_{\sigma_k,\epsilon}$ and extend it measurably to a map $\Omega \to \mathbb{S}^2$. This definition assures that $\mathbf{n}^\eta \in C^0(\Omega_{\sigma_k} \setminus \omega_\eta, \mathbb{S}^2)$ and the convergence in (2.16) holds. Furthermore, we define the set $F_\eta := F_{\sigma_k,\epsilon}$ for $\eta \in (\eta_{k+1}, \eta_k)$. Then our analysis shows that the sequence χ_{F_η} has the point wise a.e. limit χ_F, for $F = \bigcup_{k>1} F_{\sigma_k}$ since $|\chi_F - \chi_{F_\eta}| \leq |\chi_F - \chi_{F_{\sigma_k}}| + |\chi_{F_{\sigma_k}} - \chi_{F_{\sigma_k,\epsilon}}|$ and the measure of the set on which these two terms are nonzero is smaller than $C\sigma_k^2 + \frac{1}{k}$.

This finishes the proof of the first part of Theorem 2.3.1 and (2.17). □

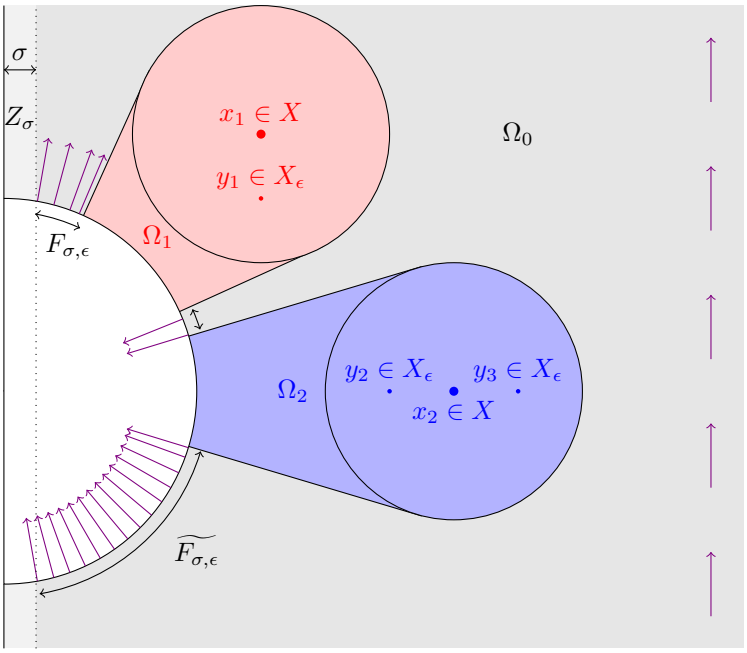

Figure 2.3: Construction made in the proof of Theorem 2.3.1. The arrows show a lifting $\mathbf{n}^\epsilon$. In the region Ω_1 the director field $\mathbf{n}^\epsilon$ has non-trivial homotopy class, around the region Ω_2, $\mathbf{n}^\epsilon$ has a trivial one.

2.5 Upper bound

In this section we are going to prove the upper bound from Theorem 2.3.1, namely (2.18). Since all functions are rotationally equivariant, it is useful to introduce the two dimensional energy for sets $\omega' \subset \Omega'$

$$\mathcal{E}^{2D}_\epsilon(Q,\omega') = \int_{\omega'} \rho \left(\frac{1}{2}|\nabla' Q|^2 + \frac{1}{\rho^2} Q_{2\times 2} : Q + \frac{1}{\epsilon^2} f(Q) + \frac{1}{\eta^2} g(Q) + C_0(\xi,\eta) \right) \mathrm{d}\rho \, \mathrm{d}\theta \,.$$

First, we show the following lemma, which gives the upper bound in the case where there are no singularities near the axis $\rho = 0$.

Remark 2.5.1. *1. The energetically relevant part of the construction in Lemma 2.5.2 away from defects is carried out with uniaxial $Q-$tensors of scalar order parameter s_*. One could also carry this out by using the physically motivated order parameter $s_{*,\xi^2/\eta^2}$ to obtain a sharper upper bound for $\xi, \eta > 0$. In our regime of the limit $\xi, \eta \to 0$, both constructions yield the same upper bound.*

2. In the construction of the singularities in (2.55), we use an isotropic core $Q = 0$. Other choices, such as an oblate uniaxial state surrounded by a biaxial region, are possible and would yield a sharper upper bound for $\xi, \eta > 0$ for certain parameters. However, our upper bound for $\xi, \eta \to 0$ is independent of this choice.

Lemma 2.5.2. *Let $\sigma > 0$ and $F \subset \mathbb{S}^2$ be a rotationally symmetric set of finite perimeter such that $\mathbb{S}^2 \cap \{\rho \leq \sigma, z > 0\}, \mathbb{S}^2 \cap \{\rho \leq \sigma, z < 0\}$ are contained in one of the sets F, F^c. Then there exists a rotationally equivariant sequence of functions $Q_\epsilon \in H^1(\Omega, \mathrm{Sym}_0)$ such that the compactness claim (2.16) holds, $\|Q_\epsilon\|_{L^\infty} \leq \sqrt{\frac{2}{3}} s_*$ and*

$$\limsup_{\epsilon \to 0} \eta \, \mathcal{E}_{\eta,\xi}(Q_\epsilon) \leq \mathcal{E}_0(F) \,.$$

Proof. The proof consists in providing an explicit definition for Q_ϵ, generalizing the construction made in [4]. The idea is the following: Let $F \subset \mathbb{S}^2 \cap \{\rho \geq \sigma\}$ be rotationally symmetric. Since we

assume F to be of finite perimeter, $|D\chi_F|(\mathbb{S}^2 \cap \{\rho \geq \sigma\}) < \infty$. Let $\overline{F} \cap \overline{F^c} \cap \Omega'_\sigma = \{\theta_0, ..., \theta_M\}$ for some $M \in \mathbb{N}$ and $\theta_i < \theta_{i+1}$ for all $i = 0, ..., M-1$. We now define the map Q_ϵ on the two dimensional domain Ω'. We divide Ω' into several regions and define Q_ϵ on each region separately (see Figure 2.4). After that, we derive the estimates that are needed to ensure that the rotated map $R_\varphi^\top Q_\epsilon R_\varphi$ satisfies the energy estimate.

Let Ω' be parametrized by polar coordinates (r, θ). As usual, we denote by $F' = F \cap \Omega'$ and $F^{c\prime} = F^c \cap \Omega'$. Note that $\rho = r \sin\theta$. Let $\mathfrak{R} > 2$ be fixed.

Step 1 (Construction on F'_η and $(F^c)'_\eta$): We define $F'_\eta = F' \setminus \bigcup_{i=0}^M B_{2\eta}(\theta_i) \subset \mathbb{S}^1 \subset \Omega'$ and $(F^c)'_\eta = F^{c\prime} \setminus \bigcup_{i=0}^M B_{2\eta}(\theta_i) \subset \mathbb{S}^1 \subset \Omega'$. For $(r, \theta) \in [1, \mathfrak{R}] \times F'_\eta$ we define

$$Q_\epsilon(r,\theta) \coloneqq s_* \left(\mathbf{n} \otimes \mathbf{n} - \frac{1}{3}\mathrm{Id} \right) \quad \text{with} \quad \mathbf{n}(r,\theta) = \begin{pmatrix} \sqrt{1 - \mathbf{n}_3^2((r-1)/\eta, \theta)} \\ 0 \\ \mathbf{n}_3((r-1)/\eta, \theta) \end{pmatrix}, \tag{2.47}$$

where $\mathbf{n}_3$ is given by Lemma 2.4.17. Analogously, for $(r, \theta) \in [1, \mathfrak{R}] \times (F^c)_\eta$ we define

$$Q_\epsilon(r,\theta) \coloneqq s_* \left(\mathbf{n} \otimes \mathbf{n} - \frac{1}{3}\mathrm{Id} \right) \quad \text{with} \quad \mathbf{n}(r,\theta) = \begin{pmatrix} -\sqrt{1 - \mathbf{n}_3^2((r-1)/\eta, \pi - \theta)} \\ 0 \\ \mathbf{n}_3((r-1)/\eta, \pi - \theta) \end{pmatrix}. \tag{2.48}$$

Since the defined Q_ϵ is uniaxial of scalar order parameter s_*, we have $f(Q_\epsilon) = 0$ and by (2.7) we can estimate the energy on $\Omega_{F'_\eta} = \{(r, \theta) : \theta \in F'_\eta, r \in [1, \mathfrak{R}]\}$

$$\begin{aligned}
&\eta \mathcal{E}_\epsilon^{2D}(Q_\epsilon, \Omega_{F'_\eta}) \\
&\quad = \eta \int_{F'_\eta} \int_1^{\mathfrak{R}} \rho \left(s_*^2 |\partial_r \mathbf{n}|^2 + \frac{s_*^2}{r^2} |\partial_\theta \mathbf{n}|^2 + \frac{1}{\rho^2} Q_{2\times 2,\epsilon} : Q_\epsilon + \frac{c_*^2}{\eta^2}(1 - \mathbf{n}_3^2) + C_0(\xi, \eta) \right) r \, \mathrm{d}r \, \mathrm{d}\theta \\
&\quad = \int_{F'_\eta} \int_0^{(\mathfrak{R}-1)/\eta} \left(s_*^2 |\partial_t \mathbf{n}|^2 + c_*^2(1 - \mathbf{n}_3^2) + C_0(\xi, \eta) \right) (1 + \eta t)^2 \sin\theta \, \mathrm{d}t \, \mathrm{d}\theta \\
&\qquad + \int_{F'_\eta} \int_0^{(\mathfrak{R}-1)/\eta} \frac{\eta^2 s_*^2}{(1+\eta t)^2} \left[|\partial_\theta \mathbf{n}|^2 + \frac{2}{\sin^2\theta}(1 - \mathbf{n}_3^2) \right] (1 + \eta t)^2 \sin\theta \, \mathrm{d}t \, \mathrm{d}\theta \,,
\end{aligned}$$

where we set $r = 1 + \eta t$ and used that $Q_{2\times 2,\epsilon} : Q = |Q_\epsilon|^2 - 6 s_*(1 - \mathbf{n}_3^2) s_* \mathbf{n}_3^2 = 2 s_*^2 (1 - \mathbf{n}_3^2)$. Estimating C_0 by Proposition 2.2.4 and using Lemma 2.4.17 we get

$$\eta \, \mathcal{E}_\epsilon^{2D}(Q_\epsilon, \Omega_{F'_\eta}) \leq \int_{F'} I(0, (\mathfrak{R}-1)/\eta, \cos\theta, 1) \sin\theta \, \mathrm{d}\theta + C\,\eta \leq 2 s_* c_* \int_{F'} (1 - \cos\theta) \sin\theta \, \mathrm{d}\theta + C\,\eta \,. \tag{2.49}$$

Applying the same steps to $(F^c)'_\eta$, we get

$$\eta \, \mathcal{E}_\epsilon^{2D}(Q_\epsilon, \Omega_{(F^c)'_\eta}) \leq 2 s_* c_* \int_{F^{c\prime}} (1 + \cos\theta) \sin\theta \, \mathrm{d}\theta + C\,\eta \,. \tag{2.50}$$

Step 2 (Construction on $(\Omega^+_{\theta_i,\eta})'$ and $(\Omega^-_{\theta_i,\eta})'$): Next, we construct Q_ϵ for $(r, \theta) \in [1 + 4\eta, \mathfrak{R}] \times \bigcup_{i=0}^M B_{2\eta}(\theta_i)$. Without loss of generality, we assume $\theta \in B_{2\eta}(\theta_0)$ and that smaller angles belong to F', while larger values lie in $F^{c\prime}$. We define $(\Omega^+_{\theta_0,\eta})' = \{(r, \theta) : \theta_0 - 2\eta \leq \theta \leq \theta_0, r \in [1 + 4\eta, \mathfrak{R}]\}$ and $(\Omega^-_{\theta_0,\eta})' = \{(r, \theta) : \theta_0 \leq \theta \leq \theta_0 + 2\eta, r \in [1 + 4\eta, \mathfrak{R}]\}$.

Since we want Q_ϵ to have H^1-regularity, we need to respect the values of Q_ϵ that we already constructed at $\theta = \theta_0 - 2\eta$ and $\theta = \theta_0 + 2\eta$. We do this by interpolating between these given values and $s_*(\mathbf{e}_3 \otimes \mathbf{e}_3 - \frac{1}{3}\mathrm{Id})$ at $\theta = \theta_0$. More precisely, for $(r, \theta) \in (\Omega^+_{\theta_0,\eta})'$ we define

$$Q_\epsilon(r,\theta) = s_* \left(\mathbf{n} \otimes \mathbf{n} - \frac{1}{3}\mathrm{Id} \right) \quad \text{with} \quad \mathbf{n}(r,\theta) = \begin{pmatrix} \sin(\phi(r,\theta)) \\ 0 \\ \cos(\phi(r,\theta)) \end{pmatrix},$$

where the phase ϕ is given by

$$\phi(r,\theta) = \frac{\theta_0 - \theta}{2\eta} \arccos\left(\mathbf{n}_3\left(r, \theta_0 - 2\eta\right)\right) . \tag{2.51}$$

Similarly, the phase for $(r,\theta) \in (\Omega^-_{\theta_0,\eta})'$ is given by

$$\phi(r,\theta) = -\frac{\theta - \theta_0}{2\eta} \arccos\left(\mathbf{n}_3\left(r, \pi - (\theta_0 + 2\eta)\right)\right) . \tag{2.52}$$

Note that Q_ϵ is indeed continuous for $\theta = \theta_0$ and that Q_ϵ coincides with our previous definition at $\theta = \theta_0 - 2\eta$ and $\theta = \theta_0 + 2\eta$.

Now we calculate the energy coming from the two regions. We assume that $(r,\theta) \in (\Omega^+_{\theta_0,\eta})'$, the estimates for $(\Omega^-_{\theta_0,\eta})'$ are similar. Since Q_ϵ is takes values in $\mathcal{N}$, $f(Q_\epsilon) = 0$ and furthermore by (2.7)

$$g(Q_\epsilon) = c_*^2(1 - \cos^2(\phi(r,\theta))) = c_*^2 \sin^2(\phi(r,\theta)) \leq c_*^2 \sin^2(\phi(r,\theta_0 - 2\eta)) .$$

For the gradient, we note that

$$\begin{aligned}
\frac{1}{2}|\nabla' Q_\epsilon(r,\theta)|^2 &= s_*^2 |\partial_r \mathbf{n}(r,\theta)|^2 + \frac{s_*^2}{r^2}|\partial_\theta \mathbf{n}(r,\theta)|^2 = s_*^2 |\partial_r \phi(r,\theta)|^2 + \frac{s_*^2}{r^2}|\partial_\theta \phi(r,\theta)|^2 \\
&= \left(\frac{\theta - \theta_0}{2\eta}\right)^2 s_*^2 |\partial_r \phi(r,\theta_0 - 2\eta)|^2 + \frac{s_*^2}{4r^2\eta^2}|\phi(r,\theta_0 - 2\eta)|^2 \\
&\leq s_*^2 |\partial_r \mathbf{n}(r,\theta_0 - 2\eta)|^2 + \frac{s_*^2}{4r^2\eta^2}|\phi(r,\theta_0 - 2\eta)|^2 .
\end{aligned}$$

Note, that for $\eta \to 0$ the phase ϕ stays bounded. Furthermore, all terms decrease exponentially in r by Lemma 2.4.17 and are thus integrable. Since $\frac{1}{2}|\partial_\varphi Q_\epsilon|^2 = Q_{2\times 2} : Q = 2s_*^2 \sin^2(\phi(r,\theta))$, this term converges to zero exponentially and is bounded for $\eta \to 0$. So finally we use the estimates on $C_0(\xi,\eta)$, the above calculations and the usual change of variables $t = 1 + \eta t$ to get

$$\eta\, \mathcal{E}^{2D}_\epsilon(Q_\epsilon, (\Omega^+_{\theta_i,\eta})') \leq C\, \eta . \tag{2.53}$$

Analogously,

$$\eta\, \mathcal{E}^{2D}_\epsilon(Q_\epsilon, (\Omega^-_{\theta_i,\eta})') \leq C\, \eta . \tag{2.54}$$

Step 3 (Construction on B' and D'): Throughout this construction, we assume that we are in the same situation as in Step 2, namely that we are switching from F' to $F^{c\prime}$ as the angle θ increases. In this situation, we are going to construct a defect of degree $-1/2$. Otherwise, one would need to define a defect of degree $1/2$, i.e. one needs to switch the sign of the angle in the definition of $Q(\alpha)$.

- We first define a map Q_B on the two dimensional ball $B_1(0)$ using polar coordinates as follows

$$Q_B(r,\alpha) = \begin{cases} 0 & r \in [0,\epsilon) \\ \left(\frac{r}{\epsilon} - 1\right) Q(\alpha) & r \in [\epsilon, 2\epsilon) \\ Q(\alpha) & r \in [2\epsilon, 1) , \end{cases} \tag{2.55}$$

  where

$$Q(\alpha) = s_* \left(\mathbf{n}(\alpha) \otimes \mathbf{n}(\alpha) - \frac{1}{3}\mathrm{Id}\right) \quad \text{with} \quad \mathbf{n}(\alpha) = \begin{pmatrix} \sin(\alpha/2) \\ 0 \\ \cos(\alpha/2) \end{pmatrix} .$$

- On $B_1 \setminus B_{2\epsilon}$ we calculate

$$\begin{aligned}\int_{B_1\setminus B_{2\epsilon}} \frac{1}{2}|\nabla' Q_B|^2 \,\mathrm{d}x &= \frac{1}{2}\int_0^{2\pi}\int_{2\epsilon}^1 \left(|\partial_r Q_B|^2 + \frac{1}{r^2}|\partial_\alpha Q_B|^2\right) r \,\mathrm{d}\alpha \,\mathrm{d}r \\ &= \frac{1}{2}\int_{2\epsilon}^1 \frac{1}{r}\,\mathrm{d}r \int_0^{2\pi} |\partial_\alpha Q_B|^2 \,\mathrm{d}\alpha \\ &= -\ln(2\epsilon)\int_0^{2\pi} s_*^2 \frac{1}{4}(\cos^2(\alpha/2)+\sin^2(\alpha/2))\,\mathrm{d}\alpha \\ &= \frac{\pi}{2}s_*^2|\ln(\epsilon)| - \frac{\ln(2)\pi}{2}s_*^2\,.\end{aligned}$$

  Furthermore, $f(Q_B) = 0$ on $B_1 \setminus B_{2\epsilon}$ and $\int_{B_1\setminus B_{2\epsilon}} |g(Q_B)|\,\mathrm{d}x \le C|B_1 \setminus B_{2\epsilon}|$. This implies

$$\int_{B_1\setminus B_{2\epsilon}} \frac{1}{2}|\nabla' Q_B|^2 + \frac{1}{\epsilon^2}f(Q_B) + \frac{1}{\eta^2}g(Q_B)\,\mathrm{d}x \le \frac{\pi}{2}s_*^2|\ln(\epsilon)| + \frac{C_1}{\eta^2}|B_1\setminus B_{2\epsilon}|\,. \tag{2.56}$$

- On $B_{2\epsilon} \setminus B_\epsilon$ we find

$$\begin{aligned}\int_{B_{2\epsilon}\setminus B_\epsilon} \frac{1}{2}|\nabla' Q_B|^2 \,\mathrm{d}x &= \frac{1}{2}\int_0^{2\pi}\int_\epsilon^{2\epsilon} \left(|\partial_r Q_B|^2 + \frac{1}{r^2}|\partial_\alpha Q_B|^2\right) r \,\mathrm{d}\alpha \,\mathrm{d}r \\ &= \frac{1}{2}\int_0^{2\pi}\int_\epsilon^{2\epsilon} \left(\frac{1}{\epsilon}-1\right)^2 |Q(\alpha)|^2 r + \frac{1}{r}\left(\frac{r}{\epsilon}-1\right)^2 |\partial_\alpha Q(\alpha)|^2 \,\mathrm{d}r\,\mathrm{d}\alpha \\ &= \frac{2}{3}\pi s_*^2\left(\frac{1}{\epsilon}-1\right)^2\int_\epsilon^{2\epsilon} r\,\mathrm{d}r + \frac{1}{2}\pi s_*^2\int_\epsilon^{2\epsilon}\frac{1}{r}\left(\frac{r}{\epsilon}-1\right)^2\,\mathrm{d}r \\ &= \pi s_*^2\left(\frac{1}{\epsilon}-1\right)^2\epsilon^2 + \frac{\pi}{2}s_*^2\left(\ln(2)-\frac{1}{2}\right) \\ &\le C\,.\end{aligned}$$

  In addition, $f(Q_B) = 0$ and $\int_{B_{2\epsilon}\setminus B_\epsilon} |g(Q_B)|\,\mathrm{d}x \le C|B_{2\epsilon}\setminus B_\epsilon|$. Together, we get

$$\int_{B_{2\epsilon}\setminus B_\epsilon} \frac{1}{2}|\nabla' Q_B|^2 + \frac{1}{\epsilon^2}f(Q_B) + \frac{1}{\eta^2}g(Q_B)\,\mathrm{d}x \le C_2\left(1+\frac{1}{\eta^2}\right)|B_{2\epsilon}\setminus B_\epsilon|\,. \tag{2.57}$$

  Finally, the gradient of Q_B on $B_\epsilon(0)$ is zero. The contributions from f and g are easily seen to be bounded by $C|B_\epsilon|$, so that

$$\int_{B_\epsilon} \frac{1}{2}|\nabla' Q_B|^2 + \frac{1}{\epsilon^2}f(Q_B) + \frac{1}{\eta^2}g(Q_B)\,\mathrm{d}x \le C_3\left(\frac{1}{\epsilon^2}+\frac{1}{\eta^2}\right)|B_\epsilon|\,. \tag{2.58}$$

Combining (2.56), (2.57) and (2.58) we get

$$\int_{B_1(0)} \frac{1}{2}|\nabla' Q_B|^2 + \frac{1}{\epsilon^2}f(Q_B) + \frac{1}{\eta^2}g(Q_B)\,\mathrm{d}x \le \frac{\pi}{2}s_*^2|\ln(\epsilon)| + C\left(1+\frac{1}{\eta^2}\right)|B_1(0)| + C\,. \tag{2.59}$$

Note that we have the same bound for $Q_{B_{\tilde r}}(r,\alpha) = Q_B(r/\tilde r,\alpha)$ on $B_{\tilde r}(0)$, where $\tilde r \le 1$. In addition, this bound is invariant under rotations and translations of the domain. Again we assume that $\theta \in B_\eta(\theta_0)$. We use the construction of Q_B to define Q_ϵ on the set $B := B_\eta(1+2\eta,\theta_0) \subset [1,1+4\eta]\times[\theta_0-2\eta,\theta_0+2\eta]$ via

$$Q_\epsilon(r,\theta) = R_{\theta_0} Q_B(\overline{r}/\eta,\alpha)\,, \tag{2.60}$$

where R_{θ_0} is the rotation matrix around the $\rho-$axis with angle θ_0, $\overline{r}^2 = (r-1-2\eta)^2 + (\theta-\theta_0)^2$ and α being the angle between the vectors $(0,1)^\top$ and $(\theta_0-\theta, r-1-2\eta)^\top$. Note, that the term $|B_1(0)|$ in (2.59) transforms to $|B|$, which can be estimated by $C\eta^2$. For the remaining term of $\mathcal{E}_\epsilon^{2D}$ we notice that $Q_{2\times2,\epsilon} : Q_\epsilon$ is bounded on B and that $\rho \ge \sigma - \eta$, thus $\int_B \rho^{-1} Q_{2\times2,\epsilon} : Q_\epsilon \le C(\sigma-\eta)^{-1}$.

Then, using $\rho \leq (1+2\eta)\sin(\theta_0)+\eta$ we get from (2.59) together with the estimate on $C_0(\xi,\eta)$ from Proposition 2.2.4 that

$$\eta\, \mathcal{E}_\epsilon^{2D}(Q_\epsilon, B) \leq ((1+2\eta)\sin(\theta_0)+\eta)\frac{\pi}{2}s_*^2\eta|\ln(\epsilon)| + C\eta + \frac{C}{\sigma-\eta}\eta\,. \tag{2.61}$$

We now want to construct the map Q_ϵ on the set $D = \{(r,\theta)\in[1,1+4\eta]\times[\theta_0-2\eta,\theta_0+2\eta]\}\setminus B$ by interpolating between the values given by Steps 1 and 2 on the one hand, and the values on ∂B on the other hand. We use the same polar coordinates $(\overline{r},\alpha)$ as for the definition of Q_ϵ on B to parametrize D. Let $\Phi_{\alpha/2}(\alpha)$ be the phase associated to the director of $Q_\epsilon(\eta,\alpha)$ and $\Phi(\alpha)$ the phase of the boundary values on $\partial(D\cup B)$. We set

$$\phi(\overline{r},\alpha) = \frac{R(\alpha)-\overline{r}}{R(\alpha)-\eta}\Phi_{\alpha/2} + \frac{\overline{r}-\eta}{R(\alpha)-\eta}\Phi(\alpha)\,,$$

where

$$R(\alpha) = \begin{cases} \frac{2\eta}{|\cos(\alpha)|} & \text{if } \alpha\in[-\pi/4,\pi/4]\cup[3\pi/4,5\pi/4]\,,\\ \frac{2\eta}{|\sin(\alpha)|} & \text{otherwise}\,.\end{cases}$$

In particular, $|R(\alpha)|\leq 2\sqrt{2}\eta$ and $|\partial_\alpha R(\alpha)|\leq 2\sqrt{2}\eta$. Then we define

$$Q_D(\overline{r},\alpha) = s_*\left(\mathbf{n}(\overline{r},\alpha)\otimes\mathbf{n}(\overline{r},\alpha)-\frac{1}{3}\mathrm{Id}\right) \quad \text{with} \quad \mathbf{n}(\overline{r},\alpha) = \begin{pmatrix}\sin(\phi(\overline{r},\alpha))\\ 0\\ \cos(\phi(\overline{r},\alpha))\end{pmatrix}.$$

Then $f(Q_\epsilon|_D)=0$ since $Q_\epsilon|_D$ is uniaxial and of scalar order parameter s_* and $|g(Q_\epsilon|_D)|$ is bounded. We can estimate the gradient

$$\begin{aligned}\int_D \frac{1}{2}|\nabla' Q_\epsilon|^2\,\mathrm{d}x &= \int_D \frac{1}{2}\left(|\partial_r Q_\epsilon|^2 + \frac{1}{r^2}|\partial_\theta Q_\epsilon|^2\right) r\,\mathrm{d}r\,\mathrm{d}\theta\\ &\leq (1+4\eta)\int_0^{2\pi}\int_\eta^{R(\alpha)}\frac{1}{2}\left(|\partial_{\overline{r}}Q_\epsilon|^2+\frac{1}{\overline{r}^2}|\partial_\alpha Q_\epsilon|^2\right)\overline{r}\,\mathrm{d}\overline{r}\,\mathrm{d}\alpha\\ &\leq (1+4\eta)s_*^2\int_0^{2\pi}\int_\eta^{R(\alpha)}\left(|\partial_{\overline{r}}\phi|^2+\frac{1}{\overline{r}^2}|\partial_\alpha\phi|^2\right)\overline{r}\,\mathrm{d}\overline{r}\,\mathrm{d}\alpha\,.\end{aligned} \tag{2.62}$$

Since $\Phi_{\alpha/2}$ and $\Phi(\alpha)$ are bounded and $\partial_{\overline{r}}\phi = \frac{-1}{R(\alpha)-\eta}\Phi_{\alpha/2} + \frac{1}{R(\alpha)-\eta}\Phi(\alpha)$, we can easily infer that $|\partial_{\overline{r}}\phi|^2\leq\frac{C}{\eta^2}$. Furthermore it is clear by definition that $|\partial_\alpha\Phi_{\alpha/2}|^2\leq C$. So it remains to derive bounds on $\partial_\alpha\Phi(\alpha)$. For $\alpha\in[0,\pi/4]$ we have $\Phi(\alpha)=\arccos(\mathbf{n}_3(1+4\eta,\theta_0-2\eta))\frac{\sqrt{R(\alpha)^2-4\eta^2}}{2\eta}$, i.e. $|\partial_\alpha\Phi(\alpha)|^2\leq C$. Similarly, $\partial_\alpha\Phi$ is bounded for $\alpha\in[-\pi/4,0]$. For $\alpha\in[\pi/4,3\pi/4]$ and $r(\alpha)=1+\sqrt{R^2(\alpha)+8\eta^2-4\sqrt{2}R(\alpha)\eta\cos(3\pi/4-\alpha)}$ one can show that $\Phi(\alpha)=\arccos(\mathbf{n}_3(r(\alpha),\theta_0-2\eta))$. An explicit calculation yields $|\partial_\alpha\Phi(\alpha)|^2\leq C$. By the same argument, $\partial_\alpha\Phi$ is also bounded for $\alpha\in[-3\pi/4,-\pi/4]$ For $\alpha\in[3\pi/4,\pi]$ we have $\Phi(\alpha)=-2\eta\tan(\pi-\alpha)+\theta_0-\frac{\pi}{2}$, so that $|\partial_\alpha\Phi(\alpha)|^2$ is also bounded by a constant. We plug this result into (2.62) and use the fact that $Q_{2\times2,\epsilon}:Q_\epsilon$ is also bounded, $\sigma\leq 1+4\eta$ and $C_0\leq C\xi^2/\eta^2$ to get

$$\mathcal{E}_\epsilon^{2D}(Q_\epsilon,D)\leq 2(1+4\eta)s_*^2\int_0^{2\pi}\int_\eta^{R(\alpha)}\left(C+\frac{C}{\sigma^2}\right)\sigma\,\mathrm{d}\sigma\,\mathrm{d}\alpha + \frac{C}{\sigma-c\eta}\leq C+\frac{C}{\sigma-c\eta}\,. \tag{2.63}$$

Hence by (2.61) and (2.63)

$$\eta\,\mathcal{E}_\epsilon^{2D}(Q_\epsilon,B\cup D)\leq((1+2\eta)\sin(\theta_0)+2\eta)\frac{\pi}{2}s_*^2\eta|\ln\epsilon| + C\eta + \frac{C}{\sigma-C\eta}\eta\,. \tag{2.64}$$

This finishes our construction of $Q_\epsilon(\rho,\theta)$.

Step 4 (Transition to $Q_\infty(\xi,\eta)$): So far, we have constructed the sequence Q_ϵ inside a ball of radius $\mathfrak{R}$ around 0. Because of the exponential convergence of the optimal profile from Lemma

2.4.17 , the function Q_ϵ is close to Q_∞ on $\partial B_\mathfrak{R}$. We will now construct a transition zone from Q_ϵ to Q_∞ for $r \in (\mathfrak{R}, \mathfrak{R}+\eta)$ and then from Q_∞ to $Q_\infty(\xi,\eta)$ for $r \in (\mathfrak{R}+\eta, \mathfrak{R}+2\eta)$. Since $Q_\epsilon(\mathfrak{R},\theta) \in \mathcal{N}$ for all $\theta \in [0,\pi]$ we can linearly interpolate the phase between $Q_\epsilon(\mathfrak{R},\theta)$ and Q_∞ as in Step 2. We estimate as in Step 2 and thus the cost of this interpolation in terms of energy is given by

$$\eta\, \mathcal{E}_\epsilon^{2D}(Q_\epsilon, B_{\mathfrak{R}+\eta} \setminus B_\mathfrak{R}) \leq C\,\eta\,. \tag{2.65}$$

For $r \in (\mathfrak{R}+\eta, \mathfrak{R}+2\eta)$ we linearly interpolate between Q_∞ and $Q_\infty(\xi,\eta)$, i.e. we define

$$Q_\epsilon(r,\theta) = \frac{1}{\eta}((\mathfrak{R}+2\eta-r)s_* + (r-\mathfrak{R}-\eta)s_{*,\xi^2/\eta^2})\left(\mathbf{e}_3\otimes\mathbf{e}_3 - \frac{1}{3}\mathrm{Id}\right).$$

Since $|s_{*,\xi^2/\eta^2} - s_*| \leq C\xi^2/\eta^2$ and by Proposition 2.2.4 we get

$$\eta\, \mathcal{E}_\epsilon^{2D}(Q_\epsilon, B_{\mathfrak{R}+2\eta} \setminus B_{\mathfrak{R}+\eta}) \leq C\,\eta^2(\frac{\xi^4}{\eta^6} + \frac{\xi^2}{\eta^4} + \frac{\xi^2}{\eta^4} + \frac{\xi^2}{\eta^2})\,. \tag{2.66}$$

Finally, if $r \geq \mathfrak{R}+2\eta$ we set $Q_\epsilon = Q_\infty(\xi,\eta)$, which has energy 0.

If we now extend Q_ϵ to Ω by using the rotated function $Q_\epsilon(\rho,\varphi,\theta) = R_\varphi^\top Q_\epsilon(\rho,\theta)R_\varphi$ and integrate $\mathcal{E}_\epsilon^{2D}$ in φ-direction, we get from (2.49), (2.50), (2.53), (2.54), (2.64), (2.65) and (2.66)

$$\begin{aligned}\eta\mathcal{E}_\epsilon(Q_\epsilon,\Omega) \leq\ & 2s_*c_*\int_0^{2\pi}\int_{F'}(1-\cos(\theta))\sin(\theta)\,\mathrm{d}\theta\,\mathrm{d}\varphi + 2s_*c_*\int_0^{2\pi}\int_{F^{c\prime}}(1+\cos(\theta))\sin(\theta)\,\mathrm{d}\theta\,\mathrm{d}\varphi\\ &+ \frac{\pi}{2}s_*^2\eta|\ln\epsilon|\sum_{i=0}^{M-1}\int_0^{2\pi}((1+2\eta)\sin(\theta_i)+2\eta)\,\mathrm{d}\varphi + C\eta + \frac{C\eta}{\sigma-c\eta}\,.\end{aligned} \tag{2.67}$$

Taking the limsup $\eta,\epsilon\to 0$ in (2.67) yields the inequality

$$\begin{aligned}\limsup_{\eta,\epsilon\to 0}\mathcal{E}_{\eta,\xi}(Q_\epsilon) &\leq 2s_*c_*\int_F(1-\cos(\theta))\,\mathrm{d}\omega + 2s_*c_*\int_{F^c}(1+\cos(\theta))\,\mathrm{d}\omega + \frac{\pi}{2}s_*^2\beta|D\chi_F|(\mathbb{S}^2)\\ &= \mathcal{E}_0(F)\,.\end{aligned}$$

It remains to show the claimed convergence. It is clear by definition of Q_ϵ that $\bigcup_{\eta>0}F_\eta = F$ and $\bigcup_{\eta>0}(F^c)_\eta = F^c$ which implies the convergence for χ_F. The continuity of $\mathbf{n}^\epsilon$ as a function with values in $\mathbb{S}^2$ outside a set ω_η is clear by construction if we choose ω_η to contain all balls B, we used in step 3. Taking ω_η as the union of all sets B and D from step 3. we can also achieve that $\Omega\setminus\omega_\eta$ is simply connected. Extending $\mathbf{n}^\epsilon$ inside B measurably, yields the compactness claim. □

Proof of the upper bound (2.18) of Theorem 2.3.1. We choose a sequence $\sigma_k > 0$ which converges to zero as $k\to\infty$. We approximate the set F by sets F_k such that the domains $\mathbb{S}^2\cap\{\rho\leq\sigma_k, z>0\}$ and $\mathbb{S}^2\cap\{\rho\leq\sigma_k, z<0\}$ are fully contained in F_k or F_k^c. By Lemma 2.5.2 there exist sequences $Q_{\epsilon,k}$ such that $\limsup_{\eta,\epsilon\to0}\mathcal{E}_{\eta,\xi}(Q_{\epsilon,k}) \leq \mathcal{E}_0(F_k)$ and (2.16) holds. We observe that

$$|D\chi_{F_k}|(\mathbb{S}^2) = |D\chi_{F_k}|(\mathbb{S}^2\cap\{\rho\geq\sigma_k\}) = |D\chi_F|(\mathbb{S}^2\cap\{\rho\geq\sigma_k\})$$

and

$$\left|\int_F\big(1-\cos(\theta)\big)\,\mathrm{d}\omega - \int_{F_k}\big(1-\cos(\theta)\big)\,\mathrm{d}\omega\right|, \left|\int_{F^c}\big(1+\cos(\theta)\big)\,\mathrm{d}\omega - \int_{F_k^c}\big(1+\cos(\theta)\big)\,\mathrm{d}\omega\right| \leq C\sigma_k^2\,.$$

Hence $\limsup_{\eta,\epsilon\to0}\mathcal{E}_{\eta,\xi}(Q_{\epsilon,k}) \leq \mathcal{E}_0(F_k) \leq \mathcal{E}_0(F) + C\sigma_k^2$ and taking a diagonal sequence $Q_\epsilon = Q_{\epsilon,k(\epsilon)}$ we get

$$\limsup_{\eta,\epsilon\to0}\mathcal{E}_{\eta,\xi}(Q_\epsilon) \leq \mathcal{E}_0(F)\,.$$

The compactness (2.16) follows by triangle inequality. □

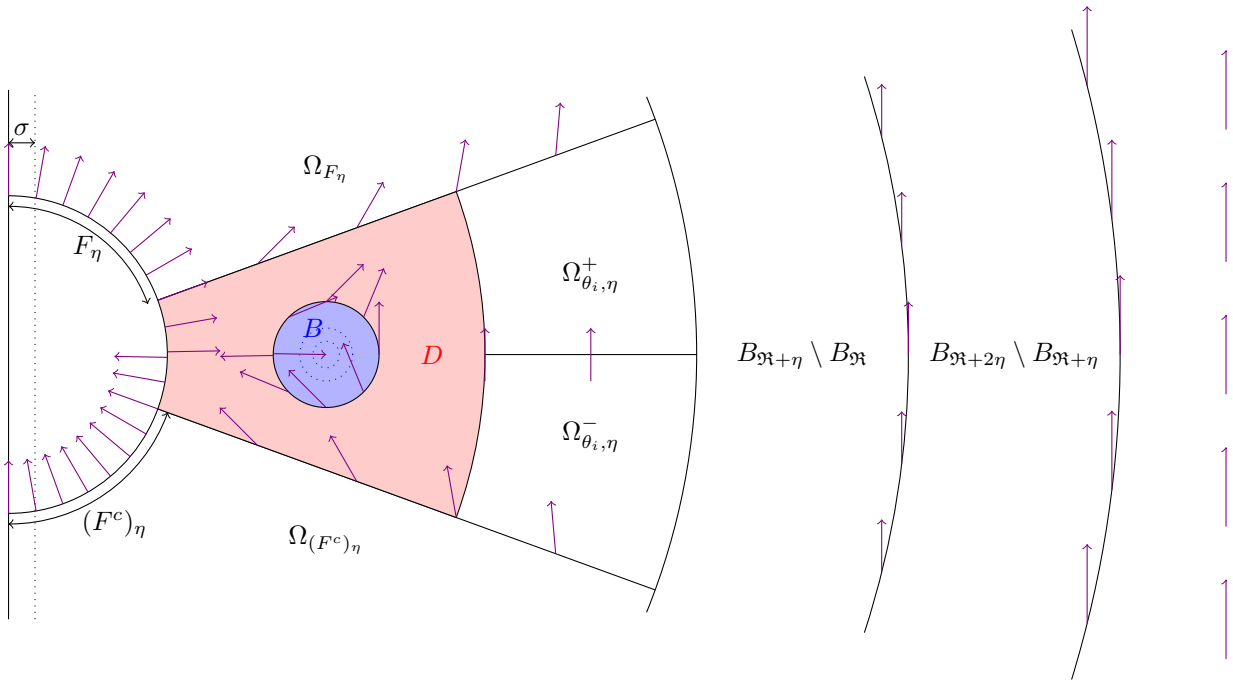

Figure 2.4: Partition of Ω' into regions for the construction of Q_ϵ (arrows show $\mathbf{n}^\epsilon$)

2.6 Limit problem, transition and hysteresis

Physicists have successfully manipulated the Saturn ring configuration by using electric fields [83] and observed a transition between dipole and Saturn ring by changing the strength of the field (see [14, p.190ff] and [113], [112]) or the radius of the particle [162]. In [112, Fig. 1] a series of images shows the accelerated shrinking of a Saturn ring defect loop around a spherical particle towards a dipole defect, once the applied electric field is switched off. The configurations intermediate between dipole and Saturn ring are observed to be unstable. Similar transitions from Saturn ring to dipole have been observed by accelerating a droplet inside a liquid crystal [95], [170].

In [154] physical reasoning, scaling arguments and numerical simulations are conducted to explain this type of transition and the occurrence of a hysteresis phenomenon. To our knowledge the hysteresis has not yet been observed, but cannot be excluded [162]. Our limit model provides an analytical setting, in which we are able to reproduce the findings derived by H. Stark from physical arguments and numerical simulations. The reduced magnetic coherence length ξ_H introduced in [154] corresponds to our parameter η in the one constant approximation. As pointed out in the first section, our limit $\xi, \eta \to 0$ corresponds to an increasing particle radius $r_0 \to \infty$ and a simultaneously decreasing field strength $h \to 0$ since $\xi \sim r_0^{-1}$ and $\eta \sim h^{-1}\xi$. The slower the decrease of h, the stronger is the influence of the magnetic field in $\eta|\ln(\xi)|$ and thus in β. It is therefore reasonable to say that small values of β correspond to strong magnetic field, relative to the size of $\xi|\ln(\xi)|$. This translates the assumption of high magnetic fields $\xi_H \ll 1$ (while keeping r_0 fixed) in [154] to smaller values of β in our limit. Although the calculations in [154] are based on the Oseen-Frank model rather than the Landau-de Gennes that we are using, we are able to reproduce the behaviour of the energy $\mathcal{E}_0$ as a function of θ_d, compare Figure 2.5 and [154, Fig. 11]. From our calculation, we also find the hysteresis for changing values of βs_*. For $\beta \gg 1$, i.e. small external fields, the dipole is the only stable configuration. Increasing the field, the system will maintain the dipole, until we reach $\beta = 0$, where a transition to the Saturn ring takes place. Decreasing the field while starting from a Saturn ring, we will retain the structure until we reach $\frac{s_*}{c_*}\beta = \frac{8}{\pi} \approx 2.546$ and the Saturn ring closes to a dipole.

The rest of this section is devoted to the calculation of the minimal energy configurations of

the limiting model which we have explained above.

In a first step, we claim that if F is a minimizer of $\mathcal{E}_0$, then F and F^c are connected. Indeed, assume that one of the two sets, say F, is not connected. Then there are two possibilities: If F^c is connected, then F also contains the point $\theta = \pi$ and we can decrease the energy $\mathcal{E}_0$ by handing over this set to F^c. If F^c is also not connected, then we can similarly exchange points between F and F^c while decreasing the energy until both sets are connected.

Now that we know that F and F^c are connected, we deduce that there can only be one angle under which the defect line separating F and F^c occurs. Let us name this angle $\theta_d \in [0, \pi]$ and let $F \subset \mathbb{S}^2$ be the set corresponding to $0 \leq \theta \leq \theta_d$. Then we can express the limit energy as

$$\begin{aligned}
\mathcal{E}_0(F) &= 2s_*c_* \int_F (1 - \cos(\theta)) \, \mathrm{d}\omega + 2s_*c_* \int_{F^c} (1 + \cos(\theta)) \, \mathrm{d}\omega + \frac{\pi}{2} s_*^2 \beta |D\chi_F|(\mathbb{S}^2) \\
&= 2s_*c_* \int_0^{2\pi} \int_0^{\theta_d} (1 - \cos(\theta)) \sin(\theta) \, \mathrm{d}\theta \, \mathrm{d}\varphi + 2s_*c_* \int_0^{2\pi} \int_{\theta_d}^{\pi} (1 + \cos(\theta)) \sin(\theta) \, \mathrm{d}\theta \, \mathrm{d}\varphi \\
&\quad + \frac{\pi}{2} s_*^2 \beta (2\pi \sin(\theta_d)) \\
&= 8\pi s_* c_* \Big(\sin^4(\theta_d/2) + \cos^4(\theta_d/2) \Big) + \pi^2 \beta s_*^2 \sin(\theta_d) \, .
\end{aligned}$$

Setting the derivative of this expression to zero gives the equation

$$\pi s_* \cos(\theta_d) \Big(\pi \beta s_* - 8 c_* \sin(\theta_d) \Big) = 0 \, ,$$

which yields the two families of solutions $\theta_1 = \pi/2 + \pi\mathbb{Z}$ and $\theta_2 = \arcsin(\frac{\pi \beta s_*}{8 c_*}) + 2\pi\mathbb{Z}$. We note:

1. For $\frac{s_*}{c_*}\beta = \frac{8}{\pi} \approx 2.546$, the two families are equal. We conclude that for $\frac{s_*}{c_*}\beta \geq \frac{8}{\pi}$ the only stable configuration is a dipole at $\theta_d = 0, \pi$ (see Figure 2.5).
2. The energy of the Saturn ring $\theta_d = \pi/2$ and the dipole $\theta_d = 0$ are equal for $\frac{s_*}{c_*}\beta = \frac{4}{\pi} \approx 1.273$, which means for greater values of $\frac{s_*}{c_*}\beta$ the dipole is the globally energy minimizing configuration, while for smaller values the Saturn ring is optimal.
3. The case where $\theta_d = \pi/2$ is the only (local) minimizer corresponds to $\beta = 0$, i.e. $\theta_2 = 0$.

In particular, we see that the only stable energy minimizing configurations are the dipole (which corresponds to $F = \emptyset$ or $F = \mathbb{S}^2$) and the Saturn ring (where F is the upper half-sphere).

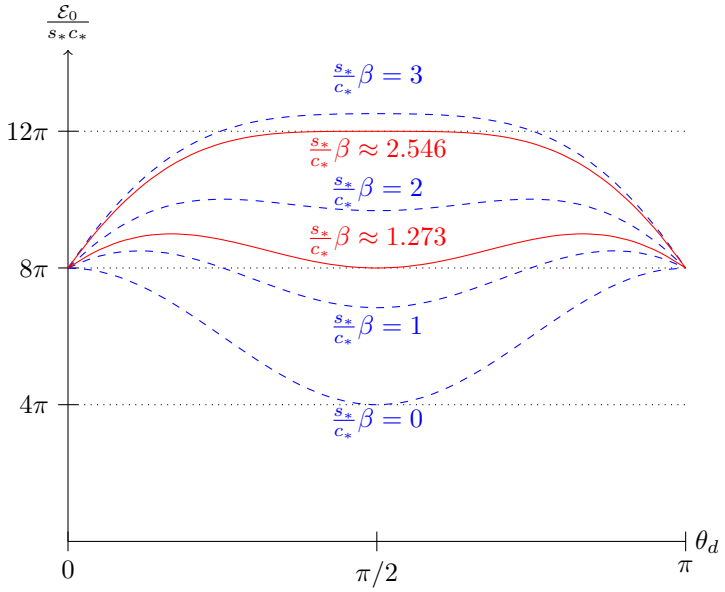

Figure 2.5: Plot of the energy $\mathcal{E}_0$ for different values of βs_* as a function of the angle θ_d

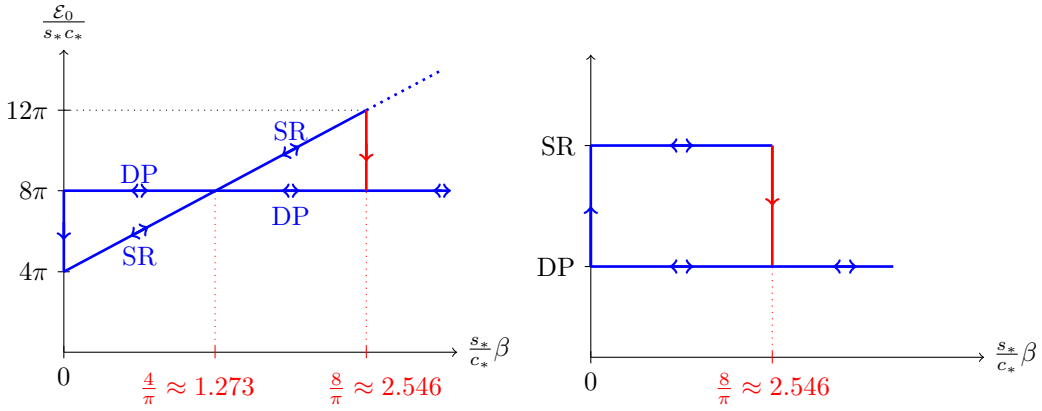

Figure 2.6: Left: Plot of the energy of the dipole and Saturn ring as a function of $\frac{s_*}{c_*}\beta$. Right: Hysteresis induced by changing $\frac{s_*}{c_*}\beta$

The available experimental and theoretical results are in agreement with these findings. Nevertheless, the conducted experiments mostly use an electric field to manipulate the orientation of the liquid crystals and were not yet able to observe the hysteresis phenomenon, described in [154] and in this work.

We hope that our analysis stimulates further research into this direction.

2.7 Conclusion

The goal of this article was to derive an effective energy of the Landau-de Gennes model for a spherical particle immersed into a nematic liquid crystals under the influence of a homogeneous external magnetic field, stated in the framework of variational convergence. We imposed strong anchoring conditions at the boundary of the particle and investigated the interplay of elastic, bulk and magnetic free energy in an intermediate regime parametrized by β that exhibits singularities of both dipole and Saturn ring type. Studying the limit energy, we show that there are no stable minimizers other than the dipole or the Saturn ring and we determine ranges for β in which either of the two is energy minimizing. We calculate values of β where a transition between the two takes place, finding a hysteresis phenomenon.

Chapter 3

The general case

This chapter is based on the article "Convergence to line and surface energies in nematic liquid crystal colloids with external magnetic field", see [9].

Abstract

We use the Landau-de Gennes energy to describe a particle immersed into nematic liquid crystals with a constant applied magnetic field. We derive a limit energy in a regime where both line and point defects are present, showing quantitatively that the close-to-minimal energy is asymptotically concentrated on lines and surfaces nearby or on the particle. We also discuss regularity of minimizers and optimality conditions for the limit energy.

3.1 Introduction

The history of interaction between variational problems and geometry has been long and of great mutual influence [81], starting from the geometrically motivated problem of the brachistochrone curve [27,137], Fermat's principle in optics [31], material science [19] to general relativity [85,122].

One particularly important problem arises when the size of geometrical objects themselves is to be minimized leading to so called *minimal surfaces* [103]. A classical example is the two dimensional soap film spanning between predefined (fixed) boundary curves, called Plateau's problem [59,140, 155]. Some solutions can be constructed explicitly [55,94] or studied through means of harmonic and complex analysis [50,93,134], but a general theory was not available until the development of geometric measure theory and its language of currents, flat chains, mass and varifolds to describe the objects and how to measure them [6,65,66,131,158].

Another question giving rise to problems involving minimal surfaces is given by the classical $\Gamma-$convergence result of Modica and Mortola [127] (see also [125]) of a weighted Dirichlet energy and a penalizing double-well potential to the perimeter functional. A constraint such as a prescribed volume ensures the problem to be non trivial. The energy typically is concentrated in regions where none of the favourable states of the potential are attained. For the limsup inequality, one constructs a one dimensional profile that minimizes the transition between the favoured states.

Another variational problem in which geometry appears is given by the Ginzburg-Landau model. In the famous work [30], the (logarithmically diverging) leading order term and (after a rescaling) a limit problem have been derived. The limit energy is stated geometrically as finding an optimal distribution of points in the plane subject to constraints coming from the topological degree of the initial problem. This approach stimulated research which lead to a large literature [5,38,44,87,108,124,145], in particular for problems in micromagnetics [89,101], superconductors [97,148,152] and liquid crystals [24,90,109].

Our work combines many of the before mentioned ideas to describe the different contributions and effects that take place in our problem. For example, we use the generalized three dimensional analogue of estimations in [30] as considered in [42, 44, 47, 92, 144] to make appear a length minimization problem for curves. Coupled with this optimization problem, we show using a Modica-Mortola type argument that the remaining part of the energy concentrates on hypersurfaces which end either on the boundary of the domain or on the described line.

The main motivation for this article was the study of the formation and transition of singularities in colloidal nematic liquid crystals, in particular the *Saturn ring effect*. It has been observed in experiments that nematic liquid crystals may exhibit line and point singularities. Those can take the form of a ring around one or several of the colloidal particles depending on the shape and size of the particles and the strength of an external electric or magnetic field [112, 113, 128, 133]. This phenomenon is caused by the incompatibility between the boundary condition at the surface of the particle where a positive topological charge is created, and the condition at infinity where an electric or magnetic field enforces a uniform alignment of the molecules in the direction of the field. While spheres are the most studied particles, there is also a considerable interest in defect structures around non-spherical inclusions [15, 143, 156]. For the study of phenomena such as self assembly [150, 151, 168] usually a large number of particles is needed. In this work however, we focus on the simpler case of a single colloidal particle as a first step for understanding the complex interaction that takes place in colloidal systems [75, 114, 133].

This article is the continuation of the work started in [8] where we studied a spherical inclusion, our main theorem (Theorem 3.3.1) is a generalisation of Theorem 3.1 in [8] (see Remark 3.3.3). In particular, our new theorem holds for an arbitrary manifold $\mathcal{M}$ of class C^2 instead of a sphere and we remove the hypothesis of rotational equivariance of Q.

Although the applied ideas could be used to carry out a similar analysis for a larger class of energy functionals, we place ourself in the context of the Landau-de Gennes model for nematic liquid crystals. A common way to describe liquid crystals is by introducing a unit vector field $\mathbf{n}$, the so called *director field*, for example in the Oseen-Frank model. The vector $\mathbf{n}$ represents the local orientation of the liquid crystal molecules. In practice, it is often not possible to distinguish between $\mathbf{n}$ and $-\mathbf{n}$, so that $\mathbf{n}$ should rather be $\mathbb{R}P^2-$valued, where $\mathbb{R}P^2$ is the two-dimensional real projective space. More generally, one can think of describing the arrangement of the molecules by a symmetric probability distribution ρ on the sphere of directions. Because of the symmetry, the first moment of ρ vanishes and the (shifted) second moment Q is a symmetric traceless matrix (also called $Q-$tensor), which is used to represent ρ in the Landau-de Gennes model. In the following we will denote Sym_0 the space of such symmetric traceless matrices. Under this identification, the uniform distribution on the sphere corresponds to the *isotropic* state in which all three eigenvalues $\lambda_1 \geq \lambda_2 \geq \lambda_3$ of Q are equal to zero or equivalently $Q = 0$. In case two eigenvalues are equal, we call Q *uniaxial*. More precisely, if $\lambda_1 = \lambda_2 > \lambda_3$ we say that Q is *prolate* (or positively) uniaxial, while if $\lambda_1 > \lambda_2 = \lambda_3$ it is called *oblate* (or negatively) uniaxial. If all three eigenvalues of Q are distinct $\lambda_1 > \lambda_2 > \lambda_3$, we speak of a *biaxial* $Q-$tensor. A particularly important role is played by the set $\mathcal{N}$ of prolate uniaxial tensors of a given norm as they are minimizers of the ordering potential in the Landau-de Gennes energy as we will see in Section 3.2.1. Elements $Q \in \mathcal{N}$ can be written as $Q = s_*(\mathbf{n} \otimes \mathbf{n} - \frac{1}{3}\mathrm{Id})$ (s_* being a constant depending on the liquid crystal) and thus allow an identification with the director field in direction $\pm\mathbf{n}$. On the other hand, singularities are described by situations in which one cannot identify a director field, e.g. if Q is isotropic or oblate uniaxial. However, the analysis carried out in this paper does not discriminate between the two different possibilities as they have asymptotically the same energetic cost in our regime. Nevertheless, in [40] it has been proven that in some situations an oblate uniaxial defect core surrounded by a biaxial region has strictly smaller energy compared to an isotopic core. We refer the interested reader to [20] for a more detailed introduction to $Q-$tensors, the Landau-de Gennes energy and related models for liquid crystals.

As we will see later in Section 3.2.1, the Landau-de Gennes model in our case comprises three contributions related to the elastic, ordering and magnetic energy. The relative strength of the individual terms are modulated by the dimensionless parameter ξ describing the ratio between elastic and bulk energy, while η couples the elastic with the magnetic term. We are concerned with the limit of $\eta, \xi \to 0$, which can be physically interpreted as a limit of large particles and weak

magnetic fields, see [8, 76]. This regime has been studied previously in [4] for a spherical particle under the assumption that $\eta|\ln(\xi)| \to 0$ as $\eta, \xi \to 0$ in which a Saturn ring structure is found. In [3] the authors treated the problem in the absence of a magnetic field, i.e. for $\eta = \infty$. For $\xi \to 0$ they deduce that a point defect occurs. Our work places itself in the intermediate regime in which $\eta|\ln(\xi)| \to \beta \in (0, \infty)$ as $\eta, \xi \to 0$. As seen in [8] for a spherical particle, this regime allows for incorporating different minimizing configurations, depending on the parameter β. In a forthcoming paper [153], we are going to develop numerical methods to calculate the minimizing configurations around non-spherical particles based on the results in this work.

3.2 Preliminaries

Before we can state our results, we give a short introduction to the Landau-de Gennes model that we use here and the concept of flat chains, stating some results that will be used later in the proof section.

3.2.1 Landau-de Gennes model for nematic liquid crystals

Our article has been motivated by the study of liquid crystal colloids with external magnetic field. Let $E \subset \mathbb{R}^3$ be a colloidal particle and let $\Omega := \mathbb{R}^3 \setminus E$ be the region occupied by the liquid crystal. The Landau-de Gennes energy with additional magnetic field term [139, Ch. 6, Secs. 3-4 and Ch. 10, Sec. 2.3] (see also [57, Ch. 3, Secs. 1-2]) can be stated in dimensionless form as

$$\mathcal{E}_{\eta,\xi}(Q) \;=\; \int_\Omega \frac{1}{2}|\nabla Q|^2 + \frac{1}{\xi^2} f(Q) + \frac{1}{\eta^2} g(Q) + C_0 \,\mathrm{d}x\,, \tag{3.1}$$

where the energy density f is given by

$$f(Q) \;=\; C - \frac{a}{2}\mathrm{tr}(Q^2) - \frac{b}{3}\mathrm{tr}(Q^3) + \frac{c}{4}\mathrm{tr}(Q^2)^2\,, \tag{3.2}$$

and g is a function taking into account the effects of the external magnetic field in a way we formalize a bit later in this section. The function $Q : \Omega \to \mathrm{Sym}_0$ is a tensorial order parameter taking values in the space of symmetric traceless matrices

$$\mathrm{Sym}_0 := \{Q \in \mathbb{R}^{3\times 3} \,:\, Q^T = Q \text{ and } \mathrm{tr}(Q) = 0\}\,,$$

equipped with the norm $\|Q\|^2 := \mathrm{tr}(Q^2)$. It is used to describe the local distribution of orientation of the liquid crystal molecules. We consider the case when the parameters η and ξ converge to zero in a regime where $\eta|\ln(\xi)| \to \beta \in (0, \infty)$. The constant $C_0 = C_0(\eta, \xi)$ (resp. C) is chosen such that the energy density (resp. f) becomes non-negative.

The following properties of f are going to be used in the sequel:

1. The function f is non-negative and $\mathcal{N} := f^{-1}(0)$ is a smooth, closed, compact, connected manifold, diffeomorphic to the real projective plane $\mathbb{R}P^2$. Note that $\mathcal{N}$ is given by

$$\mathcal{N} = \left\{ s_* \left(\mathbf{n} \otimes \mathbf{n} - \frac{1}{3}\mathrm{Id} \right) \,:\, \mathbf{n} \in \mathbb{S}^2 \right\}\,,$$

   for $s_* = \frac{1}{4c}(b + \sqrt{b^2 + 24ac})$ (cf. [119]) and in particular Q is prolate uniaxial.

2. We need f to behave uniformly quadratic close to its minima, i.e. we assume that there exist constants $\delta_0, \gamma_1 > 0$ such that for all $Q \in \mathrm{Sym}_0$ with $\mathrm{dist}(Q, \mathcal{N}) \le \delta_0$ it holds

$$f(Q) \;\ge\; \gamma_1 \mathrm{dist}^2(Q, \mathcal{N})\,.$$

3. Lastly, we need to quantify the growth of f. More precisely, we assume that there exist constants $C_1, C_2 > 0$, such that for all $Q \in \mathrm{Sym}_0$

$$f(Q) \ge C_1 \left(|Q|^2 - \frac{2}{3}s_*^2 \right)^2\,, \qquad Df(Q) : Q \ge C_1\,|Q|^4 - C_2\,.$$

It can be checked that f given in (3.2) satisfies these assumptions [8, 40, 42, 119]. The exponent 4 in the last assumption is not crucial but only needs to outweigh the growth of g.

We also recall the following facts about the geometry of Sym_0:

1. Elements $Q \in \mathrm{Sym}_0$ admit the following decomposition: There exist $s \in [0, \infty)$ and $r \in [0, 1]$ such that
$$Q = s\left(\left(\mathbf{n} \otimes \mathbf{n} - \frac{1}{3}\mathrm{Id}\right) + r\left(\mathbf{m} \otimes \mathbf{m} - \frac{1}{3}\mathrm{Id}\right)\right), \tag{3.3}$$
where $\mathbf{n}, \mathbf{m}$ are normalized, orthogonal eigenvectors of Q. The values s and r are continuous functions of Q.

2. The set where decomposition (3.3) is not unique, is given by
$$\mathcal{C} := \{Q \in \mathrm{Sym}_0 \setminus \{0\} \,:\, r(Q) = 1\} \cup \{0\}, \tag{3.4}$$
i.e. $\mathcal{C}$ consists of the isotropic as well as the oblate uniaxial states. Another characterization of $\mathcal{C}$ is $\mathcal{C} = \{Q \in \mathrm{Sym}_0 \,:\, \lambda_1(Q) = \lambda_2(Q)\}$, where the two leading eigenvalues of Q are denoted by λ_1, λ_2. Moreover, $\mathcal{C}$ has the structure of a cone over $\mathbb{R}P^2$ and $\mathcal{C} \setminus \{0\} \cong \mathbb{R}P^2 \times \mathbb{R}$.

3. There exists a continuous retraction $\mathcal{R} : \mathrm{Sym}_0 \setminus \mathcal{C} \to \mathcal{N}$ such that $\mathcal{R}(Q) = Q$ for all $Q \in \mathcal{N}$. One can choose $\mathcal{R}$ to be the nearest point projection onto $\mathcal{N}$. In this case, $\mathcal{R}(Q) = s_*(\mathbf{n} \otimes \mathbf{n} - \frac{1}{3}\mathrm{Id})$ for $Q \in \mathrm{Sym}_0 \setminus \mathcal{C}$ decomposed as in (3.3).

The energy density g in (3.1) incorporates an external magnetic field into the model. This motivates the following assumption:

1. The function g favours Q having an eigenvector equal to the direction of the external field, in our case chosen to be along $\mathbf{e}_3$. More precisely, assume g is invariant by rotations around the $\mathbf{e}_3-$axis and the function $O(3) \ni R \mapsto g(R^\top Q R)$ is minimal if $\mathbf{e}_3$ is eigenvector to the maximal eigenvalue of $R^\top Q R$. Decomposing Q as in (3.3) with $\mathbf{n} = \mathbf{e}_3$ and keeping s and $\mathbf{m}$ fixed, then $g(Q)$ is minimal for $r = 0$. For a prolate uniaxial $Q \in \mathcal{N}$, i.e. $Q = s_*(\mathbf{n} \otimes \mathbf{n} - \frac{1}{3}\mathrm{Id})$ for $s_* \geq 0$ and $\mathbf{n} \in \mathbb{S}^2$ we have
$$g(Q) = c_*^2(1 - \mathbf{n}_3^2). \tag{3.5}$$

The precise formula for g in (3.5) is not important to our analysis, but for simplicity we assume this particular form. It would be enough to assume that $g|_{\mathcal{N}}$ has a strict minimum in $Q = s_*(\mathbf{e}_3 \otimes \mathbf{e}_3 - \frac{1}{2}\mathrm{Id})$, see Remark 4.18 in [8]. Besides this physical assumption, our analysis requires g to satisfy the following hypothesis:

2. The function $g : \mathrm{Sym}_0 \to \mathbb{R}$ is of class C^2 away from $Q = 0$ and in particular satisfies the Lipschitz condition close to $\mathcal{N}$: There exist constants $\delta_1, C > 0$ such that if $Q \in \mathrm{Sym}_0$ with $\mathrm{dist}(Q, \mathcal{N}) < \delta$ for $0 < \delta < \delta_1$, then
$$|g(Q) - g(\mathcal{R}(Q))| \leq C\,\mathrm{dist}(Q, \mathcal{N}). \tag{3.6}$$

3. The growth of g is slower than f, namely
$$|g(Q)| \;\leq\; C\,(1 + |Q|^4), \tag{3.7}$$
$$|Dg(Q)| \;\leq\; C\,(1 + |Q|^3), \tag{3.8}$$
for all $Q \in \mathrm{Sym}_0$ and a constant $C > 0$.

A physically motivated example that satisfies those assumptions [8, Prop. A.1] is for example given by
$$g(Q) \;=\; \frac{2}{3}s_* - Q_{33}. \tag{3.9}$$

Under these assumptions on f and g, it has been shown in [8, Prop. 2.4 and Prop. 2.6] that g acts on f as a perturbation in the following sense:

Proposition 3.2.1. *For $\xi, \eta > 0$ with $\xi \ll \eta$, there exists a smooth manifold $\mathcal{N}_{\eta,\xi} \subset \mathrm{Sym}_0$, diffeomorphic to $\mathcal{N}$ such that*

$$f(Q) + \frac{\xi^2}{\eta^2} g(Q) + \xi^2 C_0(\xi, \eta) \geq \gamma_2 \operatorname{dist}^2(Q, \mathcal{N}_{\eta,\xi}) \tag{3.10}$$

for a constant $\gamma_2 > 0$. In addition, there exists a constant $C > 0$ such that

$$\sup_{Q \in \mathcal{N}_{\eta,\xi}} \operatorname{dist}(Q, \mathcal{N}) \leq C \frac{\xi^2}{\eta^2} \,. \tag{3.11}$$

Furthermore, there exists a unique $Q_{\infty,\xi,\eta} \in \mathcal{N}_{\eta,\xi}$ such that

$$Q_{\infty,\xi,\eta} = \operatorname*{argmin}_{Q \in \mathrm{Sym}_0} \frac{1}{\xi^2} f(Q) + \frac{1}{\eta^2} g(Q) \,,$$

given by $Q_{\infty,\xi,\eta} = s_{*,\xi^2/\eta^2}(\mathbf{e}_3 \otimes \mathbf{e}_3 - \frac{1}{3}\mathrm{Id})$, where $|s_{*,t} - s_*| \leq Ct$.

This shows that the constant C_0 in (3.1) can be chosen to be $C_0(\xi, \eta) = -\frac{1}{\xi^2} f(Q_{\infty,\xi,\eta}) - \frac{1}{\eta^2} g(Q_{\infty,\xi,\eta}) \geq 0$ and it also holds true that $C_0(\xi, \eta) \leq C\xi^2/\eta^4$.

Since $s_{*,\xi^2/\eta^2} \to s_{*,0} = s_*$ for $\xi, \eta \to 0$ in our regime, it is convenient to also introduce $Q_\infty := s_*(\mathbf{e}_3 \otimes \mathbf{e}_3 - \frac{1}{3}\mathrm{Id})$ which minimizes $\xi^{-2} f(Q) + \eta^{-2} g(Q)$ among $Q \in \mathcal{N}$.

So far we have seen that the strong weight $\frac{1}{\xi^2}$ in front of the bulk potential f (compared to $\frac{1}{\eta^2}$ for g) favours Q to be close to the manifold $\mathcal{N}$. In other words, we expect energy related to f to be concentrated in regions where Q is far from $\mathcal{N}$. In a sense that is specified in Theorem 3.3.1, this region is related to the set where Q takes values in $\mathcal{C}$. In the same spirit we remark that under prolate uniaxial constraint, g prefers the normalized eigenvector $\mathbf{n}$ corresponding to the biggest eigenvalue to have a large third component $\mathbf{n}_3$ as formalized in (3.5). Therefore we expect that the energy contribution coming from g is concentrated on domains where $|\mathbf{n}_3| \approx 0$. More precisely, we introduce

$$\mathcal{T} := \{Q \in \mathrm{Sym}_0 \,:\, s > 0 \,, 0 \leq r < 1 \,, n_3 = 0\} \,, \tag{3.12}$$

where $r, s, \mathbf{n}$ are defined as in (3.3). We study properties of $\mathcal{T}$ later on in Subsection 3.4.3 and Section A.2. Most importantly, we will show in Corollary A.2.3 that $\partial\mathcal{T} = \mathcal{C}$. This is a consequence from the fact that if $r(Q) = 1$, then Q has a two-dimensional eigenspace for the largest eigenvalue which necessarily intersects the hyperplane $\{n_3 = 0\}$.

3.2.2 Flat chains

One of the main results of this paper is that the previously described energy concentrates on lines and surfaces when $\eta, \xi \to 0$. In order to state our main theorem, we therefore need an appropriate framework to describe geometric objects such as lines, surfaces and boundaries which is provided by geometric measure theory and in particular flat chains [166,167]. The very basic idea of geometric measure theory is to represent geometric objects as elements of a vector space and therefore allows for algebraic operations such as addition. In that respect, flat chains are such elements which in our case are dedicated to represent surfaces and lines. In the following we give a quick overview of the most important results that we use subsequently. For a detailed and complete presentation of flat chains and geometric measure theory, we refer to [65–67, 131, 149].

Polyhedral flat chains. Let G be an abelian group (written additively) with neutral element 0 and $|\cdot| : G \to [0, \infty)$ a function satisfying $|g| = 0$ if and only if $g = 0$, $|-g| = |g|$ and $|g + h| \leq |g| + |h|$ for all $g, h \in G$. In this paper, we are only concerned with the easiest case of $G = \mathbb{Z}_2$ and $|\cdot|$ the normal absolute value. For $n, k \in \mathbb{N}$, $k \leq n$, we denote by $\mathcal{P}^k$ the group of polyhedral chains of dimension k with coefficients in G i.e. the set of formal sums of compact, convex, oriented polyhedra of dimension k in $\mathbb{R}^n$ with coefficients in G together with the obvious

addition. We identify a polyhedron that results from glueing along a shared face (and compatible orientation) with the sum of the individual polyhedra. Also, we identify a polyhedron of opposite orientation with the negative of the original polyhedron. An element $P \in \mathcal{P}^k$ can thus be written as

$$P \;=\; \sum_{i=1}^{p} g_i \sigma_i \,, \tag{3.13}$$

where $g_i \in G$ and σ_i are compact, convex, oriented polyhedra that can be chosen to be non-overlapping. Note that in our case of $G = \mathbb{Z}_2$, the non trivial coefficients g_i all equal 1 and that the orientational aspect of the above definition becomes trivial. This reflects the symmetry of the director field $\mathbf{n} \sim -\mathbf{n}$ in the sense that around singularities we change orientation of $\mathbf{n}$ without changing the physics. In other words, we can lift Q locally away from singularities to obtain a well-defined director $\mathbf{n}$, but in general it is not possible to combine those local liftings into a global one. The *boundary* $\partial\sigma$ of a polyhedron σ is the formal sum of the $(k-1)-$dimensional polyhedral faces of σ with the induced orientation and coefficient 1 under the above mentioned identifications. Note that $\partial(\partial\sigma) = 0$. We can linearly extend this operator to a boundary operator $\partial : \mathcal{P}^k \to \mathcal{P}^{k-1}$.

Mass and flat norm. For a polyhedral chain $P \in \mathcal{P}^k$ written as in (3.13), we define the *mass* $\mathbb{M}(P) = \sum_{i=1}^{p} |g_i| \mathcal{H}^k(\sigma_i)$ and the *flat norm* $\mathbb{F}(P)$ by

$$\mathbb{F}(P) \;=\; \inf\{\mathbb{M}(Q) + \mathbb{M}(R) \;:\; P = \partial Q + R \,, Q \in \mathcal{P}^{k+1} \,, R \in \mathcal{P}^k\} \,.$$

Obviously it holds $\mathbb{F}(P) \leq \mathbb{M}(P)$ and $\mathbb{F}(\partial P) \leq \mathbb{F}(P)$. One can show that $\mathbb{F}$ defines a norm on $\mathcal{P}^k$ [67, Ch. 2].

Flat chains and associated measures. We define the space of *flat chains* $\mathcal{F}^k$ to be the $\mathbb{F}-$completion of $\mathcal{P}^k$. The boundary operator ∂ extends to a continuous operator $\partial : \mathcal{F}^k \to \mathcal{F}^{k-1}$ and we still denote by $\mathbb{M}$ the largest lower semicontinuous extension of the mass which was defined on $\mathcal{P}^k$. Furthermore, one can show [67, Thm 3.1] that for all $A \in \mathcal{F}^k$

$$\mathbb{F}(A) \;=\; \inf\{\mathbb{M}(Q) + \mathbb{M}(R) \;:\; P = \partial Q + R \,, Q \in \mathcal{F}^{k+1} \,, R \in \mathcal{F}^k\} \,.$$

For a finite mass flat chain $A \in \mathcal{F}^k$ and a measurable set $X \subset \mathbb{R}^n$, we can define the *restriction* $A \llcorner X$ via an approximation by polyhedral chains, for which the restriction coincides with the intersection under some technical assumptions and passing to the limit. A precise definition is given in [67, Ch. 4]. To each flat chain $A \in \mathcal{F}^k$, there exists an associated measure μ_A (see [67, Ch. 4]) such that for each μ_A-measurable set X, $A \llcorner X$ is a flat chain and $\mu_A(X) = \mathbb{M}(A \llcorner X)$. The *support* of A is denoted $\mathrm{supp}\,(A)$ and given (if it exists) by the smallest closed set X such that for every open set $U \supset X$ there exists a sequence of polyhedral chains $(P_j)_j$ approximating A and such that all cells of all P_j lie inside U. If A is of finite mass, then $\mathrm{supp}\,(A) = \mathrm{supp}\,(\mu_A)$ (see [67, Thm. 4.3]).

Cartesian products and induced mappings. In the case of finite mass flat chains A, B (or one of the two chains having finite mass *and* finite boundary mass), it is possible to define the product $A \times B$ (by polyhedral approximation), see e.g. [67, Sec. 6]. In particular, it is always possible to define $[0,1] \times B$. For $U \subset \mathbb{R}^n, V \subset \mathbb{R}^m$ open sets and a Lipschitz function $f : U \to V$, one can define an induced mapping $f_\#$ on the level of flat chains, i.e. for a flat chain A supported in U, $f_\# A$ is a flat chain supported in V (see [67, Sec. 5] and [66, Sec. 2 and 3]).

Generic properties and Thom transversality theorem. A property of an object (such as a function or a set) that can be achieved by an arbitrarily small perturbation of the object is called *generic*. Examples are properties that hold in an 'almost everywhere' measure theoretic sense or that are true on a dense subset. In this work we encounter two such properties: Two dimensional planes *generically* do not contain a fixed single point (can be achieved by shifting normal to the plane). The second one is that a smooth map $f : M \to N$ *generically* intersects a submanifold $S \subset N$ transversely i.e. $\mathrm{d}f(T_x M) + T_{f(x)} S = T_{f(x)} N$ for all points $x \in f^{-1}(S)$. The latter will be used to apply Thom's transversality theorem [160] in the form given in [86, Thm. 2.7].

Deformations. In certain situations it is beneficial to approximate a flat $k-$chain A by a polyhedral $k-$chain P. The usual way to construct P is through 'pushing' A onto the $k-$skeleton of a grid in the following way. In this paper, a (cubic) grid of size h is understood to be a cell complex in $\mathbb{R}^3$ which consists of cubes of side length h. The 'pushing' operation consists of a radial projection of A from the center of each cube onto the faces of the cubes, assuming that the center does not lie on A. Then, on each face the projected flat chain gets again projected from the center of the face onto the edges (as long as the projected chain does not contain any face center point). This procedure is stopped once the projected flat $k-$chain is contained in the $k-$dimensional skeleton. This deformation procedure is a crucial ingredient to prove that every $A \in \mathcal{F}^k$ can be written as $A = P + B + \partial C$, where $P \in \mathcal{F}^k$ is a polyhedral chain, $B \in \mathcal{F}^k$ and $C \in \mathcal{F}^{k+1}$ satisfy the estimates $\mathbb{M}(P) \lesssim \mathbb{M}(A) + h\mathbb{M}(\partial A)$, $\mathbb{M}(\partial P) \lesssim \mathbb{M}(\partial A)$, $\mathbb{M}(B) \lesssim h\mathbb{M}(\partial A)$ and $\mathbb{M}(C) \lesssim h\mathbb{M}(A)$, see [166] or [67, Thm. 7.3].

Compactness. One point of importance from the perspective of calculus of variations are the compactness properties of flat chains whose mass and the mass of their boundary is bounded. We will use the result from [67, Cor. 7.5] which holds for coefficient groups G such that for all $M > 0$ the set $\{g \in G : |g| \leq M\}$ is compact. This is trivially true in our case where $G = \mathbb{Z}_2$. Let $K \subset \mathbb{R}^n$ be compact and $C_1 > 0$. Then the corollary states that

$$\{A \in \mathcal{F}^k \, : \, \text{supp}\,(A) \subset K \text{ and } \mathbb{M}(A) + \mathbb{M}(\partial A) \leq C_1\}$$

is compact.

Rectifiability. Another aspect of flat chains concerns their regularity and if one can define objects originating in smooth differential geometry such as tangent spaces. It turns out that this can be achieved a.e. provided the flat chain is rectifiable. By definition, rectifiability of a flat chain $A \in \mathcal{F}^k$ means that there exists a countable union of $k-$dimensional C^1-submanifolds N of $\mathbb{R}^n$ such that $A = A \llcorner N$ [167, Sec. 1.2]. A rectifiable flat chain admits an approximate tangent plane for $\mathcal{H}^k-$a.e. $x \in A$ [10, Thm 2.83]. Such a point x is called rectifiability point of A and we denote $\text{rect}(A)$ the set of all points of rectifiability of A. For finite groups G, finite mass $\mathbb{M}(A) < \infty$ implies rectifiability of A, see [67, Thm 10.1].

3.3 Statement of result

Our main result concerns the asymptotic behaviour of the energy $\mathcal{E}_{\eta,\xi}$ for $\eta, \xi \to 0$. Physically speaking, we consider the regime of large particles and weak magnetic fields, see [8, 76] for more discussion of the physical interpretation of our limit.

The liquid crystal occupies a region Ω outside a solid particle E, i.e. $\Omega = \mathbb{R}^3 \setminus E$. We assume the boundary of the particle $\mathcal{M} := \partial E$ to be sufficiently smooth for our analysis, that is we require $\mathcal{M}$ to be a closed, compact and oriented manifold of class at least C^2. The regularity will be needed to ensure that the outward unit normal field $\nu \in C^1$ or in other words $\mathcal{M}$ has continuous curvature. Furthermore, we assume that

$$\Gamma := \{\omega \in \mathcal{M} \, : \, \nu_3(\omega) = 0\}$$

is a C^2-curve (or a union thereof) in $\mathcal{M}$ and that $\nabla_\omega \nu_3 \neq 0$ everywhere on Γ (seen inside the tangent bundle $T\mathcal{M}$), see also Remark 3.3.2.

In order to make the minimization of the energy $\mathcal{E}_{\eta,\xi}$ non trivial, we impose the following boundary condition on $\mathcal{M}$:

$$Q \; = \; s_* \left(\nu \otimes \nu - \frac{1}{3}\text{Id} \right) \quad \text{ on } \mathcal{M}\,. \tag{3.14}$$

Indeed, without (3.14) the minimizer of $\mathcal{E}_{\eta,\xi}$ would be the constant function $Q_{\eta,\xi,\infty}$. We define the class of admissible functions $\mathcal{A} := \{Q \in H^1(\Omega, \text{Sym}_0) + Q_{\eta,\xi,\infty} \, : \, Q \text{ satisfies (3.14)}\}$. It is

convenient to define the energy $\mathcal{E}^{\mathcal{A}}_{\eta,\xi}$ for $Q \in H^1(\Omega,\mathbb{R}^{3\times 3}) + Q_{\eta,\xi,\infty}$ by

$$\mathcal{E}^{\mathcal{A}}_{\eta,\xi}(Q) \coloneqq \begin{cases} \mathcal{E}_{\eta,\xi}(Q) & \text{if } Q \in \mathcal{A}\,, \\ +\infty & \text{otherwise}\,. \end{cases}$$

We also use the notation $\mathcal{E}_{\eta,\xi}(Q,U)$ (resp. $\mathcal{E}^{\mathcal{A}}_{\eta,\xi}(Q,U)$) for the energy $\mathcal{E}_{\eta,\xi}$ (resp. $\mathcal{E}^{\mathcal{A}}_{\eta,\xi}$) of the function Q on the set U.

Theorem 3.3.1. *Suppose that*

$$\eta|\ln(\xi)| \to \beta \in (0,\infty) \qquad \text{as } \eta \to 0\,. \tag{3.15}$$

Then $\eta\,\mathcal{E}^{\mathcal{A}}_{\eta,\xi} \to \mathcal{E}_0$ in a variational sense, where the limiting energy $\mathcal{E}_0$ is given by

$$\mathcal{E}_0(T,S) = 2s_*c_*E_0(\mathcal{M},\mathbf{e}_3) + 4s_*c_*\int_{\mathcal{M}} |\cos(\theta)|\,\mathrm{d}\mu_{T\llcorner\mathcal{M}} + \frac{\pi}{2}s_*^2\beta\mathbb{M}(S) + 4s_*c_*\mathbb{M}(T\llcorner\Omega) \tag{3.16}$$

for $(T,S) \in \mathcal{A}_0 \coloneqq \{(T,S) \in \mathcal{F}^2 \times \mathcal{F}^1 \,:\, \partial T = S + \Gamma\}$ and where

$$E_0(\mathcal{M},\mathbf{e}_3) \coloneqq \int_{\{\nu_3>0\}} (1-\cos(\theta))\,\mathrm{d}\omega + \int_{\{\nu_3\le 0\}} (1+\cos(\theta))\,\mathrm{d}\omega\,.$$

The letter θ is used to denote the angle between $\mathbf{e}_3$ and the outward unit normal vector $\nu(\omega)$ at a point $\omega \in \mathcal{M}$. The variational convergence is to be understood in the following sense: Along any sequence $\eta_k, \xi_k \to 0$ with $\eta_k|\ln(\xi_k)| \to \beta$ (not labelled in the following statements):

1. *Compactness and $\Gamma-$liminf: For any sequence $Q_{\eta,\xi} \in H^1(\Omega,\mathbb{R}^{3\times 3}) + Q_{\eta,\xi,\infty}$ such that there exists a constant $C > 0$ with*

$$\eta\,\mathcal{E}^{\mathcal{A}}_{\eta,\xi}(Q_{\eta,\xi}) \le C\,, \tag{3.17}$$

there exists $(T,S) \in \mathcal{A}_0$, functions $\widetilde{Q_{\eta,\xi}} \in C^\infty(\Omega,\mathrm{Sym}_0)$ with $\lim_{\eta,\xi\to 0}\|Q_{\eta,\xi} - \widetilde{Q_{\eta,\xi}}\|_{H^1} = 0$, $\mathcal{E}^{\mathcal{A}}_{\eta,\xi}(\widetilde{Q_{\eta,\xi}}, B_R) \le \mathcal{E}^{\mathcal{A}}_{\eta,\xi}(Q_{\eta,\xi}, B_R) + C_R$ and $Y_{\eta,\xi} \in Sym$ with $\|Y_{\eta,\xi}\| \to 0$ such that $T_{\eta,\xi} = (\widetilde{Q_{\eta,\xi}} - Y_{\eta,\xi})^{-1}(\mathcal{T})$, $S_{\eta,\xi} = (\widetilde{Q_{\eta,\xi}} - Y_{\eta,\xi})^{-1}(\mathcal{C})$ for $\mathcal{T}$ and $\mathcal{C}$ given as in (3.12),(3.4) are smooth flat chains with

$$\partial T_{\eta,\xi} = S_{\eta,\xi} \;+\; \Gamma_{\eta,\xi}\,, \tag{3.18}$$

and, up to a subsequence, for any bounded measurable set $B \subset \Omega$

$$\lim_{\eta,\xi\to 0} \mathbb{F}(T_{\eta,\xi} - T, B) = 0\,, \qquad \lim_{\eta,\xi\to 0} \mathbb{F}(S_{\eta,\xi} - S, B) = 0\,. \tag{3.19}$$

Here, $\Gamma_{\eta,\xi}$ is a smooth approximation of Γ which converges to Γ in Hausdorff distance and hence also in flat norm. Furthermore, we have

$$\liminf_{\eta\to 0} \eta\,\mathcal{E}^{\mathcal{A}}_{\eta,\xi}(Q_{\eta,\xi}) \ge \mathcal{E}_0(T,S)\,. \tag{3.20}$$

2. *$\Gamma-$limsup: For any $(T,S) \in \mathcal{A}_0$, there exists a sequence $Q_{\eta,\xi} \in \mathcal{A}$ with $\|Q_{\eta,\xi}\|_{L^\infty} \le \sqrt{\frac{2}{3}}s_{\eta,\xi,*}$ such that (3.18),(3.19) hold and*

$$\limsup_{\eta\to 0} \eta\,\mathcal{E}^{\mathcal{A}}_{\eta,\xi}(Q_{\eta,\xi}) \le \mathcal{E}_0(T,S)\,. \tag{3.21}$$

Remark 3.3.2 (Assumptions in the theorem)**.** *1. We note that due to our assumptions $\beta \in (0,\infty)$, the global energy bound (3.17) can be reformulated as*

$$\mathcal{E}^{\mathcal{A}}_{\eta,\xi}(Q_{\eta,\xi}) \;\le\; \tilde{C}\,|\ln(\xi)|\,.$$

This reflects the classical behaviour of a logarithmic divergence of the energy close to singularities as already observed in earlier works e.g. in [30].

2. *If $Q_{\eta,\xi}$ is smooth enough (for example C^2) and verifies a Lipschitz estimate as in* (3.25) *for $n \sim \xi^{-1}$, we can choose $\widetilde{Q_{\eta,\xi}} = Q_{\eta,\xi}$ in the above Theorem. This is particularly true if $Q_{\eta,\xi}$ is a minimizer of* (3.1). *Indeed, from the Euler-Lagrange equations, one can deduce the regularity and the required estimate on the gradient [29, Lemma A.2].*

3. *The compactness claim holds for almost every $Y \in \mathrm{Sym}_0$ with $\|Y\|$ small enough. The norm converging to zero is needed to recover the condition $\partial T = S + \Gamma$, the stated energy densities on $T \llcorner \mathcal{M}$, and the coefficient in front of $\mathbb{M}(T \llcorner \Omega)$.*

4. *Another possibility of introducing $S_{\eta,\xi}$ is by using the operator $\mathbf{S}$ defined in [43, 44]. In our notation, this operator maps a function Q from $(L^\infty \cap W^{1,1})(\Omega, \mathrm{Sym}_0)$ to $L^1(B_{\alpha^*}(0), \mathcal{F}^1)$, where $\alpha_* > 0$ and $B_{\alpha^*}(0) \subset \mathrm{Sym}_0$. In other words, $\mathbf{S}$ allows us to define a flat $1-$chain $\mathbf{S}_Y(Q_{\eta,\xi})$ for $Q_{\eta,\xi} \in (L^\infty \cap W^{1,1})(\Omega, \mathrm{Sym}_0)$ and $Y \in B_{\alpha^*}(0)$.*

5. *The assumption of $\Gamma = \{\omega \in \mathcal{M} : \nu(\omega) \cdot \mathbf{e}_3 = 0\}$ being a C^2-curve is not very restrictive. In fact, this can already be achieved by a slight deformation of $\mathcal{M}$ which changes the energies $\mathcal{E}_{\eta,\xi}$ and $\mathcal{E}_0$ in a continuous way. The assumption that $\nabla_\omega \nu_3$ is nowhere vanishing on Γ is used as a sufficient condition to ensure that the perturbed sets $\Gamma_{\eta,\xi}$ stay regular and in a neighbourhood of Γ. In fact, since $\nu_3 = 0$ on Γ the derivative vanishes in the direction tangential to Γ, so the condition is only on the part of $\nabla_\omega \nu_3$ normal to Γ. In particular, the condition is verified if the Gaussian curvature $|\kappa_{\mathcal{M}}| > 0$ on Γ.*

Remark 3.3.3 (An alternative formulation of $\mathcal{E}_0$)**.** *1. We can express the energy* (3.16) *in a slightly different way by writing $\mu_{T \llcorner \mathcal{M}} = \chi_G \mathcal{H}^2 \llcorner \mathcal{M}$ for a mesurable set $G \subset \mathcal{M}$ and defining*

$$F := \{\omega \in \mathcal{M} \setminus G : \nu(\omega) \cdot \mathbf{e}_3 > 0\} \cup \{\omega \in \mathcal{M} \cap G : \nu(\omega) \cdot \mathbf{e}_3 \leq 0\}. \tag{3.22}$$

Then, (3.16) *reads*

$$\begin{aligned} \mathcal{E}_0(T, S) &= 2s_* c_* \int_F (1 - \cos(\theta)) \, \mathrm{d}\omega + 2s_* c_* \int_{\mathcal{M} \setminus F} (1 + \cos(\theta)) \, \mathrm{d}\omega \\ &+ \frac{\pi}{2} s_*^2 \beta \mathbb{M}(S) + 4 s_* c_* \mathbb{M}(T \llcorner \Omega). \end{aligned} \tag{3.23}$$

The idea behind this reformulation and the definition of F is the following: Assume for $\xi, \eta > 0$ that Q takes values in $\mathcal{N}$ such that (at least locally) we can lift Q to a director field $\mathbf{n}$. Because of the boundary condition, we can assume that for a given point $\omega \in \mathcal{M}$ it holds that $\mathbf{n}(\omega) = \nu(\omega)$. Following a ray in normal direction starting from ω, $\mathbf{n}$ must approach $\pm \mathbf{e}_3$ since far from the particle, Q must be close to Q_∞. If $\nu_3(\omega) > 0$, it is energetically favourable for $\mathbf{n}$ to approach $+\mathbf{e}_3$. On the other hand, the ray intersecting T means that $\mathbf{n}$ switches sign, i.e. if we start from $\nu_3(\omega) < 0$ and cross T only once, $\mathbf{n}$ converges to $+\mathbf{e}_3$. In this sense, the set F can be understood as the region on $\mathcal{M}$ in which the lifting $\mathbf{n}$ along the rays starts from ν and approach $+\mathbf{e}_3$, while on $\mathcal{M} \setminus F$ the director $\mathbf{n}$ turns from ν to $-\mathbf{e}_3$. Previously, the energy $E_0(\mathcal{M}, \mathbf{e}_3)$ describes the minimal *energy concentrated on $\mathcal{M}$, i.e. $\mathbf{n}$ always turns in the energetically favourable direction and the integral involving $\mu \llcorner \mathcal{M}$ accounts for the additional energy caused by intersecting T. See Figure 3.1 for an illustration of the different quantities appearing in* (3.23).

2. *For convex particles E, there exists an orthogonal projection $\Pi : \Omega \to \mathcal{M}$. By convexity of E, we find that $\mathcal{E}_0(\Pi_\# T, \Pi_\# S) \leq \mathcal{E}_0(T, S)$, so that we can restrict ourselves to the case $T \llcorner \Omega = 0 = S \llcorner \Omega$. Using* (3.22), *we find that $\partial F = \Pi_\# S$ and* (3.23) *becomes*

$$\mathcal{E}_0(\Pi_\# T, \Pi_\# S) = 2s_* c_* \int_F (1 - \cos(\theta)) \, \mathrm{d}\omega + 2s_* c_* \int_{\mathcal{M} \setminus F} (1 - \cos(\theta)) \, \mathrm{d}\omega + \frac{\pi}{2} s_*^2 \beta \mathbb{M}(\partial F).$$

In particular, (3.16) *is a generalization of the limit energy $\mathcal{E}_0$ defined in [8].*

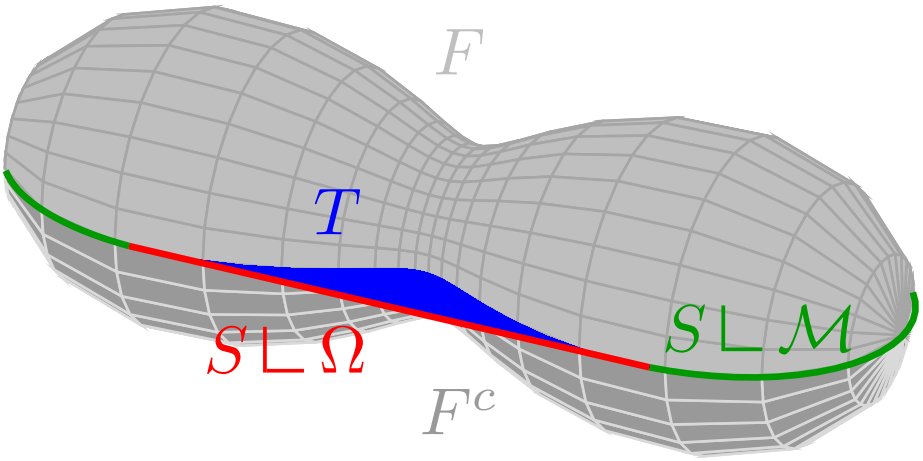

Figure 3.1: Illustration of flat chains T, S and the sets F, F^c appearing in the limit energy $\mathcal{E}_0$.

Remark 3.3.4 (Physical interpretation of T and S)**.** *The line singularity observed in physical experiments [112, 113, 128] has its origin in the isotropic or oblate uniaxial-biaxial defect core of the director field. In our mathematical framework this corresponds to the set where $Q_{\eta,\xi}$ takes values in $\mathcal{C}$ and is therefore represented by $S_{\eta,\xi}$ which tends towards S in the limit model. Note that it is a priori not possible to distinguish $+\frac{1}{2}$ and $-\frac{1}{2}$ defect lines (see Figure 3.3 (left)). But since the physical system as a whole must have a trivial topological degree, one can deduce in the situation of Figure 3.3 that one $+\frac{1}{2}$ and two $-\frac{1}{2}$ defect lines must be present. By symmetry the line in the middle must be of degree $+\frac{1}{2}$.*

Point singularities of the director $\mathbf{n}$ are represented by simply connected components of T in our model due to the following reasoning. As illustrated in Figure 3.2, the set where $\mathbf{n}_3 = 0$ attaches to Γ (yellow points on the surface of the sphere) and necessarily passes through the point singularity and creates a simply connected component. However, with this description it is not possible to determine the exact position of the point defect on the surface T. In the case of a minimizing T around a spherical inclusion, T will approach the particle surface since the nematic and magnetic exchange length become small w.r.t. the particle radius and thus T forms a half-sphere (compare with [8, Ch. 6]). In the case of a peanut-shaped particle aligned with the magnetic field we expect one of three different minimizing configurations, depending on β, see Figure 3.3. In particular, there exists a non-simply connected component of T which does not correspond to a point defect, but originates in the connection of two components of Γ. In summary, T is a surface which connects Γ to the singular set (lines and points).

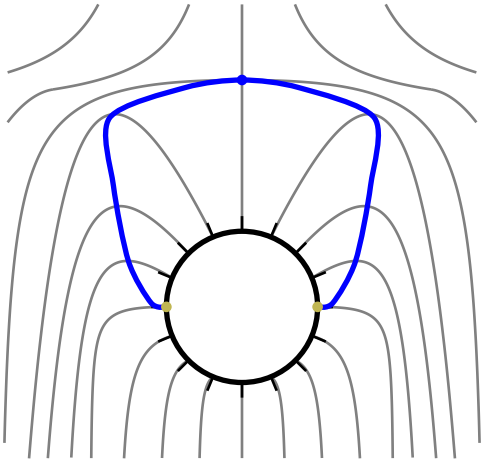

Figure 3.2: Illustration of the integral lines of the director field $\mathbf{n}$ around a spherical inclusion and the level set $\{x \in \Omega \,:\, \mathbf{n}_3(x) = 0\}$ representing T. The point defect lies on T.

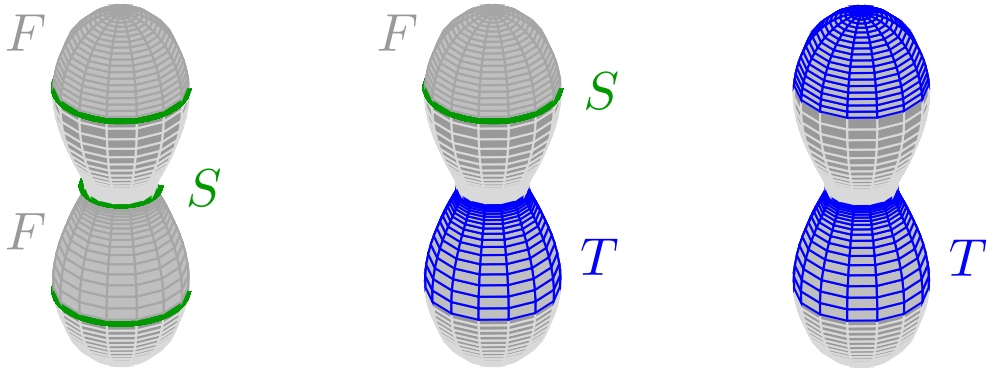

Figure 3.3: Expected minimizers of $\mathcal{E}_0$ for $\beta \ll 1$ (left), $\beta \gg 1$ (right) and intermediate β (center). For small β the line S has the tendency to stick to $\mathcal{M}$ and optimize F, thus no T appears. Here, $S = \Gamma$ and F consists of two connected components bounded by the three components of S. This configuration corresponds to three Saturn rings around the particle. For intermediate β one may find a configuration as depicted in the middle, i.e. the energy is decreased by joining two parts of S by a surface T glued to $\mathcal{M}$. This leads to the disappearance of the two rings that have been connected by T, and F contains only the part of $\mathcal{M}$ above S. Finally, for large β, the last ring disappears and we obtain a dipole configuration in which $S = 0$, $F = \emptyset$ and T has two components, see Remark 3.3.4. This last configuration has been observed experimentally, see [143, Fig. 2(a)-(c)].

3.4 Compactness

The structure of this section is as follows. We regularize the sequence $Q_{\eta,\xi}$ in the first subsection. For this new sequence $Q_{\eta,\xi,n}$, we define a 2−chains $T_{\eta,\xi,n} \in \mathcal{F}^2$ and 1−chains $S_{\eta,\xi,n} \in \mathcal{F}^1$ such that $\partial T_{\eta,\xi,n} = S_{\eta,\xi,n}$ and we have bounds on the masses to get the existence of limit objects T and S with $\partial T = S$. This construction is carried out in steps in the subsections two, three and four. We distinguish the case of $Q_{\eta,\xi,n}$ being close to $\mathcal{N}$ and hence almost prolate uniaxial and the complementary case when $Q_{\eta,\xi,n}$ is far from $\mathcal{N}$, e.g. when $Q_{\eta,\xi,n}$ is isotropic or oblate uniaxial close to the boundary S. The passage to the limit is to happen in the last subsection.

3.4.1 Approximating sequence

This section is devoted to the definition of a sequence of smooth functions $Q_{\eta,\xi,n}$, replacing $Q_{\eta,\xi}$ in our analysis and proving the properties required for the estimates in the following chapters. More precisely, we need that

- the sequence $Q_{\eta,\xi,n}$ approximates $Q_{\eta,\xi}$ in H^1,
- $Q_{\eta,\xi,n}|_{\mathcal{M}}$ approaches Q_b in C^1,
- $Q_{\eta,\xi,n}$ verifies the same energy bound $\eta\,\mathcal{E}_{\eta,\xi}(Q_{\eta,\xi,n}) \leq \tilde{C}$ and
- the estimate $\mathrm{Lip}(Q_{\eta,\xi,n}) \leq C\,n$ holds.

While n is introduced a regularization parameter, we will later choose n dependent on ξ to obtain a sequence which only depends on the original parameters η, ξ. More explicitly, we can simply take $n = \xi^{-1}$ as we will see later.

For technical reasons, we are going to extend $Q_{\eta,\xi}$ into a small neighbourhood into the interior of E. Since $\mathcal{M}$ is compact and of class C^2, we can fix a small radius $\mathbf{r}_0 > 0$ such that $\mathcal{M}$ satisfies the inner ball condition for all radii $r \leq 2\mathbf{r}_0$. In particular, $\mathbf{r}_0$ is smaller than the minimal curvature radius of $\mathcal{M}$. For $x \in E$ such that $\mathrm{dist}(x, \mathcal{M}) < 2r_0$, define

$$Q_{\eta,\xi}(x) \;=\; s_* \left(\overline{\nu}(x) \otimes \overline{\nu}(x) - \frac{1}{3}\mathrm{Id} \right),$$

where $\overline{\nu}(x) = \nu(\Pi_{\mathcal{M}}(x))$, $\Pi_{\mathcal{M}}$ the orthogonal projection onto $\mathcal{M}$, is the obvious extension of the outward normal unit vector field ν in E. Also by C^2-regularity of $\mathcal{M}$ and given $n \in \mathbb{N}$, there exists a C^2-diffeomorphism $\Phi_n : \mathbb{R}^3 \to \mathbb{R}^3$ such that

$$\Phi_n(x) \;=\; \begin{cases} x & x \in \Omega \text{ with } \mathrm{dist}(x, \mathcal{M}) > \frac{2}{n}\,, \\ x - \frac{1}{n}\,\overline{\nu}(x) & x \in \mathbb{R}^3 \text{ with } \mathrm{dist}(x, \mathcal{M}) \leq \frac{1}{n}\,, \end{cases}$$

and $|\nabla \Phi_n(x)| \leq C$.

Let $\Pi_R : \mathrm{Sym}_0 \to B_R(0) \subset \mathrm{Sym}_0$ be the orthogonal projection with $\sqrt{\frac{2}{3}} s_* \leq R < \infty$ to be fixed later. Furthermore, let $\varrho \in C_c^\infty(\mathbb{R}^3)$ be a convolution kernel with $0 \leq \varrho \leq 1$, $\varrho(x) = 0$ if $|x| > 1$, $\int_{\mathcal{R}^3} \varrho(x)\,\mathrm{d}x = 1$ and $\|\nabla \varrho\|_\infty \leq 1$. We set $\varrho_n(x) = n^3 \varrho(nx)$. Then, for $n \geq r_0^{-1}$ we define $Q_{\eta,\xi,n}(x)$ for $x \in \overline{\Omega}$ as the convolution

$$Q_{\eta,\xi,n}(x) \;:=\; \left((\Pi_R \circ Q_{\eta,\xi} \circ \Phi_n) * \varrho_n \right)(x)\,. \tag{3.24}$$

Remark 3.4.1. *1. This definition also extends $Q_{\eta,\xi,n}$ into the interior of E up to distance r_0 to $\mathcal{M}$.*

2. Through the convolution, we change the boundary values of $Q_{\eta,\xi}$, i.e. $Q_{\eta,\xi,n}$ does not necessarily satisfy (3.14)*. The diffeomorphism Φ_n ensures that the regularized sequence $Q_{\eta,\xi,n}$ defined above approximates the boundary data Q_b in C^1, although at distance from $\mathcal{M}$ we only have H^1-convergence to $Q_{\eta,\xi}$.*

3. The convolution also changes that the approximations of T that we are about to construct will not end on Γ, but on a set Γ_n (which is again a line) in the neighbourhood of Γ. Because of the C^1-convergence of $Q_{\eta,\xi,n}|_{\mathcal{M}} \to Q_b$ we can use a perturbation argument to deduce that Γ_n converges in Hausdorff distance and in flat norm to Γ. The details of this result are provided in Section 3.5.3.

The following proposition shows that this sequence has indeed the desired properties.

Proposition 3.4.2. *The sequence $Q_{\eta,\xi,n}$ defined in* (3.24) *verifies:*

1. *The functions $Q_{\eta,\xi,n}$ are smooth and there exists a constant $C > 0$ such that*

$$\|\nabla Q_{\eta,\xi,n}\|_{L^\infty} \;\leq\; C\, n\,. \tag{3.25}$$

2. *We have convergence $Q_{\eta,\xi,n} - Q_{\eta,\xi} \to 0$ in H^1 and $Q_{\eta,\xi,n}|_{\mathcal{M}} \to Q_b$ in C^1 for $n \to \infty$ and $\xi, \eta \to 0$ provided ηn diverges in the limit $n \to \infty$, $\eta \to 0$.*

3. *There exists $R \geq \sqrt{\frac{2}{3}} s_*$ and constants $C_1, C_2 > 0$ such that for all measurable sets $\Omega' \subset \Omega$ with $|\Omega'| < \infty$ the energy of $Q_{\eta,\xi,n}$ can be bounded as*

$$\begin{aligned} \eta\, \mathcal{E}_{\eta,\xi}(Q_{\eta,\xi,n}, \Omega') \;\leq\; & C_1 \left(1 + \frac{1}{n} + \frac{1+R^2}{n^2} + \frac{1+R^2}{n^2}\right) \eta\, \mathcal{E}_{\eta,\xi}\left(Q_{\eta,\xi}, B_{\frac{1}{n}}(\Omega') \cap \Omega\right) \\ & + C_2 \eta \left(\frac{1}{n} + \frac{1}{\xi^2\eta^2} R^2(1+R^2) + \frac{1}{\eta^2\sqrt{n}} R\right) \;+\; C_3 \left(\frac{|\Omega'|}{n^2} \mathcal{E}_{\eta,\xi}(Q_{\eta,\xi}, \Omega')\right)^{\frac{1}{2}}, \end{aligned} \tag{3.26}$$

where $B_r(\Omega')$ denotes the $r-$neighbourhood around Ω'.

Proof. The smoothness of the functions $Q_{\eta,\xi,n}$ is clear by standard convolution arguments, since ϱ is smooth. The bound on the gradient follows from the computation

$$|\nabla Q_{\eta,\xi,n}(x)| \;\leq\; \|\nabla \varrho_n\|_{L^\infty} \int_{B_1(x)} |\Pi_R Q_{\eta,\xi}(\Phi_n(y))|\, \mathrm{d}y \;\leq\; \frac{4}{3}\pi R\, n\,.$$

For the H^1 convergence, we note that the energy bound for $Q_{\eta,\xi}$ and Proposition 3.2.1 imply that $|\{x \in \Omega \,:\, |Q_{\eta,\xi}(x)| > R\}| \lesssim \frac{\xi^2}{\eta}(R - s\sqrt{\frac{2}{3}}s_*)^{-2}$. Hence the set on which the projection Π_R modifies $Q_{\eta,\xi}$ is asymptotically negligible. Let $U_R := \{x \in \Omega \,:\, |Q_{\eta,\xi}(x)| \leq R\}$. We can then write

$$\begin{aligned} \|Q_{\eta,\xi,n} - Q_{\eta,\xi}\|^2_{H^1(\Omega)} \;\leq\; & \|(Q_{\eta,\xi} \circ \Phi_n) * \rho_n - Q_{\eta,\xi}\|^2_{H^1(\{\mathrm{dist}(\cdot,\mathcal{M}) \leq \frac{2}{n}\} \cap U_R)} \\ & + \|Q_{\eta,\xi} * \rho_n - Q_{\eta,\xi}\|^2_{H^1(\{\mathrm{dist}(\cdot,\mathcal{M}) \geq \frac{2}{n}\} \cap U_R)} \\ & + \|Q_{\eta,\xi,n} - Q_{\eta,\xi}\|^2_{H^1(U_R^c)}\,. \end{aligned} \tag{3.27}$$

The last term in (3.27) converges to zero since the set U_R^c vanishes asymptotically as we have seen before. Since $\nabla\Phi_n$ is bounded and $\|Q_{\eta,\xi}\|^2_{H^1(\Omega)} \lesssim \eta^{-1}$, the first term vanishes as well provided $n \gg \eta^{-1}$. The second term converges to zero by the standard convolution properties.

Next, we prove the C^1-convergence on $\mathcal{M}$. For $\omega \in \mathcal{M}$ it holds that

$$|Q_{\eta,\xi,n}(\omega) - Q_b(\omega)| \;\leq\; \int_{B_{\frac{1}{n}}(0)} \left|Q_{\eta,\xi}\Big(\omega - y - \frac{1}{n}\nu_{\omega-y}\Big) - Q_b(\omega)\right| \rho_n(y)\, \mathrm{d}y\,.$$

Note that $Q_{\eta,\xi}$ does not depend on η, ξ here as it is uniquely defined by the extension $\overline{\nu}$. Since Q_b and $\overline{\nu}$ are continuous on a compact set, they are also uniformly continuous which implies C^0-convergence for $n \to 0$. Analogously,

$$|\nabla_\omega Q_{\eta,\xi,n}(\omega) - \nabla_\omega Q_b(\omega)| \;\leq\; \int_{B_{\frac{1}{n}}(0)} \left|(\nabla_\omega Q_{\eta,\xi})(\omega - y - \nu_{\omega-y})\Big(\mathrm{Id} + \frac{1}{n}\nabla_\omega\overline{\nu}\Big) - \nabla_\omega Q_b(\omega)\right| \rho_n(y)\, \mathrm{d}y\,,$$

and since $\nabla_\omega\overline{\nu}$ is bounded we can use uniform continuity of $\nabla_\omega Q_b$ to deduce C^1-convergence on $\mathcal{M}$.

It remains to prove the energy bound for $Q_{\eta,\xi,n}$. For this, we first recall that $|D\Phi_n|$ is bounded

and that for $x \in \Omega$ with $\operatorname{dist}(x, \mathcal{M}) > \frac{1}{n}$ it holds $D\Phi_n(x) = \mathrm{Id}$. This allows us to estimate

$$\begin{aligned}
\int_{\Omega'} |\nabla Q_{\eta,\xi,n}|^2 \,\mathrm{d}x &\leq \int_{\Omega'} |(\nabla(Q_{\eta,\xi} \circ \Phi_n)) * \varrho_n|^2 \,\mathrm{d}x \\
&\leq \int_{\Omega' \cap \{\operatorname{dist}(\cdot,\mathcal{M}) > \frac{2}{n}\}} \left| \int_{B_{\frac{1}{n}}(0)} (\nabla_x Q_{\eta,\xi})(x-y) n^3 \varrho(ny) \,\mathrm{d}y \right|^2 \,\mathrm{d}x + \frac{C}{n} \|Q_{\eta,\xi}\|^2_{H^1(\Omega')} \\
&\leq C|B_1| \int_{\Omega'} \int_{B_1(0)} \left| (\nabla_x Q_{\eta,\xi})\Big(x - \frac{z}{n}\Big) \right|^2 |\varrho(z)|^2 \,\mathrm{d}z \,\mathrm{d}x + \frac{C}{n} \|Q_{\eta,\xi}\|^2_{H^1(\Omega')} \\
&= C|B_1| \int_{B_1(0)} |\rho(z)|^2 \int_{\Omega'} \left| (\nabla_x Q_{\eta,\xi})\Big(x - \frac{z}{n}\Big) \right|^2 \,\mathrm{d}x \,\mathrm{d}z + \frac{C}{n} \|Q_{\eta,\xi}\|^2_{H^1(\Omega')} \\
&\leq C\Big(1 + \frac{1}{n}\Big) \int_{B_{\frac{1}{n}}(\Omega')} |(\nabla Q_{\eta,\xi})|^2 \,\mathrm{d}x \,.
\end{aligned}$$

Writing $B_{\frac{1}{n}}(\Omega') = (B_{\frac{1}{n}}(\Omega') \cap \Omega) \cup (B_{\frac{1}{n}}(\Omega') \cap E)$ and using that $|\nabla \nu(\Pi_{\mathcal{M}}(x))|$ is bounded, the integral can be further estimated by

$$\int_{B_{\frac{1}{n}}(\Omega')} \frac{1}{2} |\nabla Q_{\eta,\xi,n}|^2 \,\mathrm{d}x \;\leq\; \mathcal{E}_{\eta,\xi}(Q_{\eta,\xi}, B_{\frac{1}{n}}(\Omega') \cap \Omega) + \frac{C}{n} \,. \tag{3.28}$$

Next, we compare the bulk energy of $Q_{\eta,\xi,n}$ and $Q_{\eta,\xi}$. To this goal, we use the triangle inequality to get

$$\int_{\Omega'} F(Q_{\eta,\xi,n}) - F(Q_{\eta,\xi}) \,\mathrm{d}x \;\leq\; \int_{\Omega'} |F(Q_{\eta,\xi,n}) - F(\Pi_R Q_{\eta,\xi})| \,\mathrm{d}x + \int_{\Omega'} F(\Pi_R Q_{\eta,\xi}) - F(Q_{\eta,\xi}) \,\mathrm{d}x \,, \tag{3.29}$$

where we used the notation $F(Q) = f(Q) + \frac{\xi^2}{\eta^2} g(Q) + \xi^2 C_0$. As in [8, Prop. 4.1] we fix R such that $F(Q) \geq F(\Pi_R Q)$ for all $Q \in \mathrm{Sym}_0$. Hence $\int_\Omega f(\Pi_R Q_{\eta,\xi}) - f(Q_{\eta,\xi}) \,\mathrm{d}x \leq 0$. It remains to estimate the first integral of the RHS of (3.29). As before we split the integral into two parts depending on whether the distance to $\mathcal{M}$ is larger or smaller than $\frac{2}{n}$. We calculate

$$\begin{aligned}
\int_{\Omega'} |Q_{\eta,\xi,n} - \Pi_r Q_{\eta,\xi}|^2 \,\mathrm{d}x &= \int_{\Omega' \cap \{\operatorname{dist}(\cdot,\mathcal{M}) \geq \frac{2}{n}\}} |(\Pi_R Q_{\eta,\xi}) * \varrho_n - \Pi_R Q_{\eta,\xi}|^2 \,\mathrm{d}x + \frac{CR^2}{n} \\
&\leq \frac{1}{n^2} \int_{\Omega'} |\nabla(\Pi_R Q_{\eta,\xi})|^2 \,\mathrm{d}x + \frac{CR^2}{n} \\
&\leq \frac{C}{n^2} \mathcal{E}_{\eta,\xi}(Q_{\eta,\xi}, \Omega') + \frac{CR^2}{n} \,,
\end{aligned} \tag{3.30}$$

where we also used the $L^\infty-$bounds $|Q_{\eta,\xi,n}|, |\Pi_R Q_{\eta,\xi}| \leq R$. Applying those bounds again gives

$$\int_{\Omega'} |f(Q_{\eta,\xi,n}) - f(\Pi_R Q_{\eta,\xi})| \,\mathrm{d}x \leq \frac{C_f}{n^2}(1 + R + R^2)\, \mathcal{E}_{\eta,\xi}(Q_{\eta,\xi}, \Omega') + \frac{C}{n}(R^2 + R^3 + R^4) \,. \tag{3.31}$$

It remains the estimate of $g(Q_{\eta,\xi,n}) - g(\Pi_R Q_{\eta,\xi})$. It is enough to consider the set $\Omega'' := \Omega' \cap \{x \in \Omega \,:\, |Q_{\eta,\xi,n}(x)| \geq \frac{1}{2}\sqrt{\frac{2}{3}} s_*\}$, on $\Omega' \setminus \Omega''$ we use Proposition 4.2 in [8]. By smoothness of g on $\{Q \in \mathrm{Sym}_0 \,:\, |Q| \in [\sqrt{\frac{2}{3}} s_*, R]\}$, we find

$$\begin{aligned}
\int_{\Omega'} |g(Q_{\eta,\xi,n}) - g(\Pi_R Q_{\eta,\xi})| \,\mathrm{d}x &\lesssim \frac{\xi^2}{\eta} \mathcal{E}_{\eta,\xi}(Q_{\eta,\xi,n}, \Omega') + \|\nabla g\|_{L^\infty(\Omega'')} \int_{\Omega''} |Q_{\eta,\xi,n} - \Pi_R Q_{\eta,\xi}| \,\mathrm{d}x \\
&\lesssim \frac{\xi^2}{\eta} \mathcal{E}_{\eta,\xi}(Q_{\eta,\xi,n}, \Omega') + \left(\frac{|\Omega'|}{n^2} \mathcal{E}_{\eta,\xi}(Q_{\eta,\xi}, \Omega') + \frac{R^2}{n} \right)^{\frac{1}{2}} \,.
\end{aligned}$$

Combining this with (3.28) and (3.31), we substract $C\frac{\xi^2}{\eta} \mathcal{E}_{\eta,\xi}(Q_{\eta,\xi,n}, \Omega')$ from both sides and divide by $1 - C\frac{\xi^2}{\eta^2}$ to get the estimate (3.26). □

Having established these properties of $Q_{\eta,\xi,n}$, we are able to identify the size and structure of the set where $Q_{\eta,\xi,n}$ is close to being prolate uniaxial as stated in the next Lemma.

Lemma 3.4.3. *There exists a constant $C > 0$ such that for all $\delta > 0$, there exists a finite set $I \subset \Omega$ which satisfies*

1. *the following inclusions*

$$U_\delta \;\subset\; \bigcup_{x\in I} B_{\frac{\delta}{2n}}(x) \;\subset\; U_{\delta/2}\,, \tag{3.32}$$

   where $U_\delta := \{x \in \Omega \,:\, \mathrm{dist}(Q_{\eta,\xi,n}(x), \mathcal{N}) > \delta\}$,

2. *and*

$$\#I \;\le\; C\,\frac{n^3}{\eta\, f^\delta_{\min}\,\delta^3}\left(\xi^2 + \frac{1}{n^2}\right), \tag{3.33}$$

   where $f^\delta_{\min} = \min\{f(Q) \,:\, \mathrm{dist}(Q,\mathcal{N}) \ge \delta/2\}$.

Proof. Let $\delta > 0$ and $x_0 \in U_\delta$. By Lipschitz continuity of $Q_{\eta,\xi,n}$ (Proposition 3.4.2), we can deduce that for any $x \in B_{\frac{\delta}{2n}}(x_0)$ it holds

$$\mathrm{dist}(Q_{\eta,\xi,n}(x),\mathcal{N}) \;\ge\; \mathrm{dist}(Q_{\eta,\xi,n}(x_0),\mathcal{N}) - \|\nabla Q_{\eta,\xi,n}\|_\infty \frac{\delta}{2n} \;\ge\; \frac{\delta}{2}\,,$$

so that $x \in U_{\delta/2}$. From this, we get that

$$U_\delta \;\subset\; \bigcup_{x\in U_\delta} B_{\frac{\delta}{2n}}(x) \;\subset\; U_{\delta/2}\,.$$

By Vitali covering theorem, we find a subset $I \subset U_\delta$ with the same property and $B_{\frac{1}{3}\frac{\delta}{2n}}(x_i) \cap B_{\frac{1}{3}\frac{\delta}{2n}}(x_j) = \emptyset$ for $i \neq j$ and $x_i, x_j \in I$. Furthermore, using Proposition 3.4.2

$$\begin{aligned}
\frac{C\,\xi^2}{\eta} \;&\ge\; \int_\Omega f(Q_{\eta,\xi})\,\mathrm{d}x \;\ge\; \int_\Omega f(Q_{\eta,\xi,n})\,\mathrm{d}x - \frac{C}{\eta}\left(\xi^2 + \frac{1}{n^2}\right) \\
&\ge\; \int_{U_{\delta/2}} f(Q_{\eta,\xi,n})\,\mathrm{d}x - \frac{C}{\eta}\left(\xi^2 + \frac{1}{n^2}\right) \;\ge\; C\#I|B_{\frac{\delta}{2n}}|f_{\min} - \frac{C}{\eta}\left(\xi^2 + \frac{1}{n^2}\right) \\
&\ge\; C\#I\frac{\delta^3 f_{\min}}{n^3} - \frac{C}{\eta}\left(\xi^2 + \frac{1}{n^2}\right),
\end{aligned}$$

where we used that $f \ge f_{\min} > 0$ on $U_{\delta/2}$. From this it follows that

$$\#I \;\le\; C\frac{n^3}{\eta\, f_{\min}\delta^3}\left(\xi^2 + \frac{1}{n^2}\right).$$

□

In [8] a similar result was obtained using a regularization related to the energy and using the Euler-Lagrange equation to derive the Lipschitz continuity. This approach would also work in the new setting and one could obtain Lemma 3.4.3 with $n = \xi^{-1}$. However, our new approach has two major advantages: The first one is that the proofs are shorter and more elegant. The second (and main) reason is that we now have control over the gradient of the approximation as well, contrary to the approach in [8].

From (3.33) it follows that the volume of the union of balls in (3.32) converges to zero for $\eta, \xi \to 0$ and $n \sim \xi^{-1}$. The same holds true for the union of the surfaces of those balls. Note however that the sum of the diameters is not bounded and diverges like η^{-1}. With the tool developed in [30] and used in [8, 42] it would be possible to derive a bound, namely the sum of diameters can be shown to be bounded.

3.4.2 Definition of the line singularity

The goal of this section is to define a $1-$chain $S_{\eta,\xi,n}$ of finite length which satisfies the compactness properties announced in Theorem 3.3.1. The necessary analysis has already been carried out in [43, 44] but for the reader's convenience we recall the important steps and results.

For the construction of $S_{\eta,\xi,n}$, we follow Section 3 in [43]. We recall that $\mathcal{C}$ is the cone of oblate uniaxial $Q-$tensors which can be seen as a smooth simplicial complex of codimension 2 in Sym_0. Evoking Thom's transversality theorem, one can assume that, for almost every $Y \in \mathrm{Sym}_0$, the function $Q_{\eta,\xi,n} - Y$ is transverse to all cells of $\mathcal{C}$. Subdividing the preimages of the cells under the map $Q_{\eta,\xi,n} - Y$ if necessary, $(Q_{\eta,\xi,n} - Y)^{-1}(\mathcal{C})$ defines a smooth, simplicial, finite complex of codimension 2 which we call $S_{\eta,\xi,n}$. Note that $S_{\eta,\xi,n}$ depends on the choice of Y.

The relevant estimates on $S_{\eta,\xi,n}$ needed to prove Theorem 3.3.1 in Section 3.5.3 are formulated in Theorem C and Section 4 in [44]:

Theorem 3.4.4. *There exists a finite mass chain S such that one can choose a subsequence $S_{\eta,\xi,n}$ (not relabelled) and $\alpha > 0$ with*

$$\mathbb{F}(S_{\eta,\xi,n} - S) \;\to\; 0 \qquad \text{for almost every } Y \in B_\alpha(0)\,.$$

Furthermore, for any open subset $U \subset \mathbb{R}^3$ it holds

$$\liminf_{\xi,\eta\to 0} \eta\, \mathcal{E}_{\eta,\xi}(Q_{\eta,\xi,n}, U \cap \Omega) \;\geq\; \frac{\pi}{2} s_*^2 \beta\, \mathbb{M}(S \llcorner U)\,.$$

In our situation, by construction of $Q_{\eta,\xi,n}$ and for $Y \in B_\alpha(0)$ (α small enough) it holds that

$$(Q_{\eta,\xi,n} - Y)^{-1}(\mathcal{C}) \;\subset\; U_\delta \;\subset\; \bigcup_{x\in I} B_{\frac{\delta}{2n}}(x)\,.$$

Hence $\mathrm{supp}\,(S_{\eta,\xi,n}) \subset \bigcup_{x\in I} B_{\frac{\delta}{2n}}(x)$ and in view of the lower bound in Theorem 3.4.4 we deduce that the energy coming from $S_{\eta,\xi,n}$ in U is already contained in $U \cap \bigcup_{x\in I} B_{\frac{\delta}{2n}}(x)$.

3.4.3 Construction of T and estimates for Q close to $\mathcal{N}$

In this subsection we carry out the first steps to define the $2-$chain T. We start by defining

$$\mathcal{T} \;:=\; \{Q \in \mathrm{Sym}_0 \;:\; s > 0\,, 0 \leq r < 1\,, n_3 = 0\}\,,$$

where $r, s, \mathbf{n}$ are defined as in (3.3). From this we want to define $T_{\eta,\xi,n}$ close to $Q^{-1}_{\eta,\xi,n}(\mathcal{T})$. As carried out in [43] and described in Subsection 3.4.2, for almost every Y the set $(Q_{\eta,\xi,n} - Y)^{-1}(\mathcal{T})$ is in fact a smooth finite complex. In Lemma 3.4.6, we show that in addition for a.e. $Y \in \mathrm{Sym}_0$, the definition

$$T_{\eta,\xi,n} \;:=\; (Q_{\eta,\xi,n} - Y)^{-1}(\mathcal{T})$$

allows to control the area in regions where $Q_{\eta,\xi,n}$ is close to $\mathcal{N}$. Since both the constructions of $S_{\eta,\xi,n}$ and $T_{\eta,\xi,n}$ are valid for a.e. Y, we can choose the same Y and hence $\partial T_{\eta,\xi,n} \cap \Omega = S_{\eta,\xi,n}$. In parts of Ω where $Q_{\eta,\xi,n}$ is far from $\mathcal{N}$, e.g. close to $S_{\eta,\xi,n}$, we need to modify $T_{\eta,\xi,n}$. This will be the subject of the next subsection.

At first, we recall the (intuitively obvious) result that $\mathcal{T}$ is well behaved close to $\mathcal{N}$ in the sense that the level sets $\{n_3 = s\}$ for s small have a similar $\mathcal{H}^4-$volume as $\mathcal{T}$. This can be interpreted as control on the curvature of $\mathcal{T} \cap \mathcal{N}$.

Lemma 3.4.5. *There exists $\alpha_0, \alpha_1, C > 0$ such that for $Q \in \mathrm{Sym}_0$, $\mathrm{dist}(Q, \mathcal{N}) \leq \alpha_0$ and $\alpha \in (0, \alpha_1)$ it holds that*

$$\lim_{s\to 0} \mathcal{H}^4(\{Y \in B_\alpha(0) \;:\; n_3(Q - Y) = s\}) \;=\; \mathcal{H}^4(B_\alpha(Q) \cap \mathcal{T})\,.$$

In the smooth case this lemma follows as in [126, Lemma 3], however we give a proof here for completeness.

Proof. The parameter α_0 needs to be small enough to avoid problems far from $\mathcal{N}$ due to the non-smoothness of $\mathcal{T}$ at the singularity $0 \in \mathrm{Sym}_0$. So we choose $0 < \alpha_0 < \frac{1}{8}\mathrm{dist}(0, \mathcal{N})$. To avoid dealing with the topology of the sets involved, we pick $0 < \alpha_1 < \frac{1}{8}\mathrm{diam}\,(\mathcal{N})$. Hence, $B_\alpha(Q) \cap T$ is diffeomorphic to a $4-$dimensional ball.

We define $\phi(Y) := n_3(Y)$ for $Y \in B_\alpha(Q)$ and note that $B_\alpha(Q) \cap \mathcal{T} = \phi^{-1}(0)$. One can calculate $D\phi(Q) = D_Y n_3(Q)$ and by the calculations in the proof of Lemma A.2.4, $D\phi(Q)$ is parallel to the normal vector N_Q. Hence, for α_0, α_1 small enough $\mathrm{rank}(D\phi(Q)) = 1$. By the implicit function theorem, there exists a function ψ such that $\phi(Q + y + \psi(y)N_Q) = s$ for $y \in B_\alpha(0)$ with $y \perp N_Q$. Furthermore, $D\psi(Q+y) = (Dn_3(Q + y + \psi(y)) : N_Q)^{-1}(Dn_3(Q + y + \psi(y)))$. Since Dn_3 is parallel to N_Q in first order, for each $\epsilon > 0$ and $s_\epsilon > 0$ small enough it holds that $1 - \epsilon \leq (\det(D\psi^\top D\psi))^{\frac{1}{2}} \leq 1 + \epsilon$ on $\{\phi \leq s_\epsilon\}$. With a change of variables this becomes for $s \leq s_\epsilon$

$$(1-\epsilon)\int_{\{\phi=s\}} \psi(y)\,\mathrm{d}y \;\leq\; \mathcal{H}^4(\phi^{-1}(0)) \;\leq\; (1+\epsilon)\int_{\{\phi=s\}} \psi(y)\,\mathrm{d}y\,.$$

In the limit $s \to 0$ we obtain $(1+\epsilon)\int_{\{\phi=0\}} \psi(y)\,\mathrm{d}y \leq (1+\epsilon)^2\mathcal{H}^4(\phi^{-1}(0))$. Analogously $(1-\epsilon)\int_{\{\phi=0\}} \psi(y)\,\mathrm{d}y \geq (1-\epsilon)^2\mathcal{H}^4(\phi^{-1}(0))$. Since $\epsilon > 0$ was arbitrary, the claim follows. □

For $\delta > 0$, we introduce the set $A_\delta \subset \Omega$ in which $Q_{\eta,\xi,n}$ is close to being prolate uniaxial with norm $\sqrt{\frac{2}{3}}s_*$ as

$$A_\delta \;:=\; \{x \in \Omega \,:\, \mathrm{dist}(Q_{\eta,\xi,n}(x), \mathcal{N}) < \delta\}\,. \tag{3.34}$$

The next lemma shows that (in average) the $\mathcal{H}^2-$measure of $(Q_{\eta,\xi,n} - Y)^{-1}(\mathcal{T})$ that lies in A_δ is controlled by the energy.

Lemma 3.4.6. *There exists $\alpha_0, \delta_0 > 0$ such that for all $\alpha \in (0, \alpha_0)$, $\delta \in (0, \delta_0)$ one can find a constant $C > 0$ such that*

$$\int_{B_\alpha(0)} \mathcal{H}^2(A_\delta \cap (Q_{\eta,\xi,n} - Y)^{-1}(\mathcal{T}))\,\mathrm{d}Y \;\leq\; C\,\eta\,\mathcal{E}_{\eta,\xi}(Q_{\eta,\xi,n}, A_\delta)\,. \tag{3.35}$$

Proof. Let $\alpha, \delta > 0$ small enough such that for $Y \in B_\alpha(0)$, the map $Q \mapsto n_3(Q - Y)$ is smooth on $\{Q \in \mathrm{Sym}_0 \,:\, \mathrm{dist}(Q, \mathcal{N}) < \delta\}$. Let A_δ be defined as in (3.34). In order for the map $x \mapsto n_3(Q_{\eta,\xi,n}(x) - Y)$ to be well defined, we need to restrict ourselves to a simply connected subset of A_δ. For this, take $x_0 \in A_\delta$ and $r > 0$ such that $A_\delta \cap B_r(x_0)$ is simply connected. We carry out the analysis on $A_\delta \cap B_r(x_0)$, noting that we can cover A_δ by such balls to find the estimate (3.35). With $x_0 \in A_\delta$ and $r > 0$ fixed as described, we can calculate

$$\begin{aligned}
&\int_{B_\alpha(0)} \mathcal{H}^2(B_r(x_0) \cap A_\delta \cap (Q_{\eta,\xi,n}(x) - Y)^{-1}(\mathcal{T}))\,\mathrm{d}Y \\
&\quad= \int_{B_\alpha(0)} |D\chi_{\{x\in\Omega | n_3(Q_{\eta,\xi,n}(x)-Y)>0\}}|(B_r(x_0)\cap A_\delta)\,\mathrm{d}Y \\
&\quad\leq \liminf_{\epsilon\to 0} \int_{B_\alpha(0)} \int_{B_r(x_0)\cap A_\delta} |\nabla_x(h_\epsilon \circ n_3 \circ (Q_{\eta,\xi,n} - Y))(x)|\,\mathrm{d}x\,\mathrm{d}Y \\
&\quad= \liminf_{\epsilon\to 0} \int_{B_\alpha(0)} \int_{B_r(x_0)\cap A_\delta} |h_\epsilon'(n_3(Q_{\eta,\xi,n}(x) - Y))\nabla_Q n_3(Q_{\eta,\xi,n}(x) - Y) : \nabla_x Q(x)|\,\mathrm{d}x\,\mathrm{d}Y\,,
\end{aligned}$$

where $h_\epsilon \in C^1(\mathbb{R}, [0,1])$ is an approximation of the Heaviside function, i.e. $h_\epsilon(x) = 0$ for $x \leq 0$, $h_\epsilon(x) = 1$ for $x \geq \epsilon$ and $h_\epsilon' > 0$ on $(0, \epsilon)$. The above inequality is then just the lower semi continuity of the total variation. With the identity $h_\epsilon'(n_3(Q_{\eta,\xi,n}(x) - Y))\nabla_Q n_3(Q_{\eta,\xi,n}(x) - Y) =$

$-\nabla_Y(h_\epsilon \circ n_3 \circ (Q_{\eta,\xi,n}(x) - Y))$ and the Fubini theorem we can rewrite

$$\begin{aligned}
&\int_{B_\alpha(0)} \int_{B_r(x_0)\cap A_\delta} |h'_\epsilon(n_3(Q_{\eta,\xi,n}(x) - Y))\nabla_Q n_3(Q_{\eta,\xi,n}(x) - Y) : \nabla_x Q_{\eta,\xi,n}(x)| \, \mathrm{d}x \, \mathrm{d}Y \\
&\quad \leq \int_{B_r(x_0)\cap A_\delta} |\nabla Q_{\eta,\xi,n}| \int_{B_\alpha(0)} |\nabla_Y(h_\epsilon \circ n_3 \circ (Q_{\eta,\xi,n} - Y))| \, \mathrm{d}Y \, \mathrm{d}x \\
&\quad = \int_{B_r(x_0)\cap A_\delta} |\nabla Q_{\eta,\xi,n}| \int_0^1 \mathcal{H}^4(\{Y \in B_\alpha(0) \,:\, h_\epsilon(n_3(Q_{\eta,\xi,n}(x) - Y)) = s\}) \, \mathrm{d}s \, \mathrm{d}x \\
&\quad = \int_{B_r(x_0)\cap A_\delta} |\nabla Q_{\eta,\xi,n}| \int_0^1 \mathcal{H}^4(\{Y \in B_\alpha(0) \,:\, n_3(Q_{\eta,\xi,n}(x) - Y) = h_\epsilon^{-1}(s)\}) \, \mathrm{d}s \, \mathrm{d}x \,,
\end{aligned}$$

where we also used the coarea formula. By Lemma 3.4.5 in the liminf $\epsilon \to 0$ this equals

$$\begin{aligned}
&\liminf_{\epsilon\to 0} \int_{B_r(x_0)\cap A_\delta} |\nabla Q_{\eta,\xi,n}| \int_0^1 \mathcal{H}^4(\{Y \in B_\alpha(0) \,:\, n_3(Q_{\eta,\xi,n}(x) - Y) = h_\epsilon^{-1}(s)\}) \, \mathrm{d}s \, \mathrm{d}x \\
&\quad = \int_{B_r(x_0)\cap A_\delta} |\nabla Q_{\eta,\xi,n}| \, \mathcal{H}^4(B_\alpha(Q_{\eta,\xi,n}) \cap \mathcal{T}) \, \mathrm{d}x
\end{aligned}$$

by translation invariance of $\mathcal{H}^4$. Applying the elementary inequality $2ab \leq a^2 + b^2$ we get

$$\begin{aligned}
&\int_{B_r(x_0)\cap A_\delta} |\nabla Q_{\eta,\xi,n}| \, \mathcal{H}^4(B_\alpha(Q_{\eta,\xi,n}) \cap \mathcal{T}) \, \mathrm{d}x \\
&\qquad \leq \int_{B_r(x_0)\cap A_\delta} \frac{\eta}{2} |\nabla Q_{\eta,\xi,n}|^2 \;+\; \frac{1}{2\eta} \mathcal{H}^4(B_\alpha(Q_{\eta,\xi,n}) \cap \mathcal{T})^2 \, \mathrm{d}x \,.
\end{aligned}$$

The Dirichlet term appears in the energy, so it remains to estimate $\mathcal{H}^4(B_\alpha(Q_{\eta,\xi,n}) \cap \mathcal{T})^2$ in terms of $g(Q_{\eta,\xi,n})$. We first note that $\mathcal{T} \cap B_\alpha(Q_{\eta,\xi,n}(x)) = \emptyset$ if $\mathrm{dist}(Q_{\eta,\xi,n}(x), \mathcal{T}) > \alpha$ and since $\mathrm{dist}(Q_{\eta,\xi,n}, \mathcal{N}) < \delta$ we have $\mathcal{H}^4(B_\alpha(Q_{\eta,\xi,n}) \cap \mathcal{T}) \leq C_\delta \alpha^4$ by Proposition A.2.5. Hence, we get

$$\int_{B_r(x_0)\cap A_\delta} \mathcal{H}^4(B_\alpha(Q_{\eta,\xi,n}) \cap \mathcal{T})^2 dx \;\leq\; (C_\delta \alpha^4)^2 |B_r(x_0) \cap A_\delta \cap \{x \in \Omega \,:\, \mathrm{dist}(Q_{\eta,\xi,n}(x), \mathcal{T}) < \alpha\}| \,.$$

For $x \in A_\delta \cap \{x \in \Omega \,:\, \mathrm{dist}(Q_{\eta,\xi,n}(x), \mathcal{T}) < \alpha\}$ we can estimate

$$\begin{aligned}
g(Q_{\eta,\xi,n}(x)) \;&\geq\; g(\mathcal{R}(Q_{\eta,\xi,n}(x))) - C_g \mathrm{dist}(Q_{\eta,\xi,n}(x), \mathcal{N}) \;\geq\; \sqrt{\frac{3}{2}}(1 - n_3^2(Q_{\eta,\xi,n}(x))) - C_g\delta \\
&\geq\; \sqrt{\frac{3}{2}}(1 - C_{\mathcal{T}}\alpha) - C_g\delta \;\geq\; G > 0
\end{aligned}$$

for $\alpha, \delta \ll 1$ small enough. Hence,

$$G|B_r(x_0) \cap A_\delta \cap \{x \in \Omega \,:\, \mathrm{dist}(Q_{\eta,\xi,n}(x), \mathcal{T}) < \alpha\}| \;\leq\; \int_{B_r(x_0)\cap A_\delta} g(Q_{\eta,\xi,n}) \, \mathrm{d}x \,.$$

□

We remark that although Lemma 3.4.6 control the size for a.e. *fixed* $Y \in B_\alpha(0)$, but degenerates with α. Hence it does not provide a uniform bound in α allowing to pass to the limit $Y \to 0$. A bound independent of α will be derived in the section on the lower bound.

3.4.4 Estimates near singularities

At points $x \in \Omega$ where $\mathrm{dist}(Q_{\eta,\xi,n}(x), \mathcal{N}) > \delta$, the estimates we derived in the previous subsection are no longer available and we need new tools to bound the mass of $T_{\eta,\xi,n}$. We are concerned with two different cases: The first case is the one of $x \in T_{\eta,\xi,n}$ far from the boundary $S_{\eta,\xi,n}$. We can simply "cut out" those pieces and replace them by parts of surfaces of spheres which are controlled

in mass. This will be made precise using Lemma 3.4.3. The second case is more challenging. We will modify $T_{\eta,\xi,n}$ close to the boundary $S_{\eta,\xi,n}$ by using a construction similar to the one used in the deformation theorem (see Lemma 3.4.8). This will allow us to express the mass of the modified $2-$chain in terms of the surface of cubes and Lemma 3.4.3 permits us to control the number of such cubes.

Lemma 3.4.7 (Deformation in the interior)**.** *Let $I^{\text{int}} \subset I$ be the subset of points $x_0 \in I$ such that $\operatorname{dist}(x_0, S_{\eta,\xi,n}) > \frac{\delta}{2n}$ and $\operatorname{dist}(x_0, T_{\eta,\xi,n}) < \frac{\delta}{2n}$. Then, there exists a flat $2-$chain $\widetilde{T^{\text{int}}}$ with values in $\pi_1(\mathcal{N})$ and support in $B^{\text{int}} := \bigcup_{x\in I^{\text{int}}} \overline{B_{\frac{\delta}{2n}}(x)}$ such that*

1. $\partial\widetilde{T^{\text{int}}} = \partial(T_{\eta,\xi,n} \llcorner B^{\text{int}})$,
2. *and* $\mathbb{M}(\widetilde{T^{\text{int}}}) \lesssim \frac{n}{\eta}\left(\xi^2 + \frac{1}{n^2}\right)$.

Proof. Since $B^{\text{int}} \cap \operatorname{supp}(T_{\eta,\xi,n}) \neq \emptyset$ and $B^{\text{int}} \cap \operatorname{supp}(S_{\eta,\xi,n}) = \emptyset$ we know that $\emptyset \neq \partial(T_{\eta,\xi,n} \llcorner B^{\text{int}}) \subset \partial B^{\text{int}}$. Furthermore, since $\partial^2 = 0$ it follows that $\partial(T_{\eta,\xi,n} \llcorner B^{\text{int}})$ consists of closed curves and divides ∂B^{int} into domains. Let D be the set of these domains. Now pick any subset $D' \subset D$ such that $\partial\left(\bigcup_{U\in D'} U\right) = \partial(T_{\eta,\xi,n} \llcorner B)$. We define $\widetilde{T^{\text{int}}} := \sum_{U\in D'}[U]$. Then, by definition $T_{\eta,\xi,n} \llcorner B^{\text{int}}$ and $\widetilde{T^{\text{int}}}$ have the same boundary and since $\widetilde{T^{\text{int}}} \subset \partial B^{\text{int}}$ we also have

$$\mathbb{M}(\widetilde{T^{\text{int}}}) \;\leq\; \mathbb{M}(\partial B^{\text{int}}) \;\leq\; \sum_{x\in I^{\text{int}}} \mathbb{M}(\partial B_{\frac{\delta}{2n}}) \;\leq\; \#I\, 4\pi\, \frac{\delta^2}{n^2} \;\lesssim\; \frac{n}{\eta}\left(\xi^2 + \frac{1}{n^2}\right).$$

□

At the boundary we cannot remove a disk without the risk of creating new boundary which might not be controlled, so another method has to be used. The idea is the following: Take a cube K of size $\frac{\delta}{n}$ which contains a part of the singular line $S_{\eta,\xi,n}$ and intersects with $T_{\eta,\xi,n}$. We then modify (deform) the "surface" connecting $T_{\eta,\xi,n} \cap \partial K$ and $S_{\eta,\xi,n} \cap K$ by pushing it onto a part of ∂K (see also Figure 3.4). The result is a modified $T_{\eta,\xi,n}$ with the same boundary as before and the surface inside the cube is controlled by the surface area of K and the length of the singular line. We point out that this procedure and its proof is closely related to the deformation theorem (for flat chains) (see [166], Chapter 5 in [66], Theorem 7.3 in [67] and Chapter 4.2 in [65]) but differs in some details so that we give a full proof here.

Lemma 3.4.8 (Deformation close to the boundary)**.** *Let $I^{\text{bdry}} \subset I$ be the subset of points $x_0 \in I$ such that $\operatorname{dist}(x_0, S_{\eta,\xi,n}) < \frac{\delta}{2n}$ and $\operatorname{dist}(x_0, T_{\eta,\xi,n}) < \frac{\delta}{2n}$. Then there exists a flat $2-$chain $\widetilde{T^{\text{bdry}}}$ with values in $\pi_1(\mathcal{N})$ and support in a finite union of cubes of side length δ/n called B^{bdry} verifying $\bigcup_{x\in I^{\text{bdry}}} \overline{B_{\frac{\delta}{2n}}(x)} \subset B^{\text{bdry}}$ such that*

1. $|B^{\text{bdry}}| \lesssim \frac{1}{\eta}(\xi^2 + \frac{1}{n^2})$,
2. $\partial\widetilde{T^{\text{bdry}}} = \partial(T_{\eta,\xi,n} \llcorner B^{\text{bdry}})$,
3. *and*

$$\mathbb{M}(\widetilde{T^{\text{bdry}}}) \;\lesssim\; \frac{n}{\eta}\left(\xi^2 + \frac{1}{n^2}\right). \tag{3.36}$$

Proof. For the sake of readability we drop the dependences on ξ, η, n in the notation of this proof and simply write $\tilde{T}$ instead of $\widetilde{T^{\text{bdry}}}$. Covering S with a cubic grid of size $h = \frac{\delta}{n}$ such that S is in a general position, we can assume that the center x_K of all cubes K that contain parts of S does not intersects S or T, i.e. $x_K \notin \operatorname{supp}(T), \operatorname{supp}(S)$. Indeed, this is possible S intersects only a finite number of cubes according to Lemma 3.4.3. Let G be the set of those cubes and X the set of its centers.

Step 1 (Construction and properties of the retraction map). Let $K \in G$ be a cube and let $x_K \in X$ be its center. Let P be the central projection onto ∂K originating in x_K. We define a homotopy $\Phi : [0,1] \times (K \setminus \{x_K\}) \to K$ between the identity on K and P by simply taking $\Phi(t,x) = (1-t)x + tPx$. Note that by definition this homotopy is relative to ∂K, i.e. $\Phi(t,x) = x$ for all $t \in [0,1]$ and $x \in \partial K$. Furthermore, for all $x \in K \setminus \{x_k\}$ and $t \in [0,1]$ it holds

$$\operatorname{dist}(\Phi(t,x), x_K) \;\geq\; \operatorname{dist}(x, x_K)\,. \tag{3.37}$$

Since $|\partial_t \Phi(t,x)| = |-x+Px| \leq \sqrt{3}h$ and by (3.37) we deduce that Φ is locally Lipschitz continuous and $\operatorname{Lip}(\Phi(t,x)) \leq C\, h \operatorname{dist}(x, x_K)^{-1}$. Since Φ is relative to ∂K we can glue together all those functions defined on the cubes $K \in G$ with the identity on cubes $K \notin G$ to get a function Φ defined everywhere in $\mathbb{R}^3 \setminus X$.

Step 2 (Intermediate estimate). In this step we want to show that if we allow for a small translation of the chain S, then the mass of $\Phi_\#([0,1] \times S)$ can be bounded by $\mathbb{M}(S)$ times the size of the cube h, up to a constant.

Applying Corollary 2.10.11 in [65] (or Section 2.7 in [66]) we get as in [166, Lemma 2.1]

$$\begin{aligned}
\mathbb{M}(\Phi_\#([0,1] \times S)) \;&\leq\; \|\mathrm{Id} - P\|_\infty \int_{\mathbb{R}^3} \sup_{t\in[0,1]} \operatorname{Lip}(\Phi(t,x))\, \mathrm{d}\mu_S(x) \\
&\leq\; C\, h^2 \int_{\mathbb{R}^3} \operatorname{dist}(x,X)^{-1}\, \mathrm{d}\mu_S(x)\,.
\end{aligned}$$

Taking the mean over translation by a vector $y \in [0,1]^3$, we arrive at

$$\begin{aligned}
\int_{[0,1]^3} \mathbb{M}(\Phi_\#([0,1] \times (\tau_{hy} S))\, \mathrm{d}y \;&=\; C\, h^2 \int_{[0,1]^3} \int_{\mathbb{R}^3} \operatorname{dist}(x,X)^{-1}\, \mathrm{d}\mu_{\tau_{hy}S}(x)\, \mathrm{d}y \\
&=\; C\, h^2 \int_{[0,1]^3} \int_{\mathbb{R}^3} \operatorname{dist}(x+hy,X)^{-1}\, \mathrm{d}\mu_S(x)\, \mathrm{d}y \\
&=\; C\, h^2 \int_{\mathbb{R}^3} \int_{[0,1]^3} \operatorname{dist}(x+hy,X)^{-1}\, \mathrm{d}y\, \mathrm{d}\mu_S(x) \\
&\leq\; C\, h \int_{\mathbb{R}^3} \mathrm{d}\mu_S(x) \\
&=\; C\, h\, \mathbb{M}(S)\,.
\end{aligned}$$

Hence, we can assume that S is in a position such that

$$\mathbb{M}(\Phi_\#([0,1] \times S)) \;\leq\; C\, h\, \mathbb{M}(S)\,. \tag{3.38}$$

Step 3 (Definition of $\tilde{T}$). We define

$$\tilde{T} \;:=\; \partial(\Phi_\#([0,1] \times T)) - T\,.$$

Considering a cube $K \in G$, one can think of this construction as the boundary of the three dimensional object created by filling the space between T and its projection onto ∂K according to Step 1 and then removing the original part T. Another but equivalent point of view is to take $\tilde{T}$ as all the points along the path created by projecting $T \llcorner \partial K$, S together with the projection $P_\#(T)$, see also Figure 3.4. Indeed, one can calculate for $K \in G$

$$\begin{aligned}
\partial(\Phi_\#([0,1] \times (T \llcorner K))) &= \Phi_\#((\partial[0,1]) \times (T \llcorner K)) + \Phi_\#([0,1] \times (\partial T) \llcorner K) + \Phi_\#([0,1] \times T \llcorner (\partial K)) \\
&= P_\#(T \llcorner K) - (\mathrm{Id}_K)_\#(T) + \Phi_\#([0,1] \times (S \llcorner K)) + \Phi_\#([0,1] \times T \llcorner (\partial K))\,.
\end{aligned}$$

Thus, we have the formula

$$\tilde{T} \llcorner K \;=\; P_\#(T \llcorner K) \;+\; \Phi_\#([0,1] \times (S \llcorner K)) \;+\; \Phi_\#([0,1] \times T \llcorner (\partial K))\,.$$

Since $P_\#(T \llcorner K) + \Phi_\#([0,1] \times T \llcorner (\partial K)) \subset \partial K$ from which we derive the bound on the mass of $\tilde{T}$

$$\mathbb{M}(\tilde{T} \llcorner K) \;\leq\; \mathbb{M}(\partial K) \;+\; \mathbb{M}(\Phi_\#([0,1] \times (S \llcorner K))) \;\leq\; 6\, h^2 \;+\; C\, h\, \mathbb{M}(S \llcorner K)\,, \tag{3.39}$$

where we also used the estimate (3.38) on K of Step 2. On all cubes $K \notin G$, $\tilde{T} \llcorner K = 0$, so that we find $\mathrm{supp}\,(\tilde{T}) \subset \bigcup_{K\in G} \overline{K}$. Defining $B^{\mathrm{bdry}} := \bigcup\{\overline{K} \,:\, K \text{ is cube of the grid, } \exists x \in I^{\mathrm{bdry}} \text{ with } K \cap B_{\frac{\delta}{2n}}(x) \neq \emptyset\}$, it is clear that $\tilde{T}$ is supported in B^{bdry} since $\bigcup_{K\in G} \overline{K} \subset B^{\mathrm{bdry}}$. Furthermore, by definition of B^{bdry}, we have the claimed inclusion $\bigcup_{x\in I^{\mathrm{bdry}}} \overline{B_{\frac{\delta}{2n}}(x)} \subset B^{\mathrm{bdry}}$. The measure of B^{bdry} can easily be estimated since it is formed by cubes covering $\bigcup_{x\in I^{\mathrm{bdry}}} B_{\frac{\delta}{2n}}(x)$, the cubes having the same length scale $\frac{\delta}{n}$ as the balls. Therefore, up to a constant only depending on the space dimension, (3.33) implies that $|B^{\mathrm{bdry}}| \lesssim h^3 \frac{n^3}{\eta\delta^3}(\xi^2 + \frac{1}{n^2}) = \frac{1}{\eta}(\xi^2 + \frac{1}{n^2})$. Since $\partial \circ \partial = 0$, the boundary of $\tilde{T}$ coincides with ∂T. Since all calculations in Step 3 were local and Φ is relative to the boundaries of the cubes, (3.36) follows from summing up (3.39) over all cubes $K \in G$. □

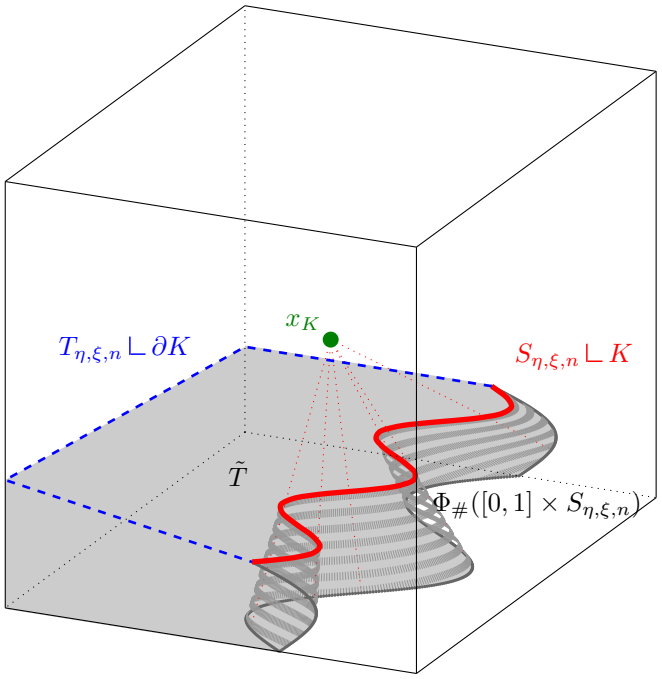

Figure 3.4: Construction near the boundary inside a cube: The newly created area (grey) is controlled by the surface of the cube and the length of the line singularity (red).

As a direct consequence of Lemma 3.4.6, Lemma 3.4.7 and Lemma 3.4.8 we have the following corollary:

Corollary 3.4.9. *There exists a flat 2−chain $\widetilde{T_{\eta,\xi,n}}$ with values in $\pi_1(\mathcal{N})$ such that*

1. $\widetilde{\partial T_{\eta,\xi,n}} = S_{\eta,\xi,n}$,
2. *for all $x_0 \in \Omega$ and $R > 0$*

$$\mathbb{M}(\widetilde{T_{\eta,\xi,n}} \llcorner B_R(x_0)) \;\lesssim\; \eta\, \mathcal{E}_{\eta,\xi}(Q_{\eta,\xi,n}, B_R(x_0)) + \frac{n}{\eta}\left(\xi^2 + \frac{1}{n^2}\right), \tag{3.40}$$

3. *and*

$$\mathbb{F}(\widetilde{T_{\eta,\xi,n}} - T_{\eta,\xi,n}) \;\lesssim\; \frac{n}{\eta}\left(\xi^2 + \frac{1}{n^2}\right). \tag{3.41}$$

Proof. Starting from $T_{\eta,\xi,n}$ and the estimate in Lemma 3.4.6, we can modify $T_{\eta,\xi,n}$ according to Lemma 3.4.7 and Lemma 3.4.8 in the region $B^{\text{int}} \cup B^{\text{bdry}}$ to obtain $\widetilde{T_{\eta,\xi,n}}$ without changing the boundary $S_{\eta,\xi,n}$ by setting

$$\widetilde{T_{\eta,\xi,n}} \;:=\; \widetilde{T^{\text{int}}} \llcorner B^{\text{int}} \;+\; \widetilde{T^{\text{bdry}}} \llcorner B^{\text{bdry}} \;+\; T_{\eta,\xi,n} \llcorner ((B^{\text{int}} \cup B^{\text{bdry}})^c)\,.$$

Estimate (3.40) is a direct consequence of the three aforementioned lemmata. Finally, by construction $T_{\eta,\xi,n} - \widetilde{T_{\eta,\xi,n}}$ is supported in $B^{\text{int}} \cup B^{\text{bdry}}$ and $\partial(T_{\eta,\xi,n} - \widetilde{T_{\eta,\xi,n}}) = 0$. Hence, $\mathbb{F}(T_{\eta,\xi,n} - \widetilde{T_{\eta,\xi,n}}) \leq |B^{\text{int}} \cup B^{\text{bdry}}|$, from which (3.41) follows for n large and η, ξ small enough. □

In the following analysis we only work with $\widetilde{T_{\eta,\xi,n}}$. In order to improve readability, we drop the tilde in our notation from now on.

3.4.5 Proof of compactness for fixed Y

Let $B \subset \Omega$ open, bounded and choose $n := \xi^{-1}$. Then, by Lemma 3.4.6 and Corollary A.2.3, we deduce that for $\alpha > 0$ and $\xi, \eta > 0$, there exist $Y_{\eta,\xi} \in B_\alpha(0) \subset \text{Sym}_0$ such that our construction yields a flat chain $T_{\eta,\xi,n} \in \mathcal{F}^2$ such that $\partial T_{\eta,\xi,n} = S_{\eta,\xi,n} + \Gamma_n$ and

$$\mathbb{M}(T_{\eta,\xi,n} \llcorner B) \;\leq\; C\left(\eta\, \mathcal{E}_{\eta,\xi}(Q_{\eta,\xi,n}, B_R(x_0)) + \frac{\xi}{\eta}\right) \;\leq\; C\left(\eta\, \mathcal{E}_{\eta,\xi}(Q_{\eta,\xi}, B_R(x_0)) + \frac{\xi}{\eta}\right),$$

where we also used (3.26) of Proposition 3.4.2. In particular the energy bound (3.17) implies that $\mathbb{M}(T_{\eta,\xi,n} \llcorner B)$ is bounded. Applying a compactness theorem for flat chains as stated in the preliminary part ([67, Cor. 7.5]), there exists a subsequence (which we do not relabel) and a flat chain $T \in \mathcal{F}^2$ with support in $\overline{\Omega}$ such that $\mathbb{F}((T_{\eta,\xi,n} - T) \llcorner B) \to 0$ for $\xi, \eta \to 0$. Extracting another subsequence if necessary we can assume that $Y_{\eta,\xi} \to Y \in \overline{B_\alpha(0)}$ for $\eta, \xi \to 0$. We note that the T constructed here depends on Y (and α). In order to keep our notation simple, we only write this dependence explicitly when necessary, i.e. when we pass to the limit $\|Y\|, \alpha \to 0$ in Subsection 3.5.3. Since the boundary operator ∂ is continuous we conclude with Theorem 3.4.4 that $\partial T = S + \Gamma$. The finite mass of T and S immediately implies rectifiability [67, Thm 10.1].

3.5 Lower bound

This section is devoted to the $\Gamma-$liminf inequality of Theorem 3.3.1. The proof necessary to deduce the line energy has already been given in [44], so that we will only state the result for completeness (Proposition 3.5.1). The energy contributions of T far from $\mathcal{M}$ are to be derived in Subsection 3.5.1. In the remaining, we are concerned with the energy of T and F close resp. on $\mathcal{M}$.

The precise cost of a singular line in our setting has been derived first in [41] based on ideas in [92, 144]. In our case, the result reads as follows.

Proposition 3.5.1. *Let $B \subset \overline{\Omega}$ be a bounded open set and $U_\eta := \{x \in \Omega : \text{dist}(x, S_{\eta,\xi,n}) \leq \sqrt{\eta}\}$. Then*

$$\liminf_{\eta,\xi \to 0} \eta\, \mathcal{E}_{\eta,\xi}(Q_{\eta,\xi,n}, U_\eta \cap B) \;\geq\; \frac{\pi}{2} s_*^2 \beta\, \mathbb{M}(S \llcorner B)\,. \tag{3.42}$$

Proof. See Theorem C and Proposition 4.1 in [44] for a proof of the version we used here. □

To derive the exact minimal energy for the lower bound related to T, we introduce the following auxiliary problem:

$$I(r_1, r_2, a, b) \;:=\; \inf_{\substack{n_3 \in H^1([r_1,r_2],[-1,1]) \\ n_3(r_1)=a,\, n_3(r_2)=b}} \int_{r_1}^{r_2} \frac{s_*^2 |n_3'|^2}{1 - n_3^2} + c_*^2(1 - n_3^2)\, \mathrm{d}r \tag{3.43}$$

for $0 \le r_1 \le r_2 \le \infty$, $a, b \in [-1,1]$. It is one dimensional and only takes into account the derivative along the integration path. Problem (3.43) is equivalent to minimizing $\int \left(\frac{1}{2}|\partial_r Q|^2 + g(Q)\right)\, \mathrm{d}r$ subject to a $\mathcal{N}-$valued function Q and fitting boundary conditions. This reflects that by Lemma 3.4.3, the regions where $Q_{\eta,\xi,n}$ is far from $\mathcal{N}$ are small. Indeed, if $Q(r) = s_*(\mathbf{n}(r) \otimes \mathbf{n}(r) - \frac{1}{3}\mathrm{Id})$ for a $\mathbb{S}^2-$valued function $\mathbf{n}$, then $\partial_r Q = s_*((\partial_r \mathbf{n}) \otimes \mathbf{n} + \mathbf{n} \otimes (\partial_r \mathbf{n}))$ and hence $|\partial_r Q|^2 = 2s_*^2 |\partial_r \mathbf{n}|^2$ since $|\mathbf{n}|^2 = 1$ and therefore $2(\partial_r \mathbf{n}) \cdot \mathbf{n} = \partial_r |\mathbf{n}|^2 = 0$. Using again that $\mathbf{n} \in \mathbb{S}^2$, we can write $\mathbf{n} = (\pm\sqrt{1-n_3}\tilde{n}_1, \pm\sqrt{1-n_3^2}\tilde{n}_2, n_3)$, where $\tilde{n} = (\tilde{n}_1, \tilde{n}_2)$ is a $\mathbb{S}^1-$valued function. One can then easily calculate that $|\partial_r \mathbf{n}|^2 \ge |\sqrt{1-n_3^2} 2 n_3 \partial_r n_3|^2 + |\partial_r n_3|^2 = |\partial_r n_3|^2/(1-n_3^2)$ (with equality if $\tilde{n}$ is constant), which is the first term in (3.43). For the second term in (3.43) we note that by (3.5) it holds that $g(s_*(\mathbf{n} \otimes \mathbf{n} - \frac{1}{3}\mathrm{Id})) = c_*^2(1-n_3^2)$. The functional in (3.43) has been previously studied in [4] and [8, Lemma 4.17] from which we need the following lemma:

Lemma 3.5.2. *Let $0 \le r_1 \le r_2 \le \infty$. Then,*

1. *$I(r_1, r_2, -1, 1) \ge 4 s_* c_*$.*
2. *Let $\theta \in [0, \pi]$. Then the minimizer $\mathtt{n}_3$ of $I(0, \infty, \cos(\theta), 1)$ is explicitly given by*

$$\mathtt{n}_3(r, \theta) = \frac{A(\theta) - \exp(-2c_*/s_* r)}{A(\theta) + \exp(-2c_*/s_* r)}, \quad A(\theta) = \frac{1 + \cos(\theta)}{1 - \cos(\theta)} \tag{3.44}$$

and

$$I(0, \infty, \cos(\theta), \pm 1) = 2 s_* c_* (1 \mp \cos(\theta)). \tag{3.45}$$

In this lemma, we use that g reduces to $c_*^2(1-n_3^2)$ for Q in $\mathcal{N}$, as demanded in (3.5). However, as pointed out in Remark 4.18 in [8], this is not necessary.

During the blow up procedure in the next subsection, we want to quantify the energy necessary for a $Q_{\eta,\xi,n}$ close to $\mathcal{N}$ to pass from $n_3(Q_{\eta,\xi,n}) \approx \pm 1$ to $n_3(Q_{\eta,\xi,n} - Y) = 0$, i.e. to intersect $T_{\eta,\xi,n}$. Since problem (3.43) does not take into account the perturbation made by subtracting $Y \in B_\alpha(0)$ from $Q_{\eta,\xi,n}$, we introduce for $\alpha > 0$ small enough

$$I_\alpha(r_1, r_2, a, b) := \inf\{I(r_1, r_2, a, \pm n_3(Q)) \,:\, Q \in \mathrm{Sym}_0,\, n_3(Q - Y) = \pm b,\, Y \in B_\alpha(0)\}. \tag{3.46}$$

Since $n_3(Q)$ and $n_3(Q-Y)$ are only defined up to a sign, it is necessary to define I_α using the infimum not only over Y but also the choice of sign. This leads to the slightly counter-intuitive situation that e.g. $I_\alpha(r_1, r_2, a, -a) = 0$ for all $a \in [-1, 1]$. As a consequence, we only have convergence of $I_\alpha(r_1, r_2, a, b) \to I(r_1, r_2, a, b)$ for $\alpha \to 0$ if $ab \ge 0$. In what follows, we will only be concerned with the case $b = 0$ as this corresponds to a point on $T_{\eta,\xi,n}$, and hence we have convergence of $I_\alpha(r_1, r_2, a, 0)$ to $I(r_1, r_2, a, 0)$ for all $a \in [-1, 1]$ for $\alpha \to 0$.

The knowledge about the optimal profile in (3.45) is also used in the construction of the upper bound, in particular the fact that $|\mathtt{n}_3| - 1$ and all derivatives of $\mathtt{n}_3$ decay fast enough (here exponentially) as $r \to \infty$. The result that for minimizers of (3.43), n_3^2 approaches 1 exponentially fast is complemented by the next lemma. It states that for a bounded energy configuration on a line, n_3^2 cannot always stay far from 1.

Lemma 3.5.3. *There exist constants $\mathfrak{C} > 0$ and $\delta_0 > 0$ such that for a line ℓ and $Q \in H^1(\ell, \mathrm{Sym}_0)$ and $K > 0$ a constant such that $\eta\, \mathcal{E}_{\eta,\xi}(Q, \ell) \le K < \infty$ it holds: For $\delta \in (0, \delta_0)$, there exist a set $I_\delta \subset \ell$ and $C_\delta > 0$ such that*

$$|\ell \setminus I_\delta| \;\le\; \frac{K+1}{C_\delta}\eta \quad \text{and} \quad |n_3(Q)| \ge 1 - \mathfrak{C}\sqrt{\delta} \text{ on } I_\delta.$$

Proof. Let

$$g_{\min} := \min\{g(Q) \,:\, Q \in \mathrm{Sym}_0,\, \mathrm{dist}(Q, \mathcal{N}) \le \delta,\, |Q - Q_\infty| \ge \mathfrak{a}\sqrt{\delta}\},$$

where $\mathfrak{a} > 0$ is chosen as in [8] and for $\delta > 0$ small enough. Proposition 2.5 in [8] then implies that $g_{\min} > 0$. Then, we can estimate

$$K \;\ge\; \eta\, \mathcal{E}_{\eta,\xi}(Q, \ell) \;\ge\; \frac{1}{\eta} g_{\min} |\{x \in \ell \,:\, \mathrm{dist}(Q(x), \mathcal{N}) \le \delta\} \cap \{x \in \ell \,:\, |Q - Q_\infty| \ge \mathfrak{a}\sqrt{\delta}\}|.$$

In view of Proposition 3.2.1, it holds that $|\ell \setminus \{\mathrm{dist}(Q,\mathcal{N}) \geq \delta/2\}| \leq C\xi^2/\eta^2$. Furthermore, a straightforward calculation shows that if $|n_3(Q)| \leq 1 - 2\frac{5}{4\sqrt{2}s_*}\mathfrak{a}\sqrt{\delta}$, then $|Q - Q_\infty| \geq \mathfrak{a}\sqrt{\delta}$. Hence,

$$K \;\geq\; \frac{1}{\eta} g_{\min} \left| \left\{ x \in \ell \,:\, |n_3(Q(x))| \leq 1 - 2\frac{5}{4\sqrt{2}s_*}\mathfrak{a}\sqrt{\delta} \right\} \right| - C\frac{\xi^2}{\eta^2} - C\frac{K}{\gamma_2\delta}\xi^2\,,$$

from which the claims follow for $\mathfrak{C} := 2\frac{5}{4\sqrt{2}s_*}\mathfrak{a}$ and $I_\delta := \{x \in \ell \,:\, |n_3(Q(x))| \geq 1 - \mathfrak{C}\sqrt{\delta}\}$. □

In the following two sections, we detail how Lemma 3.5.2 combined with Lemma 3.5.3 can be applied in the case of $T \llcorner \Omega$ and on the surface $\mathcal{M}$.

3.5.1 Blow up

We define the measure $\mu_{\eta,\xi}(U) := \eta\mathcal{E}_{\eta,\xi}(Q_{\eta,\xi}, U)$ for any open set U. Since the energy $\eta\mathcal{E}_{\eta,\xi}(Q_{\eta,\xi})$ is bounded, the measure $\mu_{\eta,\xi}$ converges (up to extracting a subsequence) weakly* to a measure μ.

Lemma 3.5.4. *For $\mathcal{H}^2-$a.e. point of rectifiability $x_0 \in \Omega$ of T it holds that*

$$\frac{\mathrm{d}\mu}{\mathrm{d}\mu_T}(x_0) \;\geq\; 2\, I_\alpha(0,\infty,0,1)\,. \tag{3.47}$$

Proof. Step 1: Notation and preliminaries. Recall that for a point of rectifiability $x_0 \in \mathrm{rect}(T)$ it holds

$$\lim_{r\to 0} \frac{\mu_T(B_r(x_0))}{\pi r^2} \;=\; \lim_{r\to 0} \frac{\mathcal{H}^2(\mathrm{rect}(T) \cap B_r(x_0))}{\pi r^2} \;=\; 1\,.$$

We note that for $\mathcal{H}^2-$a.e. point $x_0 \in \mathrm{rect}(T)$ there exists the limit

$$\lim_{r\to 0} \frac{\mu(B_r(x_0))}{\pi r^2} =: L\,. \tag{3.48}$$

In the following we assume that $x_0 \in \Omega$ is be a point of rectifiability of T which also satisfies (3.48).

Let $r_0 > 0$ such that $B_{r_0}(x_0) \subset \Omega$. Next, we introduce some notation. Let $\Phi_r(x) := (x - x_0)/r$ be a rescaling and define $T_r := (\Phi_r)_\# T$. Note that $\Phi_r(B_r(x_0)) = B_1(0) =: B_1$. The rectifiability ensures that there exists a unit vector $\nu \in \mathbb{S}^2$ such that

$$\mathbb{F}\left(T_r \llcorner B_1 - P_\nu \llcorner B_1\right) \to 0 \quad \text{ for } r \to 0\,, \tag{3.49}$$

where $P_\nu = \{\nu\}^\perp$ is the two dimensional plane perpendicular to ν passing through 0. Indeed, by Theorem 10.2 in [117] we know that $(T_{r_k} - x_0)/r_k^2$ approaches P_ν in a weak sense and by Theorem 31.2 in [149] we get the equivalence between the weak convergence and convergence in the $\mathbb{F}-$norm in our case of T having integer coefficients and $T, \partial T$ being of bounded mass.

Since $\mu_{\eta,\xi} \rightharpoonup \mu$ and $T_{\eta,\xi} \to T$ w.r.t. the flat norm for $\eta, \xi \to 0$, it holds for almost every r that

$$\begin{aligned} \mu_{\eta,\xi}(B_r(x_0)) &\to \mu(B_r(x_0)) \\ \mathbb{F}((T_{\eta,\xi} - T) \llcorner B_r(x_0)) &\to 0\,. \end{aligned} \tag{3.50}$$

We further choose a sequence $(r_k)_{k\in\mathbb{N}}$ converging to zero as $k \to \infty$ such that (3.50) holds for each r_k and

$$\left| \frac{\mu(B_r(x_0))}{\mathbb{M}(T \llcorner B_r(x_0))} - L \right| + \mathbb{F}(T_{r_k} \llcorner B_1 - P_\nu \llcorner B_1) \leq \frac{1}{k}\,. \tag{3.51}$$

Given the sequence r_k, we can extract a subsequence ξ_k, η_k such that $\eta_k/r_k \leq \frac{1}{k}$ and

$$\mathbb{F}((\Phi_{r_k})_\# T_{\eta_k,\xi_k} \llcorner B_1 - T_{r_k} \llcorner B_1) + \left| \frac{\mu_{\xi_k,\eta_k}(B_{r_k}(x_0)) - \mu(B_{r_k}(x_0))}{\mathbb{M}(T \llcorner B_{r_k}(0))} \right| \leq \frac{1}{k}\,. \tag{3.52}$$

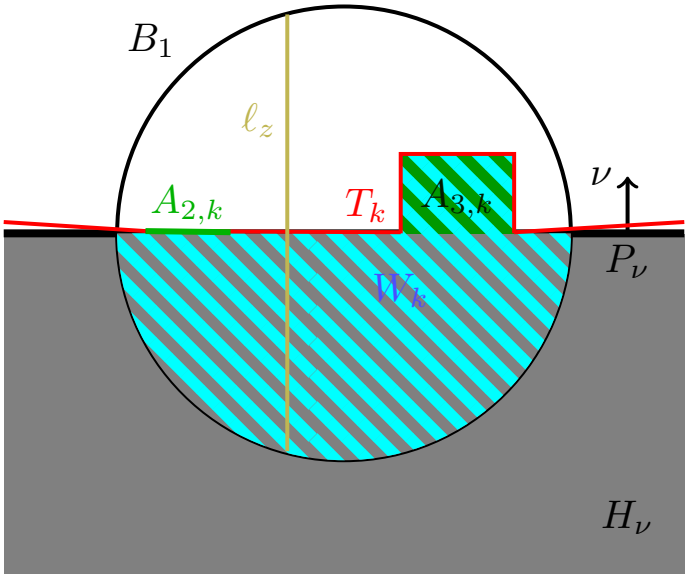

Figure 3.5: Schematic illustration of the quantities involved in Step 2 of the blow up procedure for T.

Step 2: Flat norm convergence. Denote $T_k := ((\Phi_{r_k})_\# T_{\eta_k,\xi_k}) \llcorner B_1$. By (3.49) and (3.52) it follows that $T_k \to P_\nu \llcorner B_1$ in the flat norm. Hence there exist flat chains $A_{2,k} \in \mathcal{F}^2$ and $A_{3,k} \in \mathcal{F}^3$ with $\mathbb{M}(A_{2,k}), \mathbb{M}(A_{3,k}) \to 0$ (for $k \to \infty$) such that

$$T_k - P_\nu \llcorner B_1 = A_{2,k} + \partial A_{3,k}\,. \tag{3.53}$$

This implies that $\partial(T_k - P_\nu \llcorner B_1) = \partial A_{2,k}$ or in other words $\partial(T_k - A_{2,k}) = \partial(P_\nu \llcorner B_1) = 0$ in B_1 since P_ν is the boundary of the half space $H_\nu = \{p + t\nu : p \in P_\nu, t > 0\}$, i.e. $P_\nu \llcorner B_1 = \partial(H_\nu \llcorner B_1)$ in B_1. This implies the existence of a flat chain $W_k \in \mathcal{F}^3(B_1)$ such that $T_k - A_{2,k} = \partial W_k = \partial(1 - W_k)$, where $1 \in \mathcal{F}^3(B_1)$ is the flat chain associated to the set B_1. Note that we can also choose the complement set $W_k^c = 1 - W_k$ since it has the same boundary in B_1. From (3.53) we deduce that

$$\partial(H_\nu \llcorner B_1 - W_k) = P_\nu \llcorner B_1 - A_{2,k} + T_k = \partial A_{3,k}\,.$$

This implies that

$$H_\nu \llcorner B_1 - W_k = A_{3,k} \quad \text{or} \quad H_\nu \llcorner B_1 - W_k^c = A_{3,k}\,.$$

Without loss of generality we choose W_k such that $H_\nu \llcorner B_1 - W_k = A_{3,k}$ and since $\mathbb{M}(A_{3,k}) \to 0$ as $k \to \infty$ we conclude that the symmetric difference $|W_k \Delta (H_\nu \llcorner B_1)|$ also converges to zero for $k \to \infty$.

Step 3: One dimensional estimates. For $z \in P_\nu$ we define the line $\ell_z := \{z + t\nu : t \in \mathbb{R} \text{ and } z + t\nu \in B_1\}$.

From Step 2 we recall that $|W_k \Delta (H_\nu \llcorner B_1)|, \mathbb{M}(A_{2,k}) \to 0$ as $k \to \infty$. This implies that for a subsequence (not relabelled) and almost all $z \in P_\nu$

$$|W_k \Delta (H_\nu \cap \ell_z)|, \mathcal{H}^0(A_{2,k} \cap \ell_z) \to 0 \quad \text{for } k \to \infty \tag{3.54}$$

and hence for k large enough ℓ_z crosses $T_k = \partial W_k + A_{2,k}$.

The energy in $B_{r_k}(x_0)$ can be expressed as

$$\frac{\mu_{\eta_k\xi_k}(B_{r_k}(0))}{\pi r_k^2} = \frac{1}{\pi}\int_{B_1(0)} \frac{\eta_k}{2r_k}|\nabla Q_k|^2 + \frac{r_k}{\eta_k}g(Q_k) + \frac{\eta_k r_k}{\xi_k^2}f(Q_k) + \eta r_k C_0 \,\mathrm{d}y \tag{3.55}$$

$$\geq \frac{1}{\pi}\int_{P_\nu\cap B_1}\int_{\ell_z} \frac{\eta_k'}{2}|\partial_t Q_k|^2 + \frac{1}{\eta_k'}g(Q_k) + \frac{\eta_k'}{(\xi_k')^2}f(Q_k) + \eta_k' C_0' \,\mathrm{d}t\,\mathrm{d}z\,. \tag{3.56}$$

where we introduced the notation $\eta_k' := \frac{\eta_k}{r_k}$ and $\xi_k' := \frac{\xi_k}{r_k}$ and $C_0' = C_0(\xi_k', \eta_k')$. Note that $\eta_k'/\xi_k' = \eta_k/\xi_k$.

This implies that by Fatou's lemma

$$L \;\geq\; \frac{1}{\pi}\int_{P_\nu\cap B_1} \liminf_{k\to\infty}\int_{\ell_z} \frac{\eta_k'}{2}|\partial_t Q_k|^2 + \frac{1}{\eta_k}g(Q_k) + \frac{\eta_k'}{(\xi_k')^2}f(Q_k) + \eta_k' C_0' \,\mathrm{d}t\,\mathrm{d}z\,.$$

In view of (3.47) that we want to prove, we can restrict ourselves even further to the lines ℓ_z with

$$\liminf_{k\to\infty}\int_{\ell_z} \frac{\eta_k'}{2}|\partial_t Q_k|^2 + \frac{1}{\eta_k'}g(Q_k) + \frac{\eta_k'}{(\xi_k')^2}f(Q_k) + \eta_k' C_0' \,\mathrm{d}t \;\leq\; 2I_\alpha(0,\infty,0,1)\,, \tag{3.57}$$

otherwise there is nothing to prove. By choosing another subsequence (which depends on z), we can assume this liminf is a limit and therefore that the sequence is bounded.

Using the inequality $A^2 + B^2 \geq 2AB$, the bound (3.57) implies that

$$\begin{aligned} 2I_\alpha(0,\infty,0,1) \;&\geq\; 2\int_{\ell_z}|\partial_t Q_k|\sqrt{\left(\frac{\eta_k'}{\xi_k'}\right)^2 f(Q_k) + g(Q_k) + C_0'}\,\mathrm{d}t \\ &\geq\; 2\gamma_2\frac{\eta_k'}{\xi_k'}\int_{\ell_z}|\partial_t Q_k|\mathrm{dist}(Q_k,\mathcal{N}_{\eta_k',\xi_k'})\,\mathrm{d}t\,, \end{aligned}$$

where we also used (3.10) of Proposition 3.2.1 in the last inequality. Denoting $m := \min_{\ell_z}\mathrm{dist}(Q_k,\mathcal{N}_{\eta_k,\xi_k})$ and $M := \max_{\ell_z}\mathrm{dist}(Q_k,\mathcal{N}_{\eta_k,\xi_k})$ we can estimate the energy necessary for switching from $(M+m)/2$ to M by

$$2I_\alpha(0,\infty,0,1) \;\geq\; 2\gamma_2\frac{\eta_k'}{\xi_k'}\frac{M+m}{2}\int_{\ell_z}|\partial_t Q_k|\,\mathrm{d}t \;\geq\; \frac{\gamma_2}{2}\frac{\eta_k'}{\xi_k'}(M^2-m^2)\,. \tag{3.58}$$

In order to obtain a uniform convergence of $\mathrm{dist}(Q_k,\mathcal{N}_{\eta_k,\xi_k})$, it remains to estimate m.

Again from (3.57) by using (3.10) in Proposition 3.2.1, we get that

$$2I_\alpha(0,\infty,0,1) \;\geq\; \gamma_2\frac{\eta_k'}{(\xi_k')^2}\int_{\ell_z}\mathrm{dist}^2(Q_k,\mathcal{N}_{\eta_k',\xi_k'})\,\mathrm{d}t \;\geq\; \gamma_2\frac{\eta_k'}{(\xi_k')^2}|\ell_z|m^2\,.$$

In other words, $m^2 \leq \frac{2I_\alpha(0,\infty,0,1)}{\gamma_2|\ell_z|}\frac{(\xi_k')^2}{\eta_k'}$. Plugging this estimate into (3.58) yields

$$\sup_{\ell_z}\mathrm{dist}^2(Q_k,\mathcal{N}_{\eta_k',\xi_k'}) \;=\; M^2 \;\leq\; \frac{4I_\alpha(0,\infty,0,1)}{\gamma_2}\left(\frac{\xi_k'}{\eta_k'} + \frac{(\xi_k')^2}{|\ell_z|\eta_k'}\right). \tag{3.59}$$

In view of (3.11) of Proposition 3.2.1 we can conclude that Q_k is uniformly close to $\mathcal{N}$ and converges to zero as $\xi_k', \eta_k' \to 0$.

This implies together with the convergences in (3.54) that there exists a sequence $t_k \to 0$ such that $n_3(Q_k - Y_k)(z + t_k\nu) = 0$, where $Q_k(y) := Q_{\eta_k,\xi_k}(x_0 + r_k y)$ and $Y_k := Y_{\eta_k,\xi_k}$.

We now split ℓ_z into $\ell_z^\pm$, where $\ell_z^+ := \{z + t\nu \in \ell \,:\, t \geq t_k\}$ and $\ell_z^- := \{z + t\nu \in \ell \,:\, t \leq t_k\}$ and show that on both rays there are points for which Q_k is close to Q_∞.

Applying Lemma 3.5.3 for $\delta > 0$ with the bound in (3.57) implies that for k large enough there exists $t_k^+ \in (t_k, 1)$ such that $|n_3(Q_k(t_k^+) - Y_k)| > 1 - \mathfrak{C}\sqrt{\delta}$. The goal is to take $\delta \to 0$. For

this, we choose a sequence δ_k depending on k such that δ_k and $\eta_k'/C_{\delta_k} \leq \frac{1}{k}$ converge to zero as $k \to \infty$, where C_{δ_k} is the constant from Lemma 3.5.3. Similarly, there exists $t_k^- \in (-1, t_k)$ such that $|n_3(Q_k(t_k^-) - Y_k)| > 1 - \mathfrak{C}\sqrt{\delta_k}$.

The final estimate for the integral over ℓ_z then follows by summing the contributions from $\ell_z^\pm$, both in which we pass from $n_3(Q_k - Y_k) = 0$ to $|n_3(Q_k - Y_k)| = 1$. Knowing that Q_k is uniformly close to $\mathcal{N}$, we can apply Lemma 17 in [42], the Lipschitz assumption on g in (3.6) and use the definition of I_α to determine the energetic cost on $\ell_z^\pm$. This yields

$$\begin{aligned}
L \;&\geq\; \liminf_{k\to\infty} \frac{1}{\pi} \int_{P_\nu \cap B_1} \int_{\ell_z} \frac{\eta_k'}{2} |\nabla Q_k|^2 + \frac{1}{\eta_k'} g(Q_k) + \frac{\eta_k'}{(\xi_k')^2} f(Q_k) + \eta_k' C_0' \,\mathrm{d}t \,\mathrm{d}z \\
&\geq\; \frac{1}{\pi} \int_{P_\nu \cap B_1} \liminf_{k\to\infty} \int_{\ell_z} \frac{\eta_k'}{2} |\nabla Q_k|^2 + \frac{1}{\eta_k'} g(Q_k) + \frac{\eta_k'}{(\xi_k')^2} f(Q_k) + \eta_k' C_0' \,\mathrm{d}t \,\mathrm{d}z \\
&\geq\; \frac{1}{\pi} \int_{P_\nu \cap B_1} \liminf_{k\to\infty} \int_{\ell_z} \frac{\eta_k'}{2} (1 - C\|Q_k - \mathcal{R}(Q_k)\|_{L^\infty(\ell_z)}) |\nabla \mathcal{R}(Q_k)|^2 \\
&\qquad\qquad + \frac{1}{\eta_k'} g(\mathcal{R}(Q_k)) - C|Q_k - \mathcal{R}(Q_k)| \,\mathrm{d}t \,\mathrm{d}z \\
&\geq\; \frac{1}{\pi} \int_{P_\nu \cap B_1} 2 I_\alpha(0, \infty, 0, 1) \,\mathrm{d}z \\
&\geq\; 2\, I_\alpha(0, \infty, 0, 1)\,.
\end{aligned} \tag{3.60}$$

□

3.5.2 Surface energy

In this section we do the necessary calculations to find the announced energy contribution on $\mathcal{M}$. For this, we estimate the energy in a boundary layer around $\mathcal{M}$. More precisely, we define $\mathcal{M}_{\sqrt{\eta}} := \{x \in \Omega : \mathrm{dist}(x, \mathcal{M}) \leq \sqrt{\eta}\}$. Then we proceed similarly to the previous section, the goal is to apply Lemma 3.5.2 to the rays perpendicular to $\mathcal{M}$ on which $Q_{\eta,\xi,n}$ is taking values close to $\mathcal{N}$.

We assume η small enough such that $\sqrt{\eta} < \frac{1}{2}\mathbf{r}_0$, where $\mathbf{r}_0$ was fixed in the beginning of Section 3.4 such that $\mathbf{r}_0$ is smaller than the minimal curvature radius of $\mathcal{M}$. For $\omega \in \mathcal{M}$ and $r > 0$ we define

$$L_{\omega,r} \;:=\; \{\omega + t\nu(\Omega) \;:\; t \in [0, r]\}\,. \tag{3.61}$$

We now rewrite the energy so that the line integrals over $L_{\omega,\sqrt{\eta}}$ appear. We note that for $0 < \eta \ll 1$ the map $\mathcal{M} \times [0, \sqrt{\eta}] \to \Omega$ given by $(\omega, r) \mapsto \omega + r\nu(\omega)$ is injective. The differential of this map is given by $\mathrm{Id}_{T_\omega \mathcal{M}} + r\,\mathrm{d}_\omega \nu + \nu$. Using the normalized eigenvectors $\nu, \overline{\omega_1}, \overline{\omega_2}$ corresponding to the eigenvalues $1, \kappa_1, \kappa_2$ with κ_i being the principal curvatures of $\mathcal{M}$ at ω, i.e. the eigenvalues of the Gauss map $\mathrm{d}_\omega \nu$. Then

$$\det(\mathrm{Id} + r\,\mathrm{d}_\omega \nu(\omega)) = (1 + r\kappa_1)(1 + r\kappa_2)$$

and the gradient transforms as

$$|\nabla Q_{\eta,\xi,n}|^2 = |\partial_r Q_{\eta,\xi,n}|^2 + \frac{1}{|1 + r|\kappa_1||^2} |\partial_{\overline{\omega_1}} Q_{\eta,\xi,n}|^2 + \frac{1}{|1 + r|\kappa_2||^2} |\partial_{\overline{\omega_2}} Q_{\eta,\xi,n}|^2\,.$$

In order to shorten our formulas, we still use the notation $\nabla Q_{\eta,\xi,n}$. The energy can then be rewritten as

$$\mathcal{E}_{\eta,\xi}(Q_{\eta,\xi,n}, \mathcal{M}_{\sqrt{\eta}}) \;=\; \int_{\mathcal{M}} \int_0^{\sqrt{\eta}} \left(\frac{1}{2} |\nabla Q_{\eta,\xi,n}|^2 + \frac{1}{\xi^2} f(Q_{\eta,\xi,n}) + \frac{1}{\eta^2} g(Q_{\eta,\xi,n}) \right) \prod_{i=1}^{2} (1 + r\kappa_i) \,\mathrm{d}r \,\mathrm{d}\omega\,.$$

We now distinguish two cases depending on whether the ray $L_{\omega,\sqrt{\eta}}$ intersects $T_{\eta,\xi,n}$ or not.

Case 1: $L_{\omega,\sqrt{\eta}}$ does not intersect $T_{\eta,\xi,n}$. In this case we can assume that

$$\int_0^{\sqrt{\eta}} \left(\frac{1}{2}|\nabla Q_{\eta,\xi,n}|^2 + \frac{1}{\xi^2} f(Q_{\eta,\xi,n}) + \frac{1}{\eta^2} g(Q_{\eta,\xi,n})\right) \prod_{i=1}^{2}(1+r\kappa_i)\,\mathrm{d}r \;\leq\; I_\alpha(0,\infty,1,\cos(\theta))\,,$$

otherwise there is nothing to prove. With the same argument as in (3.57)-(3.59) we can show that $\sup_{L_{\omega,\sqrt{\eta}}} \mathrm{dist}(Q_{\eta,\xi,n}, \mathcal{N}_{\eta,\xi})$ converges to zero as $\xi,\eta \to 0$. Analogously to the blow up procedure, for $\delta > 0$ we use Lemma 3.5.3 to deduce that there exists a radius $t_\omega \in [0,\sqrt{\eta}]$ such that $|n_3(Q_{\eta,\xi,n})(\omega + t_\omega \nu(\omega))| \geq 1 - \mathfrak{C}\sqrt{\delta}$. We choose a sequence $\delta_\eta \to 0$ such that $\eta/C_{\delta_\eta} \to 0$ as $\eta \to 0$. Note that $Q_{\eta,\xi,n}$ does not verify the boundary condition (3.14), but a slightly perturbed version. For $\eta,\xi \to 0$ we still obtain the right energy thanks to Proposition 3.4.2 and the uniform convergence therein. As in (3.60) we then obtain

$$\begin{aligned}
&\liminf_{\eta,\xi\to 0} \int_{L_{\omega,\sqrt{\eta}}} \frac{\eta}{2}|\nabla Q_{\eta,\xi,n}|^2 + \frac{1}{\eta} g(Q_{\eta,\xi,n}) + \frac{\eta_k}{\xi^2} f(Q_{\eta,\xi,n}) + \eta C_0'\,\mathrm{d}t \\
&\quad\geq\; \liminf_{\eta,\xi\to 0} \int_{L_{\omega,\sqrt{\eta}}} \frac{\eta}{2}(1 - C\|Q_k - \mathcal{R}(Q_k)\|_{L^\infty(\ell_z)})|\nabla \mathcal{R}(Q_{\eta,\xi,n})|^2 \\
&\qquad\qquad + \frac{1}{\eta} g(\mathcal{R}(Q_{\eta,\xi,n})) - C|Q_{\eta,\xi,n} - \mathcal{R}(Q_{\eta,\xi,n})|\,\mathrm{d}t \\
&\quad\geq\; I(0,\infty,1,|\cos(\theta)|)\,.
\end{aligned} \tag{3.62}$$

Case 2: $L_{\omega,\sqrt{\eta}}$ intersects $T_{\eta,\xi,n}$. Let $t'_\omega \in (0,\sqrt{\eta})$ denote the radius of intersection between $L_{\omega,\sqrt{\eta}}$ and $T_{\eta,\xi,n}$. The only difference to Case 1 is that we estimate the two parts $t \leq t'_\omega$ and $t \geq t'_\omega$ separately.

With the same reasoning as before we can assume that the energy on the ray is bounded and that $\mathrm{dist}(Q_{\eta,\xi,n}, \mathcal{N}_{\eta,\xi})$ is uniformly converging to zero on the ray. On L_{ω,t'_ω} we obtain just like in Step 1 the estimate

$$\liminf_{\eta,\xi\to 0} \int_{L_{\omega,t'_\omega}} \frac{\eta}{2}|\nabla Q_{\eta,\xi,n}|^2 + \frac{1}{\eta} g(Q_{\eta,\xi,n}) + \frac{\eta_k}{\xi^2} f(Q_{\eta,\xi,n}) + \eta C_0'\,\mathrm{d}t \;\geq\; I_\alpha(0,\infty,\cos(\theta),0)\,. \tag{3.63}$$

On the remaining part of the ray $L_{\omega,\sqrt{\eta}}$ we want to find the energy $I_\alpha(0,\infty,1,0)$. Since t'_ω might be arbitrarily close to $\sqrt{\eta}$, we cannot apply Lemma 3.5.3 to conclude that $n_3(Q_{\eta,\xi,n})$ is close to ± 1 somewhere. Extending the ray up to a distance $t = 2\sqrt{\eta}$ from $\mathcal{M}$ and repeating the above reasoning, we can find for $\delta > 0$ and η small enough $t_\omega \in [\sqrt{\eta}, 2\sqrt{\eta}]$ such that $|n_3(Q_{\eta,\xi,n})(\omega + t_\omega\nu(\omega))| \geq 1 - \mathfrak{C}\sqrt{\delta}$. Now we proceed again as in (3.62) and combine with (3.63) to obtain

$$\begin{aligned}
&\liminf_{\eta,\xi\to 0} \int_{L_{\omega,2\sqrt{\eta}}} \frac{\eta}{2}|\nabla Q_{\eta,\xi,n}|^2 + \frac{1}{\eta} g(Q_{\eta,\xi,n}) + \frac{\eta_k}{\xi^2} f(Q_{\eta,\xi,n}) + \eta C_0'\,\mathrm{d}t \\
&\qquad\geq\; I_\alpha(0,\infty,\cos(\theta),0) + I_\alpha(0,\infty,1,0)\,.
\end{aligned} \tag{3.64}$$

3.5.3 Proof of compactness and lower bound

We now need to combine the estimates (3.42), (3.47), (3.62) and (3.64). To this aim, we use the localization technique for $\Gamma-$convergence as described for example in [33, Ch. 16]. Let U_i, $i = 1,2,3$ be three pairwise disjoint sets open in $\overline{\Omega}$. Then it holds that

$$\begin{aligned}
\liminf_{\eta,\xi\to 0} \eta\,\mathcal{E}_{\eta,\xi}(Q_{\eta,\xi}) \;&\geq\; \liminf_{\eta,\xi\to 0} \sum_{i=1}^{3} \eta\,\mathcal{E}_{\eta,\xi}(Q_{\eta,\xi}, U_i) \;\geq\; \sum_{i=1}^{3} \liminf_{\eta,\xi\to 0} \eta\,\mathcal{E}_{\eta,\xi}(Q_{\eta,\xi}, U_i) \\
&\geq\; \frac{\pi}{2} s_*^2 \beta\, \mathbb{M}(S \llcorner U_1) + 2I_\alpha(0,\infty,1,0)\mathbb{M}(T \llcorner (\Omega \cap U_2)) \\
&\quad + \int_{\mathcal{M}} I(0,\infty,1,|\cos(\theta)|)\,\mathrm{d}\mu_{(1-T\llcorner\mathcal{M})\llcorner U_3} \\
&\quad + \int_{\mathcal{M}} I_\alpha(0,\infty,1,0) + I_\alpha(0,\infty,\cos(\theta),0)\,\mathrm{d}\mu_{T\llcorner(\mathcal{M}\cap U_3)}\,.
\end{aligned}$$

Since the LHS does not depend on the sets U_i, we can take the supremum over all pairwise disjoint open sets. For $\epsilon > 0$ and by inner regularity we can approximate the measure $\mathbb{M}(S)$ by a compact set $A_{1,\epsilon} \subset \mathrm{rect}(S)$ and an open set $U_{1,\epsilon} \supset A_{2,\epsilon}$ such that $\mathbb{M}(S) - \mathbb{M}(S \llcorner A_{1,\epsilon}) \leq \epsilon$, $\mathcal{H}^2(\mathcal{M} \cap \overline{U_{1,\epsilon}}) \leq \epsilon/2$ and $\mathbb{M}(T \llcorner \overline{U_{1,\epsilon}}) \leq \epsilon/2$ since the measures μ_S and μ_T are mutually singular. Furthermore, we find another compact set $A_{2,\epsilon} \subset (\mathrm{rect}(T) \cap \Omega) \setminus U_{1,\epsilon}$ such that $\mathbb{M}(T \llcorner \Omega) - \mathbb{M}(T \llcorner A_{2,\epsilon}) \leq \epsilon$. Then, by construction there exists an open set $U_{2,\epsilon} \supset A_{2,\epsilon}$ such that $U_{2,\epsilon} \cap U_{1,\epsilon} = \emptyset$ and $\mathrm{dist}(\mathcal{M}, U_{2,\epsilon}) > 0$. Finally, taking an open neighbourhood of $\mathcal{M}$ disjoint from $\overline{U_{2,\epsilon}}$ and removing $\overline{U_{1,\epsilon}}$ from it, we find a third open set $U_{3,\epsilon}$ which satisfies $\mathcal{H}^2(\mathcal{M} \setminus U_{3,\epsilon}) \leq \epsilon$. By monotonicity we then find

$$\begin{aligned}
\liminf_{\eta,\xi \to 0} \eta\, \mathcal{E}_{\eta,\xi}(Q_{\eta,\xi}) \;\geq\; & \sup_{U_1,U_2,U_3} \frac{\pi}{2} s_*^2 \beta\, \mathbb{M}(S \llcorner U_1) + 2I_\alpha(0,\infty,1,0)\mathbb{M}(T \llcorner (\Omega \cap U_2)) \\
& + \int_{\mathcal{M}} I(0,\infty,1,|\cos(\theta)|)\, \mathrm{d}\mu_{(1-T\llcorner\mathcal{M})\llcorner U_3} \\
& + \int_{\mathcal{M}} I_\alpha(0,\infty,1,0) + I_\alpha(0,\infty,\cos(\theta),0)\, \mathrm{d}\mu_{T\llcorner(\mathcal{M}\cap U_3)} \\
\geq\; & 2I_\alpha(0,\infty,1,0)\mathbb{M}(T \llcorner \Omega) + \frac{\pi}{2} s_*^2 \beta\, \mathbb{M}(S) \\
& + \int_{\mathcal{M}} I(0,\infty,1,|\cos(\theta)|)\, \mathrm{d}\mu_{(1-T\llcorner\mathcal{M})} \\
& + \int_{\mathcal{M}} I_\alpha(0,\infty,1,0) + I_\alpha(0,\infty,\cos(\theta),0)\, \mathrm{d}\mu_{T\llcorner\mathcal{M}}\,.
\end{aligned} \tag{3.65}$$

We now want to pass to the limit $\alpha \to 0$. In order to mark the dependence of T and S on α, we add the index α in our notation for the rest of the proof. Since $I_\alpha(0,\infty,1,0) \geq s_* c_* > 0$, the mass of $T_\alpha \llcorner \Omega$ is bounded uniformly in α and since $\mathcal{M}$ has finite surface area it follows that $\mathbb{M}(T_\alpha)$ is bounded independent of α. Since the mass of S_α and the length of the curves Γ_α are also uniformly bounded, we conclude that the flat chains T_α as well as their boundaries $\partial T_\alpha = S_\alpha + \Gamma_\alpha$ have finite mass. Choosing a sequence $\alpha_k \to 0$, (3.65) holds and we can apply the compactness theorem for flat chains [67, Cor. 7.5] as stated in Subsection 3.2.2. From this we get that there exists a subsequence (not relabelled) and flat chains $T \in \mathcal{F}^2$, $S \in \mathcal{F}^2$ such that $\mathbb{F}(T_{\alpha_k} - T) \to 0$ and $\mathbb{F}(S_{\alpha_k} - S) \to 0$ as $k \to \infty$. Since boundaries are preserved under flat convergence and $\Gamma_\alpha \to \Gamma$ uniformly, it holds that $\partial T = S + \Gamma$. We note that $I_{\alpha_k}(0,\infty,\pm 1,0) \to I(0,\infty,\pm 1,0)$, and $I_{\alpha_k}(0,\infty,\cos(\theta),0) \to I(0,\infty,\cos(\theta),0)$ as $\alpha_k \to 0$. Passing to the limit $\alpha_k \to 0$ in (3.65) thus yields

$$\begin{aligned}
\liminf_{\eta,\xi \to 0} \eta\, \mathcal{E}_{\eta,\xi}(Q_{\eta,\xi}) \;\geq\; & 2I(0,\infty,1,0)\mathbb{M}(T \llcorner \Omega) + \frac{\pi}{2} s_*^2 \beta\, \mathbb{M}(S) \\
& + \int_{\mathcal{M}} I(0,\infty,1,|\cos(\theta)|)\, \mathrm{d}\mu_{(1-T\llcorner\mathcal{M})} \\
& + \int_{\mathcal{M}} I(0,\infty,1,0) + I(0,\infty,\cos(\theta),0)\, \mathrm{d}\mu_{T\llcorner\mathcal{M}} \\
=\; & 4s_* c_* \mathbb{M}(T \llcorner \Omega) + \frac{\pi}{2} s_*^2 \beta\, \mathbb{M}(S) \\
& + 2s_* c_* \int_{\mathcal{M}} (1 - |\cos(\theta)|)\, \mathrm{d}\omega + 4s_* c_* \int_{\mathcal{M}} |\cos(\theta)|\, \mathrm{d}\mu_{T\llcorner\mathcal{M}}\,.
\end{aligned} \tag{3.66}$$

Combining the compactness result from Subsection 3.4.5 for fixed α with the above estimates, we can choose a diagonal sequence $\alpha_{k(\xi,\eta)} \to 0$ as $\eta, \xi \to 0$ such that

$$\lim_{\eta,\xi \to 0} \mathbb{F}(T_{\eta,\xi,n,\alpha_{k(\xi,\eta)}} - T) = 0 \qquad \lim_{\eta,\xi \to 0} \mathbb{F}(S_{\eta,\xi,n,\alpha_{k(\xi,\eta)}} - S) = 0$$

and (3.66) holds.

It remains to verify that $\partial T = S + \Gamma$ as claimed by Theorem 3.3.1. We recall from the boundary condition (3.14) that

$$Q_{\eta,\xi}(\omega) \;=\; Q_b(\omega) = s_* \left(\nu(\omega) \otimes \nu(\omega) - \frac{1}{3}\mathrm{Id} \right) \qquad \text{for all } \omega \in \mathcal{M}\,.$$

This implies that on Γ

$$n_3(Q_{\eta,\xi}(\omega)) = n_3(Q_b(\omega)) = \nu_3(\omega) = 0\,. \tag{3.67}$$

by definition. Furthermore, we assumed that the derivative of ν_3 on Γ is non-degenerate, i.e. $\nabla_\omega \nu_3(\omega) \neq 0$ for all $\omega \in \Gamma$. Hence, on Γ it holds

$$\nabla_\omega n_3(Q_{\eta,\xi}(\omega)) \;=\; \nabla_\omega \nu_3(\omega) \;\neq\; 0\,. \tag{3.68}$$

Next, we consider the function $F(\omega, n, Y) \;:=\; n_3(Q_{\eta,\xi,n}(\omega) + Y)$ for $n \in \mathbb{N}$ and $Y \in B_\alpha(0) \subset \mathrm{Sym}_0$ for $0 < \alpha \ll 1$. Note that we can rewrite

$$\begin{aligned} F(\omega, n, Y) \;&=\; n_3(Q_{\eta,\xi}(\omega) + (Q_{\eta,\xi,n}(\omega) - Q_{\eta,\xi}(\omega)) + Y) \\ &=\; n_3(Q_b(\omega) + (Q_{\eta,\xi,n}(\omega) - Q_{\eta,\xi}(\omega)) + Y)\,. \end{aligned}$$

Since on $\mathcal{M}$, $Q_{\eta,\xi,n}$ is by construction an approximation by convolution of Q_b, it holds that $Q_{\eta,\xi,n} \to Q_b$ in C^1 on $\mathcal{M}$ for $n \to 0$. In other words, from (3.67) we get that $F(\omega, \infty, 0) = 0$.

For the rest of the proof we argue locally on $\mathcal{M}$. Let (u, v) be a local parametrization on $\mathcal{M}$ such that ∇u is parallel to Γ and ∇v is in direction of the normal vector of the curve Γ, called ν_Γ. We can choose (u, v) such that $\omega_0 = (u(0), v(0)) \in \Gamma$ and $(u, v(0))$ locally parametrizes Γ. Then

$$\begin{aligned} \partial_v F(\omega, n, Y)|_{\omega_0,\infty,0} \;&=\; \partial_v F((u, v), n, Y)|_{(0,0),\infty,0} \\ &=\; Dn_3(Q_b(\omega_0))(\partial_v Q_b(\omega_0) + \partial_v(Q_{\eta,\xi,n}(\omega) - Q_{\eta,\xi}(\omega)))\,. \end{aligned}$$

For n large enough we can assume that $\|Dn_3\|_{C^0(\mathcal{N})}\|Q_{\eta,\xi,n} - Q_{\eta,\xi}\|_{C^1(\mathcal{M})} \leq \frac{1}{2}\inf_\omega |\partial_v n_3(Q_b(\omega))|$ by Proposition 3.4.2. Since $Dn_3(Q_b(\omega_0))\partial_v Q_b(\omega_0) = \partial_v n_3(Q_b(\omega))|_{\omega=\omega_0}$ it follows from (3.68) that $\partial_v F(\omega, n, Y)|_{\omega_0,\infty,0} \neq 0$.

The assumptions of the implicit function theorem are therefore satisfied and there exists an open neighbourhood V of $(u(0), \infty, 0)$ and a function $\tilde{v}$ defined on V such that $F((u, \tilde{v}(u, n, Y)), n, Y) = 0$ on V. In other words,

$$0 \;=\; F((u, \tilde{v}(u, n, Y)), n, Y) \;=\; n_3(Q_{\eta,\xi,n}((u, \tilde{v}(u, n, Y))) + Y)$$

So $(u, \tilde{v}(u, n, Y))$ serves as a local parametrization of the set $\Gamma_{n,Y} := \{\omega \in \mathcal{M} : n_3(Q_{\eta,\xi,n}(\omega) + Y) = 0\}$. Noting that $\mathcal{M}$ is of class C^2 and hence $\nu \in C^1$, it holds that $\tilde{v}$ and $\Gamma_{n,Y}$ are also of class C^1 and in particular $\Gamma_{n,Y}$ has finite length.

Since $\tilde{v} \to 0$ uniformly as $n \to \infty$ and $Y \to 0$, it holds that $n_3(Q_{\eta,\xi,n} + Y)$ also uniformly converges to $n_3(Q_b)$. By Theorem 3.3 in [51] it follows the Hausdorff convergence of $\Gamma_{n,Y}$ to Γ, i.e.

$$\mathrm{dist}_{\mathcal{H}}(\Gamma, \Gamma_{n,Y}) \;:=\; \max\left\{\sup_{\omega\in\Gamma} \mathrm{dist}(\omega, \Gamma_{n,Y}),\; \sup_{\omega'\in\Gamma_{n,Y}} \mathrm{dist}(\omega', \Gamma)\right\} \to 0 \text{ for } n \to \infty \text{ and } Y \to 0\,.$$

Using the parametrization $\tilde{v}$ to link Γ to $\Gamma_{n,Y}$, we can also build a flat 2−chain $G_{n,Y}$ with boundary $\partial G_{n,Y} = \Gamma - \Gamma_{n,Y}$. It then holds

$$\mathbb{F}(\Gamma - \Gamma_{n,Y}) \;\leq\; \mathbb{M}(G_{n,Y}) \;\leq\; \sup_{(\omega,m,Z)\in V} \mathcal{H}^1(\Gamma_{m,Z})\,\mathrm{dist}_{\mathcal{H}}(\Gamma, \Gamma_{n,Y})\,.$$

3.6 Upper bound

This section is devoted to the construction of the recovery sequence of Theorem 3.3.1. Essentially, there are three steps in this construction:

1. We approximate T by a sequence T_n, solution to a minimization problem. The advantage of replacing T by T_n is the gain of regularity. Indeed, as we will see in Subsection 3.6.1, T and its boundary inside Ω will be of class $C^{1,1}$. Furthermore, by a comparison argument, we can show that $\partial(T_n \llcorner \mathcal{M})$ is a line of finite length.

2. We introduce local coordinate systems in which we can define $Q_{\eta,\xi,n}$ and estimate its energy.
3. Choosing a diagonal sequence $n(\xi,\eta)$ we find the recovery sequence.

3.6.1 A first regularity result for (almost) minimizers

In this subsection, we rewrite the limit energy $\mathcal{E}_0$ in a way that it only depends on T:

$$\mathcal{E}_0(T) \;=\; E_0(\mathcal{M},\mathbf{e}_3) + 4s_*c_* \int_{\mathcal{M}} |\cos(\theta)|\, \mathrm{d}\mu_{T\llcorner\mathcal{M}} + 4s_*c_*\mathbb{M}(T\llcorner\Omega) + \frac{\pi}{2}s_*^2\beta\mathbb{M}(\partial T - \Gamma)\,, \quad (3.69)$$

where $\Gamma \in \mathcal{F}^1$ is given by the curve $\{\nu_3 = 0\} \subset \mathcal{M}$. For the approximation of a flat chain $T \in \mathcal{F}^2$ we are going to study the following minimization problem:

$$\min_{\tilde{T}\in\mathcal{F}^2} \mathcal{E}_0(\tilde{T}) + n\,\mathbb{F}(\tilde{T} - T)\,, \quad (3.70)$$

for $n \in \mathbb{N}$. The existence of a minimum of (3.70) is imminent since by assumption T verifies $\mathcal{E}_0(T) + n\mathbb{F}(T-T) = \mathcal{E}_0(T) < \infty$, the energy is non-negative and lower semi-continuous with respect to convergence in the flat norm. We have the following result:

Proposition 3.6.1. *Let $T \in \mathcal{F}^2$ with $\mathcal{E}_0(T) < \infty$. For all $n \in \mathbb{N}$, the problem (3.70) has a solution $T_n \in \mathcal{F}^2$. The minimizer T_n verifies*

1. *$T_n \to T$ for $n \to \infty$ in the flat norm.*
2. *$T_n \llcorner \Omega$ is of class C^1 up to the boundary $\partial(T_n \llcorner \Omega)$.*
3. *$(\partial T_n)\llcorner\Omega$ is of class $C^{1,1}$.*

We note that the above Proposition also holds true for $n = 0$, i.e. minimizers of (3.69) and hence of our limit problem are of class C^1 up to the boundary in Ω which is of class C^2. As we will see later, the minimizers of $\mathcal{E}_0$ are in fact smooth (see Proposition 3.7.1). In order to make this subsection more readable and simplify notation, we divide (3.69) by $4s_*c_*$ and redefine the parameter β to replace the constant $\frac{1}{8}\frac{s_*}{c_*}\beta$. Also, we will simply write n instead of $\frac{n}{4c_*s_*}$. Since in this subsection we are only concerned with the regularity of minimizers, this change of notation does not impact our results.

The proof of Proposition 3.6.1 makes use of a series of lemmas which we are going to state and prove first. The main ideas for the regularity of T_n and ∂T_n have already been developed in earlier papers [52,53,129,158], so it remains to check that we can apply them in our case. For the sake of simple notation, we drop the subscript n for the rest of this section and define $S := \partial T - \Gamma$. We recall from Subsection 3.2.2 that $\mathrm{rect}(S)$ is the set of all points of rectifiability of S. In particular, for $x_0 \in \mathrm{rect}(S)$ the density $\lim_{r\to 0}\mu_S(B_r(x_0))/(2r)$ exists and is strictly positive.

Lemma 3.6.2. *It holds that* $\mathrm{supp}\,(S) = \overline{\mathrm{rect}(S)}$ *and* $\mathcal{H}^1(\mathrm{supp}\,(S)\setminus \mathrm{rect}(S)) = 0$.

Proof. Let's show first that S is supported by a closed 1-dimensional set.

For this, we prove that S cannot contain subcycles of arbitrary small length. Assume that S_1 is a subcycle of S, i.e. $\mathbb{M}(S) = \mathbb{M}(S_1) + \mathbb{M}(S - S_1)$ and $\partial S_1 = 0$, and that S_1 is supported in $B_r(x_0)$ for $r \in (0, \frac{1}{2}\mathbf{r}_0)$. By (7.6) in [67], there exists a constant $b > 0$ and $T_1 \in \mathcal{F}^2$ such that $S_1 = \partial T_1$ and $\mathbb{M}(T_1) \le b\mathbb{M}(S_1)^2$. By projecting T_1 onto $B_r(x_0)\cap\overline{\Omega}$, we can furthermore assume that T_1 is supported in $B_r(x_0)$ and lies within $\overline{\Omega}$. Projecting onto $B_r(x_0)$ does not affect the previous estimate since it decreases the mass. Projecting $T_1 \llcorner E$ onto $\mathcal{M}$ has Lipschitz constant less than $1 + 4\frac{r}{\mathbf{r}_0}$ and hence, the estimate stays true with an additional factor of $1 + 4\frac{r}{\mathbf{r}_0}$. We estimate by minimality of T

$$\begin{aligned}
\mathcal{E}_0(T) + n\mathbb{F}(T - T_0) \;&\le\; \mathcal{E}_0(T + T_1) + n\mathbb{F}(T + T_1 - T_0)\\
&\le\; \mathcal{E}_0(T) + \mathbb{M}(T_1) - \beta\mathbb{M}(S_1) + n\mathbb{F}(T - T_0) + n\mathbb{M}(T_1)\\
&\le\; \mathcal{E}_0(T) - \beta\mathbb{M}(S_1) + n\mathbb{F}(T - T_0) + (n+1)(1 + 4\frac{r}{\mathbf{r}_0})b\mathbb{M}(S_1)^2\,,
\end{aligned}$$

and thus $\beta\mathbb{M}(S_1) - b(n+1)(1+4\frac{r}{\mathbf{r}_0})\mathbb{M}(S_1)^2 \leq 0$. We hence find that either $\mathbb{M}(S_1) = 0$ or that $\mathbb{M}(S_1) \geq \beta/(3b(n+1))$.

Now, let x_0 be a point of rectifiability of S and $r \leq \beta/(6b(n+1))$. Assume that $\mu_S(B_r(x_0)) < 2r$. Then, since

$$\int_0^r \mu_S(\partial B_s(x_0))\,\mathrm{d}s \leq \mu_S(B_r(x_0)) < 2r\,,$$

we can evoke Theorem 5.7 of [67] to deduce that there exists a set of positive measure $I \subset [0,r]$ such that $\mu_S(\partial B_s(x_0)) < 2$ for all $s \in I$. Thus, we can find radii $s < r$ such that $\mathbb{M}(\partial(S \llcorner B_s(x_0))) \leq 1$. But a bounded 1-chain cannot have just one end, so that for $S_1 := S \llcorner B_s(x_0)$ we conclude that $\partial S_1 = 0$. In addition $\mathbb{M}(S_1) < 2r$ by assumption. Hence, we have $\mathbb{M}(S_1) < \beta/(3b(n+1))$ and the above calculation shows that necessarily $\mathbb{M}(S_1) = 0$. In particular, x_0 is not in the support of S which is a contradiction.

Let us conclude now that S is indeed a closed set. Let $\mathrm{rect}(S)$ be the rectifiability set of S. Since S has coefficients in a finite group, it is rectifiable [167] with $\mu_S = \mathcal{H}^1 \llcorner \mathrm{rect}(S)$. Now, take a sequence $x_k \in \mathrm{rect}(S)$ and assume $x_k \to x$. By the above reasoning it holds $\mu_S(B_r(x_k)) \geq 2r$ for all $r \leq \beta/(6b(n+1))$ and in the limit $k \to \infty$ also $\mu_S(B_r(x)) \geq 2r$. It follows that $\mu_S(\Omega \setminus \mathrm{rect}(S)) = 0$. From this, Theorem 2.56 in [10] allows us to conclude that $\mathcal{H}^1(\mathrm{supp}\,(S) \setminus \mathrm{rect}(S)) = 0$. □

After having established this basic property of S, we can state a first regularity result:

Lemma 3.6.3. *The flat chain S is supported on a finite union of closed $C^{1,\frac{1}{2}}-$curves.*

Proof. Our goal is to prove that $S \llcorner \Omega$ is an almost minimizer of the length functional $\mathbb{M}$ and apply Theorem 3.8 in [129] to deduce $C^{1,\frac{1}{2}}-$regularity.

Let $x_0 \in \Omega$ and $\overline{r} \in (0, \frac{1}{2}\mathbf{r}_0)$ such that $B_{\overline{r}}(x_0) \subset \Omega$. Let $r \in (0,\overline{r})$. Consider $T' \in \mathcal{F}^2$ with $\mathrm{supp}\,(T - T') \subset B_r(x_0) \subset \Omega$. For almost every $r \in (0,\overline{r})$, it holds that $S_r := S \llcorner B_r(x_0)$ is a flat chain with boundary $\partial S_r = S \llcorner \partial B_r(x_0)$. In this case, $S'_r := \partial T' \llcorner B_r(x_0)$ has the same boundary. Hence, the flat chain $A := S_r + S'_r = \partial T + \partial T'$ is a cycle, i.e. verifies $\partial A = 0$ and is supported inside $B_r(x_0)$. We can construct the cone C' with vertex x_0 over A. Then, $\partial C' = A$ and $\mathbb{M}(C') \leq cr\mathbb{M}(A)$. Now, we distinguish two cases: It holds either $\mathbb{M}(S_r) \leq \mathbb{M}(S'_r)$ (which is enough for our conclusion as we will see below) or $\mathbb{M}(S_r) \geq \mathbb{M}(S'_r)$ and hence $\mathbb{M}(A) \leq 2\mathbb{M}(S_r)$. Comparing T to $T + C'$ and by minimality of T we get that

$$\beta\mathbb{M}(S_r) \;\leq\; \beta\mathbb{M}(S'_r) + (n+1)\mathbb{M}(C') \;\leq\; \beta\mathbb{M}(S'_r) + 2c(n+1)r\mathbb{M}(S_r)\,.$$

For r small enough we conclude that

$$\mathbb{M}(S_r) \;\leq\; \left(1 + \frac{4c(n+1)}{\beta}\,r\right)\mathbb{M}(S'_r)\,. \tag{3.71}$$

In case T' is not entirely contained in Ω, we need to project those parts of T' and of the boundary S'_r onto $\mathcal{M}$. Since we assumed $r < \overline{r} \leq \frac{1}{2}\mathbf{r}_0$, the Lipschitz constant of the projection can be estimated by $1 + 4\frac{r}{\mathbf{r}_0}$, i.e. our analysis and in particular (3.71) holds true if we replace $\mathbb{M}(S'_r)$ by $(1 + 4\frac{r}{\mathbf{r}_0})\mathbb{M}(S'_r)$. This shows that there exists a constant $C = C_{n,\beta,\mathbf{r}_0} > 0$ such that S is $(\mathbb{M}, Cr, \overline{r})-$minimal in the sense of Almgren. Together with Lemma 3.6.2, (3.71) allows us to apply Theorem 3.8 in [129] which gives the $C^{1,1/2}-$regularity and the decomposition of $\mathrm{supp}\,(S)$ into a finite union of curves, possibly meeting at triple points. Finally, since our flat chains take values only in $\pi_1(\mathcal{N}) = \{0,1\}$, we can exclude the existence of triple points since they would create boundary. Hence, S is a union of curves. □

The regularity of S in Lemma 3.6.3 is not optimal. The following Lemma provides us with the smoothness we announced in Proposition 3.6.1:

Lemma 3.6.4. *The flat chain S is supported on a finite union of closed $C^{1,1}-$curves. In particular, the curvature of S is bounded.*

Proof. Let $x_0 \in \operatorname{supp}(S)$ and take $r > 0$ such that $B_r(x_0) \subset \Omega$ and $\mu_S(\partial B_r(x_0)) = 2$. Let $\{x_1, x_2\} := \operatorname{supp}(S) \cap \partial B_r(x_0)$ and define $S_r := S \llcorner B_r(x_0)$. We compare S_r (and $T \llcorner B_r(x_0)$) to two competitors.

The first one is the geodesic segment S_g joining x_1 and x_2 in $\partial B_r(x_0)$. For the corresponding T_g we use a piece of $\partial B_r(x_0)$ between $T \llcorner (\partial B_r(x_0))$ and S_g. By minimality of S_r we find

$$\beta \mathbb{M}(S_r) \;\leq\; 2\pi r \left(\beta + 4(n+1)r\right) . \tag{3.72}$$

Our second competitor is the flat chain supported on the straight line segment joining x_1 to x_2 which we call S'. Then $S' + S_r$ is supported in $B_r(x_0)$ and is closed, i.e. $\partial(S' + S_r) = 0$. By the construction (7.6) in [67], we get the existence of a flat chain $T' \in \mathcal{F}^2$ supported in Ω and a constant $b > 0$ (depending only on the dimensions of the flat chains and the ambient space) such that $\partial T' = S' + S_r$ and $\mathbb{M}(T') \leq b(\mathbb{M}(S') + \mathbb{M}(S_r))^2$. Since $x_0 \in \operatorname{supp}(S)$ it also holds that $\mathbb{M}(S_r) \geq 2r$. This, together with the minimality of S_r and (3.72) implies that

$$\begin{aligned} 2\beta r \;\leq\; \beta \mathbb{M}(S_r) \;&\leq\; \beta \mathbb{M}(S') + b(n+1)(\mathbb{M}(S') + \mathbb{M}(S_r))^2 \\ &\leq\; \beta \mathbb{M}(S') + b(n+1)\left(\mathbb{M}(S') + 2\pi r\left(1 + \frac{4(n+1)}{\beta} r\right)\right)^2 \\ &\leq\; \beta \mathbb{M}(S') + C_1 r^2 , \end{aligned} \tag{3.73}$$

for $C_1 = 2(2+2\pi)^2 b(n+1)$ and r small enough. Hence, (3.73) implies $(2 - (C_1/\beta)r)r \leq \mathbb{M}(S')$. If we now choose r even smaller to assure $r \leq r_1 := (C_1)^{-1}\beta$, one gets even $\mathbb{M}(S') \geq r$, i.e. the points x_1 and x_2 must not be too close.

Our goal is now to show that S_r is in fact close to S' and that S' is almost a diameter of $B_r(x_0)$, in the sense that S_r lies in a small neighbourhood of S' and the distance between x_0 and S' is of order r^2. Let's denote $\ell := \mathbb{M}(S') = |x_2 - x_1|$. Suppose $\mathbb{M}(S_r) \leq \ell + \alpha$ for a $\alpha > 0$ and let $\rho > 0$ be the smallest positive number such that S_r lies within a $\rho-$neighbourhood of S'. Then, $\mathbb{M}(S_r) \geq \sqrt{\ell^2 + 4\rho^2}$ and hence $\ell^2 + 4\rho^2 \leq \mathbb{M}(S_r) \leq (\ell + \alpha)^2$ which yields the bound

$$\rho \;\leq\; \sqrt{\frac{\ell\alpha}{2} + \frac{\alpha^2}{4}} \;\leq\; \sqrt{2r\alpha}\,, \tag{3.74}$$

provided $\alpha \leq 4r$ and $\ell \leq 2r$. Applying this result to our case where $\alpha = \beta^{-1} C_1 r^2$, we get S_r is contained in a neighbourhood of S' of radius $\rho \leq \sqrt{2\beta^{-1} C_1 r^3}$.

In addition, if S_r is supported in a $\rho-$cylinder around S', there exists a $T_\rho \in \mathcal{F}^2$ and a constant c (depending only on the space dimension) such that $\mathbb{M}(T_\rho) \leq c\rho \mathbb{M}(S_r)$ and $\partial T_\rho = S' + S_r$. This implies that $\mathbb{M}(S_r) \leq \ell + \beta^{-1}(n+1)c\rho \mathbb{M}(S_r)$. Previously, we have also shown that $\mathbb{M}(S_r) \leq \ell + \beta^{-1} C_1 r^2 \leq 3r$, leading to

$$\mathbb{M}(S_r) \;\leq\; \ell + C_2 \rho r\,, \quad \text{where } C_2 = 3c\frac{n+1}{\beta}\,. \tag{3.75}$$

Now, we want to iterate this procedure. Let $\alpha_0 := \beta^{-1} C_1 r^2$ as start of our induction.

1. Knowing that $\mathbb{M}(S_r) \leq \ell + \alpha_k$ (either by (3.73) or by induction hypothesis) and by (3.74) we can deduce that S_r lies in a ρ_k-neighbourhood of S', for $\rho_k = \sqrt{2r\alpha_k}$.
2. Since S_r lies in a ρ_k-neighbourhood of S', one can use (3.75) with $\rho = \rho_k$ to obtain $\mathbb{M}(S_r) \leq \ell + \alpha_{k+1}$, where $\alpha_{k+1} := C_2 r \rho_k$.

Throughout this iteration, α_k and ρ_k verify $\rho_{k+1} = \sqrt{2r\alpha_{k+1}} = \sqrt{2C_2\rho_k}\, r$. Thus, ρ_k converges to $2C_2 r^2$ in the limit $k \to \infty$. We can conclude that the distance between a point in S_r and S' is at most $2C_2 r^2$. In particular, since $x_0 \in \operatorname{supp}(S_r)$, it holds that $\operatorname{dist}(x_0, \operatorname{supp}(S'))$ is of order r^2 which shows that the line S' is close to being a diameter.

Let us turn now to the assertion of the lemma. For $x_0 \in \operatorname{supp}(S)$ and $r > 0$ chosen small enough, we denote $\tau_r(x_0)$ the vector $\frac{x_2 - x_1}{\|x_2 - x_1\|}$, where x_1, x_2 are constructed as before. By our

previous calculations, we know that the corresponding points for $\frac{r}{2}$ are at most at distance $2C_2r^2$ from the line connecting x_1 and x_2 which gives $\|\tau_r(x_0) - \tau_{\frac{r}{2}}(x_0)\| \leq C_3 r$. This shows that the limit $\tau(x_0) = \lim_{r\to 0} \tau_r(x_0)$ exists and that $\|\tau_r(x_0) - \tau(x_0)\| \leq 2C_3 r$. The triangle inequality then yields the existence of another constant $C_4 > 0$, depending on β and n, such that for $x, y \in \operatorname{supp}(S)$ with $|x - y| =: r$ small enough we have $\|\tau(x) - \tau(y)\| \leq C_4 r$.

□

Having reached the optimal regularity for S, we now turn to the properties of T.

Lemma 3.6.5. *The flat chain $T \llcorner \Omega$ is supported on a hypersurface of class C^1 up to the boundary.*

Proof. We first discuss the regularity in the interior of $T \llcorner \Omega$. Let $x_0 \in \Omega$, $r > 0$ such that $B_r(x_0) \cap \operatorname{supp}(T \llcorner \Omega) \neq \emptyset$ and consider a variation T' of T in $B_r(x_0)$. Then, by minimality of T we find

$$\mathbb{M}(T) \;\leq\; \mathbb{M}(T') \;+\; n\mathbb{F}(T - T') \;\leq\; \mathbb{M}(T') \;+\; \frac{4}{3}\pi n r^3 \,.$$

We can then apply the result of Taylor [158], or more general Theorem 1.15 in [52] to obtain $C^{1,\alpha}-$regularity in Ω, for some $\alpha > 0$.

For the regularity up to the boundary we want to apply Theorem 31.1 in [53]. In order to do this we need to show that on a certain scale, the boundary S is close to a straight line and T is almost flat.

Take a point of rectifiability $x_0 \in S$. We define a blow-up sequence $r_k \searrow 0$. Since S is supported by $C^{1,1}-$curves, a blow up of S converges to a straight line. We claim that a blow up of T converges to a limit T_0 which is a half plane. For this, we use the minimality of T to deduce for $r > 0$ small enough that

$$\begin{aligned}
\mathbb{M}(T \llcorner B_r(x_0)) + 2\beta r \;&\leq\; \mathbb{M}(T \llcorner B_r(x_0)) + \beta \mathbb{M}((\partial T) \llcorner B_r(x_0)) \\
&\leq\; \mathbb{M}(\operatorname{cone}(T \llcorner \partial B_r(x_0))) + \beta \mathbb{M}(\operatorname{cone}((\partial T) \llcorner \partial B_r(x_0))) \\
&\leq\; \frac{r}{2}\mathbb{M}(T \llcorner \partial B_r(x_0)) + \beta r \mathbb{M}((\partial T) \llcorner \partial B_r(x_0)) \\
&=\; \frac{r}{2}\mathbb{M}(T \llcorner \partial B_r(x_0)) + 2\beta r \,.
\end{aligned}$$

This implies that $\mathbb{M}(T \llcorner B_r(x_0))/r^2$ is monotonically increasing and thus admits a unique limit d. We define $T_{r_k} = (T - x_0)/r_k$ and by monotonicity we get for $s_1 < s_2$ that $\mathbb{M}(T_{r_k} \llcorner B_{s_1})/s_1^2 \leq \mathbb{M}(T_{r_k} \llcorner B_{s_2})/s_2^2$. For $r_k \to 0$ both sides converge to the same limit πd. But this means that $\mathbb{M}(T_0 \llcorner B_{s_1})/s_1^2 = \mathbb{M}(T_0 \llcorner B_{s_2})/s_2^2$, i.e. T_0 is a cone and hence a half-plane. Since a half plane has density $\frac{1}{2}$, we find $d = \frac{1}{2}$. In particular, we have for k large enough

$$\mathbb{M}\left(\frac{T_{r_k} - x_0}{r_k} \llcorner B_1\right) \;=\; \frac{\pi}{2} + o(1)\,,$$

from which it follows that condition (31.6) in [53] holds and thus we can apply Theorem 31.1 on a length scale $R \leq r_k$. We remark that by convergence in the flat norm, following [123], we also verify the condition (31.4) of Theorem 31.1 in [53]. By compactness of the boundary $(\partial T) \llcorner \Omega$, we find a finite cover with balls of uniformly positive radius to which we can apply Theorem 31.1. This allows us to conclude. □

Proof of Proposition 3.6.1. We have already established the existence of a minimizer of (3.70). The convergence $\mathbb{F}(T_n - T_0) \to 0$ for $n \to \infty$ is obvious since $n\,\mathbb{F}(T_n - T_0) \leq \mathcal{E}_0(T_0) < \infty$ for all $n \in \mathbb{N}$.

The regularity of T_n follows from Lemma 3.6.4 and Lemma 3.6.5. □

3.6.2 Construction of the recovery sequence

In this section we will use the approximation of T given by the minimizer of (3.70) to construct our recovery sequence. First we establish the following Proposition which yields additional control over $\partial(T \llcorner \mathcal{M}) \setminus \partial T$ and its boundary which will be necessary for the final construction in Proposition 3.6.9.

Proposition 3.6.6. *Let $T \subset \overline{\Omega}$ be a flat $2-$chain of finite mass and $S \subset \overline{\Omega}$ be a flat $1-$chain of finite mass such that $\partial S = 0$ and $\partial T = S + \Gamma$. Then, there exist finite mass flat chains $T_n \in \mathcal{F}^2$ of class* Lip *up to the boundary and $S_n \in \mathcal{F}^1$ of class $C^{1,1}$ such that*

1. *$\partial S_n = 0$ and $\partial T_n = S_n + \Gamma$,*
2. *$\mathbb{F}(T_n - T) \to 0$ and $\mathcal{E}_0(T_n) \to \mathcal{E}_0(T)$ as $n \to \infty$,*
3. *and there exists a constant $C_n > 0$ such that $\mathbb{M}(\partial(T_n \llcorner \mathcal{M}) \setminus \partial T_n) \leq C_n$ and $\mathbb{M}(\partial(\partial(T_n \llcorner \mathcal{M}) \setminus \partial T_n)) \leq C_n$.*

Essentially, the first two parts of Proposition are proved by Proposition 3.6.1, saying that the minimizer T_n of (3.70) fulfils our claims. It remains to prove the last assertion i.e. that we can modify T_n to control the length of the set where the T_n attaches to $\mathcal{M}$. For this, we need the following average argument stating that we can find radii r such that the corresponding sets $T_n \llcorner \mathcal{M}_r$, for $\mathcal{M}_r := \{x \in \Omega : \operatorname{dist}(x, \mathcal{M}) = r\}$, are of finite length.

Lemma 3.6.7. *Let T_n be as constructed in the previous subsection. There exist a constant $c > 0$ and a radius $r \in (0, \frac{1}{2}\mathbf{r}_0)$ such that*

$$\mathbb{M}(T_n \llcorner \mathcal{M}_r) \;\leq\; \frac{4c\mathbb{M}(T_n)}{\mathbf{r}_0}\,. \tag{3.76}$$

Proof. Assume that $\mathbb{M}(T_n \llcorner \mathcal{M}_r) > \frac{4c\mathbb{M}(T_n)}{\mathbf{r}_0}$ for all $r \in (0, \frac{1}{2}\mathbf{r}_0)$ and some $c > 0$. This implies

$$\int_0^{\mathbf{r}_0/2} \mu_{T_n}(\mathcal{M}_r)\,\mathrm{d}r \;>\; 2c\mathbb{M}(T_n)\,.$$

Now, there exists a constant $c > 0$ such that $\int_0^{\mathbf{r}_0/2} \mu_{T_n}(\mathcal{M}_r)\,\mathrm{d}r \leq c\mathbb{M}(T_n)$ (see (5.7) in [67]). Hence, the lemma is proved. □

Now, we can modify T_n by replacing a small part close to $\mathcal{M}$ by a projection to control the boundary of $T_n \llcorner \mathcal{M}$ which is not included in S.

Proof of Proposition 3.6.6. We construct T_n as in Proposition 3.6.1. To ensure the additional estimate, we choose a radius r and a slice $\mathcal{M}_r$ as in Lemma 3.6.7. With the same argument as in Lemma 3.6.7 for S_n one can choose $r \in (0, \frac{1}{2}\mathbf{r}_0)$ for which additionally $\mathbb{M}(S_n \llcorner \mathcal{M}_r)$ is finite. Let $\Pi : \Omega_{\mathbf{r}_0} \to \mathcal{M}$ be the projection onto $\mathcal{M}$. We define $\Phi : \mathcal{M}_r \times [0,1] \to \overline{\Omega}$ by $\Phi(x,t) := (1-t)x + t\Pi x$. Then, by [66, Sec. 2.7], [65, Cor. 2.10.11], $\mathbb{M}(\Phi_\#(T_n \llcorner \mathcal{M}_r \times [0,1])) \leq Cr\mathbb{M}(T_n \llcorner \mathcal{M}_r)$ and also $\mathbb{M}(\Pi_\#(T_n \llcorner \mathcal{M}_r)) \leq C\mathbb{M}(T_n \llcorner \mathcal{M}_r)$. Again by the same argument, we get $\mathbb{M}(\partial\Pi_\#(T_n \llcorner \mathcal{M}_r)) \leq C\mathbb{M}(\partial(T_n \llcorner \mathcal{M}_r))$. This procedure can be applied to almost every $r \in (0, \frac{1}{2}\mathbf{r}_0)$, in particular, we can choose a sequence $r_n \to 0$ as $n \to \infty$. Replacing T_n close to $\mathcal{M}$ with these projections, we get the desired estimates.

The convergence of the energy $\mathcal{E}_0(T_n)$ to $\mathcal{E}_0(T)$ is a consequence of the convergence statements in Proposition 3.6.1 and the fact that $T_n \llcorner \mathcal{M}$ approaches $T \llcorner \mathcal{M}$. □

The recovery sequence $Q_{\eta,\xi}$ for our problem will be constructed around the regularized sequence of T. The gained regularity permits us to define $Q_{\eta,\xi}$ directly and without the need to write T as a complex and 'glue' together the parts of $Q_{\eta,\xi}$ on each simplex.

Before starting, we need one final ingredient as stated in the following lemma stating that the normal field on $\mathcal{M}$ can be extended to Ω. It will be used to fix choices of orientation consistently across Ω. The only crucial point is that the gradient of the extension must be bounded in order for our estimates to work out.

Lemma 3.6.8. *Let $\mathcal{M}$ be a closed compact manifold of class C^2. Then, there exists a Lipschitz continuation v of the outward normal field ν on $\mathcal{M}$ to Ω with the same Lipschitz constant.*

Proof. Since $\mathcal{M} \in C^2$, the outward normal ν is Lipschitz continuous. Then, the existence of a Lipschitz extension with the same Lipschitz constant is a direct consequence from Kirszbraum's theorem [98] (see also Theorem 7.2 in [117] or in full generality Theorem 1.31 in [146]). □

Proposition 3.6.9. *There exists a recovery sequence $Q_{\eta,\xi}$ for the problem* (3.21).

The construction relies on the approximation and regularisation made in the previous subsection. We will construct $Q_{\eta,\xi}$ step by step: The straightforward parts are the profile on F and $\mathcal{M} \setminus F$ away from ∂F, as well as the transition across T. In order to be compatible with the latter, we have to adjust the construction made in [8] for the singular line S. The profile of the part of S that approaches the surface $\mathcal{M}$ can be chosen as in [8]. Last, we need to connect $\partial F \setminus S$ to the profile of T already constructed. This last part is a bit subtle since the $\partial F \setminus S$ does not appear in the energy. The control we obtained in Proposition 3.6.6 is artificial and indeed we do not control the length of $\partial F \setminus S$. Hence, we will choose n depending on η, ξ in a way to allow this length to slowly grow to infinity while the energy contribution of $Q_{\eta,\xi}$ in this region vanishes.

Proof. From now on we choose n depending on ξ, η such that $\mathbb{M}(\partial(T_n \llcorner \mathcal{M})), \mathbb{M}(\partial(\partial(T_n \llcorner \mathcal{M}) \setminus \partial T_n)) \leq C|\ln(\eta)|$ and that the curvature of S_n is bounded by $C/\sqrt{\eta}$. Indeed, if the constant C_n in Proposition 3.6.6 is bounded in n, then for η small enough this condition is trivial. If $C_n \to \infty$ for $n \to \infty$ (choosing a subsequence we can furthermore assume that $C_n \nearrow \infty$), we can define $n(\eta) := \sup\{m \in \mathbb{N} : C_m \leq -\ln(\eta)\}$. Since $-\ln(\eta) \to \infty$ for $\eta \to 0$, it also holds that $n(\eta) \to \infty$ and the bound $\mathbb{M}(\partial(T_{n(\eta)} \llcorner \mathcal{M})), \mathbb{M}(\partial(\partial(T_{n(\eta)} \llcorner \mathcal{M}) \setminus \partial T_{n(\eta)})) \leq C|\ln(\eta)|$ holds.

Furthermore, whenever this doesn't lead to confusion, we drop the subscript parameters η, ξ and n in order to make the construction more readable.

Step 1: Adaptation of the optimal profile. The goal of this step is to construct a one dimensional profile close to the optimal one in Lemma 3.5.2, but where the transition takes place on a finite length and which gives the correct energy density (3.45) for $\eta \to 0$. To this goal, we introduce the "artificial" length scale η^γ for $\gamma \in (\frac{1}{2}, 1)$ and define

$$\Phi^\pm_\eta(t,\theta,v) := \begin{cases} s_*(\mathbf{n}^\pm(t/\eta,\theta) \otimes \mathbf{n}^\pm(t/\eta,\theta) - \frac{1}{3}\mathrm{Id}) & t \in [0,\eta^\gamma]\,, \\ s_*(\mathbf{n}^\pm(\eta^\gamma/\eta,\theta) \otimes \mathbf{n}^\pm(\eta^\gamma/\eta,\theta) - \frac{1}{3}\mathrm{Id})(2\eta^\gamma - t) + (t-\eta^\gamma)Q_\infty & t \in (\eta^\gamma, 2\eta^\gamma]\,, \\ (3\eta^\gamma - t)Q_\infty + (t-2\eta^\gamma)Q_{\eta,\xi,\infty} & t \in (2\eta^\gamma, 3\eta^\gamma]\,, \end{cases} \tag{3.77}$$

with $\mathbf{n}^\pm = (\sqrt{1-\mathfrak{n}_3^2}(v_1,v_2), \pm\mathfrak{n}_3)$, where $\mathfrak{n}_3(t,\theta)$ is the optimal profile from (3.44) and $(v_1,v_2) \in \mathbb{S}^1$. The choice of η^γ permits us to conclude that $\mathbf{n}^\pm(\eta^\gamma/\eta) \to \pm\mathbf{e}_3$ for $\eta \to \infty$. On the other hand, η^γ is large enough to verify $(\eta^\gamma)^2/\eta \to 0$ which ensures that undesired energy contributions vanish, as we will see in the following steps.

Step 2: Construction on F and F^c. Let $\omega \in F_{3\eta^\gamma} := \{\omega \in F : \mathrm{dist}(\omega, \partial F) \geq 3\eta^\gamma\} \subset \mathcal{M}$ and let $0 \leq r < 3\eta^\gamma \leq \frac{1}{2}\mathbf{r}_0$. We define

$$Q_{\eta,\xi}(\omega + r\nu(\omega)) := \Phi^+(r,\theta,v(x)) \quad \text{where } \theta = \arccos(\nu(\omega)\cdot\mathbf{e}_3)\,. \tag{3.78}$$

Since $|\nabla v|$ is bounded, one can then easily calculate

$$\begin{aligned}\eta\,\mathcal{E}_{\eta,\xi}(Q_{\eta,\xi},F_{3\eta^\gamma,3\eta^\gamma}) &= \int_{F_{3\eta^\gamma}}\int_0^{3\eta^\gamma}\left(\frac{\eta}{2}|\nabla Q_{\eta,\xi}|^2+\frac{\eta}{\xi^2}f(Q_{\eta,\xi})+\frac{1}{\eta}g(Q_{\eta,\xi})+\eta C_0\right)\prod_{i=1}^2(1+r\kappa_i)\,\mathrm{d}r\,\mathrm{d}\omega\\ &\le \int_{F_{3\eta^\gamma}}\int_0^{\eta^\gamma}\left(\frac{\eta}{2}|\partial_r Q_{\eta,\xi}|^2+\frac{1}{\eta}g(Q_{\eta,\xi})\right)\prod_{i=1}^2(1+r\kappa_i)\,\mathrm{d}r\,\mathrm{d}\omega+C\eta\\ &\le \int_{F_{3\eta^\gamma}} I\left(0,\frac{\eta^\gamma}{\eta},\cos(\theta),+1\right)\,\mathrm{d}\omega+o(1)\,,\end{aligned}$$

where $F_{3\eta^\gamma,R}:=\{x\in\Omega\,:\,x=\omega+r\nu(\omega),\,\omega\in F_{3\eta^\gamma},\,r\in[0,R]\}$ for $R>0$. Note that $\frac{\eta^\gamma}{\eta}\to\infty$ for $\eta\to 0$ since we chose $\gamma\in(\frac12,1)$. Analogously, we can define $Q_{\eta,\xi}$ on F^c away from ∂F by using Φ^- and estimate its energy. Note that this construction may already create the part of T that attaches to the surface $\mathcal{M}$ in the limit $\eta,\xi\to 0$. Indeed, if a point ω is contained in F although the energy density corresponding to F^c would be lower, the profile constructed passes trough $n_3=0$ within a distance η^γ from $\mathcal{M}$ and hence is included in the limiting T.

Step 3: Construction on T. Let $x\in T_\eta:=\{x\in\operatorname{supp}(T)\,:\,\operatorname{dist}(x,\mathcal{M})>3\eta^\gamma$ and $\operatorname{dist}(x,S)>3\eta^\gamma\}$. For each connected component of T (and thus of T_η) we can associate a sign depending on the sign of the degree of the singularity line S (if the component of T has such). This must be compatible with the part of T that reaches $\mathcal{M}$ and already has been constructed in Step 2. The compatibility corresponds to the choice of the signs of $\phi_\eta^\pm$ and of the distance function, viewing T_η as a boundary, locally. Assuming that in Step 2 we chose Φ_η^+ whenever $\operatorname{dist}(\cdot,T_\eta)>0$ and Φ_η^- for $\operatorname{dist}(\cdot,T_\eta)<0$, we define

$$Q_{\eta,\xi,n}(x) \;:=\; \Phi_\eta^+(\operatorname{dist}(x,T),\frac{\pi}{2},v(x))\,.$$

Since $|\nabla v|$ is bounded, and writing $T_{\eta,t}:=\{x\in\Omega\,:\,\operatorname{dist}(x,T_\eta)=\operatorname{dist}(x,T)$ and $\operatorname{dist}(x,T_\eta)\le t\}$ for $t\ge 0$ we can estimate by Lemma (3.5.2) and the coarea formula

$$\begin{aligned}&\int_{T_{\eta,3\eta^\gamma}}\frac{\eta}{2}|\nabla Q_{\eta,\xi,n}|^2+\frac{\eta}{\xi^2}f(Q_{\eta,\xi,n})+\frac{1}{\eta}g(Q_{\eta,\xi,n})+\eta C_0\,\mathrm{d}x\\ &\quad\le \int_{T_{\eta,\eta^\gamma}}\frac{\eta}{2}|\nabla Q_{\eta,\xi,n}|^2+\frac{1}{\eta}g(Q_{\eta,\xi,n})\,\mathrm{d}x+C\eta\,\mathbb{M}(T)\\ &\quad= 2s_*c_*\int_{T_{\eta,\eta^\gamma}}|\mathtt{n}_3'(\operatorname{dist}(x,T_n)/\eta)|\,\mathrm{d}x+C\eta\,\mathbb{M}(T)\\ &\quad= 2s_*c_*\int_0^{\eta^\gamma}\int_{T_{\eta,\eta^\gamma}\cap\{\operatorname{dist}(\cdot,T)=s\}}|\mathtt{n}_3'(s/\eta)|\,\mathrm{d}s+o(1)\\ &\quad= 2s_*c_*\int_0^{\eta^\gamma}\mathcal{H}^2(T_{\eta,\eta^\gamma}\cap\{\operatorname{dist}(\cdot,T)=s\})|\mathtt{n}_3'(s/\eta)|\,\mathrm{d}s+o(1)\\ &\quad\le 2s_*c_*\big(2\mathbb{M}(T)+o(1)\big)\int_0^{\eta^\gamma}|\mathtt{n}_3'(s/\eta)|\,\mathrm{d}s+o(1)\\ &\quad= 4s_*c_*|\mathtt{n}_3(\eta^\gamma/\eta)|\,\mathbb{M}(T)+o(1)\,,\end{aligned}$$

where we also used that $\mathcal{H}^2(T_{\eta,\eta^\gamma}\cap\{\operatorname{dist}(\cdot,T)=s\})\to 2\mathbb{M}(T)$ for $s\to 0$. Note that $|\mathtt{n}_3(t)|\to 1$ as $t\to\infty$. Hence, for $\eta,\xi\to 0$ we end up with

$$\begin{aligned}\limsup_{\eta,\xi\to0}\int_{T_{\eta,3\eta^\gamma}}&\frac{\eta}{2}|\nabla Q_{\eta,\xi,n}|^2+\frac{\eta}{\xi^2}f(Q_{\eta,\xi,n})+\frac{1}{\eta}g(Q_{\eta,\xi,n})+\eta C_0\,\mathrm{d}x\\ &\le\; 4s_*c_*\mathbb{M}(T_n)\,.\end{aligned}$$

Step 4: Construction on $S\llcorner\Omega$. Following the notation we used in Step 2 and 3, we introduce the region

$$S_{3\eta^\gamma}\;:=\;\{x\in\Omega\,:\,\exists y\in T\text{ with }\operatorname{dist}(y,S)\le 3\eta^\gamma\text{ and }\operatorname{dist}(x,T)=\|x-y\|\le 3\eta^\gamma\}\qquad(3.79)$$

around the singular line S (see also Figure 3.7). We will construct $Q_{\eta,\xi,n}$ as follows: Depending on the sign attributed to the connected component of T in Step 3 or the change between F and F^c in Step 2, we place a singularity of degree $-\frac{1}{2}$ (resp. $\frac{1}{2}$) as in Lemma 5.2 in [8] in the center of $S_{3\eta^\gamma}$. We do so by setting $Q=0$ in a disk of radius ξ (perpendicular to S) and oblate Q uniaxial with director field $(\sin(\phi/2),0,\cos(\phi/2))$ on the annulus between the radii 2ξ and η, interpolating linearly in radial direction between these two regions. From the circle of radius η to the boundary of the region (3.79), we use the profile $\Phi_\eta^\pm$ to make a transition to Q_∞ along $\nabla \mathrm{dist}(\cdot,T)$. By doing so, we get the compatibility between the construction made for T and S.

More precisely, we define as in [8](Lemma 5.2, Step 3, Equation (55))

$$Q_B(r,\phi) \;:=\; \begin{cases} 0 & r\in[0,\xi)\,,\\ \left(\frac{r}{\xi}-1\right)Q(\phi) & r\in[\xi,2\xi)\,,\\ Q(\phi) & r\in[2\xi,\eta)\,, \end{cases}$$

where $r\in[0,\eta)$, $\phi\in[0,2\pi)$ and

$$Q(\phi) \;=\; s_*\left(\mathbf{n}(\phi)\otimes\mathbf{n}(\phi)-\frac{1}{3}\mathrm{Id}\right) \quad \text{with} \quad \mathbf{n}(\phi) \;=\; \begin{pmatrix}\sin(\phi/2)\\ 0\\ \cos(\phi/2)\end{pmatrix}.$$

We use this to define $Q_{\eta,\xi}$ on a small $\eta-$neighbourhood of S as follows. For η small enough, we can assume that the $\eta-$neighbourhood is parametrized by the projection onto S, the radius $\mathrm{dist}(\cdot,S)$ and an angle ϕ.

Modifying T close to S if necessary, we can furthermore assume that on each (small) plane disk perpendicular to S, the restriction of T to this disk is given by a straight line segment. Indeed, as in Lemma 3.6.7 we can select a radius $r\in(\eta,2\eta)$ and a slice T_r of T at $\mathrm{dist}(\cdot,S)=r$ such that T_r is of finite length. One can then replace T by a $\tilde{T}$ inside the tubular neighbourhood $\{\mathrm{dist}(x,S)\le r\}$ where $\tilde{T}$ is defined by the straight lines connecting S to T_r on each disk perpendicular to S.

Consider $x_0\in S$. By applying rotations if necessary, we can assume that a normal vector of T_n in x_0 is $\nu_T=\mathbf{e}_3$ and the outward normal vector of S seen as boundary of T verifies $\nu_S=\mathbf{e}_1$. We then set

$$Q_{\eta,\xi,n}(x) \;:=\; Q_B(\mathrm{dist}(x,S),\phi(x))\,,$$

where

$$\phi(x)=\begin{cases}\arccos\left(\nu_S\cdot\frac{x-x_0}{\|x-x_0\|}\right) & \text{if } \nu_T\cdot\frac{x-x_0}{\|x-x_0\|}\ge 0\,,\\ 2\pi-\arccos\left(\nu_S\cdot\frac{x-x_0}{\|x-x_0\|}\right) & \text{otherwise.}\end{cases}$$

Note that if $\phi(x)\in(\frac{\pi}{2},\frac{3\pi}{2})$, then $\mathrm{dist}(x,T)<\mathrm{dist}(x,S)$ and thus we can also write

$$\phi(x) \;=\; \arccos\left(\frac{\mathrm{dist}(x,T)}{\mathrm{dist}(x,S)}\right)+\frac{\pi}{2}\,.$$

It remains the transition from the set $\{\mathrm{dist}(\cdot,S)=\eta\}$ to the boundary of (3.79). Let Π be the projection along $\nabla\mathrm{dist}(\cdot,T)$ onto $\{\mathrm{dist}(\cdot,S)=\eta\}\cup(T\cap\{\mathrm{dist}(\cdot,S)\ge\eta\})$. The function $Q_{\eta,\xi}$ is already defined on the first set in the union, for the second we simply pose $Q_{\eta,\xi}(x)=s_*((v(x),0)\otimes(v(x),0)-\frac{1}{3}\mathrm{Id})$ in order to be compatible with Step 3. For $x\in S_{3\eta^\gamma}\setminus(\{\mathrm{dist}(\cdot,S)\le\eta\}\cup(T\cap\{\mathrm{dist}(\cdot,S)\ge\eta\}))$ we then define

$$Q_{\eta,\xi}(x) \;:=\; \Phi_\eta^+(\|x-\Pi x\|,\theta(x),v(x))\,,$$

where $\theta(x)$ is the angle between $\mathbf{e}_3$ and the director field that we have already constructed in Πx, i.e. $\theta(x)=\arccos(\mathbf{n}(\phi(x))\cdot\mathbf{e}_3)$ or $\theta(x)=\arccos(v(\Pi x)\cdot\mathbf{e}_3)$ depending on which set contains Πx.

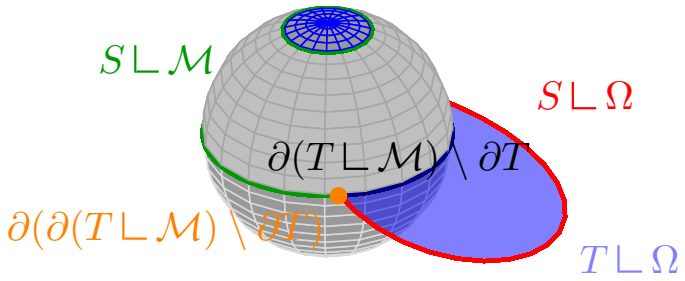

Figure 3.6: Schematic view of the different parts of T and S that are constructed in Step 2 to 6

It is easy to see that since f, g and C_0 are uniformly bounded and the curvature of S is bounded by Lemma 3.6.4, we get

$$\begin{aligned}
&\int \frac{\eta}{2}|\nabla Q_{\eta,\xi,n}|^2 + \frac{\eta}{\xi^2} f(Q_{\eta,\xi,n}) + \frac{1}{\eta} g(Q_{\eta,\xi,n}) + \eta C_0 \, \mathrm{d}x \\
&\leq \frac{\eta}{2} \int_{2\xi}^{\eta} \int_{\{\mathrm{dist}(\cdot,S)=r\}} |\nabla Q(\phi(x))|^2 \, \mathrm{d}r \; + \; C \frac{\eta}{\xi^2} \mathcal{H}^3(\{\mathrm{dist}(\cdot,S) \leq 2\xi\}) \; + \; C \frac{\eta}{\eta^2} \mathcal{H}^3(\{\mathrm{dist}(\cdot,S) \leq \eta\}) \\
&\leq \frac{\eta}{2} \int_{2\xi}^{\eta} \int_{\{\mathrm{dist}(\cdot,S)=r\}} |\nabla Q(\phi(x))|^2 \, \mathrm{d}r \; + \; C\eta \, (1 + K_S) \, \mathbb{M}(S) \, .
\end{aligned}$$

Estimating the gradient at distance $r := \mathrm{dist}(\cdot, S) \in [2\xi, \eta)$ yields

$$\begin{aligned}
\frac{1}{2}|\nabla Q(\phi(x))|^2 \; &= \; s_*^2 |\nabla \mathbf{n}(\phi(x))|^2 \; \leq \; \frac{s_*^2}{4} \left| \frac{1}{r} \partial_\phi \mathbf{n}(\phi(x)) \nabla \phi(x) \right|^2 + \frac{s_*^2}{4} |\partial_r \mathbf{n}(x)|^2 + C(|\nabla \tau_S|^2 + |\nabla \nu_S|^2) \\
&\leq \; \frac{s_*^2}{4r^2} \, (1 + Cr) + C \, .
\end{aligned}$$

Hence, we get

$$\begin{aligned}
\frac{\eta}{2} \int_{2\xi}^{\eta} \int_{\{\mathrm{dist}(\cdot,S)=r\}} |\nabla Q(\phi(x))|^2 \, \mathrm{d}r \; &\leq \; \frac{s_*^2 \pi}{2} \mathbb{M}(S) \int_{2\xi}^{\eta} \frac{1}{r} \, \mathrm{d}r + o(1) \\
&\leq \; \frac{\pi}{2} s_*^2 \eta |\ln(\xi)| \mathbb{M}(S) + o(1) \, .
\end{aligned}$$

For the remaining part of the domain defined in (3.79) we get that

$$\eta \int \frac{1}{2}|\nabla Q_{\eta,\xi,n}|^2 + \frac{1}{\xi^2} f(Q_{\eta,\xi,n}) + \frac{1}{\eta^2} g(Q_{\eta,\xi,n}) + C_0 \, \mathrm{d}x \; \leq \; C\eta \frac{(\eta^\gamma)^2}{\eta^2} \mathbb{M}(S) + o(1) \, .$$

Since we chose $\gamma > \frac{1}{2}$, we get that $\eta^{2\gamma-1} \to 0$ as $\eta \to 0$ and the energy contribution vanishes in the limit.

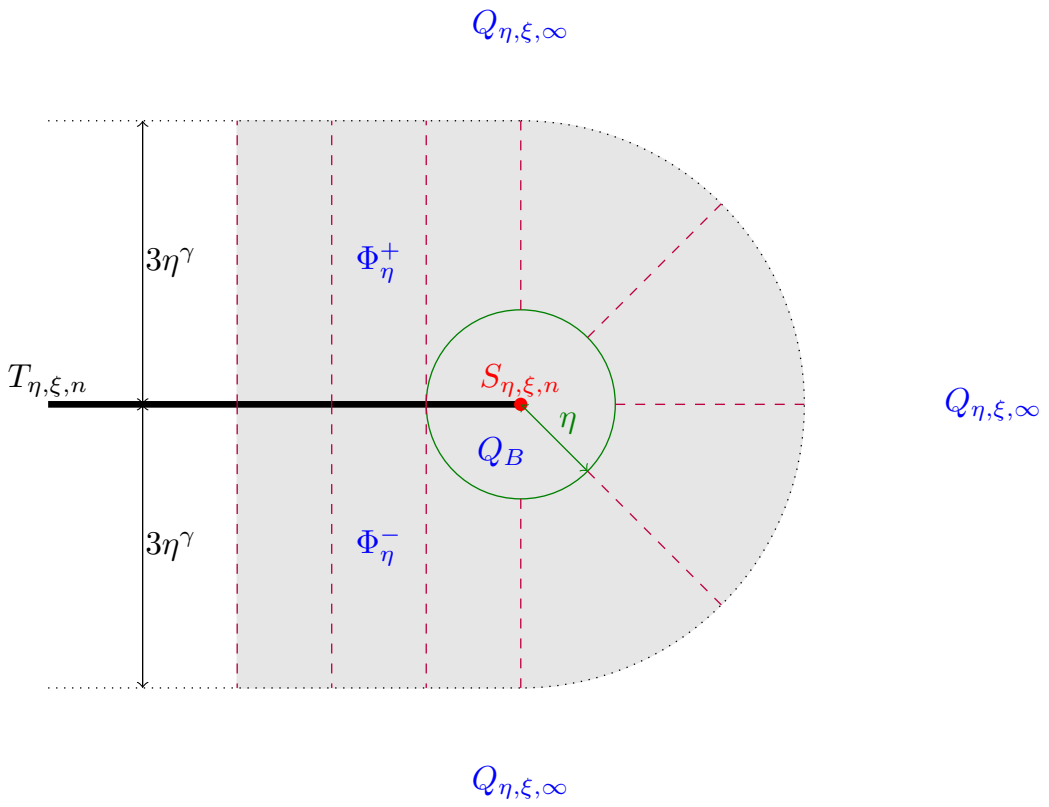

Figure 3.7: Sketch of the construction for $Q_{\eta,\xi,n}$ in Step 5 in the region $S_{3\eta^\gamma}$ defined in (3.79) (grey shaded area). Dashed lines indicate the direction of the projection Π.

Step 5: Construction on $S \llcorner \mathcal{M}$. The domain

$$S_{0,3\eta^\gamma} := \{x \in \Omega : \operatorname{dist}(x,S) \leq 3\eta^\gamma, \operatorname{dist}(x,M) \leq 3\eta^\gamma \text{ and } \operatorname{dist}(x, \partial(\partial(T \llcorner \mathcal{M}) \setminus \partial T)) \geq 3\eta^\gamma\}$$

can essentially be treated in the same manner as in Step 4 or as in [8, p.1444, Step 3]. To give some more details, we can reuse the profile Q_B from the previous step (assuming a $+\frac{1}{2}-$singularity) for defining $Q_{\eta,\xi}$ in a ball of radius η centered in x_S in the middle of $S_{0,3\eta^\gamma}$, seen as family of plane sets perpendicular to S. Note that $Q_{\eta,\xi}$ has already been defined on the boundary on each of those plane sets. Thus, a simple two dimensional interpolation of the phase angle along $\nabla \operatorname{dist}(\cdot, x_S)$ as in [8, eq (56-64)] shows that the energy contribution is

$$\mathcal{E}_{\eta,\xi}(Q_{\eta,\xi}, S_{0,3\eta^\gamma}) \leq (1 + C\eta)\frac{\pi}{2} s_*^2 |\ln(\xi)| \mathbb{M}(S \llcorner \mathcal{M}) + C\frac{(\eta^\gamma)^2}{\eta^2}.$$

Step 6: Construction on $\partial F \setminus S$. It remains to fill the "gaps" left by the Steps 2 to 5. The important part is the transition between the part of T that approaches $\mathcal{M}$ (and which was constructed in Step 2) and the part that stays bounded away, including the region where S detaches from $\mathcal{M}$. At distance larger than $3\eta^\gamma$ from $\mathcal{M}$, we set $Q_{\eta,\xi} = Q_{\eta,\xi,\infty}$ for all points where we haven't defined $Q_{\eta,\xi}$ so far. Note that this is compatible with the previous constructions.

Let's consider the set $\Upsilon_{3\eta^\gamma} := \{x \in \Omega : \operatorname{dist}(x, \partial(T \llcorner \mathcal{M}) \setminus \partial T) \leq 3\eta^\gamma \text{ and } \operatorname{dist}(x, \partial(\partial(T \llcorner \mathcal{M}) \setminus \partial T)) \geq 3\eta^\gamma\}$. Considering the slices of $\Upsilon_{3\eta^\gamma}$ orthogonal to and parametrized by $\partial(T \llcorner \mathcal{M})$, we note that Steps 2 to 5 ensure that $Q_{\eta,\xi}$ takes values in $\mathcal{N}$ whenever meeting the boundary of the slice and $Q_{\eta,\xi}$ having trivial homotopy class. For an arbitrary $Q \in N$, we can define $Q_{\eta,\xi} := Q$ on a disk of size η in the middle of the slice and again by linear interpolation of the phase towards the boundary of the disk. We thus get a function $Q_{\eta,\xi} \in H^1(\Upsilon_{0,3\eta^\gamma}, \mathcal{N})$ respecting the previous constructions and $Q = Q_b$ on $\mathcal{M}$. Furthermore, the interpolation allows us to estimate $|\nabla Q|^2 \leq C((\eta^\gamma)^{-2} + \eta^{-2})$

and since g is bounded, $f(Q) = 0$ (because Q takes values in $\mathcal{N}$) the energy contribution can be estimated

$$\begin{aligned}\eta\mathcal{E}_{\eta,\xi}(Q, \Upsilon_{0,3\eta^\gamma}) &\leq C\,\eta\,|\Upsilon_{0,3\eta^\gamma}|\left(\frac{1}{(\eta^\gamma)^2}+\frac{1}{\eta^2}+1\right)\\ &\leq C\,\mathbb{M}(\partial(T\llcorner\mathcal{M})\setminus\partial T)\left(\eta+\frac{(\eta^\gamma)^2}{\eta}+\eta(\eta^\gamma)^2\right),\end{aligned}$$

which vanishes in the limit $\eta, \xi \to 0$ due to our hypothesis about the size of $\partial(T\llcorner\mathcal{M})\setminus\partial T$.

It remains the region where S detaches from $\mathcal{M}$ or in other words $\Upsilon_{1,3\eta^\gamma} := \{x \in \Omega : \operatorname{dist}(x, \partial(\partial(T\llcorner\mathcal{M})\setminus S)) \leq 3\eta^\gamma\}$. We can also use interpolation to construct $Q_{\eta,\xi}$ and estimate its energy but we need to be a bit more careful since this time $f(Q_{\eta,\xi})$ cannot be chosen to be zero. This is due to the isotropic core of our construction around S. So we connect the 'core' parts from Step 4 and 5 where we defined S in Ω and close to $\mathcal{M}$ that is the profile Q_B which has been used in both steps. Around this tube, we can again apply the previous idea of linear interpolation of the phase, this time on slices perpendicular to the tube. We end up with

$$\mathcal{E}_{\eta,\xi}(Q_{\eta,\xi}, \Upsilon_{1,3\eta^\gamma}) \leq C\eta^\gamma\mathbb{M}(\partial(\partial(T\llcorner\mathcal{M})\setminus\partial T)),$$

which vanishes in the limit $\eta \to 0$ in view of the bound $\mathbb{M}(\partial(\partial(T\llcorner\mathcal{M})\setminus\partial T)) \leq C|\ln(\eta)|$. □

3.7 Regularity and optimality conditions for the limit problem

Let us first state an improved regularity results for minimizers of the energy $\mathcal{E}_0$:

Proposition 3.7.1. *Let T be a minimizer of (3.16) and $S = \partial T - \Gamma$. Then each component of $T\llcorner\Omega$ is an embedded manifold-with-boundary of class C^∞.*

Proof. The main work has been already carried out in the proof of Proposition 3.6.1 for $n = 0$. The higher regularity can be obtained by Schauder theory. For details we refer to Theorem 2.1 in [130]. □

Next, we give a characterization of minimizers of the limit energy. Because of the regularity given by Proposition 3.7.1, we can take variations of $T\llcorner\Omega$ and $S\llcorner\Omega$ in the classical sense to derive the optimality conditions. Furthermore, we can obtain a version of Young's law [138, 159]

Proposition 3.7.2. *Let T be a minimizer of (3.16) and $S = \partial T - \Gamma$. Then $T\llcorner\Omega$ has zero mean curvature and $S\llcorner\Omega$ is of constant curvature $\frac{8}{\pi}\frac{c_*}{s_*}\beta^{-1}$. Furthermore, Young's law holds*

$$\nu_{\partial(T\cap\Omega)}\cdot\nu_{\partial F^+} = \nu_{\mathcal{M}}\cdot\mathbf{e}_3 \quad \text{on } \partial(T\llcorner\Omega)\setminus S,$$

i.e. T meets $\mathcal{M}$ in an angle $\theta = \arccos(\nu_{\mathcal{M}}\cdot\mathbf{e}_3)$.

Proof. The first claim is a well known fact since the variation of $\mathbb{M}(T\llcorner\Omega)$ along a smooth vector field Ξ in Ω yields [111, Proposition 2.1.3]

$$(\mathbb{M}(T\llcorner\Omega))'(\Xi) = \int_{T\cap\Omega} H_T(\Xi\cdot\nu_T)\,\mathrm{d}x + \int_{\partial(T\cap\Omega)}(\Xi\cdot\nu_{\partial T})\,\mathrm{d}x, \tag{3.80}$$

where H_T is the mean curvature of T, ν_T is a normal vector of T and $\nu_{\partial T}$ is the inward normal vector of $\partial(T\llcorner\Omega)$ in the tangent space of T. With the same argument and since $\partial S = 0$, we get that

$$(\mathbb{M}(S))'(\Xi) = \int_S K_S(\Xi\cdot\nu_S)\,\mathrm{d}x, \tag{3.81}$$

where K_S is the curvature of S and ν_S is the normal vector of S in $\mathbb{R}^3$, such that the plane for the circle of maximal curvature is spanned by ν_S and a tangent vector to S. This yields for the boundary that

$$0 \;=\; \int_S \Xi \cdot \left(4 s_* c_* \nu_{\partial T} + \frac{\pi}{2} s_*^2 \beta K_S \nu_S \right) \, \mathrm{d}x \,,$$

from which we deduce $\nu_{\partial T} = \pm \nu_S$ and $K_S = \pm \frac{8}{\pi} \frac{c_*}{s_*} \beta^{-1}$. In particular, the circle of maximal curvature for S lies in the plane spanned by the tangent space of T. Finally, taking variations on $\mathcal{M}$ we get

$$\left(\int_{F^\pm} 1 \mp \cos(\theta) \, \mathrm{d}\omega \right)' (\Xi) \;=\; \int_{\partial F^\pm} (1 \mp \cos(\theta)) \, (\Xi \cdot \nu_{\partial F^\pm}) \, \mathrm{d}\omega \,.$$

Since $\nu_{\partial F^-} = -\nu_{\partial F^-}$, we hence get

$$\left(\int_{F^+} 1 - \cos(\theta) \, \mathrm{d}\omega + \int_{F^-} 1 + \cos(\theta) \, \mathrm{d}\omega \right)' (\Xi) \;=\; - \int_{\partial F^+} 2 \cos(\theta) (\Xi \cdot \nu_{\partial F^+}) \, \mathrm{d}\omega \,. \tag{3.82}$$

As in the proof of Theorem 19.8 in [117], (3.80) and (3.82) combine to

$$0 \;=\; \int_{\partial F^+} \Xi \cdot (4 s_* c_* \nu_T|_{\mathcal{M}} - 4 s_* c_* \cos(\theta) \nu_{\partial F^+}) \, \mathrm{d} \,.$$

If we take a variation with $\Xi \cdot \nu_{\mathcal{M}} = 0$ and write

$$\Xi \cdot \nu_T|_{\mathcal{M}} \;=\; \Xi \cdot ((\nu_{\partial T} \cdot \nu_{\partial F^+}) \nu_{\partial F^+}) \;+\; \Xi \cdot ((\nu_T|_{\mathcal{M}} \cdot \tau) \tau)$$

where τ is a unit tangent vector to $\mathcal{M}$, perpendicular to $\nu_{\partial F^+}$, we get

$$\Xi \cdot ((\nu_{\partial T} \cdot \tau) \tau) \;=\; 0 \qquad \text{and} \qquad \nu_{\partial T} \cdot \nu_{\partial F^+} \;=\; \cos(\theta) \,.$$

The first equality is automatically true since $\nu_{\partial T} \cdot \tau = 0$ ($\nu_{\partial T}$ can only have a component in direction $\nu_{\partial F^+}$ and one in direction $\nu_{\mathcal{M}}$) and the second one implies that

$$\nu_{\partial T} \cdot \nu_{\partial F^+} \;=\; \nu_{\mathcal{M}} \cdot \mathbf{e}_3 \,.$$

□

Chapter 4

Numerical minimization of the limit energy

4.1 Introduction

Finding a surface with minimal area and a given boundary is a classical problem since its introduction by Lagrange [103]. Solutions to this so-called *Plateau problem* are *minimal surfaces* and have been studied extensively since then [59, 140, 155]. In some particular cases, analytic tools allow for explicit solutions or characterizations, see [50, 55, 93, 94, 134].

Whenever the boundary and ambient space do not disclose an exact solution, the question of numerical approximation arises. Different approaches have been developed to represent surfaces and how to ensure their minimality. Most famous is the *mean curvature flow* [35, 60], based on the vanishing mean curvature optimality condition for minimal surfaces. Although originally developed for hypersurfaces, the concept has been rapidly generalized to arbitrary codimension [11]. While the standard approach consists in representing the surface via a level set, more recently varifolds constituted by point clouds are also used [39]. In addition to classical algorithms, it is also possible to employ machine learning techniques such as training neural networks to simulate a mean curvature flow [36]. Another very successful ansatz is to model the surface as jump set of a BV−function and therefore minimizing the total variation leads to minimal surfaces. The total variation is then discretized via finite difference or finite elements [46, 48, 84, 164], although other choices also prove to be useful [1].

Compared to all of the aforementioned methods, the treatment of our limit energy $\mathcal{E}_0$ exhibits the major challenge of optimizing a surface *and* its boundary simultaneously. While mean curvature flows of both objects independently are known and implemented, their joint minimization might cause conflict due to possible contradicting movements close to the boundary. In the following, we will use an approach related to the minimization of the total variation.

4.2 Theoretical background

As a first step, we consider a toy problem without particle. Let K be an open Lipschitz domain of finite measure in which we will state our problem. The goal is to find a flat chain T supported in K which minimizes $\mathbb{M}(T) + \beta\mathbb{M}(\partial T)$, i.e. formally, we want to solve

$$\min_{\substack{T\in\mathcal{F}^2,\\ \operatorname{supp}(T)\subset K}} \quad \mathbb{M}(T) \;+\; \beta\,\mathbb{M}(\partial T)\,. \tag{4.1}$$

Note that this problem is trivial since we did not include the line Γ into our problem. The main simplification we are going to apply is to take the objects $T, \partial T$ in the space of currents rather than flat chains resulting in a convex optimization problem. Then, we reformulate Problem (4.1)

in terms of vector fields. If we assume that T and ∂T are regular enough, let ν_T be a unit normal vector field on T and $\tau_{\partial T}$ a normal tangent vector field on ∂T (with induced orientation). Then, it holds that

$$\mathbb{M}(T) \;=\; \int_T 1 \,\mathrm{d}\mathcal{H}^2 \;=\; \sup_{\substack{p\in L^\infty(K,\mathbb{R}^3)\\ \|p\|_{L^\infty}\le 1}} \int_T p\cdot\nu_T \,\mathrm{d}\mathcal{H}^2\,,$$

and

$$\mathbb{M}(\partial T) \;=\; \sup_{\substack{q\in L^\infty(K,\mathbb{R}^3)\\ \|q\|_{L^\infty}\le 1}} \int_{\partial T} q\cdot\tau_{\partial T} \,\mathrm{d}\mathcal{H}^1\,.$$

By Stokes' Theorem it holds that (at least formally, if q is smooth enough)

$$\int_{\partial T} q\cdot\tau_{\partial T}\,\mathrm{d}x \;=\; \int_T \mathrm{curl}(q)\cdot\nu_T\,\mathrm{d}x\,.$$

If we think of u, a $\mathbb{R}^3-$valued measure compactly supported on K, i.e. $u\in\mathbf{M}(K)^3$, as representation of T, the above reasoning justifies the definition of

$$\mathbf{C}(u,K) \;:=\; \sup\Big\{\int_K \mathrm{curl}(\phi)\cdot\,\mathrm{d}u \;:\; \phi\in C_c^\infty(K,\mathbb{R}^3),\,\|\phi\|_\infty\le 1\Big\}\,, \tag{4.2}$$

as proxy for the boundary ∂T. With this definition, we may replace problem (4.1) by

$$\inf_{u\in\mathbf{M}(K)^3}\int_K \mathrm{d}\|u\| \;+\; \beta\;\mathbf{C}(u,K)\,, \tag{4.3}$$

In order to incorporate Γ, we need to replace ∂T in the energy by $\partial T+\Gamma$ and to add the tangential vector field of Γ. If formally $\mathrm{curl}(u_0)$ is the vector-valued measure $\tau_\Gamma\mathcal{H}^1\llcorner\Gamma$, for some $u_0\in\mathbf{M}(K)^3$, then we can modify the preceding problem as

$$\inf_{u\in\mathbf{M}(K)^3}\int_K \mathrm{d}\|u\| \;+\; \beta\;\mathbf{C}(u+u_0,K)\,. \tag{4.4}$$

It remains to include the particle $E\subset\subset K$ and the energy coming from its surface $\mathcal{M}=\partial E$. Let $\Omega := K\setminus\overline{E}$. We then write

$$\inf_{u\in\mathbf{M}(K)^3}\int_\Omega \mathrm{d}\|u\| \;+\; \int_{\mathcal{M}} |\nu_3|\,\mathrm{d}\|u\| \;+\; \beta\;\mathbf{C}(u+u_0,K)\,. \tag{4.5}$$

Remark 4.2.1 (Well-posedness)**.** *It is not imminent that the problem in* (4.5) *is well posed. This is due to the fact that $|\nu_3|=0$ on Γ, and hence a minimizing sequence of* (4.5) *might accumulate mass on Γ and the limiting object is not a current any more despite being of finite energy. We overcome this issue in the following by introducing a small parameter $0<\varepsilon\ll 1$ and replacing $|\nu_3|$ by $\max\{|\nu_3|,\varepsilon\}$, i.e. we consider*

$$\inf_{u\in\mathbf{M}(K)^3}\int_\Omega \mathrm{d}\|u\| \;+\; \int_{\mathcal{M}} \max\{|\nu_3|,\varepsilon\}\,\mathrm{d}\|u\| \;+\; \beta\;\mathbf{C}(u+u_0,K)\,. \tag{4.6}$$

With this modification, the mass of u is controlled by the constant ε^{-1} times the energy from (4.6).

Remark 4.2.2 (Relation to total variation minimization)**.** *The fundamental idea in what follows is to represent T by a vector field u and its boundary by* $\mathrm{curl}(u)$*. Inside T,* $\mathrm{curl}(u)$ *vanishes and u can be seen as a (local) gradient of some scalar potential ϕ. Minimizing the mass of T (represented by the L^1-norm of u) and hence the L^1-norm of $\nabla\phi$ can be interpreted as minimizing the total variation of ϕ.*

The problem of minimizing a total variation has attracted a lot of attention in recent years [1, 46, 48, 84]. Our problem differs since we consider a general vector field u (in contrast to the classical total variation problems where $u=\nabla\phi$) and we have an additional L^1-term in our minimization that depends on the derivative of u. The latter fact contrasts with problems e.g. from image reconstruction where terms like $\|\phi-\phi_0\|_{L^2}^2$ are considered. We point out that the subject of [164] is the case when $\mathrm{curl}(u)=\mathrm{curl}(u_0)$ is prescribed. This can be seen as a total variation minimization for solving the classical Plateau problem.

Remark 4.2.3 (Differential forms). *In the smooth case, problem* (4.4) *can also be stated via differential forms. Let* $\Omega^k(K)$ *denote the space of differential* $k-$*forms. We can identify* $\Omega^1(K)$ *with vector fields in* K *and* (4.4) *can be reformulated as finding a* $1-$*form* ω_T *with* $\int_K \omega_T \wedge \eta = \int_T \eta$ *for all* $\eta \in \Omega^2(K)$ *minimizing the mass norm*

$$\|\omega_T\|_{\text{Mass}} \;=\; \sup_{\substack{\eta\in\Omega^2(K)\\ \|\eta\|_\infty\le 1}} \int_K \eta\wedge\omega_T\,.$$

The boundary ∂T *corresponds to a* $2-$*form* $\omega_{\partial T}$ *with* $\omega_{\partial T} = \mathrm{d}\omega_T$. *Indeed, by Stokes' Theorem it holds that for any* $\eta \in \Omega^1(K)$ *which vanishes on* ∂K

$$\int_K \eta\wedge\omega_{\partial T} \;=\; \int_{\partial T}\eta \;=\; \int_T \mathrm{d}\eta \;=\; \int_K \mathrm{d}\eta\wedge\omega_T \;=\; \int_K \eta\wedge\,\mathrm{d}\omega_T\,.$$

Hence, Problem (4.4) *is essentially the same as to minimize* $\|\omega\|_{\text{Mass}} + \beta\|\mathrm{d}\omega + \mathrm{d}\omega_0\|_{\text{Mass}}$ *among all* $\omega \in \Omega^1(K)$, *where* ω_0 *is* $1-$*form with boundary* Γ.

4.3 Numerical simulation

In order to solve Problem (4.3) we use a finite element discretization and then employ an Alternating Direction Method of Multipliers (ADMM) algorithm for the optimization.

4.3.1 Finite element discretization

We start by introducing the finite element spaces that we will use in the further course of this chapter. The definition we give here is standard and can be found in many books on finite elements, for example [64] or [110, Ch. 3].

Definition 4.3.1 (Finite element spaces). *Let* $\mathcal{T}_h$ *be a tetrahedral mesh of* K *consisting of a set of nodes* $\mathcal{N}_h$, *edges* $\mathcal{E}_h$, *faces* $\mathcal{F}_h$ *and tetrahedra* $\mathcal{T}_h$. *We call a* finite element space *a finite dimensional function space* $\mathcal{V}$ *(in our case a subspace of polynomials) defined on a domain* $\mathcal{D}$ *(here the tetrahedra of* $\mathcal{T}_h$*) and a set of degrees of freedom* $\mathcal{L}$ *which form a basis of the dual space of* $\mathcal{V}$ *(unisolvence). For* $T \in \mathcal{T}_h$, *let* $\mathcal{P}_q(T)$ *be the space of polynomials on* T *with degree smaller or equal to* $q \ge 0$ *and* $\overline{\mathcal{P}}_q(T)$ *the polynomials over* T *with degree equal to* q.

1. *The* Lagrange-element *of order* 1 *is given by*

$$\mathcal{D} = T\,, \qquad \mathcal{V} = \mathcal{P}_1(T)\,,$$

where $T \in \mathcal{T}_h$ *and* $\mathcal{L}$ *consists of function evaluations at the nodes of* T. *We call* P^1 *the corresponding finite element space defined on* $\mathcal{T}_h$.

2. *The* discontinuous Lagrange-element *of order* 0 *is given by*

$$\mathcal{D} = T\,, \qquad \mathcal{V} = \mathcal{P}_0(T)\,,$$

where $T \in \mathcal{T}_h$ *and* $\mathcal{L}$ *consists of the function evaluation at the center of mass of* T. *The corresponding finite element space defined on* $\mathcal{T}_h$ *is denoted by* P^0 *and the vector valued version* $\mathbb{P}^0 := (P^0)^3$.

3. *Next, the* Nédélec-element *of the first kind of order* 1 *is given by*

$$\mathcal{D} = T\,, \qquad \mathcal{V} = (\mathcal{P}_0(T))^3 + x\times\overline{\mathcal{P}}_0(T)\,,$$

for $T \in \mathcal{T}_h$. *The degrees of freedom* $\mathcal{L}$ *for a function* $v \in \mathcal{V}$ *are given by the integrals of* $v\cdot t_e$ *over the edges* $e \in \mathcal{E}_h$ *that are included in the boundary* ∂T, t_e *denoting the tangential vector of* e. *The finite element space consisting of Nédélec-elements of order* 0 *is denoted by* Ned.

4. *We define the* Raviart-Thomas-element *of order* 0 *as*

$$\mathcal{D} = T\,, \qquad \mathcal{V} = (\mathcal{P}_0(T))^3 + x\overline{\mathcal{P}}_0(T)\,,$$

for $T \in \mathcal{T}_h$. The degrees of freedom $\mathcal{L}$ for a function $v \in \mathcal{V}$ are given by the integrals of $v \cdot n_F$ over the facets $F \in \mathcal{F}_h$ that are included in the boundary ∂T, n_F denoting the normal vector of F. The finite element space consisting of Raviart-Thomas-elements of order 0 *is denoted by* RT.

Each finite element space V comes with a projection operator Π_V which allows us to pass from functions defined on Ω to finite element approximations over $\mathcal{T}_h$.

We note that $\nabla v \in \text{Ned}$ if $v \in P^1$, $\text{curl}(v) \in \text{RT}$ if $v \in \text{Ned}$ and $\text{div}(v) \in P^0$ if $v \in \text{RT}$. More precisely, we have the following proposition:

Proposition 4.3.2. *The diagram*

$$\begin{array}{ccccccccccc}
\mathbb{R} & \longrightarrow & H^1 & \xrightarrow{\nabla} & H(\text{curl}) & \xrightarrow{\text{curl}} & H(\text{div}) & \xrightarrow{\text{div}} & L^2 & \longrightarrow & 0 \\
 & & \downarrow{\scriptstyle \Pi_{P^1}} & & \downarrow{\scriptstyle \Pi_{\text{Ned}}} & & \downarrow{\scriptstyle \Pi_{\text{RT}}} & & \downarrow{\scriptstyle \Pi_{P^0}} & & \\
\mathbb{R} & \longrightarrow & P^1 & \xrightarrow{\nabla} & \text{Ned} & \xrightarrow{\text{curl}} & \text{RT} & \xrightarrow{\text{div}} & P^0 & \longrightarrow & 0
\end{array}$$

commutes and the rows are short exact sequences.

Proof. The upper row is just the usual de Rham-complex for a simply connected Lipschitz domain in $\mathbb{R}^3$. The lower row is its discrete analogue, see Prop. 16.15 in [64]. For the commutation properties, we refer to Chapter 16.1.2 and Chapter 16.2.2 and Lemma 16.16 in [64]. □

Since T and ∂T are measures, we cannot assume regularity and need to discretize them with finite elements of lowest possible order, e.g. $\mathbb{P}^0-$elements. We therefore choose to represent u as a Nédélec function, noting that its curl belongs to RT and can be seen as a subset of $\mathbb{P}^0$. We thus rewrite Problem (4.4) as

$$\inf_{u \in \text{Ned}} \int_K |\Pi_{P^0}(u)|\,\mathrm{d}x \;+\; \beta \int_K |\text{curl}(u) + \text{curl}(u_0)|\,\mathrm{d}x\,, \tag{4.7}$$

where $u_0 \in \text{Ned}$ is an approximation for the tangential vector field τ_Γ.

Note that the choice of Nédélec elements is not canonic and other choices are possible. For example in [45], Crouzeix-Raviart elements are used for a total variation minimization problem. The approximation of the solutions obtained there is sharper compared to the Nédélec/P^1 elements. Also other finite elements could be used as long as they verify a variant of Proposition 4.3.2 and in particular the image and kernel of the discrete curl$-$operator are known, see [16, Ch. 7]. In order to decide which elements to use one must then balance the quality of the approximations for T and S given by the size of ker(curl) and im(curl), as well as the computational cost required by the finite elements.

Remark 4.3.3 (Relation to discrete total variation minimization)**.** *In view of Proposition 4.3.2, Remark 4.2.2 can be translated into the finite element setting as follows: If $u \in$* Ned *such that* $\text{curl}(u) = 0 \in \text{RT}$*, then by exactness of the sequence there exists $\phi \in P^1$ such that $u = \nabla\phi$.*

In order to find a finite element representation of (4.6), we introduce a density function $\rho_\delta \in C^0(\overline{\Omega})$, defined for $0 < \delta \ll 1$ and $x \in \overline{\Omega}$ as $\rho_\delta(x) = \max\{|\nu_3(\Pi_{\mathcal{M}}(x))|, \varepsilon\}$ if $\text{dist}(x, \mathcal{M}) \leq \delta$ and $\rho_\delta(x) = 1$ if $\text{dist}(x, \mathcal{M}) > 2\delta$, $\varepsilon > 0$ being the parameter introduced in Remark 4.2.1. The parameter δ determines the size of the boundary layer $\mathcal{M}_\delta := \{x \in \overline{\Omega} \,:\, x = \omega + r\nu(\omega) \text{ for } \omega \in \mathcal{M}, r \in [0, \delta]\}$ which will serve as proxy for $\mathcal{M}$. We choose the approximation $u_{0,\delta}$ of u_0 to be centred at distance $\frac{\delta}{2}$ from $\mathcal{M}$ and supported in $\mathcal{M}_\delta \setminus \mathcal{M}_{\delta/4}$ such that $u_{0,\delta,h} \overset{*}{\rightharpoonup} u_0$ in $\mathbf{M}(K)^3$. We

furthermore use the notation $\Omega_\delta := \Omega \setminus \mathcal{M}_\delta$. For $u_h \in \mathrm{Ned}$ and $u_{0,\delta,h} := \Pi_{\mathrm{Ned}}(u_{0,\delta})$ we then define

$$\mathcal{E}_{h,\delta}(u_h) = \begin{cases} \int_K \rho_\delta |\Pi_{P^0}(u_h)| \,\mathrm{d}x + \beta \int_K |\mathrm{curl}(u_h) + \mathrm{curl}(u_{0,\delta,h})| \,\mathrm{d}x & \text{if } u_h \equiv 0 \text{ in } E\,, \\ +\infty & \text{otherwise.} \end{cases} \tag{4.8}$$

We next show that for $\delta = \sqrt{h}$, the functional $\mathcal{E}_{h,\delta}$ approaches (4.4) in a variational sense when $h \to 0$.

Proposition 4.3.4. *Let $\delta := \sqrt{h}$. Then, the energy $\mathcal{E}_{h,\delta}$ $\Gamma-$converges to the energy in* (4.6) *with respect to the weak*-topology of measures.*

Proof. Let $\varepsilon > 0$ be fixed, $\delta > 0$, $u_h \in \mathrm{Ned}$ and $u_{0,\delta,h} \in \mathrm{Ned}$ be the previously described approximation for the tangential vector field τ_Γ w.r.t. the weak*-topology of vector valued measures. We note that a function v of the Nédélec space on a tetrahedron $T \in \mathcal{T}_h$ can be written as

$$v|_T(x) = v(c_T) + \mathrm{curl}(v|_T) \times (x - c_T)\,, \tag{4.9}$$

where c_T is the center of mass of the cell T, $\mathrm{curl}(v|_T)$ is a constant vector on each cell and $v(c_T) = \fint_T v \,\mathrm{d}x$. We can hence estimate $|u_h|_T - \Pi_{P^0}(u_h)|_T| \le Ch|\mathrm{curl}(u_h)|_T|$ which gives

$$\begin{aligned} \int_K |u_h - \Pi_{P^0}(u_h)| \,\mathrm{d}x &= \sum_{T\in\mathcal{T}_h} \int_T |u_h|_T - \Pi_{P^0}(u_h)|_T| \,\mathrm{d}x \\ &\le Ch \sum_{T\in\mathcal{T}_h} \int_T |\mathrm{curl}(u_h)|_T| \,\mathrm{d}x = Ch \int_K |\mathrm{curl}(u_h)| \,\mathrm{d}x\,. \end{aligned}$$

This allows to conclude that $u_h - \Pi_{P^0}(u_h) \overset{*}{\rightharpoonup} 0$ in the space of measures as $h \to 0$ and

$$\begin{aligned} \int_K |u_h| \,\mathrm{d}x &\le \int_K |\Pi_{P^0}(u_h)| \,\mathrm{d}x + \int_K |u_h - \Pi_{P^0}(u_h)| \,\mathrm{d}x \\ &\le C\Big(1 + \frac{1}{\varepsilon}\Big)\mathcal{E}_{h,\delta}(u_h) + C\delta\mathcal{H}^2(\mathcal{M}) + C\mathcal{H}^1(\Gamma)\,. \end{aligned}$$

We can therefore assume that (up to a subsequence) $u_h \overset{*}{\rightharpoonup} u$ as measures for some $u \in \mathbf{M}(K)^3$ with support outside of E.

For the liminf inequality, take $\phi \in C_c^\infty(K)^3$ with $|\phi|_\infty \le 1$ to get

$$\int_K \phi \cdot \mathrm{curl}(u_h + u_{0,\delta,h}) \,\mathrm{d}x = \sum_{T\in\mathcal{T}_h} \int_T \phi \cdot \mathrm{curl}(u_h + u_{0,\delta,h}) \,\mathrm{d}x\,.$$

Integration by parts on each mesh cell $T \in \mathcal{T}_h$ yields

$$\begin{aligned} \sum_{T\in\mathcal{T}_h} \int_T \phi \cdot \mathrm{curl}(u_h + u_{0,\delta,h}) \,\mathrm{d}x &= \sum_{T\in\mathcal{T}_h} \int_T \mathrm{curl}(\phi) \cdot (u_h + u_{0,\delta,h}) \,\mathrm{d}x \\ &\quad + \sum_{T\in\mathcal{T}_h} \int_{\partial T} \phi \cdot ((u_h + u_{0,h}) \times \nu_{\partial T}) \,\mathrm{d}x\,. \end{aligned}$$

We note that on boundary faces it holds $u_h = u_{0,\delta,h} = 0$. Furthermore, in the sum over all cells boundaries of the above calculation each interior face appears exactly twice but with opposite signs for the normal vector. Since the tangential components of Nédélec-functions are continuous across faces, it follows that the second sum on the right hand side vanishes. Thus,

$$\int_K \phi \cdot \mathrm{curl}(u_h + u_{0,\delta,h}) \,\mathrm{d}x = \int_K \mathrm{curl}(\phi) \cdot (u_h + u_{0,\delta,h}) \,\mathrm{d}x\,. \tag{4.10}$$

By choosing the size of the regularization δ much larger than than the discretization h, e.g. by setting $\delta(h) := \sqrt{h}$, we can use the weak*-convergence of u_h and $u_{0,\delta,h}$ and take the supremum in ϕ to get

$$\liminf_{h,\delta(h)\to 0} \int_K |\mathrm{curl}(u_h) + \mathrm{curl}(u_{0,\delta,h})| \,\mathrm{d}x \;\geq\; \mathbf{C}(u+u_0, K)\,.$$

Now, we estimate

$$\int_K \rho_\delta |\Pi_{P^0}(u)| \,\mathrm{d}x \;\geq\; \int_{\mathcal{M}_\delta} \rho_\delta |\Pi_{P^0}(u)| \,\mathrm{d}x \;+\; \int_{\Omega\setminus\mathcal{M}_{2\delta}} |\Pi_{P^0}(u)| \,\mathrm{d}x\,.$$

Since Ω is open and $\Omega = \bigcup_{\delta>0}(\Omega \setminus \mathcal{M}_{2\delta})$, it holds that

$$\liminf_{h,\delta(h)\to 0} \int_{\Omega\setminus\mathcal{M}_{2\delta}} |\Pi_{P^0}(u_h)| \,\mathrm{d}x \;\geq\; \int_\Omega \mathrm{d}\|u\|\,.$$

For the integral over $\mathcal{M}_\delta$, it holds

$$\int_{\mathcal{M}_\delta} \rho_\delta |\Pi_{P^0}(u_h)| \,\mathrm{d}x \;\geq\; \int_{\mathcal{M}} \max\{|\nu_3|, \varepsilon\} \int_0^\delta |\Pi_{P^0}(u_h)| \,\mathrm{d}r \,\mathrm{d}\omega - C\delta h\,.$$

In the limit $h, \delta(h) \to 0$ we recover $\int_{\mathcal{M}_\delta} \rho_\delta |\Pi_{P^0}(u_h)| \,\mathrm{d}x \geq \int_{\mathcal{M}} \max\{|\nu_3|, \varepsilon\} \,\mathrm{d}\|u\|$ which concludes the proof of the lower bound.

For the upper bound, let u be a vector valued measure. We assume that $u \equiv 0$ in E, otherwise the result is trivial. We regularize u on a scale $0 < \kappa \ll 1$ through a convolution with $\zeta_\kappa = \frac{1}{\kappa^3}\zeta(\cdot/\kappa)$, where ζ is a standard convolution kernel with $\zeta \in [0,1]$, $\mathrm{supp}\,(\zeta) \subset B_1(0)$, $\int \zeta = 1$ and smoothly shift the support of the resulting function by κ in direction normal to $\mathcal{M}$ so that the function sequence is supported in Ω. We discretise the regularized functions u_κ in Ω, i.e. we pose $u_{h,\kappa} := \Pi_{\mathrm{Ned}}(u_\kappa)$. Note that by the properties of the Nédélec interpolation operator Π_{Ned} it holds the estimate

$$\|u_{h,\kappa} - u_\kappa\|_{L^1} \;\lesssim\; h|u_\kappa|_{H^1} \;\lesssim\; \frac{h}{\kappa}\int \mathrm{d}\|u\|\,. \tag{4.11}$$

In view of this estimate, we choose $\kappa(h) := h^{\frac{3}{4}}$ such that $h/\kappa \to 0$ as $h \to 0$. Furthermore, it is natural to demand that the regularization of $u \llcorner \mathcal{M}$ is contained in $\mathcal{M}_\delta$. By our choices of $\kappa(h) = h^{\frac{3}{4}} \ll \delta(h) = h^{\frac{1}{2}}$ this is satisfied for h small enough.

For the integral $\int_K |\mathrm{curl}(u_{h,\kappa} + u_{0,\delta,h})| \,\mathrm{d}x$, we want to use the same idea as in the lower bound. We hence rewrite the absolute values as a supremum using functions $\phi \in C_c^\infty(K)^3$ with $|\phi|_\infty \leq 1$ and use the formula in (4.10). We then get

$$\limsup_{h,\kappa(h),\delta(h)\to 0} \int_K |\mathrm{curl}(u_{h,\kappa} + u_{0,\delta,h})| \,\mathrm{d}x \;=\; \sup_{\substack{\psi\in\mathcal{C}_c^\infty(K)\\ \|\phi\|_\infty\leq 1}} \int_K \mathrm{curl}(\phi)\cdot(u+u_0) \,\mathrm{d}x \;=\; \mathbf{C}(u+u_0, K)\,,$$

where we used (4.11) and the weak* convergences $u_\kappa \overset{*}{\rightharpoonup} u$ and $u_{0,\delta} \overset{*}{\rightharpoonup} u_0$ as $\delta, \kappa, h \to 0$.

The integral $\int_{\Omega_\delta} |\Pi_{P^0}(u_{h,\kappa})| \,\mathrm{d}x$ passes to the limit $h, \kappa(h), \delta(h) \to 0$ again due to (4.11) and the weak* convergence of u_κ. It remains the estimate of $\int_{\mathcal{M}_\delta} \rho_\delta |\Pi_{P^0}(u_{h,\kappa})| \,\mathrm{d}x$. For this we note that since $h \ll \kappa(h) \ll \delta(h)$, it holds

$$\limsup_{h,\kappa(h),\delta(h)\to 0} \int_{\mathcal{M}_\delta} \rho_\delta |\Pi_{P^0}(u_{h,\kappa})| \,\mathrm{d}x \;\leq\; \int_{\mathcal{M}} \max\{|\nu_3|, \varepsilon\} \,\mathrm{d}\|u\|\,.$$

□

4.3.2 ADMM-algorithm

To minimize the energy in (4.8) numerically, we employ the Alternating Direction Method of Multipliers (ADMM) [74]. This algorithm requires our problem to be of the form [32, Sec. 3]

$$\min_{x\in\mathbb{R}^{n_x},\, y\in\mathbb{R}^{n_y}} F(x)+G(y) \quad \text{subject to } Ax+By=c\in\mathbb{R}^{n_c}\,. \tag{4.12}$$

Then, one performs alternating minimizations in x and y as well as updates of the dual variable z of the augmented Lagrangian

$$L(x,y,z) \;=\; F(x)+G(y)+z^\top(Ax+By-c)+\frac{\varpi}{2}\|Ax+By-c\|^2\,.$$

We first reformulate (4.8) to fit into this scheme. With a little abuse of notation, we identify the finite element functions and their vectors of degrees of freedom. We set $x := u$, $y := (p,q)$, $z := (\lambda,\mu)$ and define the density functions

$$p_{\max} := \begin{cases} 1 & \text{if } x\in\Omega_h\,,\\ \max\{|\nu_3(x)|,\varepsilon\} & \text{if } x\in\mathcal{M}_h\,,\\ +\infty & \text{otherwise,}\end{cases} \qquad \text{and} \qquad q_{\max} := \begin{cases}\beta & \text{if } x\in\Omega\,,\\ +\infty & \text{otherwise.}\end{cases}$$

Defining the objective functions F and G by

$$F(u) := 0 \qquad G(p,q) := \|p_{\max}p\|_{L^1} \;+\; \|q_{\max}q\|_{L^1}\,,$$

subject to the constraints

$$\begin{pmatrix}1\\ \mathrm{curl}\end{pmatrix}u \;+\; \begin{pmatrix}-1 & 0\\ 0 & -1\end{pmatrix}\begin{pmatrix}p\\ q\end{pmatrix} \;=\; \begin{pmatrix}0\\ \mathrm{curl}(u_0)\end{pmatrix}\,,$$

we transformed the minimization of (4.8) into a problem suitable for ADMM. We furthermore write $\varpi=(\gamma_M,\gamma_C)$ for the stepsizes used inside the algorithm. Our ADMM scheme is summarized in Algorithm 1.

The minimization procedures in Algorithm 1 are carried out using the optimality conditions and solving the associated linear systems. More precisely, for the minimization in line 2 of Algorithm 1 we solve the weak formulation

$$0 \;=\; \gamma_C\langle\mathrm{curl}(u),\mathrm{curl}(v)\rangle+\gamma_M\langle u,v\rangle-\langle(\lambda+\gamma_C p),\mathrm{curl}(v)\rangle-\langle(\mu+\gamma_M q),v\rangle \quad \forall v\in\mathrm{Ned}\,. \tag{4.13}$$

Line 3 and 4 are computed by

$$\begin{cases} p \;=\; \frac{1}{\gamma_M}\left(\Big(\max\{|\overline{p}|/p_{\max},1\}\Big)^{-1}-1\right)\overline{p}\,, & \overline{p}=\lambda-\gamma_M\Pi_{\mathbb{P}^0}(u)\,,\\ q \;=\; \frac{1}{\gamma_C}\left(\Big(\max\{|\overline{q}|/q_{\max},1\}\Big)^{-1}-1\right)\overline{q}\,, & \overline{q}=\mu-\gamma_C\mathrm{curl}(u)\,.\end{cases}$$

Numerous modifications for speeding up ADMM are known [96]. We tested the "Accelerated Alternating Direction Method of Multipliers" from [96], the Nesterov acceleration as described in [80] as well as a simple over-relaxation scheme, finding that the latter leads to a faster convergence, while the others two had no noticeable influence on the speed.

Algorithm 1 ADMM algorithm for minimizing $\mathcal{E}_0$

Parameter: $\gamma_M, \gamma_C > 0$ (step sizes), $h > 0$ (mesh size), $\beta \geq 0$ (weight for $\mathbb{M}(S)$), $\phi \in [0, \pi]$ (angle of rotation), $w_E \gg 1$ (penalization weight inside E), $\varepsilon > 0$ (to avoid zero divisions)
Initialize: $p, q, \lambda, \mu \leftarrow 0 \in \mathbb{P}^0$
Initialize: $u \leftarrow 0 \in \mathrm{Ned}$
Initialize: $q_{\max} \leftarrow \Pi_{\mathbb{P}^0}(\beta \chi_\Omega + w_E \chi_E)$
Initialize: $p_{\max} \leftarrow \Pi_{\mathbb{P}^0}(1\, \chi_{\Omega \setminus \mathcal{M}_h} + \max\{|\nu \cdot \mathbb{H}|, \varepsilon\} \chi_{\mathcal{M}_h} + w_E \chi_E)$
1: **for** $k = 1, 2, \ldots$ **do**
2: $\quad u \leftarrow \arg\min_u \left\{ -\langle \lambda, u \rangle - \langle \mu, \mathrm{curl}(u) \rangle + \frac{\gamma_C}{2} \|q - \mathrm{curl}(u)\|_{L^2}^2 + \frac{\gamma_M}{2} \|p - u\|_{L^2}^2 \right\}$
3: $\quad q \leftarrow \arg\min_q \left\{ \|q_{\max} q\|_{L^1} + \langle \lambda, q \rangle + \frac{\gamma_C}{2} \|q - \mathrm{curl}(u)\|_{L^2}^2 \right\}$
4: $\quad p \leftarrow \arg\min_p \left\{ \|p_{\max} p\|_{L^1} + \langle \mu, p \rangle + \frac{\gamma_M}{2} \|p - u\|_{L^2}^2 \right\}$
5: $\quad \lambda \leftarrow \lambda + \gamma_C (q - \mathrm{curl}(u) - \mathrm{curl}(u_0))$
6: $\quad \mu \leftarrow \mu + \gamma_M (p - \Pi_{\mathbb{P}^0}(u))$
7: **end for**
Output: $E_h = \|p_{\max} p\|_{L^1(\Omega)} + \beta \|q\|_{L^1(\Omega)}$

4.3.3 Implementation

The finite element discretization and implementation of Algorithm 1 has been carried out using *FEniCS* [7,110], see also [104] for an introduction. For generating the meshes we use the program GMSH [78]. The visualization of the results is realised using ParaView [17].

Solving equations and projections. We perform the projections in Algorithm 1 by solving the linear system associated to the L^2-orthogonality relation verified by the projection. All matrices for the linear systems, including (4.13) are independent of the iteration step, and hence we assemble them only once before the iteration starts. For solving the system, we apply a solver using a $LU-$decomposition also calculated once in the beginning and assembling only the right hand side in each iteration.

Mesh and representation of Γ. From Chapter 3 we know that minimal configurations of T and S are concentrated inside the convex envelope of the particle. This is why we decided to create a mesh adapted to this situation, i.e. a fine mesh close to the surface $\mathcal{M}$ and inside the convex envelope, while far from $\mathcal{M}$ the mesh can be coarser, see Figure 4.1. In our case we choose the mesh size h to be between 0.03 on $\mathcal{M}$ and 0.3 at the boundary of the box. The simulations in which we investigate the influence of the angle between particle orientation and external field $\mathbf{H}$ are conducted by changing the vector $\mathbf{H}$, thus allowing to use the same mesh for all simulations of a particle. In order to obtain an accurate approximation, we also include the boundary layer $\mathcal{M}_h$ into the mesh generation. We choose the thickness of $\mathcal{M}_h$ to be equal to h, which gives satisfactory results from our experiences, see Figure 4.1b. We can furthermore perform a cut-out of our mesh, i.e. remove the cells inside E from our simulation, which significantly increases the speed of our code. In the case of the peanut mesh, this reduces the number of cells by more than 40%, see Figure 4.1a. We maintain a small layer inside E which is used to prevent the surface and its boundary to enter the particle and to create the initial condition: Using the level-set function of the shape, we calculate the normal field ν which allows us to define the function $\nu \cdot \mathbf{H}$. Then, we set $u_0 := \chi_E \nabla(\nu \cdot \mathbf{H})$. The vector field $\mathrm{curl}(u_0)$ serves as approximation for τ_Γ.

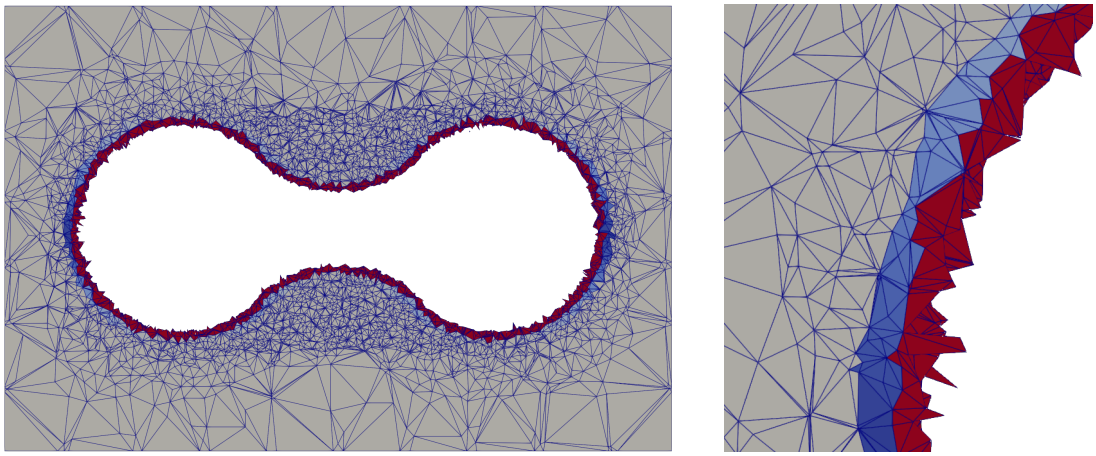

(a) (b)

Figure 4.1: Left: Mesh after removing the interior cells. The colors represent the values of $p_{\max}$: 10^5 inside the particle (red), $|\nu_3|$ in the boundary layer (shades of blue), 1 otherwise (grey). Right: Magnification of a part of the mesh.

Breaking symmetry: the parameter d_Γ. In the first simulations, we observed the behaviour that the algorithm converges, but the solution surface has holes or covers the whole of $\mathcal{M}$, see Figure 4.2. This phenomenon seems to be related to the non-uniqueness of the solution. By mirror symmetry of the particle, there are two distinct configurations which have the same energy and seem to superpose each other. Note that the curl we obtain in this situation is of order 10^{-2}, i.e. close to zero. To overcome this issue, we introduce the parameter d_Γ which acts as a shift for the initial condition in direction $\mathbf{H}$ and breaks the symmetry. Choosing $d_\Gamma := h$ is enough to eliminate this phenomenon, see e.g. Figure 4.5.

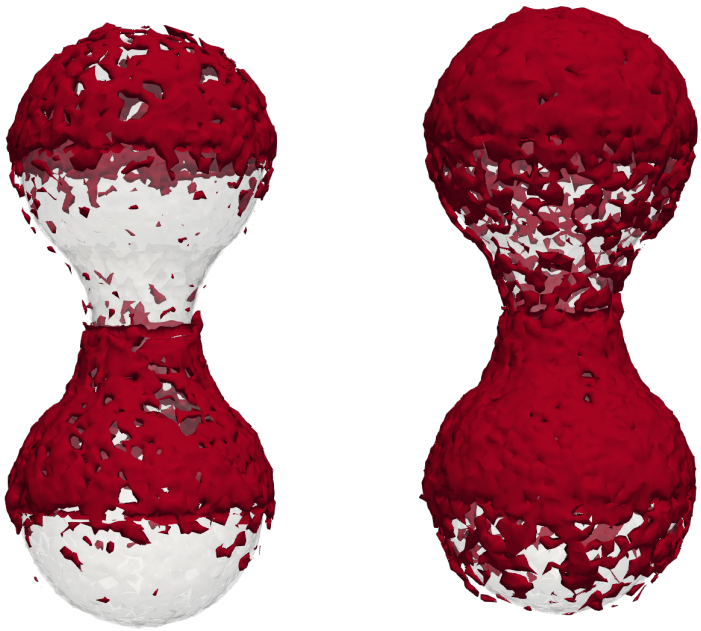

Figure 4.2: Different isosurfaces of a terminal configuration obtained for $\beta = 1$ after 4000 iterations with $d_\Gamma = 0$.

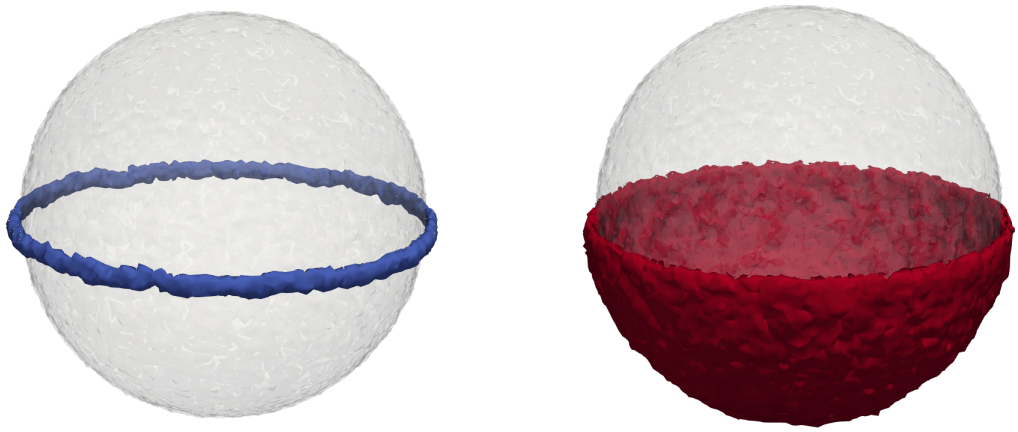

(a) (b)

Figure 4.3: Observed defect configurations: Saturn ring (a) for small values of β and dipole (b) for large β. The line S is indicated in red and T in blue.

4.4 Results

In this section we detail and comment on the numerical simulations we conducted to the three particle geometries: Sphere, Peanut and Croissant. In the case of the sphere, the minimizers of $\mathcal{E}_0$ are known to be the Saturn ring around the equator and the dipole, see Chapter 2. This case can thus serve as validation of our algorithm and the numerical implementation. The peanut-shape has been chosen because the rotational symmetry is broken along an axis. It is therefore possible to study the defect structures and the energy as function of a single angle ϕ between this axis and the external field $\mathbf{H}$. Since the peanut is also non-convex, one could hope to see a non-trivial $T \llcorner \Omega$. However, this is not observed in our simulations. Finally, the croissant is another non-convex particle for which certain parameter choices do result in a non-vanishing $T \llcorner \Omega$.

4.4.1 Spherical particle

The simulation of the spherical particle serves mainly as validation case for our algorithm. Running simulations for values of β between 0.01 and 1.1, we observe only a Saturn ring at the equator or a dipole, as expected from the theoretical analysis, see Figure 4.3.

Furthermore, the numerically calculated energy as function of the parameter β is linearly increasing for a Saturn ring configuration and constant (independent of β) for a dipole, see Figure 4.4. These findings are consistent with the behaviour calculated in Section 2.6, compare with Figure 2.6. Note that since we are calculating the globally energy minimizing configuration, it is not possible to reproduce the hysteresis phenomenon.

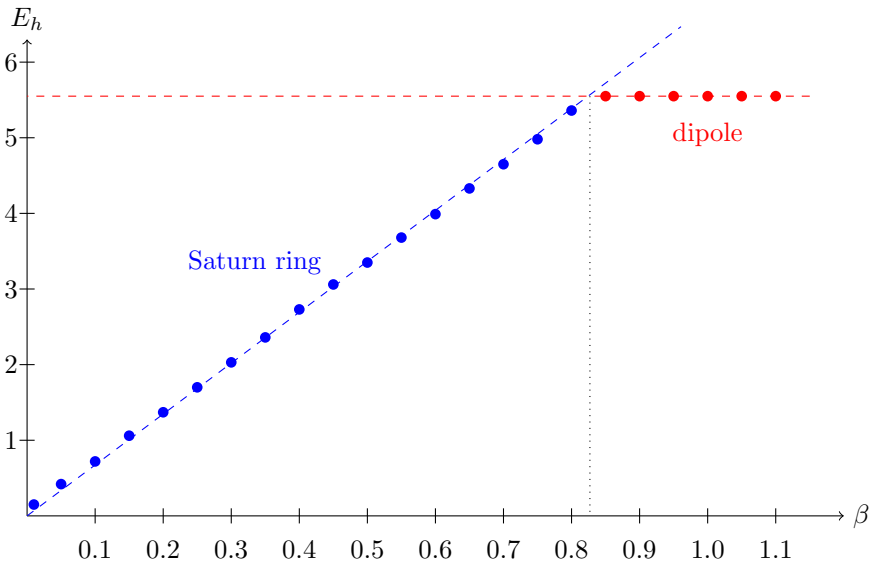

Figure 4.4: Energy of minimizers for different values of β around a sphere of radius 1. The mesh consists of around 449 000 cells of size $h = 0.03$ around the particle surface.

4.4.2 Peanut-shaped particle

In this subsection we present out findings about a non-spherical particle. The shape is constructed by combining three circle arcs (two bending outwards which are mirror images of each other, and one inwards) and then rotating the resulting curve to obtain a surface of revolution. The resulting object is therefore rotationally symmetric around an axis and exhibits additionally a mirror symmetry. We are interested how the angle ϕ between the symmetry axis of the peanut and the eternal field $\mathbf{H}$ influences the defect structures and energy.

For $\phi = \frac{\pi}{2}$, the results resemble the spherical case: There are only two observed configurations, Saturn ring and dipole, see Figure 4.5 (d) and (e). The plot of the energy as function of β in Figure 4.7 has the same qualitative behaviour as Figure 4.4. If $\phi = 0$ the situation is quite different: since Γ consists of three disjoint circle arcs, for β small, we see three Saturn rings surrounding the peanut, see Figure 4.5 (a). Note that the outer two Saturn rings are of type $-\frac{1}{2}$, while the inner one has to be a $+\frac{1}{2}-$defect for orientability reasons. In our program the difference of a $\pm\frac{1}{2}-$defect is represented by the fact that the vector field $\operatorname{curl}(u)$ (and q) have different orientations. Before attaining a dipole configuration for large β which consists of two disjoint components of $T \llcorner \mathcal{M}$ (as in Figure 4.5 (c)), there exists a regime for β in which two of the components of Γ are joined together by $T \llcorner \mathcal{M}$ and the third component still appears as a Saturn ring, see Figure 4.5 (b).

Comparing the found defect structures, we observe that depending on the number of connected components of Γ, we observe 1 or 3 Saturn rings for small β.

As the total length of Γ for different angles ϕ is not equal (in fact the length decreases when ϕ increases), it is natural to expect the slope of the energy as function of β to be monotonically decreasing as function of ϕ, being minimal for $\phi = \frac{\pi}{2}$. This is indeed the observed behaviour in Figure 4.7. Also the dipoles have different energy even though they always cover half of the particle. This can be explained through the weight $|\nu \cdot \mathbf{H}|$ in the integration over the surface, since for $\phi = 0$ a larger part of $\mathcal{M}$ is oriented perpendicular to $\mathbf{H}$, while for $\phi = \frac{\pi}{2}$ ν is close to parallel to $\mathbf{H}$ on a larger portion of the particle surface. We observe again a monotone behaviour of the energy w.r.t. ϕ, the minimal energy being given for $\phi = 0$. We conclude that $\phi = 0$ (resp. $\phi = \frac{\pi}{2}$) is the energetically preferred orientations for β large (resp. small). Notice that in the experiments conducted in [143, Fig. 1] these are by far the most frequently observed orientations.

As the peanut is non-convex, one could hope for the surface T to form outside the boundary layer $\mathcal{M}_h$. We did not observe this in our simulations which can heuristically be explained by the

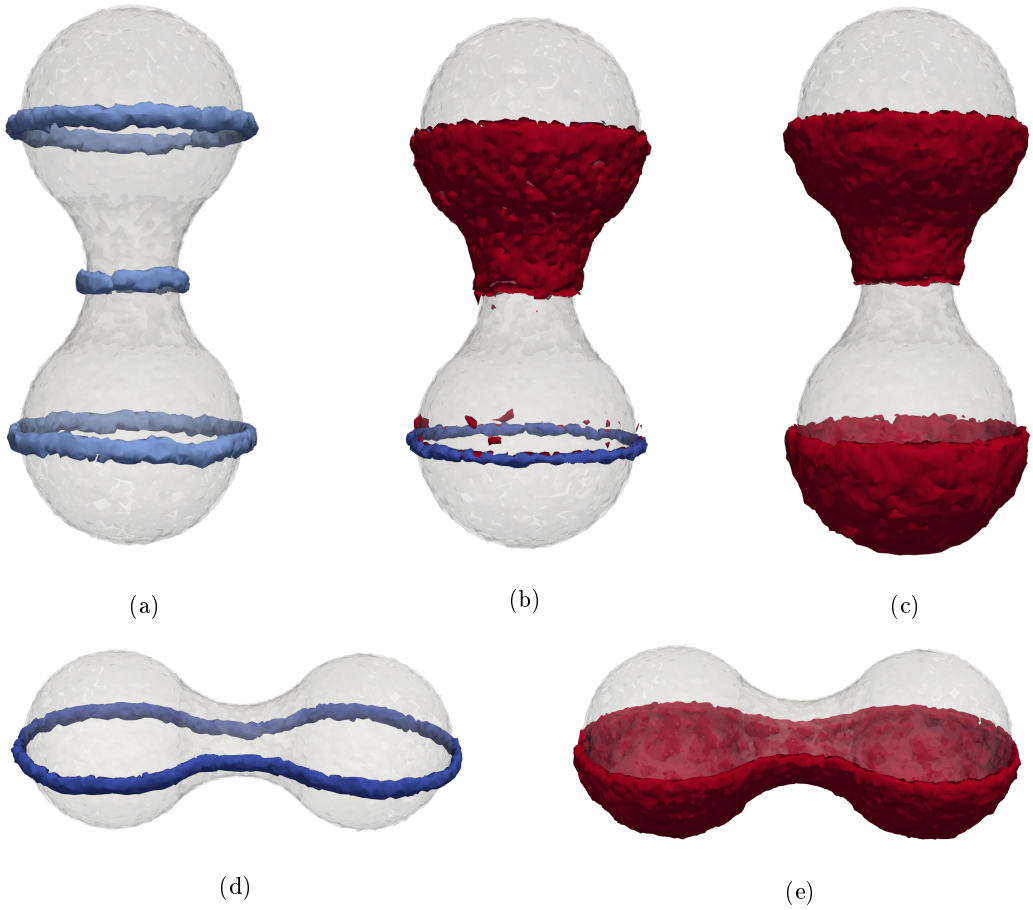

Figure 4.5: The observed defect configurations for $\phi = 0$ (a)-(c) are three Saturn rings (a), two components of Γ joined together leaving one Saturn ring (b) and dipole (c). For $\phi = \frac{\pi}{2}$ (d)-(e), we find a Saturn ring (d) and dipole (e).

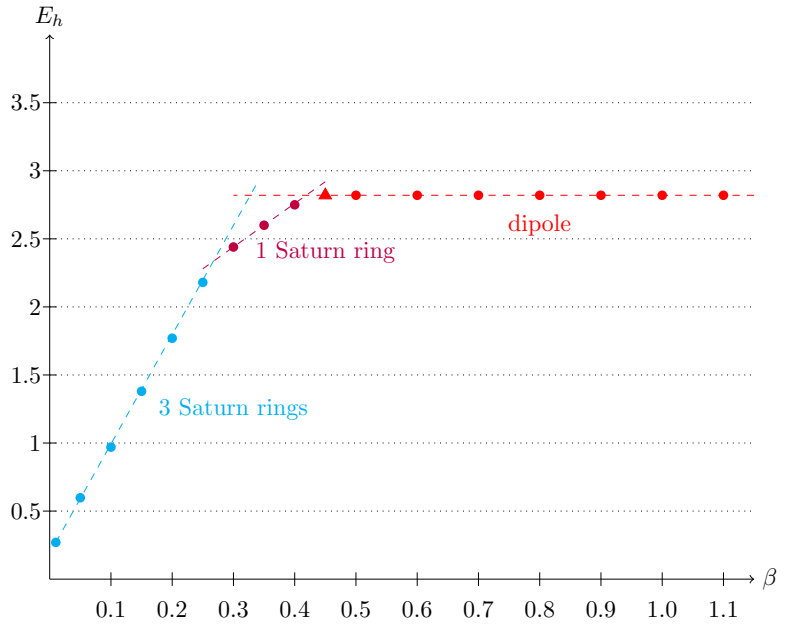

Figure 4.6: Energy of minimizers for different values of β around the peanut shape for $\phi = 0$. Dashed lines indicate the regression line for each of the three observed configurations.

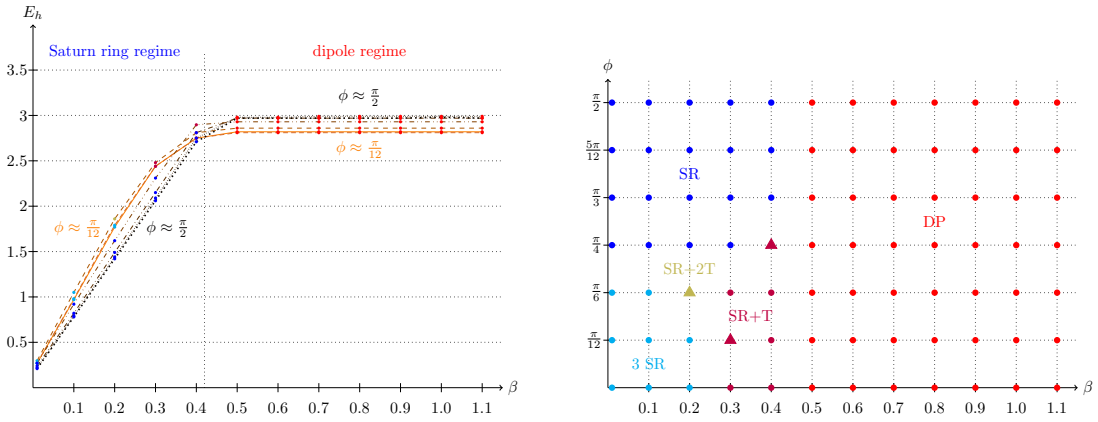

Figure 4.7: Left: Energy of minimizers as function of β around the peanut shape for different values of ϕ between 0 (solid line) and $\frac{\pi}{2}$ (dotted line). The mesh consists of around 485 000 cells of size $h = 0.03$ around the particle surface. Right: Defect configuration corresponding to the minimal energy for given ϕ and β. Dots indicate simulations with 2 000, triangles with 4 000 iterations. We observe dipoles (DP), Saturn rings with one (SR) or three components (3 SR) and Saturn rings with non-trivial surface T of one (SR+T) or two components (SR+2T).

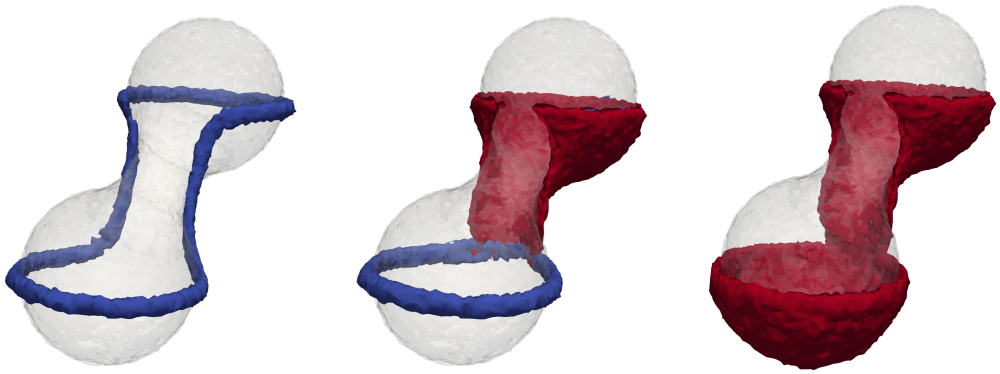

Figure 4.8: Configurations obtained for $\phi = \frac{\pi}{4}$ and $\beta = 0.3, 0.4, 0.5$.

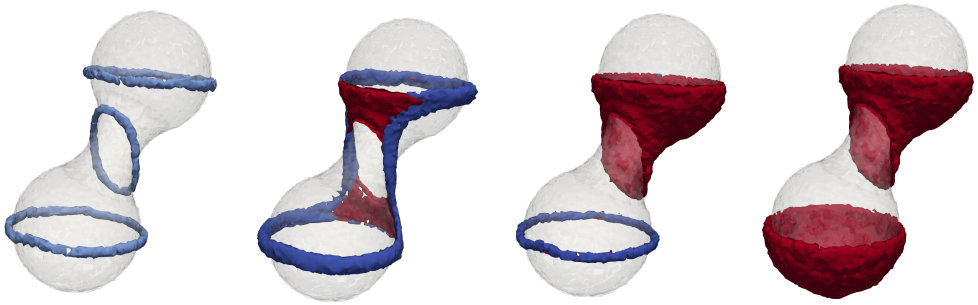

Figure 4.9: Configurations obtained for $\phi = \frac{\pi}{6}$ and $\beta = 0.1, 0.2, 0.4, 0.5$.

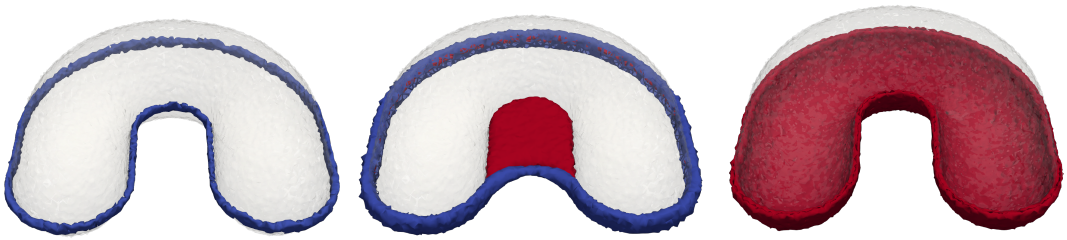

Figure 4.10: Configurations obtained for $\beta = 0.01, 0.33, 0.67$ and $\phi = \psi = 0$ after 4 000 iterations.

fact that the line S detaching from the surface at distance d would only be shortened by a term of order d^2 while the additional $\mathbb{M}(T \llcorner \Omega)$ would be of order d. We therefore expect the line S to always stay at the surface of $\mathcal{M}$ unless the dipole becomes energetically favourable.

4.4.3 Croissant-shaped particle

Our interest in croissant-shaped particles is twofold:

1. Until now, both S and T have been entirely included in the boundary layer $\mathcal{M}_h$. We would therefore like to give an example of when T and S detach from $\mathcal{M}$ and have parts inside Ω. The examples given here illustrate the variety and complexity of minimizers (T, S) of the limit problem.

2. From the point of view of applications it appears that particles similar to our croissant shape ("horse shoe") are interesting since they are able to self-assemble into two- and three-dimensional nematic colloidal crystals [15]. The precise understanding of defect structure could therefore be valuable e.g. for tunable metamaterials.

The particle we use in our simulations is made from five components. The central piece is a half-torus to which two cylindrical parts are attached. The remaining open ends of the cylinders are closed using two half-spheres. Since the croissant has less symmetries than the peanut, we describe its orientation relative to the external field by the two angles ϕ (rotation around the x_1-axis) and ψ (rotation around the x_2-axis). The two radii R, r of the torus and the length L of the cylinders are chosen as $R = 0.7$, $r = 0.4$ and $L = 0.5$. Those values are obtained heuristically as we expect for well chosen orientation and β to observe a non-trivial surface $T \llcorner \Omega$. Indeed, if the torus lies parallel to the x_1x_2-plane, then in order to shorten the length of S, we expect the line S to directly connect the two half-spheres and hence a surface T outside the boundary layer $\mathcal{M}_h$ connects Γ to $S \llcorner \Omega$. Varying the parameter β for $\phi = \psi = 0$, we obtain the expected intermediate configuration, see Figure 4.10. The values of β for which these transitions occur are contained in the two intervals $(0.25, 0.29)$ and $(0.4, 0.42)$.

It is therefore possible to qualitatively study the optimality conditions from Proposition 3.7.2.

1. The curvature of S should behave like β^{-1} and indeed we find qualitatively that for increasing β the curvature of $S \llcorner \Omega$ decreases, see Figure 4.11.

2. We also observe a surface T that has a non-trivial components $T \llcorner \mathcal{M}$ and $T \llcorner \Omega$ and detaches from $\mathcal{M}$ in a line other than Γ, see Figure 4.12. We observe that the angle formed by the normal vectors of $\mathcal{M}$ and T do not form a right angle as predicted by Young's law. This can also be observed in Figure 4.13 (a).

3. The surface $T \llcorner \Omega$ in Figure 4.12 and 4.10 appears to be flat, verifying the optimality condition of vanishing mean curvature. In Figure 4.13 we give an example where $T \llcorner \Omega$ has non-vanishing curvature but the curvature in the two depicted slices have opposite sign.

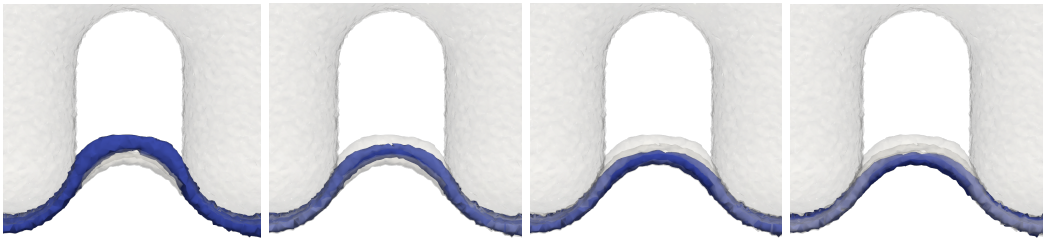

Figure 4.11: Evolution of the singularity line $S \llcorner \Omega$ as β increases, from left to right $\beta = 0.33, 0.375, 0.39, 0.4$. For comparison all four lines are indicated in all four images. Configurations obtained for $\phi = \psi = 0$ and 4 000 iterations.

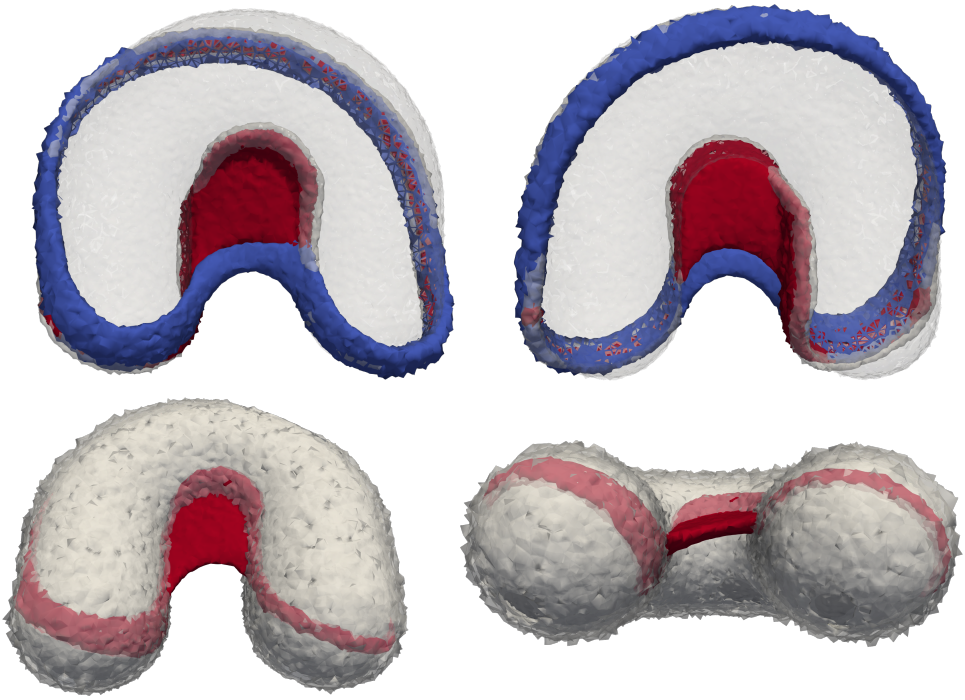

Figure 4.12: Four views on the configuration after 8 000 iterations for $\phi = \frac{\pi}{4}$, $\psi = \frac{\pi}{8}$ and $\beta = 0.31$. The line Γ is indicated transparently in the images of the upper row. The bottom row shows the transparent boundary layer $\mathcal{M}_h$ around the solid particle E, allowing to distinguish $T \llcorner \mathcal{M}$ and $T \llcorner \Omega$.

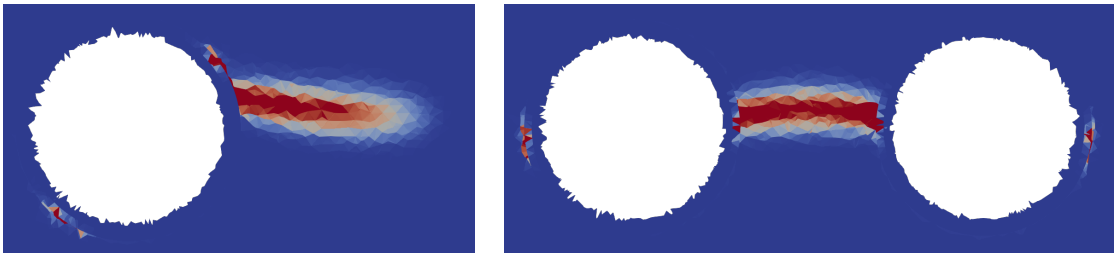

(a) (b)

Figure 4.13: Section though the x_2x_3-plane (left) and x_1x_3-plane(right) of T after 4 000 iterations for $\phi = \frac{\pi}{4}$, $\psi = 0$ and $\beta = 0.3$. The part of T inside Ω is curved into opposite directions in the two images.

Chapter 5

Conclusion and perspectives

The goal of this thesis was to investigate the complex interaction between a nematic liquid crystal, an immersed particle and an applied external magnetic field focusing on the type, shape and position of possible singularities. We used a reasonably rescaled version of the Landau-de Gennes model enriched with an energy density that allows to include anisotropies such as a homogeneous magnetic field which is the interpretation we focused on. The rescaled model contains two non-dimensional parameters, ξ and η, and we placed ourself in a regime where both tend to zero. We specified the relative speed by assuming that $\eta|\ln(\xi)| \to \beta \in (0, \infty)$ as $\xi, \eta \to 0$. This physically corresponds to an increasingly large immersed particle and a field of decreasing strength.

In the case of a single spherical particle, we derived an effective energy stated on the surface of the particle. We are able to explicitly calculate the minimizers of this limiting energy, giving a rigorous description and explanation of the different defect structures as well as the transition between them. In particular, we find that the only possible (locally) minimizing configurations are the Saturn ring around the equator and a dipole at one of the two poles of the sphere. We postulate that the transition between the two minimizers occurs while increasing and decreasing the parameter β, described by a hysteresis loop. Our findings are in accordance with [154] but unfortunately the hysteresis has not yet been observed experimentally. The observation would contribute to further validate our model and might also be interesting from a physical point of view as to describe different behaviour in a small range for the parameters.

In the second part we have seen how our limit model can be generalised to also describe singularities around an arbitrary but regular particle. We saw that if the particle is convex, then the energy asymptotically concentrates at the surface of the particle and the generalized model reduces to the minimization of the energy on the surface stated previously in the spherical particle case. In the non-convex case there may or may not be defects present in the interior of the liquid crystal material. We derived optimality conditions for those defect structures, also showing that they are smooth.

The last chapter then introduces a numerical algorithm that enables us to calculate the shape and energy of globally minimizing configurations. This last part is necessary since we are not able to find the minimizers of the limit energy explicitly, even for relatively simple particle such as the peanut shape. Exploring the structures appearing for different relative orientations ϕ between particle and magnetic field, we find a rich landscape of possible minimizers which one should observe also in experiments. The physical results on colloids involving peanut shaped particle in [143] focus on the dynamical behaviour. In order to observe the 'exotic' structures described in Chapter 4, one would need to consider a static situation in which the particle cannot move or rotate freely. If we only fix the direction of the external field (and hence the director field at infinity) and allow the peanut to rotate, we recover that the optimal angle ϕ is close to 0 or $\frac{\pi}{2}$ confirmed by [143]. Our model and the numerical simulations can therefore help in understanding which singularities and what shapes we observe in reality.

Of course this is only a first step on the way to understand liquid crystal colloids which would pave the way to manipulate liquid crystal properties itself or assemble microstructures within a liquid crystal medium.

Several future directions could be envisaged from here onwards:

1. As we're interested in colloids, a natural question would be to ask if it is possible to describe arrangements of several particles in the same framework we used in this thesis. It is known that if the particles are close enough, singularity lines can form in a way to entangle several of them and to form chains or layers. Moreover, the topology of those lines becomes interesting as in experiments one observes knots and links [116, 133] in contrast to the Saturn rings of trivial topology we described in this work. In [114], a formalism is explained how knotted configurations can be described, but it remains open how one can relate this to an energetic formulation such as the Landau-de Gennes model.

2. From a theoretical point of view it would be desirable to derive a model of higher order. Indeed, our model only takes into account the highest order terms, while some phenomena cannot be captured in this expansion. For example, in reality the Saturn ring might stay at a certain distance from a spherical particle [3, 71, 83, 128], in our first order model it is always confined to the sphere. An energy including linear order terms in η might be able to provide estimates on the distance of the defect from the surface.

3. The numerical algorithm we're proposing here needs to be studied and improved. In order to be justified, a full and general proof of consistency is needed in addition to the results we give here. It would also be of interest to prove convergence of our method and get some estimates on the convergence rate which seems a challenging task in view of the results for related total variation minimization problems [46]. Trying to create an analogous "phase diagram" (see Figure 4.7) for the croissant or any other more complicated particle requires considerable computing power or time. One can therefore seek to further accelerate and parallelise our implementation.

4. Seen as a part of the modelisation for liquid crystals, one could also investigate how our results depend on the chosen Landau-de Gennes model. One could try to reprove analogous statements for a different potential f, going beyond the one constant approximation, varying the temperature or considering a non-homogeneous external field [21, 23, 56, 99, 132]. Already for an electric field, the assumption of homogeneity throughout the liquid crystal sample is not justified any more and one would need to consider a model where the influence of the director on the field is taken into account [12, 77]. As we are interested in the transition between singularities, one might also ask if one could derive a dynamical version of our results, describing the evolution of the singularities by those of S and T, see e.g. the description in [112] and simulations in [68]. In the same spirit, one might be able to include a flow field replacing or supplementing the magnetic field into the model. It has been observed that a flow field can also induce a dipole-Saturn ring transition [95].

Appendix A

Appendix

A.1 Two examples for the function g

In this section we check that the two functions g_1 and g_2 as defined in (2.9) verify the assumptions on g, in particular (2.5), (2.6), (2.7) and (2.8). All calculations are straightforward.

Proposition A.1.1 (Properties of g_1)**.** *Let g_1 be given as in* (2.9)*.*

1. *If $Q \in \mathcal{N}$ is given by $Q = s_*(\mathbf{n}\otimes\mathbf{n} - \frac{1}{3}\mathrm{Id})$ with $\mathbf{n}\in\mathbb{S}^2$, then*

$$g_1(Q) = s_*\left(1-\mathbf{n}_3^2\right)\,,$$

   i.e. $c_*^2 = s_*$.

2. *There exists a constant $C>0$ such that for all $Q\in\mathrm{Sym}_0$*

$$|g_1(Q) - g_1(\mathcal{R}(Q))| \le C\,\mathrm{dist}(Q,\mathcal{N})\,. \tag{A.1}$$

3. *The function g_1 satisfies the growth assumptions* (3.7),(3.8) *and is invariant by rotations around the e_3-axis. For fixed $|Q|$, $g_1(Q)$ is minimal if $\mathbf{e}_3$ is the eigenvector corresponding to the maximal eigenvalue of Q. For $Q = s((\mathbf{e}_3\otimes\mathbf{e}_3 - \frac{1}{3}\mathrm{Id}) + r(\mathbf{m}\otimes\mathbf{m} - \frac{1}{3}\mathrm{Id}))$ (using the notation of* (2.4)*), $g_1(Q)$ is minimized for $r=0$.*

Proof. For $Q = s_*(\mathbf{n}\otimes\mathbf{n} - \frac{1}{3}\mathrm{Id})$ with $\mathbf{n}\in\mathbb{S}^2$ and $s_*\ge 0$ one easily checks that

$$g_1(Q) = \frac{2}{3}s_* - s_*\Big(\mathbf{n}_3^2 - \frac{1}{3}\Big) = s_* - s_*\mathbf{n}_3^2\,.$$

For the second assertion, we take a $Q\in\mathrm{Sym}_0$ and use Proposition 2.2.3 to write

$$Q = s\left(\left(\mathbf{n}\otimes\mathbf{n} - \frac{1}{3}\mathrm{Id}\right) + r\left(\mathbf{m}\otimes\mathbf{m} - \frac{1}{3}\mathrm{Id}\right)\right)\,,$$

with $s>0$, $0\le r<1$ and $\mathbf{n},\mathbf{m}$ orthonormal eigenvectors of Q and $\mathcal{R}(Q) = s_*\left(\mathbf{n}\otimes\mathbf{n} - \frac{1}{3}\mathrm{Id}\right)$. Then we can estimate

$$\begin{aligned}|g_1(Q) - g_1(\mathcal{R}(Q))| &= \Big|s\Big(\mathbf{n}_3^2 - \frac{1}{3}\Big) + sr\Big(\mathbf{m}_3^2 - \frac{1}{3}\Big) - s_*\Big(\mathbf{n}_3^2 - \frac{1}{3}\Big)\Big| \\ &\le |s-s_*|\Big|\mathbf{n}_3^2 - \frac{1}{3}\Big| + |sr|\Big|\mathbf{m}_3^2 - \frac{1}{3}\Big|\,.\end{aligned}$$

On the other hand, as in (2.38)

$$\mathrm{dist}^2(Q,\mathcal{N}) = |Q-\mathcal{R}(Q)|^2 \ge \frac{1}{3}|s-s_*|^2 + \frac{1}{3}|sr|^2\,.$$

Combining these two expressions, we find

$$|g_1(Q) - g_1(\mathcal{R}(Q))| \leq \frac{4}{\sqrt{3}} \operatorname{dist}(Q, \mathcal{N}),$$

which completes the proof of the second assertion for the choice $C = \frac{4}{\sqrt{3}}$.

The function g_1 is smooth and obviously satisfies (2.5) and (2.6). Furthermore, since g_1 only depends on Q_{33}, it is invariant under rotations around the $\mathbf{e}_3-$axis. Writing once again $Q \in \mathrm{Sym}_0$ in the form of Proposition 2.2.3, we get

$$g_1(Q) \;=\; \frac{2}{3}s_* - s\Big(\Big(\mathbf{n}_3^2 - \frac{1}{3}\Big) + r\Big(\mathbf{m}_3^2 - \frac{1}{3}\Big)\Big).$$

For fixed $s, r, \mathbf{m}$ this is minimized by $\mathbf{n}_3^2 = 1$, which corresponds to the principal eigenvector $\mathbf{n}$ equal to $\mathbf{e}_3$. We also see that for $\mathbf{n} = \mathbf{e}_3$ and s fixed, g becomes minimal if $r = 0$, since $\mathbf{m} \perp \mathbf{n}$. □

Proposition A.1.2 (Properties of g_2)**.** *Let g_2 be given as in* (2.9).

1. *$g_2(Q) \geq 0$ for all $Q \in \mathrm{Sym}_0$ with equality of and only if $Q = t(\mathbf{e}_3 \otimes \mathbf{e}_3 - \frac{1}{3}\mathrm{Id})$ for some $t \geq 0$.*
2. *If $Q \in \mathcal{N}$ is given by $Q = s_*(\mathbf{n} \otimes \mathbf{n} - \frac{1}{3}\mathrm{Id})$ with $\mathbf{n} \in \mathbb{S}^2$, then*

$$g_2(Q) = \sqrt{\frac{3}{2}}\left(1 - \mathbf{n}_3^2\right),$$

   i.e. $c_*^2 = \sqrt{\frac{3}{2}}$.
3. *There exist constants $\delta_1, C > 0$ such that if $Q \in \mathrm{Sym}_0$ with $\operatorname{dist}(Q, \mathcal{N}) \leq \delta$ for $0 < \delta < \delta_1$, then*

$$|g_2(Q) - g_2(\mathcal{R}(Q))| \leq C \operatorname{dist}(Q, \mathcal{N}). \tag{A.2}$$

4. *The function g_2 satisfies the growth assumptions* (2.5),(2.6) *and is invariant by rotations around the e_3-axis. For fixed $|Q|$, $g_2(Q)$ is minimal if $\mathbf{e}_3$ is the eigenvector corresponding to the maximal eigenvalue of Q. For $Q = s((\mathbf{e}_3 \otimes \mathbf{e}_3 - \frac{1}{3}\mathrm{Id}) + r(\mathbf{m} \otimes \mathbf{m} - \frac{1}{3}\mathrm{Id}))$ (using again the notation of* (2.4)*), $g_2(Q)$ is minimized for $r = 0$.*

Proof. Minimizing g_2 under the tracelessness constraint, we get the necessary conditions

$$-\frac{1}{|Q|} + \frac{Q_{33}^2}{|Q|^3} - \lambda = 0, \quad \frac{Q_{33}Q_{jj}}{|Q|^3} - \lambda = 0 \text{ for } j = 1, 2, \quad \frac{Q_{33}Q_{ij}}{|Q|^3} = 0 \text{ for } i \neq j$$

for a Lagrange multiplier λ. For $Q = 0$ the claim is clear by definition. So let $Q \in \mathrm{Sym}_0 \setminus \{0\}$. If $Q_{33} = 0$ we get a contradiction. Hence we can assume $Q_{33} \neq 0$. Then the third equation from above implies $Q_{ij} = 0$ for $i \neq j$ and the second $Q_{11} = Q_{22}$. By $\operatorname{tr}(Q) = 0$, we have $Q_{33} = -2Q_{11}$. Then the first equation reads $0 = \frac{3}{2}Q_{33}^2 - |Q|^2$, i.e. $Q_{33} = \sqrt{2/3}|Q|$. Inserting this into g_2 we get $\min_{\mathrm{Sym}_0} g_2 = 0$. Our conditions also imply the claimed representation $Q = t(\mathbf{e}_3 \otimes \mathbf{e}_3 - \frac{1}{3}\mathrm{Id})$. Reversely, it is obvious that $g_2 = 0$ for such Q.

For the second claim, it is straightforward to check that for $Q = s_*(\mathbf{n} \otimes \mathbf{n} - \frac{1}{3}\mathrm{Id}) \in \mathcal{N}$ we have $|Q|^2 = \frac{2}{3}s_*^2$. Thus

$$g_2(Q) = \sqrt{\frac{2}{3}} - \frac{s_*(\mathbf{n}_3^2 - \frac{1}{3})}{\sqrt{\frac{2}{3}}s_*} = \sqrt{\frac{2}{3}} + \frac{1}{3}\sqrt{\frac{3}{2}} - \sqrt{\frac{3}{2}}\mathbf{n}_3^2 = \sqrt{\frac{3}{2}}\left(1 - \mathbf{n}_3^2\right).$$

For the next property we use the same notation as before (from Proposition 2.2.3) to write

$$Q = s\left(\left(\mathbf{n} \otimes \mathbf{n} - \frac{1}{3}\mathrm{Id}\right) + r\left(\mathbf{m} \otimes \mathbf{m} - \frac{1}{3}\mathrm{Id}\right)\right),$$

with $s > 0$, $0 \leq r < 1$ and $\mathbf{n}, \mathbf{m}$ orthonormal eigenvectors of Q. From the second part of this proposition, we infer that $g_2(\mathcal{R}(Q)) = \sqrt{\frac{3}{2}}(1 - \mathbf{n}_3^2)$. In order to calculate $g_2(Q)$, we note that

$$\begin{aligned} |Q|^2 &= s^2 \left| \mathbf{n} \otimes \mathbf{n} - \frac{1}{3}\mathrm{Id} \right|^2 + (sr)^2 \left| \mathbf{m} \otimes \mathbf{m} - \frac{1}{3}\mathrm{Id} \right|^2 + 2s^2 r \left(\mathbf{n} \otimes \mathbf{n} - \frac{1}{3}\mathrm{Id} \right) : \left(\mathbf{m} \otimes \mathbf{m} - \frac{1}{3}\mathrm{Id} \right) \\ &= \frac{2}{3} s^2 \left(r^2 - r + 1 \right) . \end{aligned}$$

This implies

$$\begin{aligned} |g_2(Q) - g_2(\mathcal{R}(Q))| &= \left| \sqrt{\frac{2}{3}} - \frac{s(n_3^2 - \frac{1}{3}) + sr(m_3^2 - \frac{1}{3})}{\sqrt{\frac{2}{3}} s \sqrt{1 - r + r^2}} - \sqrt{\frac{2}{3}} + \frac{s_*(n_3^2 - \frac{1}{3})}{s_* \sqrt{\frac{2}{3}}} \right| \\ &\leq \frac{n_3^2 - \frac{1}{3}}{\sqrt{\frac{2}{3}}} \left(\frac{1}{\sqrt{1 - r + r^2}} - 1 \right) + \frac{m_3^2 - \frac{1}{3}}{\sqrt{\frac{2}{3}}} \frac{r}{\sqrt{1 - r + r^2}} . \end{aligned}$$

Note, that the Taylor expansion at $r = 0$ is given by $\frac{1}{\sqrt{1 - r + r^2}} - 1 = \frac{r}{2} + \mathcal{O}(r^2)$ and $\frac{r}{\sqrt{1 - r + r^2}} = r + \mathcal{O}(r^2)$. Hence

$$|g_2(Q) - g_2(\mathcal{R}(Q))| \leq \frac{3}{2} r + \mathcal{O}(r^2) . \tag{A.3}$$

As in Proposition A.1.1 we get that $\mathrm{dist}^2(Q, \mathcal{N}) \geq \frac{1}{3}|s - s_*|^2 + \frac{1}{3}|sr^2|$ and hence $|s - s_*| \leq \sqrt{3}\,\mathrm{dist}(Q, \mathcal{N})$ and $|r| \leq \frac{\sqrt{3}\,\mathrm{dist}(Q, \mathcal{N})}{|s|}$. We define $\delta_1 = \frac{1}{2\sqrt{3}} s_*$ and together with (A.3) we get

$$|g_2(Q) - g_2(\mathcal{R}(Q))| \leq Cr \leq \frac{\sqrt{3}\mathrm{dist}(Q, \mathcal{N})}{|s|} \leq C \frac{2\sqrt{3}}{s_*} \mathrm{dist}(Q, \mathcal{N}) .$$

It remains to prove the last assertion. Again the growth assumptions (2.5) and (2.6) are trivially satisfied. With the same arguments as in Proposition A.1.1 (since $|Q|$ is fixed), we get that $g_2(Q)$ is minimal for $\mathbf{n} = \mathbf{e}_3$. Finally, we can compute

$$g_2(s((\mathbf{e}_3 \otimes \mathbf{e}_3 - \frac{1}{3}\mathrm{Id}) + r(\mathbf{m} \otimes \mathbf{m} - \frac{1}{3}\mathrm{Id}))) \;=\; \sqrt{\frac{2}{3}} - \frac{\frac{2}{3}s + sr(\mathbf{m}_3^2 - \frac{1}{3})}{\sqrt{\frac{2}{3}} s \sqrt{1 - r + r^2}}$$

and see that this is indeed minimal if $r = 0$. □

A.2 The complex $\mathcal{T}$

In this section, we collect and prove all results in connection to the structure of $\mathcal{T}$ as defined in Section 3.4.3. Recall that

$$\mathcal{T} \coloneqq \{ Q \in \mathrm{Sym}_0 \,:\, s > 0 \,, 0 \leq r < 1 \,, n_3 = 0 \} .$$

Our first result is a characterization of $\mathcal{T}$ that provides us with a more accessible parametrization.

Proposition A.2.1. *Every matrix $Q \in \mathcal{T}$ can be written as*

$$Q = \lambda(\mathbf{n} \otimes \mathbf{n} - R_{\mathbf{n}}^\top M R_{\mathbf{n}}) ,$$

where $\lambda > 0$, $\mathbf{n} = (n_1, n_2, 0) \in \mathbb{S}^2$, $R_{\mathbf{n}}$ is the rotation around $\mathbf{n} \wedge \mathbf{e}_3$, such that $R_{\mathbf{n}}\mathbf{n} = \mathbf{e}_3$ and

$$M \;=\; \begin{pmatrix} M' & & 0 \\ & & 0 \\ 0 & 0 & 0 \end{pmatrix}$$

with $M' \in \mathbb{R}^{2\times 2}$ symmetric, $\mathrm{tr}(M') = 1$ and $\langle M'v, v \rangle > -1$ for all $v \in \mathbb{S}^1$. The matrix Q is oblate uniaxial if and only if $M' = \frac{1}{2}\mathrm{Id}$.

Proof. A matrix Q of the above form $Q = \lambda(\mathbf{n}\otimes\mathbf{n} - R_{\mathbf{n}}^\top M R_{\mathbf{n}})$ has $\mathbf{n}$ as an eigenvector to the eigenvalue λ and $\mathbf{n}_3 = 0$ by definition. Furthermore, since $\min_{v\in\mathbb{S}^1}\langle M'v, v\rangle > -1$ the eigenvalue λ is strictly bigger than the other eigenvalues, thus $r < 1$ and $Q \in \mathcal{T}$. Conversely, we can write every $Q \in \mathrm{Sym}_0$ as

$$Q \;=\; \lambda_1 \mathbf{n}\otimes\mathbf{n} + \lambda_2 \mathbf{m}\otimes\mathbf{m} + \lambda_3 \mathbf{p}\otimes\mathbf{p}\,,$$

with $\lambda_1 \geq \lambda_2 \geq \lambda_3$ and $\mathbf{n}, \mathbf{m}, \mathbf{p} \in \mathbb{S}^2$ pairwise orthogonal eigenvectors of Q to $\lambda_1, \lambda_2, \lambda_3$. By definition of $\mathcal{T}$, $n_3 = 0$ as required for our parametrization and clearly we can identify $\lambda = \lambda_1$. Setting $M = -R_{\mathbf{n}}(\frac{\lambda_2}{\lambda_1}\mathbf{m}\otimes\mathbf{m} + \frac{\lambda_3}{\lambda_1}\mathbf{p}\otimes\mathbf{p})R_{\mathbf{n}}^\top$, it is obvious that M is of the above form and that $Q \in \mathcal{T}$ can be written as claimed.

If $M' = \frac{1}{2}\mathrm{Id}$ then

$$Q \;=\; \lambda(\mathbf{n}\otimes\mathbf{n} - R_{\mathbf{n}}^\top M R_{\mathbf{n}}) \;=\; \frac{3}{2}\lambda(\mathbf{n}\otimes\mathbf{n} - \frac{1}{3}\mathrm{Id})\,,$$

i.e. Q is oblate uniaxial. The reversed implication follows similarly, since the matrices $R_{\mathbf{n}}^\top, R_{\mathbf{n}}$ are invertible.

□

Remark A.2.2. *Given a vector $u \in \mathbb{R}^3$ as axis of rotation and an angle θ, then this rotation is described by the matrix R with*

$$R = \begin{pmatrix} \cos\theta + u_1^2(1-\cos\theta) & u_1u_2(1-\cos\theta) - u_3\sin\theta & u_1u_3(1-\cos\theta) + u_2\sin\theta \\ u_1u_2(1-\cos\theta) + u_3\sin\theta & \cos\theta + u_2^2(1-\cos\theta) & u_2u_3(1-\cos\theta) - u_1\sin\theta \\ u_1u_3(1-\cos\theta) - u_2\sin\theta & u_2u_3(1-\cos\theta) + u_1\sin\theta & \cos\theta + u_3^2(1-\cos\theta) \end{pmatrix}.$$

Corollary A.2.3. *$\mathcal{T}$ is a four dimensional smooth complex and $\partial\mathcal{T} = \mathcal{C}$.*

Proof. From the characterization in Proposition A.2.1, it is clear that one can use the map $Q \mapsto (\lambda, \mathbf{n}, m_{11}, m_{12})$ to make $\mathcal{T}$ a four dimensional manifold with a conical singularity in $Q = 0$. In particular, $\mathcal{T}$ is a smooth complex.

Proposition A.2.1 furthermore implies that the boundary of $\mathcal{T}$ consists of matrices of the form $\lambda = 0$ (from which follows directly $Q = 0$) or M' has the eigenvalue -1 (which corresponds to $r = 1$). In particular, the matrices with $r = 0$ are not included in $\partial\mathcal{T}$ as one may think from the definition in (3.12). This implies the inclusion $\partial\mathcal{T} \subset \mathcal{C}$. For the inverse inclusion, take $Q \in \mathcal{C}$ with orthogonal eigenvectors $\mathbf{m}, \mathbf{p} \in \mathbb{S}^2$ associated to the biggest eigenvalue $\lambda_1 = \lambda_2$. So in fact we have a two dimensional subspace of eigenvectors to this eigenvalue spanned by $\mathbf{m}$ and $\mathbf{p}$. Since the hyperplane defined through $\{n_3 = 0\}$ is of codimension one, there exists a unit vector $\mathbf{n} \in \{n_3 = 0\} \cap \mathrm{span}\{\mathbf{m}, \mathbf{p}\}$ which we were looking for. The unit eigenvector orthogonal to $\mathbf{n}$ in the plane $\mathrm{span}\{\mathbf{m}, \mathbf{p}\}$ requires M' to have the eigenvalue -1 or in other words $\min_{v\in\mathbb{S}^1}\langle M'v, v\rangle = -1$, so that $Q \in \partial\mathcal{T}$. □

Lemma A.2.4. *Let $Q \in \mathcal{T} \cap \mathcal{N}$. Then, the normal vector N_Q on $\mathcal{T}$ at Q is given by*

$$N_Q = \frac{3}{2}\lambda \begin{pmatrix} 0 & 0 & n_1 \\ 0 & 0 & n_2 \\ n_1 & n_2 & 0 \end{pmatrix},$$

where $\mathbf{n} = (n_1, n_2, 0) \in \mathbb{S}^2$ is the eigenvector associated to the biggest eigenvalue λ_1.

Proof. We are going to prove a slightly more general result by first considering $Q \in \mathcal{T}$ and calculating the tangent vectors to $\mathcal{T}$ in Q. We use the representation from Proposition A.2.1 and vary $\lambda, \mathbf{n}, m_{11}, m_{12}$ one after another.

- First, we can easily take the derivative with respect to λ and obtain $\mathbf{T}_1 = (\mathbf{n}\otimes\mathbf{n} - R_{\mathbf{n}}^\top M R_{\mathbf{n}})$.

- Second, we vary the parameter $\mathbf{n}$. So, let's consider $\mathbf{n} = (n_1, n_2, 0) \in \mathbb{S}^2$. Without loss of generality we assume that $n_2 \neq 0$ and write $\mathbf{n}(t) = (n_1 + t, n_2 - \frac{n_1}{n_2}t)$. Then $|\mathbf{n}(t)|^2 = 1 + O(t^2)$ and

$$\mathbf{n}(t) \otimes \mathbf{n}(t) \;=\; \mathbf{n} \otimes \mathbf{n} + tD_{\mathbf{n}\otimes\mathbf{n}} + O(t^2)\,, \qquad D_{\mathbf{n}\otimes\mathbf{n}} = \begin{pmatrix} 2n_1 & n_2 - \frac{n_1^2}{n_2} & 0 \\ n_2 - \frac{n_1^2}{n_2} & -2n_1 & 0 \\ 0 & 0 & 0 \end{pmatrix}.$$

  The derivative of the second term $R_{\mathbf{n}(t)}^\top M R_{\mathbf{n}(t)}$ can be calculated using Remark A.2.2 with the axis $\mathbf{n}^\perp(t) := \mathbf{n}(t) \wedge \mathbf{e}_3$. Since $\mathbf{n}(t) \perp \mathbf{e}_3$ we can write

$$R_{\mathbf{n}(t)} \;=\; R_{\mathbf{n}} + tD_{R_{\mathbf{n}}} + O(t^2)\,, \qquad D_{R_{\mathbf{n}}} = \frac{1}{n_2}\begin{pmatrix} -2n_1n_2 & -n_2^2 + n_1^2 & -n_2 \\ -n_2^2 + n_1^2 & 2n_1n_2 & n_1 \\ n_2 & -n_1 & 0 \end{pmatrix}.$$

  The second tangent vector $\mathbf{T}_2$ is thus given by $\mathbf{T}_2 = \lambda(D_{\mathbf{n}\otimes\mathbf{n}} - D_{R_{\mathbf{n}}}^\top M R_{\mathbf{n}} - R_{\mathbf{n}}^\top M D_{R_{\mathbf{n}}})$.

- Third, we can take the derivative with respect to m_{11}. This is straightforward and we obtain

$$\mathbf{T}_3 = \lambda R_{\mathbf{n}}^\top \begin{pmatrix} 1 & 0 & \\ 0 & -1 & \\ & & 0 \end{pmatrix} R_{\mathbf{n}}\,.$$

- Last, varying m_{12} we easily calculate

$$\mathbf{T}_4 = \lambda R_{\mathbf{n}}^\top \begin{pmatrix} 0 & 1 & \\ 1 & 0 & \\ & & 0 \end{pmatrix} R_{\mathbf{n}}\,.$$

Before proceeding, we want to calculate a fifth vector by varying $\mathbf{n}_3$. As it will turn out later, this is indeed the normal vector.

- Writing once again $\mathbf{n} = (n_1, n_2, 0)$ and defining $\mathbf{n}(t) := (n_1\sqrt{1-t^2}, n_2\sqrt{1-t^2}, t)$ we can express

$$\mathbf{n}(t) \otimes \mathbf{n}(t) \;=\; \mathbf{n} \otimes \mathbf{n} + t(\mathbf{n} \otimes \mathbf{e}_3 + \mathbf{e}_3 \otimes \mathbf{n}) + O(t^2)\,.$$

  As for the second tangent vector, we use Remark A.2.2 and the rotation around $\mathbf{n}^\perp(t) = \mathbf{n}(t) \wedge \mathbf{e}_3$. Unlike previously, $\mathbf{n}(t)$ is no longer orthogonal to $\mathbf{e}_3$ for $t \neq 0$, namely $\theta = \arccos(\langle \mathbf{n}(t), \mathbf{e}_3 \rangle) = t$. Substituting this our expression of the rotation matrix we get

$$R_{\mathbf{n}(t)} \;=\; R_{\mathbf{n}} + tD_3 + O(t^2)\,, \qquad D_3 = \begin{pmatrix} 1 - n_2^2 & n_1n_2 & 0 \\ n_1n_2 & 1 - n_1^2 & 0 \\ 0 & 0 & 1 \end{pmatrix}.$$

  Adding the two partial results, we get

$$N \;:=\; \lambda(\mathbf{n} \otimes \mathbf{e}_3 + \mathbf{e}_3 \otimes \mathbf{n} - D_3^\top M R_{\mathbf{n}} - R_{\mathbf{n}}^\top M D_3)\,.$$

It remains to show that $\{\mathbf{T}_1, \mathbf{T}_2, \mathbf{T}_3, \mathbf{T}_4, N\}$ are pairwise orthogonal if Q is oblate uniaxial. Indeed, then it follows that N is a normal vector, since it is orthogonal to $T_Q\mathcal{T}$.

It is easy to see that since the trace is invariant by change of basis and since $R_{\mathbf{n}}^\top = R_{\mathbf{n}}^{-1}$

$$\langle \mathbf{T}_3, \mathbf{T}_4 \rangle \;=\; \lambda^2 \mathrm{tr}\left(\begin{pmatrix} 1 & 0 \\ 0 & -1 \end{pmatrix}\begin{pmatrix} 0 & 1 \\ 1 & 0 \end{pmatrix}\right) \;=\; \lambda^2 \mathrm{tr}\left(\begin{pmatrix} 0 & 1 \\ -1 & 0 \end{pmatrix}\right) \;=\; 0\,.$$

Noting that $\mathbf{n}\otimes\mathbf{n}R_{\mathbf{n}}^{\top}MR_{\mathbf{n}}=0$ for $M\in\mathrm{Sym}_0$ with $m_{ij}=0$ if $i=3$ or $j=3$, we get

$$\begin{aligned}\langle\mathbf{T}_1,\mathbf{T}_3\rangle &= \lambda\mathrm{tr}\Big((\mathbf{n}\otimes\mathbf{n}-R_{\mathbf{n}}^{\top}MR_{\mathbf{n}})(R_{\mathbf{n}}^{\top}\begin{pmatrix}1&0&\\0&-1&\\&&0\end{pmatrix}R_{\mathbf{n}})\Big)\\ &= \lambda\mathrm{tr}(M\begin{pmatrix}1&0&\\0&-1&\\&&0\end{pmatrix}) = \lambda\mathrm{tr}(\begin{pmatrix}m_{11}&-m_{12}&\\m_{12}&-m_{22}&\\&&0\end{pmatrix}) = \lambda(2m_{11}-1)\,.\end{aligned}$$

With the same argument we also find

$$\begin{aligned}\langle\mathbf{T}_1,\mathbf{T}_4\rangle &= \lambda\mathrm{tr}\Big((\mathbf{n}\otimes\mathbf{n}-R_{\mathbf{n}}^{\top}MR_{\mathbf{n}})(R_{\mathbf{n}}^{\top}\begin{pmatrix}0&1&\\1&0&\\&&0\end{pmatrix}R_{\mathbf{n}})\Big)\\ &= \lambda\mathrm{tr}(M\begin{pmatrix}0&1&\\1&0&\\&&0\end{pmatrix}) = \lambda\mathrm{tr}(\begin{pmatrix}m_{12}&m_{11}&\\m_{22}&m_{12}&\\&&0\end{pmatrix}) = 2\lambda m_{12}\,.\end{aligned}$$

Furthermore, we claim that

$$\langle\mathbf{T}_1,\mathbf{T}_2\rangle = \lambda\,\mathrm{tr}((\mathbf{n}\otimes\mathbf{n}-R_{\mathbf{n}}^{\top}MR_{\mathbf{n}})(D_{\mathbf{n}\otimes\mathbf{n}}-D_{R_{\mathbf{n}}}^{\top}MR_{\mathbf{n}}-R_{\mathbf{n}}^{\top}MD_{R_{\mathbf{n}}})) = 0\,.$$

Indeed, one can check that

$$\begin{aligned}\mathrm{tr}(\mathbf{n}\otimes\mathbf{n}D_{\mathbf{n}\otimes\mathbf{n}}) &= 0 = \mathrm{tr}(\mathbf{n}\otimes\mathbf{n}D_{R_{\mathbf{n}}}^{\top}MR_{\mathbf{n}})\,,\\ \mathrm{tr}(\mathbf{n}\otimes\mathbf{n}R_{\mathbf{n}}^{\top}MD_{R_{\mathbf{n}}}) &= 0 = \mathrm{tr}(R_{\mathbf{n}}^{\top}MR_{\mathbf{n}}D_{\mathbf{n}\otimes\mathbf{n}})\,,\\ \mathrm{tr}(R_{\mathbf{n}}^{\top}MR_{\mathbf{n}}D_{R_{\mathbf{n}}}^{\top}MR_{\mathbf{n}}) &= 0 = \mathrm{tr}(R_{\mathbf{n}}^{\top}MR_{\mathbf{n}}R_{\mathbf{n}}^{\top}MD_{R_{\mathbf{n}}})\,.\end{aligned}$$

This implies that

$$\langle N,\mathbf{T}_3\rangle = \lambda^2\mathrm{tr}\Big((\mathbf{n}\otimes\mathbf{e}_3+\mathbf{e}_3\otimes\mathbf{n}-D_3^{\top}MR_{\mathbf{n}}-R_{\mathbf{n}}^{\top}MD_3)(R_{\mathbf{n}}^{\top}\begin{pmatrix}1&0&\\0&-1&\\&&0\end{pmatrix}R_{\mathbf{n}})\Big) = 0\,,$$

since again the traces of all cross terms vanish. Similarly,

$$\langle N,\mathbf{T}_4\rangle = 0\,.$$

Next, we have the equality

$$\langle\mathbf{T}_2,\mathbf{T}_3\rangle = -4\lambda^2\frac{m_{12}}{n_2}\,.$$

This follows since $\mathrm{tr}(D_{\mathbf{n}\otimes\mathbf{n}}\mathbf{T}_3)=0$ and $\mathrm{tr}(D_3MR_{\mathbf{n}}\mathbf{T}_3)=\frac{2m_{12}}{n_2}$. The latter fact is evident if one calculates $M\begin{pmatrix}1&0&\\0&-1&\\&&0\end{pmatrix}=\begin{pmatrix}m_{11}&-m_{12}&\\m_{12}&-m_{22}&\\&&0\end{pmatrix}$ and $R_{\mathbf{n}}D_3^{\top}=\begin{pmatrix}0&-1/n_2&1\\1/n_2&0&-n_1/n_2\\-1&n_1/n_2&0\end{pmatrix}$.
This also permits us to derive

$$\langle\mathbf{T}_2,\mathbf{T}_4\rangle = 2\lambda^2\frac{2m_{11}-1}{n_2}\,.$$

Again, we simply calculate the traces of all cross terms. For example

$$\begin{aligned}
\operatorname{tr}(\mathbf{n}\otimes\mathbf{e}_3 D_{\mathbf{n}\otimes\mathbf{n}}) &= 0\,,\\
\operatorname{tr}(\mathbf{n}\otimes\mathbf{e}_3 R_{\mathbf{n}}^\top M D_{R_{\mathbf{n}}}) &= 0\,,\\
\operatorname{tr}(\mathbf{n}\otimes\mathbf{e}_3 D_{R_{\mathbf{n}}}^\top M R_{\mathbf{n}}) &= \frac{m_{12}}{n_2}(n_1^2-n_2^2)-n_1(2m_{11}-1)\,,\\
\operatorname{tr}(D_{R_{\mathbf{n}}}^\top M R_{\mathbf{n}} D_{\mathbf{n}\otimes\mathbf{n}}) &= 2\frac{m_{11}n_1}{n_2}+\frac{1}{n_2^2}(n_1^2(2m_{11}-1)+m_{11})\,,\\
\operatorname{tr}(D_{R_{\mathbf{n}}}^\top M R_{\mathbf{n}} R_{\mathbf{n}}^\top M D_{R_{\mathbf{n}}}) &= -2\frac{n_1 m_{12}}{n_2}+\frac{1}{n_2^2}\left(3(m_{11}^2+m_{12}^2)-(1+n_1^2)(2m_{11}-1)\right)\,,\\
\operatorname{tr}(D_{R_{\mathbf{n}}}^\top M R_{\mathbf{n}} D_{R_{\mathbf{n}}}^\top M R_{\mathbf{n}}) &= 2\frac{m_{11}m_{22}+m_{12}^2}{n_2^2}\,,
\end{aligned}$$

We end up with

$$\langle N,\mathbf{T}_2\rangle = \frac{6\lambda^2 m_{12}(n_1^2-n_2^2)}{n_2}-6\lambda^2 n_1(2m_{11}-1)\,.$$

Another straightforward calculation shows that

$$\begin{aligned}
\langle N,\mathbf{T}_1\rangle = {}& \lambda 2 n_1 m_{12}(n_1^5 m_{12}-2n_1^4 n_2 m_{11}-2n_1^3 m_{12}-2n_1^2 n_2^3 m_{11}+3n_1^2 n_2 m_{11}\\
&-2n_1^2 n_2-n_1 n_2^4 m_{12}+n_1 m_{12}+n_2^3 m_{11}-n_2 m_{11}-2n_2^3+2n_2)\,.
\end{aligned}$$

After these calculations, it is apparent that for prolate uniaxial $Q\in\mathrm{Sym}_0$ (and in particular $Q\in\mathcal{N}$), i.e. $M'=\frac{1}{2}\mathrm{Id}$ all inner products vanish. In order to form a basis, we must prove that the vectors themselves never vanish. We find

$$\begin{aligned}
\|\mathbf{T}_1\|^2 &= 2(m_{11}^2-m_{11}+m_{12}+1)\,,\\
\|\mathbf{T}_2\|^2 &= \frac{2}{n_2^2}(6n_1^2(1-2m_{11})-6m_{12}n_1n_2+5m_{11}^2-2m_{11}+5m_{12}+2)\,,\\
\|\mathbf{T}_3\|^2 &= 2\lambda^2\,,\\
\|\mathbf{T}_4\|^2 &= 2\lambda^2\,,\\
\|N\|^2 &= \lambda^2(12m_{11}n_1^2-6n_1^2+12m_{12}n_1n_2+2m_{11}^2-8m_{11}+2m_{12}^2+8)\,,
\end{aligned}$$

and thus for $M'=\frac{1}{2}\mathrm{Id}$ it holds that $\|\mathbf{T}_1\|^2=\frac{6}{4}$, $\|\mathbf{T}_2\|^2=\frac{9}{2}\lambda^2 n_2^{-2}$ and $\|N\|^2=\frac{9}{2}\lambda^2$.

This concludes the proof that $\{\mathbf{T}_1,\mathbf{T}_2,\mathbf{T}_3,\mathbf{T}_4\}$ form indeed a basis of $T_Q\mathcal{T}$, and since N is orthogonal to $T_Q\mathcal{T}$, the result follows. □

Proposition A.2.5. *There exists $C,\alpha_0>0$ such that for all $\alpha\in(0,\alpha_0)$ and $Q\in\mathcal{N}$ it holds*

$$\mathcal{H}^4(B_\alpha(Q)\cap\mathcal{T}) \le C\alpha^4\,.$$

Proof. As seen before, $\mathcal{T}$ has the structure of a smooth manifold around $\mathcal{N}$. By invariance of $\mathcal{N}$ under rotations, it is enough to show that the claim holds around one $Q\in\mathcal{N}$. The Ricci curvature κ of $\mathcal{N}$ is bounded so that we can choose $\alpha_0>0$ small enough such that $B_\alpha(Q)\cap\mathcal{T}$ is contained in the geodesic ball in $\mathcal{T}$ of size 2α around Q for all $\alpha\in(0,\alpha_0)$. Furthermore, if needed, we can choose $\alpha_0>0$ even smaller such that $1-\frac{\kappa}{36\alpha_0^2}\le 2$. Theorem 3.1 in [82] then implies that

$$\mathcal{H}^4(B_\alpha(Q)\cap\mathcal{T}) \le \mathrm{vol}_{\mathcal{T}}(B_{2\alpha}(Q)) \le 16\pi^2\alpha^4\,.$$

□

Bibliography

[1] R. Abergel and L. Moisan. The shannon total variation. *Journal of Mathematical Imaging and Vision*, 59(2):341–370, may 2017.

[2] S. Alama, L. Bronsard, D. Golovaty, and X. Lamy. Saturn ring defect around a spherical particle immersed in nematic liquid crystal. Preprint, 2020.

[3] S. Alama, L. Bronsard, and X. Lamy. Minimizers of the Landau–de Gennes energy around a spherical colloid particle. *Arch. Ration. Mech. Anal.*, 222(1):427–450, 2016.

[4] S. Alama, L. Bronsard, and X. Lamy. Spherical particle in nematic liquid crystal under an external field: The saturn ring regime. *J. Nonlinear Sci.*, 28(4):1443–1465, 2018.

[5] G. Alberti, S. Baldo, and G. Orlandi. Variational convergence for functionals of ginzburg-landau type. *Indiana University Mathematics Journal*, 54(5):1411–1472, 2005.

[6] F. Almgren. *Plateau's Problem: An Invitation to Varifold Geometry*. American Mathematical Society, aug 2001.

[7] M. Alnæs, J. Blechta, J. Hake, A. Johansson, B. Kehlet, A. Logg, C. Richardson, J. Ring, M. E. Rognes, and G. N. Wells. The fenics project version 1.5. *Archive of Numerical Software*, Vol 3:Starting Point and Frequency: Year: 2013 , 2015.

[8] F. Alouges, A. Chambolle, and D. Stantejsky. The saturn ring effect in nematic liquid crystals with external field: Effective energy and hysteresis. *Arch Ration Mech Anal*, 2021.

[9] F. Alouges, A. Chambolle, and D. Stantejsky. Convergence to line and surface energies in nematic liquid crystal colloids with external magnetic field. *Preprint*, 2022.

[10] L. Ambrosio, N. Fusco, and D. Pallara. *Functions of Bounded Variation and Free Discontinuity Problems*. OXFORD UNIVERSITY PRESS, 2000.

[11] L. Ambrosio and H. M. Soner. Level set approach to mean curvature flow in arbitrary codimension. *Journal of Differential Geometry*, 43(4), jan 1996.

[12] A. Amoddeo, R. Barberi, and G. Lombardo. Electric field-induced fast nematic order dynamics. *Liq. Cryst.*, 38(1):93–103, 2011.

[13] D. Andrienko. Introduction to liquid crystals. *J. Mol. Liq.*, 267:520–541, 2018.

[14] M. Antonietti, editor. *Colloid Chemistry I*. Springer Berlin Heidelberg, 2003.

[15] J. Aplinc, A. Pusovnik, and M. Ravnik. Designed self-assembly of metamaterial split-ring colloidal particles in nematic liquid crystals. *Soft Matter*, 15(28):5585–5595, 2019.

[16] D. N. Arnold. *Finite Element Exterior Calculus*. Society for Industrial and Applied Mathematics, dec 2018.

[17] U. Ayachit. *The ParaView Guide: A Parallel Visualization Application*. Kitware, Inc., 2015.

[18] R. Badal, M. Cicalese, L. De Luca, and M. Ponsiglione. Γ-convergence analysis of a generalized XY model: fractional vortices and string defects. *Commun. Math. Phys.*, 358(2):705–739, 2018.

[19] J. M. Ball. The calculus of variations and materials science. *Quarterly of Applied Mathematics*, 56(4):719–740, 1998.

[20] J. M. Ball. Liquid crystals and their defects. In *Mathematical thermodynamics of complex fluids*, volume 2200 of *Lecture Notes in Math.*, pages 1–46. Springer, Cham, 2017.

[21] J. M. Ball. Mathematics and liquid crystals. *Mol. Cryst. Liq. Cryst.*, 647(1):1–27, 2017.

[22] J. M. Ball and S. J. Bedford. Discontinuous order parameters in liquid crystal theories. *Mol. Cryst. Liq. Cryst.*, 2014.

[23] J. M. Ball and A. Majumdar. Nematic liquid crystals: From Maier-Saupe to a continuum theory. *Mol. Cryst. Liq. Cryst.*, 525(1):1–11, 2010.

[24] J. M. Ball and A. Zarnescu. Orientability and energy minimization in liquid crystal models. *Archive for Rational Mechanics and Analysis*, 202(2):493–535, may 2011.

[25] S. Bedford. Function spaces for liquid crystals. *Arch. Ration. Mech. Anal.*, 219(2):937–984, 2016.

[26] A. N. Beris and B. J. Edwards. *Thermodynamics of Flowing Systems: with Internal Microstructure*. Oxford University Press, aug 1994.

[27] J. Bernoulli. Problema novum ad cujus solutionem mathematici invitantur. *Acta Eruditorum*, 18:269, June 1696.

[28] F. Bethuel. Variational methods for ginzburg-landau equations. In *Lecture Notes in Mathematics*, pages 1–43. Springer Berlin Heidelberg, 1999.

[29] F. Bethuel, H. Brezis, and F. Hélein. Asymptotics for the minimization of a Ginzburg-Landau functional. *Calc. Var. Partial Differential Equations*, 1(2):123–148, 1993.

[30] F. Bethuel, H. Brezis, and F. Hélein. *Ginzburg-Landau Vortices*. Birkhäuser Boston, 1994.

[31] M. Born and E. Wolf. *Principles of Optics*. Cambridge University Press, 2019.

[32] S. Boyd, N. Parikh, E. Chu, B. Peleato, and J. Eckstein. Distributed optimization and statistical learning via the alternating direction method of multipliers. *Foundations and Trends® in Machine Learning*, 3(1):1–122, 2010.

[33] A. Braides. *Gamma-Convergence for Beginners*. OXFORD UNIV PR, 2002.

[34] A. Braides, M. Cicalese, and F. Solombrino. Q-tensor continuum energies as limits of head-to-tail symmetric spin systems. *SIAM J. Math. Anal.*, 47(4):2832–2867, 2015.

[35] K. A. Brakke. The surface evolver. *Experimental Mathematics*, 1(2):141–165, jan 1992.

[36] E. Bretin, R. Denis, S. Masnou, and G. Terii. Learning phase field mean curvature flows with neural networks. *Preprint*, 2021.

[37] H. Brezis, J.-M. Coron, and E. H. Lieb. Harmonic maps with defects. *Commun. Math. Phys.*, 107(4):649–705, 1986.

[38] H. Brezis and L. Nirenberg. Degree theory and BMO part I: Compact manifolds without boundaries. *Selecta Mathematica*, 1(2):197–263, sep 1995.

[39] B. Buet, G. P. Leonardi, and S. Masnou. Weak and approximate curvatures of a measure: A varifold perspective. *Nonlinear Analysis*, 222:112983, sep 2022.

[40] G. Canevari. Biaxiality in the asymptotic analysis of a 2D Landau–de Gennes model for liquid crystals. *ESAIM. Control Optim. Calc. Var.*, 21(1):101–137, 2015.

[41] G. Canevari. *Defects in the Landau-de Gennes model for liquid crystals*. PhD thesis, Université Pierre et Marie Curie - Paris VI, 2015.

[42] G. Canevari. Line defects in the small elastic constant limit of a three-dimensional Landau–de Gennes model. *Arch. Ration. Mech. Anal.*, 223(2):591–676, 2017.

[43] G. Canevari and G. Orlandi. Topological singular set of vector-valued maps, I: applications to manifold-constrained sobolev and BV spaces. *Calculus of Variations and Partial Differential Equations*, 58(2), mar 2019.

[44] G. Canevari and G. Orlandi. Topological singular set of vector-valued maps, II: γ-convergence for ginzburg–landau type functionals. *Archive for Rational Mechanics and Analysis*, 241(2):1065–1135, jun 2021.

[45] A. Chambolle and T. Pock. Crouzeix–raviart approximation of the total variation on simplicial meshes. *Journal of Mathematical Imaging and Vision*, 62(6-7):872–899, feb 2020.

[46] A. Chambolle and T. Pock. Approximating the total variation with finite differences or finite elements. In *Geometric Partial Differential Equations - Part II*, pages 383–417. Elsevier, 2021.

[47] D. Chiron. *Etude mathématique de modèles issus de la physique de la matière condensée.* PhD thesis, Université Pierre et Marie Curie - Paris VI, 2004.

[48] L. Condat. Discrete total variation: New definition and minimization. *SIAM Journal on Imaging Sciences*, 10(3):1258–1290, jan 2017.

[49] A. Contreras and X. Lamy. Singular perturbation of manifold-valued maps with anisotropic energy. Preprint, 2018.

[50] R. Courant. *Dirichlet's principle, conformal mapping, and minimal surfaces : reprint.* Springer Verlag, New York, 1977.

[51] M. Dambrine and B. Puig. Oriented distance point of view on random sets. *ESAIM: Control, Optimisation and Calculus of Variations*, 26:84, 2020.

[52] G. David. $C^{1+\alpha}$-regularity for two-dimensional almost-minimal sets in $\mathbb{R}^n$. *J. Geom. Anal.*, 2010.

[53] G. David. A local description of 2-dimensional almost minimal sets bounded by a curve. 2019. hal-01996231.

[54] T. S. David Dunmur. *Soap, Science, and Flat-Screen TVs: A History of Liquid Crystals.* OXFORD UNIV PR, 2010.

[55] F. W. David Hoffman, Hermann Karcher. The genus one helicoid and the minimal surfaces that led to its discovery. *Global Analysis and Modern Mathematics*, pages 119–170, 1993.

[56] T. A. Davis and E. C. Gartland. Finite element analysis of the landau-de gennes minimization problem for liquid crystals. *SIAM Journal on Numerical Analysis*, pages 336–362, 1998.

[57] P. G. de Gennes and J. Prost. *The Physics of Liquid Crystals.* International Series of Monographs on Physics, 1993.

[58] D. Demus, J. W. Goodby, G. W. Gray, H.-W. Spiess, and V. Vill. *Handbook of Liquid Crystals.* Wiley VCH Verlag GmbH, 2014.

[59] J. Douglas. Solution of the problem of plateau. *Transactions of the American Mathematical Society*, 33(1):263–321, 1931.

[60] G. Dziuk. An algorithm for evolutionary surfaces. *Numerische Mathematik*, 58(1):603–611, dec 1990.

[61] J. L. Ericksen. Conservation laws for liquid crystals. *Transactions of the Society of Rheology*, 5(1):23–34, mar 1961.

[62] J. L. Ericksen. Hydrostatic theory of liquid crystals. *Archive for Rational Mechanics and Analysis*, 9(1):371–378, jan 1962.

[63] J. L. Ericksen. Liquid crystals with variable degree of orientation. *Arch. Ration. Mech. Anal.*, 113(2):97–120, 1991.

[64] A. Ern and J.-L. Guermond. *Finite Elements I: Approximation and Interpolation*. Springer International Publishing, 2021.

[65] H. Federer. *Geometric Measure Theory*. Springer Berlin Heidelberg, 1996.

[66] H. Federer and W. H. Fleming. Normal and integral currents. *The Annals of Mathematics*, 72(3):458, nov 1960.

[67] W. H. Fleming. Flat chains over a finite coefficient group. *Transactions of the American Mathematical Society*, 121(1):160–160, jan 1966.

[68] G. Foffano, J. Lintuvuori, A. Tiribocchi, and D. Marenduzzo. The dynamics of colloidal intrusions in liquid crystals: a simulation perspective. *Liquid Crystals Reviews*, 2(1):1–27, jan 2014.

[69] M. G. Forest, Q. Wang, and H. Zhou. Homogeneous pattern selection and director instabilities of nematic liquid crystal polymers induced by elongational flows. *Phys. Fluids*, 12(3):490–498, 2000.

[70] F. C. Frank. I. liquid crystals. on the theory of liquid crystals. *Discuss. Faraday Soc.*, 25:19–28, 1958.

[71] J. Fukuda, H. Stark, M. Yoneya, and H. Yokoyama. Dynamics of a nematic liquid crystal around a spherical particle. *J. Phys.: Condens. Matter*, 16(19):S1957–S1968, 2004.

[72] J. Fukuda and H. Yokoyama. Stability of the director profile of a nematic liquid crystal around a spherical particle under an external field. *Eur. Phys. J. E*, 21(4):341–347, 2006.

[73] J. Fukuda, M. Yoneya, and H. Yokoyama. Director configuration of a nematic liquid crystal around a spherical particle: Numerical analysis using adaptive mesh refinement. *Mol. Cryst. Liq. Cryst.*, 413(1):221–229, 2004.

[74] D. Gabay and B. Mercier. A dual algorithm for the solution of nonlinear variational problems via finite element approximation. *Computers & Mathematics with Applications*, 2(1):17–40, 1976.

[75] Y. A. Garbovskiy and A. V. Glushchenko. Liquid crystalline colloids of nanoparticles. In *Solid State Physics*, pages 1–74. Elsevier, 2010.

[76] E. C. Gartland. Scalings and limits of Landau-deGennes models for liquid crystals: A comment on some recent analytical papers. *Math. Modelling and Anal.*, 23(3):414–432, 2018.

[77] E. C. Gartland. Forces and variational compatibility for equilibrium liquid crystal director models with coupled electric fields. *Continuum Mech. Thermodyn.*, 32(6):1559–1593, 2020.

[78] C. Geuzaine and J.-F. Remacle. Gmsh. *Available at: http://http://gmsh.info/*, 2020.

[79] M. Goldman, B. Merlet, and V. Millot. A Ginzburg-Landau model with topologically induced free discontinuities. *Ann. Inst. Fourier*, 2017.

[80] T. Goldstein, B. O'Donoghue, S. Setzer, and R. Baraniuk. Fast alternating direction optimization methods. *SIAM Journal on Imaging Sciences*, 7(3):1588–1623, jan 2014.

[81] H. H. Goldstine. *A History of the Calculus of Variations from the 17th through the 19th Century*. Springer New York, 1980.

[82] A. Gray. The volume of a small geodesic ball of a riemannian manifold. 20(4), apr 1974.

[83] Y. Gu and N. L. Abbott. Observation of saturn-ring defects around solid microspheres in nematic liquid crystals. *Physical Review Letters*, 85(22):4719–4722, nov 2000.

[84] M. Herrmann, R. Herzog, S. Schmidt, J. Vidal-Núñez, and G. Wachsmuth. Discrete total variation with finite elements and applications to imaging. *Journal of Mathematical Imaging and Vision*, 61(4):411–431, oct 2018.

[85] D. Hilbert. Die grundlagen der physik. *Mathematische Annalen*, 92(1-2):1–32, mar 1924.

[86] M. W. Hirsch. *Differential Topology*. Springer New York, 1976.

[87] R. Ignat and R. L. Jerrard. Renormalized energy between vortices in some Ginzburg–Landau models on 2-dimensional riemannian manifolds. *Archive for Rational Mechanics and Analysis*, 239(3):1577–1666, jan 2021.

[88] R. Ignat and X. Lamy. Lifting of $\mathbb{RP}^{d-1}$-valued maps in BV and applications to uniaxial Q-tensors. With an appendix on an intrinsic BV-energy for manifold-valued maps. *Calc. Var. Partial Differential Equations*, 58(2):Art. 68, 26, 2019.

[89] R. Ignat and R. Moser. Interaction energy of domain walls in a nonlocal ginzburg–landau type model from micromagnetics. *Archive for Rational Mechanics and Analysis*, 221(1):419–485, jan 2016.

[90] R. Ignat, L. Nguyen, V. Slastikov, and A. Zarnescu. Stability of point defects of degree $\pm\frac{1}{2}$ in a two-dimensional nematic liquid crystal model. *Calculus of Variations and Partial Differential Equations*, 55(5), sep 2016.

[91] B. Jerome. Surface effects and anchoring in liquid crystals. *Reports on Progress in Physics*, 54(3):391–451, mar 1991.

[92] R. L. Jerrard. Lower bounds for generalized Ginzburg–Landau functionals. *SIAM J. Math. Anal.*, 30(4):721–746, 1999.

[93] J. Jost. *Two-dimensional geometric variational problems*. Wiley, Chichester New York, 1991.

[94] H. Karcher. Construction of minimal surfaces. *Surveys in Geometry*, pages 1–96, 1989.

[95] S. Khullar. An experimental study of bubbles and droplets rising in a nematic liquid crystal. Master's thesis, Faculty of Chemical and Biological Engineering, University of British Columbia, 2007.

[96] D. Kim. Accelerated proximal point method for maximally monotone operators. *Mathematical Programming*, 190(1-2):57–87, mar 2021.

[97] K. I. Kim and Z. Liu. Global minimizer for the Ginzburg-Landau functional of an inhomogeneous superconductor. *Journal of Mathematical Physics*, 43(2):803–817, feb 2002.

[98] M. Kirszbraun. Über die zusammenziehende und Lipschitzsche Transformationen. *Fundamenta Mathematicae*, 22(1):77–108, 1934.

[99] G. Kitavtsev, J. M. Robbins, V. Slastikov, and A. Zarnescu. Liquid crystal defects in the landau–de gennes theory in two dimensions — beyond the one-constant approximation. *Mathematical Models and Methods in Applied Sciences*, 26(14):2769–2808, dec 2016.

[100] M. Kléman and O. D. Lavrentovich. Topological point defects in nematic liquid crystals. *Philos. Mag.*, 86(25-26):4117–4137, 2006.

[101] M. Kurzke, C. Melcher, R. Moser, and D. Spirn. Ginzburg-Landau vortices driven by the Landau-Lifshitz-Gilbert equation. *Archive for Rational Mechanics and Analysis*, 199(3):843–888, sep 2010.

[102] J. P. Lagerwall and G. Scalia. A new era for liquid crystal research: Applications of liquid crystals in soft matter nano-, bio- and microtechnology. *Current Applied Physics*, 12(6):1387–1412, nov 2012.

[103] J. L. Lagrange. Essai d'une nouvelle méthode pour détérminer les maxima et les minima des formules intégrales indéfinies. *Miscellanea Taurinensia*, pages 335–362, 1760-1761.

[104] H. P. Langtangen and A. Logg. *Solving PDEs in Python*. Springer International Publishing, 2016.

[105] O. Lavrentovich, P. Pasini, C. Zannoni, and S. Zumer, editors. *Defects in Liquid Crystals: Computer Simulations, Theory and Experiments*. Springer Netherlands, 2001.

[106] O. Lehmann. Über fliessende krystalle. *Zeitschrift für Physikalische Chemie*, 4U(1):462–472, jul 1889.

[107] F. M. Leslie. Some constitutive equations for liquid crystals. *Archive for Rational Mechanics and Analysis*, 28(4):265–283, jan 1968.

[108] F. H. Lin. Solutions of Ginzburg-Landau equations and critical points of the renormalized energy. *Annales de l'Institut Henri Poincaré C, Analyse non linéaire*, 12(5):599–622, sep 1995.

[109] C. Liu and N. J. Walkington. Approximation of liquid crystal flows. *SIAM Journal on Numerical Analysis*, 37(3):725–741, jan 2000.

[110] A. Logg, K.-A. Mardal, and G. Wells, editors. *Automated Solution of Differential Equations by the Finite Element Method*. Springer Berlin Heidelberg, 2012.

[111] R. López. *Constant Mean Curvature Surfaces with Boundary*. Springer Berlin Heidelberg, 2013.

[112] J. Loudet, O. Mondain-Monval, and P. Poulin. Line defect dynamics around a colloidal particle. *Eur. Phys. J. E*, 7(3):205–208, 2002.

[113] J. C. Loudet and P. Poulin. Application of an electric field to colloidal particles suspended in a liquid-crystal solvent. *Phys. Rev. Lett.*, 87(16), 2001.

[114] T. Machon. The topology of knots and links in nematics. *Liquid Crystals Today*, 28(3):58–67, jul 2019.

[115] T. Machon, H. Aharoni, Y. Hu, and R. D. Kamien. Aspects of Defect Topology in Smectic Liquid Crystals. *Commun. Math. Phys.*, 372(2):525–542, 2019.

[116] T. Machon and G. P. Alexander. Knotted defects in nematic liquid crystals. *Physical Review Letters*, 113(2), jul 2014.

[117] F. Maggi. *Sets of Finite Perimeter and Geometric Variational Problems*. Cambridge University Press, 2009.

[118] W. Maier and A. Saupe. Eine einfache molekulare theorie des nematischen kristallinflüssigen zustandes. *Zeitschrift für Naturforschung A*, 13(7):564–566, jul 1958.

[119] A. Majumdar. Equilibrium order parameters of nematic liquid crystals in the Landau-de Gennes theory. *Eur. J. Appl. Math.*, 21(2):181–203, 2010.

[120] A. Majumdar. The radial-hedgehog solution in Landau-de Gennes' theory for nematic liquid crystals. *Eur. J. Appl. Math.*, 23(1):61–97, 2012.

[121] A. Majumdar and A. Zarnescu. Landau-de Gennes theory of nematic liquid crystals: the Oseen-Frank limit and beyond. *Arch. Ration. Mech. Anal.*, 196(1):227–280, 2009.

[122] A. Masiello. Applications of calculus of variations to general relativity. In *Recent Developments in General Relativity*, pages 173–195. Springer Milan, 2000.

[123] R. Matveev and J. W. Portegies. Intrinsic flat and Gromov-Hausdorff convergence of manifolds with Ricci curvature bounded below. *The Journal of Geometric Analysis*, 27(3):1855–1873, sep 2016.

[124] P. Mironescu. On the stability of radial solutions of the Ginzburg-Landau equation. *Journal of Functional Analysis*, 130(2):334–344, jun 1995.

[125] L. Modica. Gradient theory for phase transitions and the minimal interface criterion. *Arch. Rat. Mech. Anal.*, 98:123–142, 1987.

[126] L. Modica. The gradient theory of phase transitions and the minimal interface criterion. *Archive for Rational Mechanics and Analysis*, 98(2):123–142, jun 1987.

[127] L. Modica and S. Mortola. Un esempio di Γ-convergenza. *Boll. Un. Mat. Ital. B*, 5(14):285–299, 1977.

[128] O. Mondain-Monval, J. Dedieu, T. Gulik-Krzywicki, and P. Poulin. Weak surface energy in nematic dispersions: Saturn ring defects and quadrupolar interactions. *The European Physical Journal B*, 12(2):167–170, nov 1999.

[129] F. Morgan. $(\mathbf{M}, \epsilon, \delta)$-minimal curve regularity. *Proceedings of the American Mathematical Society*, 120(3):677–677, mar 1994.

[130] F. Morgan. Surfaces minimizing area plus length of singular curves. *Proceedings of the American Mathematical Society*, 122(4):1153–1153, apr 1994.

[131] F. Morgan. *Geometric measure theory : a beginner's guide*. Elsevier Ltd, Amsterdam, 2016.

[132] N. J. Mottram and C. J. P. Newton. Introduction to Q-tensor theory. Working Paper, 2014.

[133] I. Muševič. Nematic liquid-crystal colloids. *Materials*, 11(1):24, 2018.

[134] J. C. C. Nitsche. *Lectures on Minimal Surfaces*. Cambridge University Press, 2011.

[135] L. Onsager. The effects of shape on the interaction of colloidal particles. *Annals of the New York Academy of Sciences*, 51(4):627–659, may 1949.

[136] C. W. Oseen. The theory of liquid crystals. *Trans. Faraday Soc.*, 29:883–899, 1933.

[137] M. G. Paolo Freguglia. *The Early Period of the Calculus of Variations*. Springer-Verlag GmbH, 2016.

[138] G. D. Philippis and F. Maggi. Regularity of free boundaries in anisotropic capillarity problems and the validity of Young's law. *Archive for Rational Mechanics and Analysis*, 216(2):473–568, nov 2014.

[139] E. B. Priestley, P. J. Wojtowicz, and P. Sheng, editors. *Introduction to Liquid Crystals*. Plenum Press, 1974.

[140] T. Radó. *On the Problem of Plateau*. Springer Berlin Heidelberg, 1933.

[141] F. Reinitzer. Beiträge zur kenntniss des cholesterins. *Monatshefte für Chemie - Chemical Monthly*, 9(1):421–441, dec 1888.

[142] T. Rivière. Everywhere discontinuous harmonic maps into spheres. *Acta Math.*, 175(2):197–226, 1995.

[143] D. K. Sahu, T. G. Anjali, M. G. Basavaraj, J. Aplinc, S. Čopar, and S. Dhara. Orientation, elastic interaction and magnetic response of asymmetric colloids in a nematic liquid crystal. *Scientific Reports*, 9(1), jan 2019.

[144] E. Sandier. Lower bounds for the energy of unit vector fields and applications. *J. Funct. Anal.*, 152(2):379–403, 1998.

[145] E. Sandier and S. Serfaty. Gamma-convergence of gradient flows with applications to Ginzburg-Landau. *Communications on Pure and Applied Mathematics*, 57(12):1627–1672, 2004.

[146] J. Schwartz. *Nonlinear functional analysis*. Gordon and Breach, New York, 1969.

[147] B. Senyuk, Q. Liu, S. He, R. D. Kamien, R. B. Kusner, T. C. Lubensky, and I. I. Smalyukh. Topological colloids. *Nature*, 493(7431):200–205, dec 2012.

[148] S. Serfaty. Vorticity for the Ginzburg-Landau model of superconductors in a magnetic field. *Nonlinear Dynamics and Renormalization Group*, 2001.

[149] L. Simon. *Lectures on geometric measure theory.* Centre for Mathematical Analysis, Australian National University, Canberra, 1983.

[150] I. I. Smalyukh. Liquid crystals enable chemoresponsive reconfigurable colloidal self-assembly. *Proceedings of the National Academy of Sciences*, 107(9):3945–3946, feb 2010.

[151] N. V. Solodkov, J. uk Shim, and J. C. Jones. Self-assembly of fractal liquid crystal colloids. *Nature Communications*, 10(1), jan 2019.

[152] B. H. Søren Fournais. *Spectral Methods in Surface Superconductivity.* SPRINGER NATURE, 2010.

[153] D. Stantejsky. A finite element approach for minimizing line and surface energies arising in the study of singularities in liquid crystals. *In preparation*, 2022.

[154] H. Stark. Director field configurations around a spherical particle in a nematic liquid crystal. *Eur. Phys. J. B*, 10(2):311–321, 1999.

[155] M. Struwe. *Plateau's Problem and the Calculus of Variations.* Princeton University Press, 2014.

[156] D. V. Sudhakaran, R. K. Pujala, and S. Dhara. Orientation dependent interaction and self-assembly of cubic magnetic colloids in a nematic liquid crystal. *Advanced Optical Materials*, 8(7):1901585, jan 2020.

[157] X. Tang and J. V. Selinger. Orientation of topological defects in 2d nematic liquid crystals. *Soft Matter*, 13(32):5481–5490, 2017.

[158] J. E. Taylor. The structure of singularities in soap-bubble-like and soap-film-like minimal surfaces. *The Annals of Mathematics*, 103(3):489, may 1976.

[159] J. E. Taylor. Boundary regularity for solutions to various capillarity and free boundary problems. *Communications in Partial Differential Equations*, 2(4):323–357, jan 1977.

[160] R. Thom. Un lemme sur les applications différentiables. *Boletín de la Sociedad Matemática Mexicana. Segunda Serie*, 1:59–71, 1956.

[161] E. G. Virga. *Variational Theories for Liquid Crystals.* Chapman and Hall/CRC, 1994.

[162] C. Völtz, Y. Maeda, Y. Tabe, and H. Yokoyama. Director-configurational transitions around microbubbles of hydrostatically regulated size in liquid crystals. *Phys. Rev. Lett.*, 97(22), 2006.

[163] M. A. C. Vollmer. Critical points and bifurcations of the three-dimensional Onsager model for liquid crystals. *Arch. Ration. Mech. Anal.*, 226(2):851–922, 2017.

[164] S. Wang and A. Chern. Computing minimal surfaces with differential forms. *ACM Transactions on Graphics*, 40(4):1–14, aug 2021.

[165] X. Wang. *Wave Propagation in Liquid-Crystal Materials.* PhD thesis, Technische Universität, Darmstadt, 2014.

[166] B. White. The deformation theorem for flat chains. *Acta Mathematica*, 183(2):255–271, 1999.

[167] B. White. Rectifiability of flat chains. *The Annals of Mathematics*, 150(1):165, jul 1999.

[168] Y. Xie, Y. Li, G. Wei, Q. Liu, H. Mundoor, Z. Chen, and I. I. Smalyukh. Liquid crystal self-assembly of upconversion nanorods enriched by depletion forces for mesostructured material preparation. *Nanoscale*, 10(9):4218–4227, 2018.

[169] Y. Yu. Disclinations in limiting Landau-de Gennes theory. *Arch. Ration. Mech. Anal.*, 237(1):147–200, 2020.

[170] C. Zhou, P. Yue, and J. J. Feng. The rise of Newtonian drops in a nematic liquid crystal. *J. Fluid Mech.*, 593:385–404, 2007.

ECOLE
DOCTORALE
DE MATHEMATIQUES
HADAMARD

Titre : Limite asymptotique du modèle de Landau-de Gennes pour des cristaux liquides autour d'une inclusion

Mots clés : cristaux liquides, modèle de Landau-de Gennes, $\Gamma-$convergence, défauts topologiques, effet de l'anneau de Saturne

Résumé : Les cristaux liquides sont des matériaux avec des propriétés intermédiaires entre celles des liquides et des solides cristallins, c'est-à-dire les molécules peuvent se déplacer mais montrent un ordre de position et d'orientation. L'une de leurs caractéristiques les plus remarquables est la formation naturelle de structures de défauts, en particulier des singularités ponctuelles ou en lignes. Dans ce travail on considère une version du modèle de Landau-de Gennes pour les cristaux liquides nématiques avec un champ magnétique externe modélisant l'effet de l'anneau de Saturne autour d'une particule immergée. Dans un régime asymptotique où les singularités ponctuelles et de lignes se produisent, nous dérivons une énergie effective décrivant la formation et la transition entre les différentes singularités.
Le premier chapitre porte sur le cas physique le plus étudié d'une particule sphérique. Après une remise à l'échelle de l'énergie physique, une énergie limite au sens de la $\Gamma-$convergence, énoncée à la surface de la particule, est dérivée. En étudiant le problème limite, nous expliquons la transition entre la configuration du dipôle et de l'anneau de Saturne ainsi que l'apparition d'un phénomène d'hystérésis.
Dans le deuxième chapitre, nous considérons le cas général d'une particule quelconque fermée et suffisamment lisse. Contrairement à une particule sphérique (ou plus générale convexe), nous obtenons un terme supplémentaire dans l'énergie limite, montrant quantitativement que l'énergie proche du minimum est asymptotiquement concentrée sur des lignes et des surfaces proches de la particule voire collées à sa surface. Nous discutons également la régularité des minimiseurs et les conditions d'optimalité de l'énergie limite.
Le troisième chapitre est consacré à l'étude numérique de l'énergie limite et au développement et à la mise en œuvre de méthodes numériques adaptées. Nous vérifions les résultats du premier chapitre pour la sphère, puis nous étudions les structures de défauts dans le cas d'une particule en forme de cacahuète ou de croissant.

Title : Asymptotic Limit of the Landau-de Gennes Model for Liquid Crystals Around an Inclusion

Keywords : liquid crystals, Landau-de Gennes model, $\Gamma-$convergence, topological defects, Saturn ring effect

Abstract : Liquid crystals are a type of matter which share properties with both liquids and crystalline solids, i.e. the molecules of such materials can move but exhibit a positional and orientational order. One of the most remarkable characteristics is the formation of defect structures, in particular point and line singularities. In this work we use a version of the Landau-de Gennes model for nematic liquid crystals with an external magnetic field to describe the Saturn ring effect around an immersed particle. In an asymptotic regime where both point and line singularities occur, we derive an effective energy describing the formation and transition between different singularities.
The first chapter deals with the physically relevant case of a spherical particle. After a rescaling of the physical energy, a limit energy in the sense of $\Gamma-$convergence, stated on the particle surface, is derived. Studying the limit problem, we explain the transition between the dipole and Saturn ring configurations and the occurrence of a hysteresis phenomenon.
In the second chapter we consider the general case of an arbitrary closed and sufficiently smooth particle. In contrast to spherical (or more general convex) particle, we obtain an additional term in the limit energy, showing quantitatively that the close-to-minimal energy is asymptotically concentrated on lines and surfaces nearby or on the particle. We also discuss regularity of minimizers and optimality conditions for the limit energy.
The third chapter is dedicated to the numerical investigation of the limit energy and the development and implementation of adapted numerical methods. We verify the results of the first chapter for the sphere and then study the defect structures in the case of a peanut and croissant-like particle.

Institut Polytechnique de Paris
91120 Palaiseau, France